CHALLENGING THE FUNCTIONAL CONNECTIVITY DISRUPTION IN NEURODEGENERATIVE DISEASES: NEW THERAPEUTIC PERSPECTIVES THROUGH NON-INVASIVE NEUROMODULATION AND CUTTING-EDGE TECHNOLOGIES

EDITED BY: Giancarlo Zito, Takashi Hanakawa, Luca Berdondini, Lorenzo Masia and Lorenzo Natale

PUBLISHED IN: Frontiers in Neuroscience

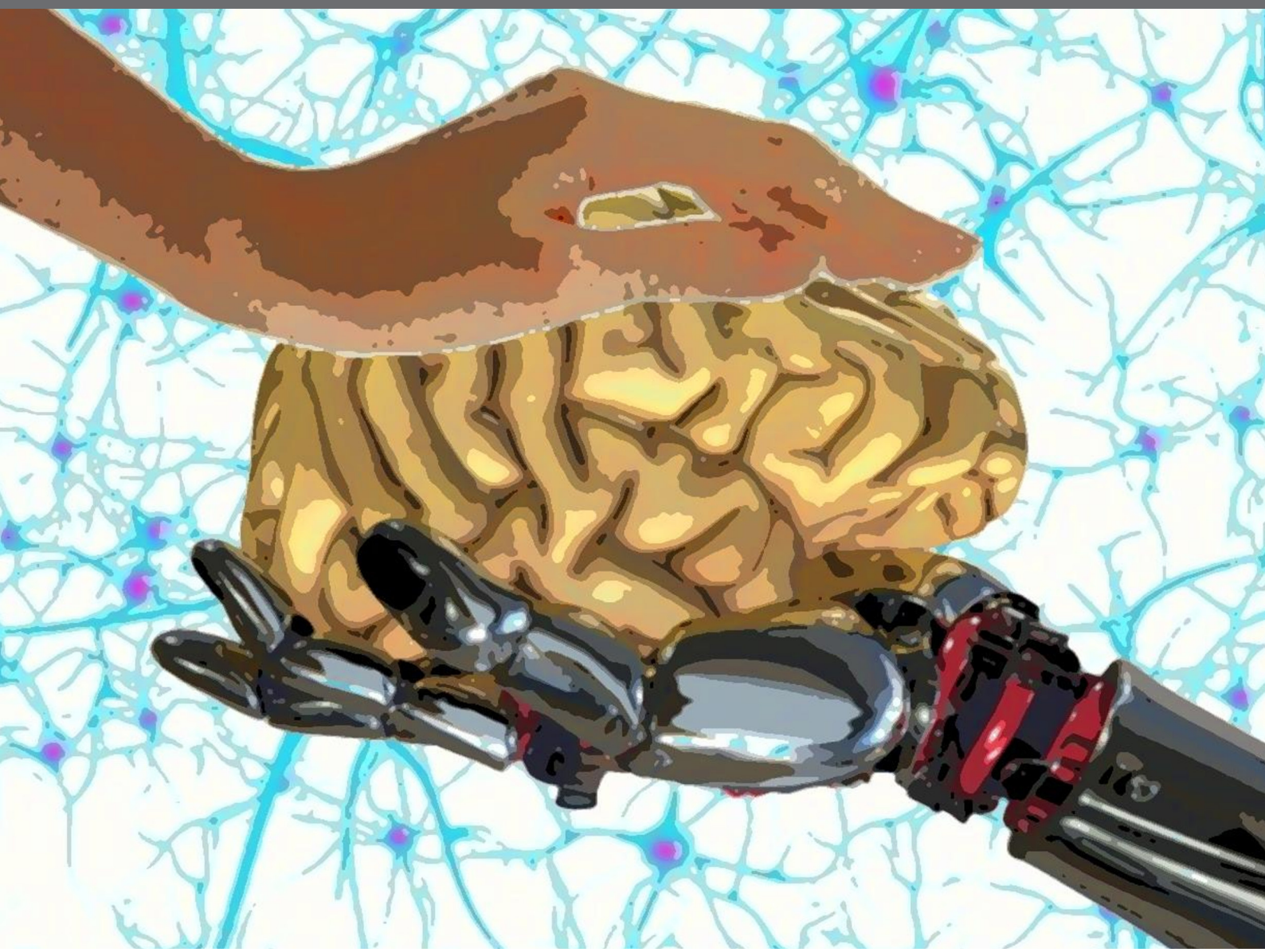

frontiers Research Topics

ISSN 1664-8714
ISBN 978-2-88945-593-5
DOI 10.3389/978-2-88945-593-5

About Frontiers

Frontiers is more than just an open-access publisher of scholarly articles: it is a pioneering approach to the world of academia, radically improving the way scholarly research is managed. The grand vision of Frontiers is a world where all people have an equal opportunity to seek, share and generate knowledge. Frontiers provides immediate and permanent online open access to all its publications, but this alone is not enough to realize our grand goals.

Frontiers Journal Series

The Frontiers Journal Series is a multi-tier and interdisciplinary set of open-access, online journals, promising a paradigm shift from the current review, selection and dissemination processes in academic publishing. All Frontiers journals are driven by researchers for researchers; therefore, they constitute a service to the scholarly community. At the same time, the Frontiers Journal Series operates on a revolutionary invention, the tiered publishing system, initially addressing specific communities of scholars, and gradually climbing up to broader public understanding, thus serving the interests of the lay society, too.

Dedication to Quality

Each Frontiers article is a landmark of the highest quality, thanks to genuinely collaborative interactions between authors and review editors, who include some of the world's best academicians. Research must be certified by peers before entering a stream of knowledge that may eventually reach the public - and shape society; therefore, Frontiers only applies the most rigorous and unbiased reviews.
Frontiers revolutionizes research publishing by freely delivering the most outstanding research, evaluated with no bias from both the academic and social point of view. By applying the most advanced information technologies, Frontiers is catapulting scholarly publishing into a new generation.

What are Frontiers Research Topics?

Frontiers Research Topics are very popular trademarks of the Frontiers Journals Series: they are collections of at least ten articles, all centered on a particular subject. With their unique mix of varied contributions from Original Research to Review Articles, Frontiers Research Topics unify the most influential researchers, the latest key findings and historical advances in a hot research area! Find out more on how to host your own Frontiers Research Topic or contribute to one as an author by contacting the Frontiers Editorial Office: researchtopics@frontiersin.org

CHALLENGING THE FUNCTIONAL CONNECTIVITY DISRUPTION IN NEURODEGENERATIVE DISEASES: NEW THERAPEUTIC PERSPECTIVES THROUGH NON-INVASIVE NEUROMODULATION AND CUTTING-EDGE TECHNOLOGIES

Topic Editors:
Giancarlo Zito, Italian Medicines Agency (AIFA), Italy
Takashi Hanakawa, National Center of Neurology and Psychiatry, Japan
Luca Berdondini, Fondazione Istituto Italiano di Tecnologia, Italy
Lorenzo Masia, University of Twente, Netherlands
Lorenzo Natale, Fondazione Istituto Italiano di Tecnologia, Italy

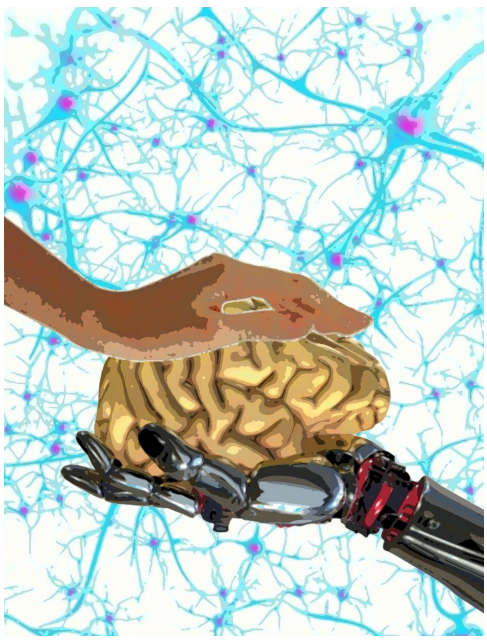

The growing affinity between human and cutting-edge technologies, including biorobotics is becoming a landmark for improving the potential of rehabilitation after multifactorial insults to the brain and nervous system. Image: Giancarlo Zito.

The neurorehabilitation field is increasingly focused on understanding how to efficiently revert the effects that acute (i.e., stroke or traumatic brain injury) or chronic (i.e., neurodegenerative diseases) insults play either on small or large-scale networks, encompassing motor, sensory and cognitive domains. The link between the disrupted neuronal pulse generators and their effectors is being re-shaped through a wide scenario that embraces biorobotics, robot-aided rehabilitation, non-invasive neurostimulation, nanoprosthetics and neuroengineering. For the past decade and at an amazing speed, large investments and efforts allowed enthusiastic and only apparently heterogeneous researchers to borrow theories from neurophysiology, pharmacology, physics and quantum mechanics in order to generate together highly

sophisticated tools that restore, resemble or even substitute the basic biological architecture. The idea of actually reverting weakened functions and/or replacing the faulty parts either of the human body or the central and peripheral nervous system is becoming a new reality, opening a fascinating era in this field.

In this Research Topic, several researchers showed how the above principles became reality, from theory to the bedside of patients, providing full explanations of the whole mechanistic processes and how they were implemented, up to the final stage.

Citation: Zito, G., Hanakawa, T., Berdondini, L., Masia, L., Natale, L., eds (2018). Challenging the Functional Connectivity Disruption in Neurodegenerative Diseases: New Therapeutic Perspectives through Non-Invasive Neuromodulation and Cutting-Edge Technologies. Lausanne: Frontiers Media. doi: 10.3389/978-2-88945-593-5

Table of Contents

SECTION III

PHYSIOLOGICAL AND PHARMACOLOGICAL NEUROMODULATION FOR NEUROLOGICAL CONDITIONS

frontiers in Neuroscience

EDITORIAL
published: 08 August 2018
doi: 10.3389/fnins.2018.00554

Editorial: Challenging the Functional Connectivity Disruption in Neurodegenerative Diseases: New Therapeutic Perspectives Through Non-invasive Neuromodulation and Cutting-Edge Technologies

Giancarlo Zito [1,2*] *and Takashi Hanakawa* [3]

[1] *Unit of Neurology, Ospedale San Giovanni Calibita Fatebenefratelli, Rome, Italy,* [2] *Innovation and Pharmaceutical Strategy Division, Italian Medicines Agency, Rome, Italy,* [3] *Department of Advanced Neuroimaging, Integrative Brain Imaging Center, National Center of Neurology and Psychiatry, Tokyo, Japan*

Keywords: rehabilitation, Biorobotics, Translational research, Neurophysiology, neuroprostheses, virtual reality environment, non-invasive brain stimulation, personalized treatment

OPEN ACCESS

Edited by:
Hari S. Sharma,
Uppsala University, Sweden

Reviewed by:
Asya Ozkizilcik,
University of Arkansas, United States
Jose Vicente Lafuente,
University of the Basque Country (UPV/EHU), Spain

****Correspondence:***
Giancarlo Zito
giancarlo.zito@afar.it

Specialty section:
This article was submitted to Neural Technology, a section of the journal Frontiers in Neuroscience

Received: *08 June 2018*
Accepted: *20 July 2018*
Published: *08 August 2018*

Citation:
Zito G and Hanakawa T (2018) Editorial: Challenging the Functional Connectivity Disruption in Neurodegenerative Diseases: New Therapeutic Perspectives Through Non-invasive Neuromodulation and Cutting-Edge Technologies. Front. Neurosci. 12:554. doi: 10.3389/fnins.2018.00554

Editorial on the Research Topic

Challenging the Functional Connectivity Disruption in Neurodegenerative Diseases: New Therapeutic Perspectives Through Non-invasive Neuromodulation and Cutting-Edge Technologies

A growing body of work indicates that in several acute and chronic neurological conditions, including stroke and neurodegenerative diseases, pathophysiological events may introduce functional alterations over small- and large-scale functional network dynamics. These phenomena occur ever since, or even before, the appearance of the first, distinct symptoms, and involve brain connectivity under either a resting or active task condition. The alterations of network dynamics can affect the outcome of subsequent therapeutic interventions and re-learning mechanisms during rehabilitation (Krakauer, 2006). Hence, an in-depth knowledge of early predictors of such network changes is crucial to address the most effective therapeutic and rehabilitation strategies, and to help reduce the burden on neurological patients and health care systems. To disentangle how changes of network dynamics take place in the brain, several functional domains, including motor, sensory, and cognitive ones, should be considered. It is also important to parse not only the extent and distribution of network damage across different conditions, but also to implement cutting-edge methods that are able to integrate specific information of networks on a broader perspective (Pievani et al., 2014). In this research topic, we will see how investigators highlighted the value of continuous and mutual osmosis between clinical research and technology, such as bio-robotics, robot-aided rehabilitation, non-invasive neurostimulation, neuroimaging, and neuroengineering, which can give rise to innovations in the field of neurorehabilitation.

MONITORING EFFECTS OF INTERVENTION OR DISEASE-RELATED BRAIN STATES

The combination of different neuroscientific techniques provides new opportunities for researchers to address new questions. Das et al. developed a mouse model to study neuroplasticity induced by transcranial direct current stimulation (tDCS) and showed polarity- and genetics-dependent effects of anodal tDCS-induced decreases in vestibulo-ocular reflex gain after cerebellar stimulation. Seewoo et al. explored possible ways to translate knowledge about the actions of repetitive transcranial magnetic stimulation (rTMS) from pre-clinical research in rodents to clinically plausible neuromodulation techniques in humans. In particular, they indicate that the combination of rTMS with fMRI requires specific adjustments to experimental protocols to efficiently scale and interchange paradigms borrowed from rTMS in rodents to fMRI in humans, and vice versa. Neuromodulation with simultaneous electroencephalography (EEG), functional MRI (fMRI), or positron emission tomography (PET) would shed light on a deeper characterization of the complexities behind connectivity dynamics induced by therapeutic or neuromodulatory rTMS.

Yamasaki et al. discussed the "connectopathy," which might underlie multifaceted deficits in social and behavioral domains in children with autistic spectrum disorders (ASD). Their contribution focused on how visual-evoked and event-related potentials (VEP/ERP) and diffusion tensor imaging (DTI) might reveal tiny alterations of visual and attentional networks in this condition. The ASD "connectopathy" likely arises from abnormal functional and structural connectivity in cortical networks involved in social information processing.

Machine learning methods are being extensively used for extracting neurophysiological features allowing individual categorization of patients with many neurologic conditions. Ogata et al. successfully trained a Support Vector Machine (SVM) on resting-state fMRI images to isolate specific functional connectivity features in idiopathic normal pressure hydrocephalus (iNPH). Moreover, the SVM was able to grade severity of the classical triad in iNPH (cognitive, gait, and urinary disturbances) using resting-state connectivity.

VIRTUAL REALITY AND ROBOTICS

Over the past 25 years, robotics and virtual reality have been increasingly used either to measure human movement or to gain knowledge on how the brain learns and controls voluntary movement (Reinkensmeyer et al., 2004). Robot-aided paradigms enable participants to conveniently tune several physical factors involved in movement simultaneously, thus allowing researchers to examine realistic motor cortex physiology, while minimizing mental frustration and physical harm in patients with motor dysfunctions (Woldag and Hummelsheim, 2002). Despite the great progress in the field of both computer science and engineering, however, much can be done to improve the contribution of virtual reality and robotics to the strategies behind functional recovery of damaged nervous functions (Holden, 2005). Marchal-Crespo et al. introduced fMRI-compatible robot-aided training strategies in a complex locomotor learning task—involving the coordination of the legs in a gait-like pattern to track a Lissajous figure presented on a screen, during fMRI. This is a nice experiment that showed the existence of a mathematical relationship between the error reduction induced by training and the initial skill level, with an error-amplification dependent engagement of cerebral reward circuits. Benyoucef et al. proposed highly realistic virtual simulations to study mental disorders. Although the concept needs to be proved, virtual reality could enhance active participation of patients with mental disorders in experimental studies, overcoming intrinsic communicative, emotional, and affective barriers.

PHYSIOLOGICAL AND PHARMACOLOGICAL NEUROMODULATION FOR NEUROLOGICAL CONDITIONS

Pinto et al. discussed in detail how pharmacological interventions with selective serotonin reuptake inhibitors (SSRI), which are widely used for the treatment of depression, may influence recovery after stroke.

Along with pharmacological methodology, non-invasive brain stimulation has been extensively studied in many neuro-psychiatric conditions as a physiological method to induce changes across regions of the nervous system. Quartarone et al. discusses the therapeutic potential of rTMS and tDCS and their neurophysiologic effects ("after effects") in dystonia. They also pointed out the limitation of the current techniques due to high variability of the outcomes. It is thus necessary to gather all the relevant information from overwhelmingly heterogeneous study protocols and then to convert them into a more harmonized protocol, which would make the interpretation of different studies easier. In this regard, Marceglia et al. proposed a new protocol for focal hand dystonia, using cathodal tDCS bilaterally over the primary motor cortex for 20 min daily for 5 consecutive days. Focal hand dystonia is a movement disorder that can be highly disabling since it often affects body parts essential for professional activity such as the fingers and wrists in pianists. tDCS seems to be a potentially effective non-invasive approach to revert cortical excitability to the normal state, thereby improving dystonic symptoms.

The damage induced by inflammation in multiple sclerosis (MS) represents another important model of functional disruption of networks. MS is a pathological entity in which inflammatory demyelination within the central nervous system leads to an ever-increasing depletion of synaptic transmission and effective plasticity due to a dissemination of lesions in both time and space. For unknown reasons, imaging and clinical findings are not well correlated in MS (known as "clinico-radiological paradox"). This morpho-functional disconnection prevents clinicians from formulating an accurate prognostic judgment about recovery. Stampanoni Bassi et al. give an

overview of several non-invasive techniques used in the study of MS, with the aim of clarifying how the choice of targeted brain areas influences the evaluation for the extent of recovery, while providing a holistic organizational view of brain networks in a comprehensive biochemical and neurophysiologic perspective. They also rehearse the interesting concept of diaschisis and extend it to the functional connectome (Carrera and Tononi, 2014) to explain the paradox.

It is important to be aware of the individual variations of the brain anatomy undergoing stimulation. Cancelli et al. extended their technology for personalizing neuromodulatory intervention using transcranial electrical stimulation (tES), aiming at better fitting the electrodes' shape over the cerebral cortical foldings. Their innovative technique achieved individually tailored electrode positioning without a neuronavigation system. This development may allow patients to undergo convenient, yet accurate and affordable tES treatment at home in the future.

Moving toward a better comprehension of mechanisms underlying gait impairment in Parkinson's disease (PD)-the most prevalent movement disorder-Cai et al. applied sinusoidal or stochastic galvanic vestibular stimulation (GVS) to a small group of patients with PD. GVS was able to enhance the functional connectivity between cortical/subcortical regions of interests and the putative pedunculopontine nucleus, which regulates locomotion at the supraspinal level.

CONCLUDING REMARKS

The editors of this topic really hope that the innovative neural technology as introduced here is effectively implemented in clinical practice to help patients with neuro-psychiatric disorders.

AUTHOR CONTRIBUTIONS

GZ launched the topic, drafted the Editorial. TH handled six contributions of the topic, critically and constructively revised the Editorial.

FUNDING

This work was in part supported by the Brain Mapping by Integrated Neurotechnologies for Disease Studies (Brain/MINDS) and Health Labor Science Research Grants from Japan Agency for Medical Research and development (AMED), and by KAKENHI grants (26120008, 18H04960, and 16H03306) from JSPS to TH.

REFERENCES

Carrera, E., and Tononi, G. (2014). Diaschisis: past, present, future. *Brain* 137, 2408–2422. doi: 10.1093/brain/awu101

Holden, M. K. (2005). Virtual environments for motor rehabilitation: review. *Cyberpsychol. Behav*. 8, 187–211; discussion: 212–219. doi: 10.1089/cpb.2005.8.187

Krakauer, J. W. (2006). Motor learning: its relevance to stroke recovery and neurorehabilitation. *Curr. Opin. Neurol.* 19, 84–90. doi: 10.1097/01.wco.0000200544.29915.cc

Pievani, M., Filippini, N., van den Heuvel, M. P., Cappa, S. F., and Frisoni, G. B. (2014). Brain connectivity in neurodegenerative diseases—from phenotype to proteinopathy. *Nat. Rev. Neurol.* 10, 620–633. doi: 10.1038/nrneurol.2014.178

Reinkensmeyer, D. J., Emken, J. L., and Cramer, S. C. (2004). Robotics, motor learning, and neurologic recovery. *Annu. Rev. Biomed. Eng.* 6, 497–525. doi: 10.1146/annurev.bioeng.6.040803.140223

Woldag, H., and Hummelsheim, H. (2002). Evidence-based physiotherapeutic concepts for improving arm and hand function in stroke patients: a review. *J. Neurol.* 249, 518–528. doi: 10.1007/s0041502 00058

Conflict of Interest Statement: The authors declare that the research was conducted in the absence of any commercial or financial relationships that could be construed as a potential conflict of interest.

frontiers in Neuroscience

REVIEW
published: 23 March 2018
doi: 10.3389/fnins.2018.00180

Combined rTMS/fMRI Studies: An Overlooked Resource in Animal Models

Bhedita J. Seewoo[1,2], *Sarah J. Etherington*[3], *Kirk W. Feindel*[2,4] *and Jennifer Rodger*[1,5]*

[1] *Experimental and Regenerative Neurosciences, School of Biological Sciences, The University of Western Australia, Perth, WA, Australia,* [2] *Centre for Microscopy, Characterization and Analysis, Research Infrastructure Centers, The University of Western Australia, Perth, WA, Australia,* [3] *School of Veterinary and Life Sciences, Murdoch University, Perth, WA, Australia,* [4] *School of Biomedical Sciences, University of Western Australia, Perth, WA, Australia,* [5] *Brain Plasticity Group, Perron Institute for Neurological and Translational Research, Perth, WA, Australia*

Repetitive transcranial magnetic stimulation (rTMS) is a non-invasive neuromodulation technique, which has brain network-level effects in healthy individuals and is also used to treat many neurological and psychiatric conditions in which brain connectivity is believed to be abnormal. Despite the fact that rTMS is being used in a clinical setting and animal studies are increasingly identifying potential cellular and molecular mechanisms, little is known about how these mechanisms relate to clinical changes. This knowledge gap is amplified by non-overlapping approaches used in preclinical and clinical rTMS studies: preclinical studies are mostly invasive, using cellular and molecular approaches, while clinical studies are non-invasive, including functional magnetic resonance imaging (fMRI), TMS electroencephalography (EEG), positron emission tomography (PET), and behavioral measures. A non-invasive method is therefore needed in rodents to link our understanding of cellular and molecular changes to functional connectivity changes that are clinically relevant. fMRI is the technique of choice for examining both short and long term functional connectivity changes in large-scale networks and is becoming increasingly popular in animal research because of its high translatability, but, to date, there have been no reports of animal rTMS studies using this technique. This review summarizes the main studies combining different rTMS protocols with fMRI in humans, in both healthy and patient populations, providing a foundation for the design of equivalent studies in animals. We discuss the challenges of combining these two methods in animals and highlight considerations important for acquiring clinically-relevant information from combined rTMS/fMRI studies in animals. We believe that combining rTMS and fMRI in animal models will generate new knowledge in the following ways: functional connectivity changes can be explored in greater detail through complementary invasive procedures, clarifying mechanism and improving the therapeutic application of rTMS, as well as improving interpretation of fMRI data. And, in a more general context, a robust comparative approach will refine the use of animal models of specific neuropsychiatric conditions.

Keywords: translational studies, non-invasive animal models, neuromodulation, rTMS, fMRI, resting-state, functional connectivity

OPEN ACCESS

Edited by:
Takashi Hanakawa, National Center of Neurology and Psychiatry (Japan), Japan

Reviewed by:
Mitsunari Abe, Fukushima Medical University, Japan
Ken-Ichiro Tsutsui, Tohoku University, Japan

***Correspondence:**
Jennifer Rodger
jennifer.rodger@uwa.edu.au

Specialty section:
This article was submitted to Neural Technology, a section of the journal Frontiers in Neuroscience

Received: *19 October 2017*
Accepted: *06 March 2018*
Published: *23 March 2018*

Citation:
Seewoo BJ, Etherington SJ, Feindel KW and Rodger J (2018) Combined rTMS/fMRI Studies: An Overlooked Resource in Animal Models. Front. Neurosci. 12:180. doi: 10.3389/fnins.2018.00180

INTRODUCTION

An exciting approach for the treatment of neuropsychiatric conditions is to use neuronal activity itself to encourage repair and improve brain function. This method can be used as an adjuvant with other interventions and might prove to be more effective and specific than a pharmacological approach, which often has side-effects and might not induce lasting changes. Several lines of evidence suggest that dysfunctional connectivity within specific neural networks may underpin many neurological and psychiatric conditions (Seeley et al., 2009; van den Heuvel and Hulshoff Pol, 2010). Transcranial magnetic stimulation (TMS) is a non-invasive neuromodulation technique that uses magnetic fields to induce electrical currents in the brain, thereby modulating neuronal activity, and networks (Barker and Freeston, 2007; Wassermann and Zimmermann, 2012). TMS works according to the principle of electromagnetic induction: pulses of current flowing through a TMS coil generate a controllable, pulsatile magnetic field that passes into the brain unimpeded by skin, muscle or skull (basic principles described in Walsh, 1998). This time-dependent magnetic field induces transient electrical currents within the brain. TMS is able to stimulate the human brain and deep peripheral nerves without causing pain because current is not induced in the skin, i.e., pain fiber nerve endings are not activated. This lack of discomfort enables the technique to be used readily on patients and volunteers for research and therapeutic purposes (Barker and Freeston, 2007).

Repetitive transcranial magnetic stimulation (rTMS) delivers trains of closely spaced pulses to the brain to induce transient modulation of neural excitability and brain function. Although transient, the modulation can outlast the stimulation period leading to long-term changes in synaptic plasticity and behavior (for review, see Lenz and Vlachos, 2016). George et al. (1995) were the first to use rTMS as a treatment for depression and its efficacy in medication-resistant patients has been validated by numerous clinical trials (Gaynes et al., 2014). In 2008, an rTMS device developed by Neuronetics was approved by the Food and Drug Administration in the United States for the treatment of patients with major depressive disorder who are resistant to at least one antidepressant drug (O'Reardon et al., 2007). rTMS has since been shown to have therapeutic potential for a range of psychiatric disorders, including unipolar (Xia et al., 2008; Gaynes et al., 2014) and bipolar depression (Xia et al., 2008), schizophrenia (Dlabac-de Lange et al., 2010), obsessive-compulsive disorder (Jaafari et al., 2012), and post-traumatic stress disorder (Clark et al., 2015) as well as in neurological conditions such as Parkinson's disease (Arias-Carrión, 2008), dystonia (Machado et al., 2011), tinnitus (Soleimani et al., 2015), epilepsy (Pereira et al., 2016), and stroke (Corti et al., 2012). rTMS has also shown promising results in the treatment of pain syndromes such as migraine (Lipton and Pearlman, 2010) and chronic pain (Galhardoni et al., 2015). However, there is significant inter- and intra-individual variability in the after-effects induced by rTMS and increasing evidence suggests that subject-related variables such as gender, age, exercise, diet, use of neuropharmacological drugs, the state of the subject, and genetic background might affect the stimulation-induced effects of rTMS in both healthy individuals and patient populations (for review, see Ridding and Ziemann, 2010). To improve the safety and efficacy of rTMS in a clinical setting, a better understanding of how rTMS affects the brain is required (Müller-Dahlhaus and Vlachos, 2013).

Animal models have been useful in elucidating some of the mechanisms of rTMS as they allow us to perform invasive studies of molecular and genetic changes that are not ethically possible in humans. These studies have been reviewed extensively elsewhere (e.g., Tang et al., 2015; Lenz and Vlachos, 2016). However, to align the different experimental approaches used in preclinical animal studies (invasive: cellular and molecular outcomes) and in human studies (non-invasive: e.g., TMS and motor-evoked potentials, MEPs; electroencephalography, EEG; optical imaging, positron emission tomography, PET; functional magnetic resonance imaging, fMRI, behavior) is difficult. Although MEPs (electrical signals induced in muscles following cortical stimulation), which are currently the most common outcome measure used in humans, can also be measured in animals (Rotenberg et al., 2010; Sykes et al., 2016), this approach lacks sensitivity and can be applied only to motor cortical areas. The vast majority of TMS research and clinical treatments target non-motor regions such as the prefrontal or sensory cortex (e.g., Schneider et al., 2010; Liston et al., 2014; Jansen et al., 2015; Valchev et al., 2015), with effects that extend to deeper regions that are not accessible to MEPs (e.g., Komssi et al., 2004). Similarly, EEG (e.g., Komssi et al., 2004; Benali et al., 2011) and optical imaging (e.g., Allen et al., 2007; Kozel et al., 2009) have restricted depth of recording and can detect rTMS-induced functional changes only in the most superficial regions of the brain.

The ability to measure whole-brain functional connectivity before and after rTMS is important because rTMS can induce widespread changes both in cortical and subcortical networks. Currently, PET and fMRI are the only techniques capable of measuring functional effects of rTMS in the whole brain. Combined rTMS/PET have been used in humans (e.g., Paus et al., 1997; Kimbrell et al., 1999; Speer et al., 2000; Mintun et al., 2001; Conchou et al., 2009) and animal models (e.g., Gao et al., 2010; Salinas et al., 2013). However, a major disadvantage of PET with regards to safety is the use of radiotracers, exposing subjects to ionizing radiation. A single PET scan using a standard radiotracer dose leads to radiation exposure up to an order of magnitude greater than that received annually from background radiation. Therefore, longitudinal rTMS/PET studies requiring repeated measurements are not ethically feasible. fMRI, on the other hand, does not require the use of ionizing radiation and therefore, is a safe imaging tool appropriate for repeated long-term experiments.

Therefore, in this review, we suggest that fMRI will be a powerful tool amenable to visualizing and comparing rTMS-induced short and long term neural connectivity changes throughout the brain at high spatio-temporal resolutions in both humans and animals. This method could potentially help unravel the physiological processes underlying the rTMS-induced changes in the cortex and in functionally connected brain regions. Comparison of rTMS effects in human and

animal studies will also provide insight into the usefulness of animal models in understanding and improving rTMS based treatments for humans. Here, we review findings from combined rTMS/fMRI studies in humans and consider potential insights from, and limitations of, using fMRI in animal rTMS studies.

INFORMATION OBTAINED FROM COMBINED RTMS AND FMRI TECHNIQUES IN HUMANS

Ability of fMRI to Detect Network-Level Effects of rTMS on Healthy Volunteers

Bohning et al. (1998) were the first to demonstrate the feasibility of combining TMS and fMRI protocols, by performing TMS stimulation inside an MRI scanner. TMS applied to the primary motor cortex (M1) in humans resulted in a significant increase in activity in M1 as detected by the fMRI scan. Soon after, the same authors demonstrated that there was a significant increase in activity not only in M1 but also in areas distal to the stimulation site (e.g., the contralateral M1 and ipsilateral cerebellum), illustrating the potential of this technique for mapping connectivity patterns between brain areas (Bohning et al., 1999). The ability of rTMS to target both local and remote brain regions was confirmed by Bestmann et al. (2004), who used interleaved rTMS/fMRI to compare different intensities of rTMS (**Figure 1**). They showed that fMRI can detect effects of rTMS delivered at an intensity that does not elicit a motor response (i.e, MEP). Therefore, fMRI provides a significant improvement in terms of sensitivity and resolution over MEPs.

Since then, a range of combined rTMS/fMRI human studies have been conducted to record the rTMS-induced changes in hemodynamic activity both in healthy subjects and subjects with neurological disorders (Schneider et al., 2010; Fox et al., 2012b). In healthy subjects, for example, fMRI was used to detect plastic changes induced in the brain after 5 Hz rTMS was applied to the right dorsolateral prefrontal cortex (DLPFC) (Esslinger et al., 2014). No change in activation was detected at the stimulation site, but there was increased connectivity within the right DLPFC as well as from the stimulated DLPFC to the ipsilateral superior parietal lobule, which is functionally associated with the right DLPFC during working memory (Esslinger et al., 2014). This increased connectivity was associated with a decrease in reaction time during a working memory task (*n*-back task). These results suggested the presence of rTMS-induced plasticity in prefrontally connected networks downstream of the stimulation site (Esslinger et al., 2014). Similar results were found when Valchev et al. (2015) delivered a continuous train of theta burst stimulation (cTBS) to the left primary somatosensory cortex of healthy volunteers. Functional connectivity between the stimulated brain region and several functionally-connected brain regions, including the dorsal premotor cortex, cerebellum, basal ganglia, and anterior cingulate cortex, decreased. Another study applying high-frequency (10 Hz) rTMS to the right DLPFC in healthy volunteers while passively viewing emotional faces found significant right amygdala activity attenuation when evaluating negatively valenced visual stimuli (Baeken et al., 2010). Taken together, these studies show that rTMS can have widespread effects, not limited to the stimulated brain area and demonstrate that brain stimulation studies and treatment plans need to take network-level effects into account. Although the hippocampus

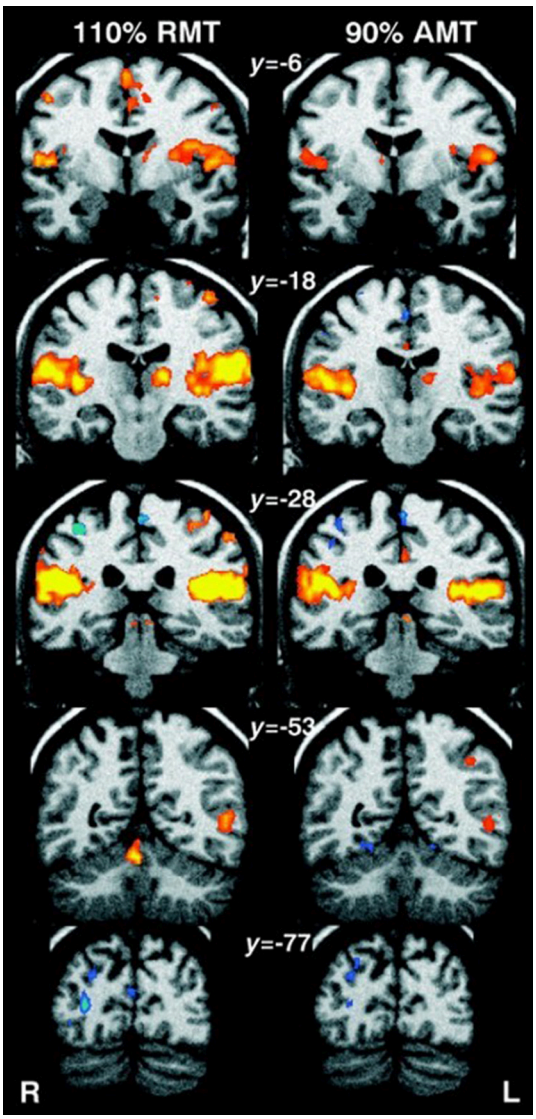

FIGURE 1 | Human fMRI data showing whole-brain effects of **(Left)** high-intensity rTMS at 110% resting motor threshold (RMT), and **(Right)** low-intensity rTMS at 90% active motor threshold (AMT). Coronal standard MNI brain sections (Talairach coordinates indicated) with superimposed fMRI results are shown. Areas of significant ($n = 11$, corrected $p < 0.01$) activations during rTMS compared to rest have been colored red-yellow, and decrease in fMRI signal in blue. Suprathreshold rTMS induced an increase in activity in the stimulated left sensorimotor cortex, medial supplementary and cingulate motor area, auditory cortex, lateral postcentral region, and left thalamus. Decrease in activity was observed in the right sensorimotor cortex and occipital cortex. Subthreshold rTMS produced similar but smaller activations, with no significant changes in the stimulated brain region. Image from Bestmann et al. (2004). Permission to reuse Figure 7 from the article was granted by John Wiley and Sons and Copyright Clearance Center through their RightsLink® service on 17th of August 2017.

as a deep brain structure is unlikely to be directly modulated by rTMS, which affects only superficial regions immediately beneath the coil, an ipsilateral change in the hippocampus was detected following multiple-session high-frequency (20 Hz) stimulation to the left lateral parietal cortex of healthy adults (Wang et al., 2014). Increased functional connectivity was observed and this change was correlated with improved associative memory performance. The effects of rTMS on these brain regions (e.g., cerebellum, basal ganglia, cingulate cortex, amygdala, hippocampus) are interesting because they have therapeutic implications which will be summarized in section Potential Applications of Combined rTMS/fMRI Studies in Human Diseases, along with more detailed effects of rTMS on functional connectivity in the intact normal state vs. diseased states.

Activation Patterns in Healthy vs. Diseased States in Humans

While fMRI detects changes in brain activity during an active task, resting-state fMRI (rs-fMRI) provides information about connectivity between brain regions at rest, i.e., when no specific stimulus or task is presented. Rs-fMRI detects brain regions whose patterns of spontaneous blood oxygen level dependent (BOLD) contrast fluctuations are temporally correlated when the subject is at rest. These brain regions with coherent spontaneous fluctuations in activity form an organized network called the resting-state network (Biswal et al., 1995). The default mode network (DMN), a resting-state network with a synchronized activity pattern, shows highest activation when the subject is at rest and is deactivated in goal-oriented tasks (Raichle et al., 2001). The DMN has been associated with cognitive performance and is thought to play an important role in neuroplasticity through the consolidation and maintenance of brain functions (Marcotte et al., 2013). For example, a higher resting-state activity within the DMN is hypothesized to favor network efficiency (Kelly et al., 2008), while decreased connectivity between the frontal and posterior DMN brain regions is associated with functional deficits (Davis et al., 2009). Consistent with these hypotheses, patients with neurological and psychiatric disorders show DMN dysregulation compared with healthy individuals (for review, see van den Heuvel and Hulshoff Pol, 2010). Disruptions in functional connectivity between brain regions forming part of the DMN have been implicated, *inter alia*, in patients with conditions like Alzheimer's disease (Greicius et al., 2004), multiple sclerosis (Lowe et al., 2002; Sbardella et al., 2015), autism (Cherkassky et al., 2006; Kennedy et al., 2006), epilepsy (Waites et al., 2006), depression (Greicius et al., 2007), schizophrenia (Bluhm et al., 2007; Whitfield-Gabrieli et al., 2009), aphasia (Marcotte et al., 2013), and addiction (Sutherland et al., 2012; Lerman et al., 2014).

Given that the pathophysiology of many psychiatric and neurological disorders is believed to be related to altered neural connectivity and network dynamics, interleaved rTMS/fMRI protocols provide an opportunity to investigate altered patterns of neural activity in these disorders (for review, see Hampson and Hoffman, 2010). The activation patterns in healthy individuals and patients with neurological or psychiatric conditions can be compared after an rTMS session to determine how these patterns are disrupted in the disease state (Hampson and Hoffman, 2010). For example, Schneider et al. (2010) examined the effect of 5 Hz rTMS on the primary somatosensory cortex in patients with dystonia (a condition associated with impaired somatosensory ability) and healthy controls based on their ability to discriminate between two stimulation frequencies applied to the right index finger before and after the rTMS session. An fMRI scan was carried out together with the tactile discrimination task. Without rTMS application, patients showed relative overactivity in the basal ganglia compared to healthy controls (**Figure 2A**). rTMS led to an improved performance in this task in healthy controls but not in the patients. There was increased activity detected in the stimulated primary somatosensory cortex and bilateral premotor cortex in both groups (**Figures 2B,C**) but fMRI detected an increase in activity in the basal ganglia in healthy subjects only (**Figure 2D**), suggesting an abnormal functional connectivity in the cortico-basal network in dystonia. The authors hypothesized that this could be related to altered sensory circuits and sensorimotor integration in patients with dystonia.

Interestingly, rTMS has been shown to modulate functional connectivity in humans, but the direction (increase or decrease in activity) and extent of this modulation depend on the rTMS protocol used, as we review below (Fox et al., 2012b; more recent articles: Popa et al., 2013; Glielmi et al., 2014; Jansen et al., 2015; Li et al., 2016). Using fMRI, increases and decreases in functional activity have been found depending on the stimulated brain region and the frequency of rTMS, allowing insight into how rTMS affects complex brain circuits (Bohning et al., 1999; Kimbrell et al., 1999).

rTMS PROTOCOLS AND THEIR SPECIFIC EFFECTS IN HUMANS

Simple Stimulation Protocols

There is considerable evidence from MEP and animal studies that that low-frequency (<5 Hz) rTMS has long-term synaptic depression (LTD) like effects and thereby decreases brain excitability (Klomjai et al., 2015; Wilson and St George, 2016). The inhibitory effect of low-frequency rTMS has been confirmed in studies of the DMN. For example, van der Werf et al. (2010) applied 1 Hz rTMS for two sessions over the left DLPFC of healthy volunteers. The rTMS sessions appeared to decrease resting-state network activity within the DMN, with the reductions happening in the temporal lobes, distant from the stimulated region. More specifically, they found that the hippocampus had reduced activation bilaterally following the application of low-frequency rTMS. They hypothesized that this change in neuronal activity of the hippocampus could arise from a change in cortical excitability or the transcallosal spread of rTMS effects inducing bilateral inhibition. The inhibitory effect of low-frequency rTMS was also confirmed in a resting-state connectivity study between motor regions in healthy individuals (Glielmi et al., 2014). Interestingly, 1 Hz, an inhibitory frequency, is thought to decrease the activity of inhibitory neurones in the stimulated hemisphere, causing a reduction in the inhibitory

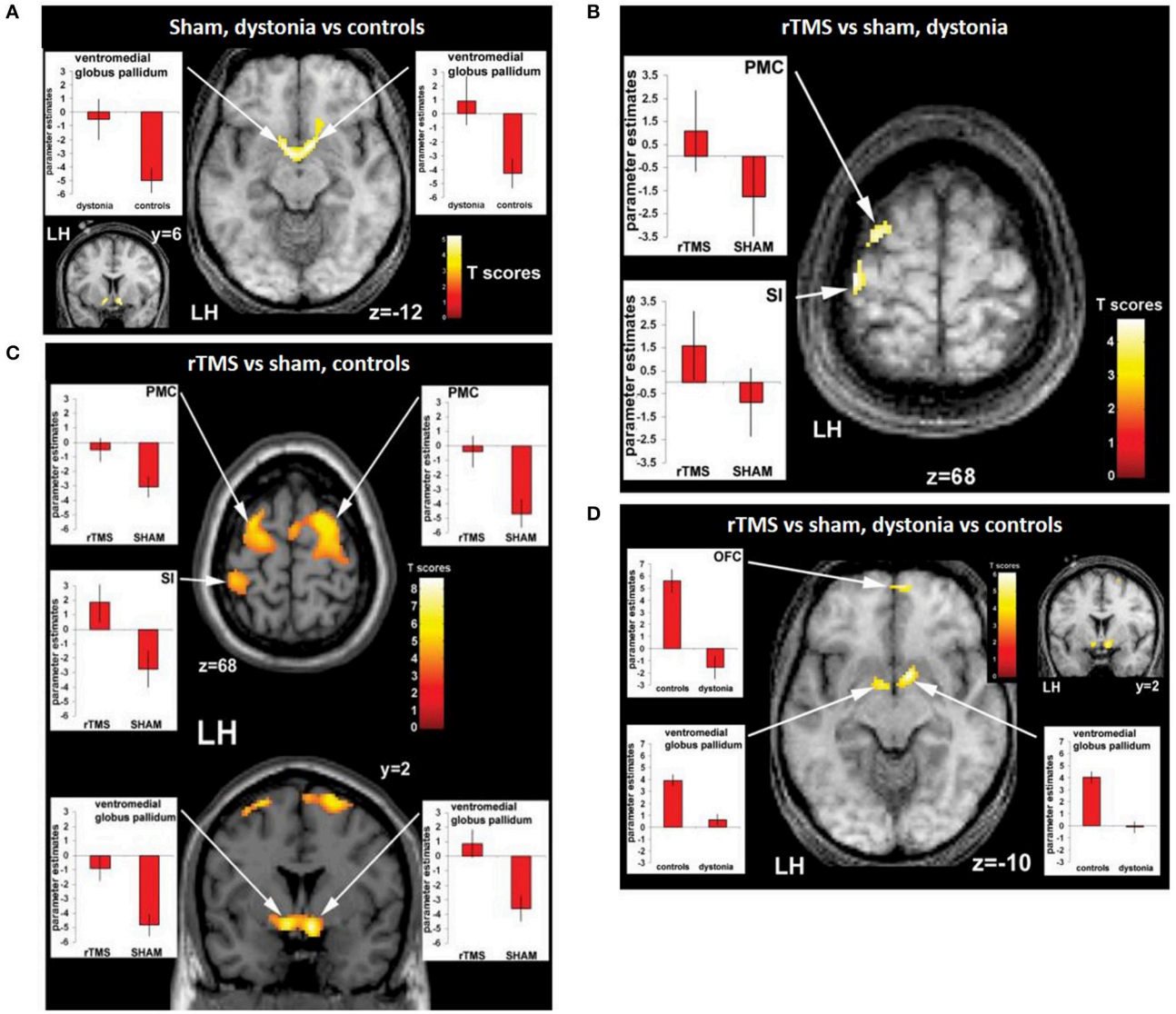

FIGURE 2 | Evidence of functional connectivity abnormalities in patients with dystonia and changes following rTMS. **(A)** Connectivity maps of patients vs. controls during the sham condition showing bilaterally greater activity in the ventromedial pallidum of patients compared to healthy controls. Effects of rTMS (real versus sham condition) on neuronal activity during sensory discrimination task in dystonia patients **(B)** and controls **(C)**. Both patients with dystonia **(B)** and healthy controls **(C)** show relatively greater activity ipsilaterally in the left premotor cortex (PMC) and the left sensorimotor cortex (S1) following after real-rTMS compared to sham stimulation. In addition, there is activation of the ventromedial pallidum bilaterally in healthy controls, but not in patients with dystonia. **(D)** Interaction (group × condition) during rTMS in patients with dystonia compared to controls. Compared to controls, dystonia patients show reduced activity in the left oribtofrontal cortext (OFC) and the ventromedial pallidum bilaterally after real-rTMS compared to sham stimulation **(D)**. Image from Schneider et al. (2010). Permission to reuse Figures 3 and 4 from the article was granted by John Wiley and Sons and Copyright Clearance Center through their RightsLink® service on 13th of February 2018.

interhemispheric drive, which in turn leads to an increase in excitability of the contralateral hemisphere. For example, O'Shea et al. (2007) found that even when 1 Hz stimulation over the left dorsal premotor cortex had no effect on behavior, there was a compensatory increase in activity in the right dorsal premotor cortex and connected medial premotor areas. This contralateral effect of 1 Hz rTMS has been utilized to treat patients with stroke by applying low-frequency stimulation to the unaffected hemisphere to decrease transcallosal inhibition of the lesioned hemisphere and consequently improve motor function in such patients. An rTMS/fMRI study by Grefkes et al. (2010) recruited patients with mild to moderate unilateral hand weakness after a first-ever subcortical ischemic stroke in the middle cerebral artery. Each subject underwent a baseline fMRI scan, a post-sham stimulation scan, and a post 1 Hz stimulation scan. rTMS applied over contralesional M1 significantly improved the motor performance of the paretic hand, and the improvement in symptoms was correlated with the functional connectivity results. The fMRI data showed a decrease in negative transcallosal influences from the contralesional M1 and an increase in

functional connectivity between the ipsilesional supplementary motor area (SMA) and M1.

In contrast to low-frequency stimulation, high-frequency (≥5 Hz) rTMS has long-term synaptic potentiation (LTP) like effects and increases brain excitability (Klomjai et al., 2015; Wilson and St George, 2016). In patients with stroke, high-frequency rTMS is sometimes applied directly to the affected hemisphere to increase excitability and promote plasticity of the lesioned hemisphere. For example, rs-fMRI demonstrated a bilateral increase in M1 connectivity in such patients after 10 days of 5 Hz rTMS applied ipsilesionally (Li et al., 2016). There was also an increased connectivity between the stimulated ipsilesional M1 and the SMA, bilateral thalamus, contralesional postcentral gyrus, and superior temporal gyrus and decreased connectivity between the stimulated ipsilesional M1 and the ipsilesional postcentral gyrus, M1, middle frontal gyrus, and superior parietal gyrus. An improved interhemispheric functional connectivity was also found in a case study of post-stroke apathy by Mitaki et al. (2016) when 5 Hz rTMS was applied to the SMA of each hemisphere of the patient over the course of two weeks. The improvement in the interhemispheric functional disconnection was correlated with the patient's recovery from post-stroke apathy.

Even though the studies tend to have small sample sizes (Watrous et al., 2013), these results show that understanding the effects of rTMS on multiple brain regions is important and that the effects can be determined to some extent by specific rTMS protocols. Information about the extent to which the functional connectivity within and between different networks can be modulated by different rTMS protocols may prove helpful in the development of treatment options for dysfunctional connectivity.

Complex Stimulation Patterns

In contrast to the simple frequencies described above, theta burst stimulation (TBS) uses a composite stimulation pattern, consisting of repeating bursts of stimuli (Larson et al., 1986). Each burst consists of three pulses of stimulation at 50 Hz, and the bursts are repeated at 5 Hz (0.2 s) (for review, see Cárdenas-Morales et al., 2010). This pattern of stimulation is based on the endogenous brain oscillations observed in the hippocampus (Huang et al., 2005), with human hippocampal theta oscillations being at a lower frequency (around 3 Hz) than the hippocampal theta oscillations of rats (8 Hz) (Watrous et al., 2013; Jacobs, 2014). The effect of TBS on the brain depends on the pattern of stimulation (Ljubisavljevic et al., 2015). For example, when cTBS is applied for 40 s (i.e., 600 stimuli) to M1 in humans, there is a decrease in brain excitability (Green et al., 1997). In contrast, when intermittent TBS (iTBS), with a 2 s train of TBS repeated every 10 s for 190 s (i.e., 600 stimuli), there is an increase in brain excitability (Green et al., 1997). Even though recent studies show evidence of substantial inter- and intra-individual variability in response to TBS (Zangen and Hyodo, 2002; Cho et al., 2012), the two main modalities, in general, have opposite effects on brain excitability.

Research on the DMN extends our understanding of the effects of TBS. iTBS applied over the left and right lateral cerebellum in patients with progressive supranuclear palsy for 10 sessions over the course of two weeks lead to an increased signal in the caudate nucleus bilaterally within the DMN (Brusa et al., 2014). iTBS also increased the efficiency of the impaired functional connectivity between the cerebellar hemisphere and the contralateral M1 observed in these patients compared with healthy individuals and patients with Parkinson's disease. The enhanced functional connectivity between the cerebellar hemisphere, the caudate nucleus, and the cortex was accompanied by an improvement of dysarthria in all patients. iTBS was also shown to have a dose-dependent effect on excitability and functional connectivity within the motor system (Nettekoven et al., 2014). When applied over the M1 of healthy volunteers, iTBS increased the resting-state functional connectivity between the stimulated M1 and premotor regions bilaterally. iTBS also increased connectivity between M1 and the ipsilateral dorsal premotor cortex when the number of stimuli was increased. The authors hypothesized that dense connections between M1 and the regions showing increased functional connectivity might facilitate simultaneous stimulation of these interconnected brain areas by the iTBS protocol, thereby modulating the synchrony of the resting activity in those regions.

There have also been studies of the inhibitory action of cTBS on brain activity using fMRI. Following eight sessions of 30 Hz cTBS applied to the SMA over two consecutive days, patients with Tourette syndrome or chronic tic disorder showed a significant reduction in the activity of SMA and left and right M1 activation during a finger-tapping exercise, suggesting inhibition in the motor network. However, improvement in symptoms was not significantly different between test and control subjects, perhaps because of the small sample size. Similar to 1 Hz rTMS, cTBS has been shown to dis-inhibit contralateral targets; in healthy individuals, cTBS application to the right Heschl's gyrus did not induce changes in the stimulated brain region, but significantly increased activity in the contralateral Heschl's gyrus, postcentral gyrus, and left insula and in the bilateral lateral occipital cortex (Andoh and Zatorre, 2012). The mechanisms underlying this interhemispheric interaction are not well understood but could be related to short-term plasticity or compensatory mechanisms to preserve function by increasing the activity of homologous brain regions in the contralateral hemisphere (Andoh and Zatorre, 2012).

In summary, a range of frequencies and stimulation patterns have been tested in human subjects and have specific impacts on brain function and network connectivity. There is significant opportunity to develop other stimulation paradigms systematically, which might have different neuronal effects, and to produce precise and reproducible effects in the brains of patients.

POTENTIAL APPLICATIONS OF COMBINED rTMS/fMRI STUDIES IN HUMAN DISEASES

Change in Connectivity Post rTMS Linked to Improvement in Symptoms

Change in functional connectivity achieved using rTMS as a treatment method can be used to determine the neural

mechanisms of improvement in symptoms in patients. For example, a longitudinal study by González-García et al. (2011) used fMRI to investigate the mechanisms by which 25 Hz rTMS (10 trains of 100 pulses) over M1 for three months improves the motor symptoms of patients with Parkinson's disease. rTMS was found to cause an increase in activity in the caudate nucleus during a simple motor task (finger-tapping test). fMRI also showed a decline in activity in the SMA, which was accompanied by an increase in its functional connectivity to the prefrontal areas. These changes substantiated the beneficial effect of rTMS on the symptoms of Parkinson's disease observed in these patients.

Another way to analyze the link between rTMS therapy and improvement in symptoms is to use rs-fMRI to detect the change in functional connectivity after rTMS. Popa et al. (2013) found that the connectivity within both the cerebello-thalamo-cortical network and the DMN was compromised in patients with essential tremor. Application of 1 Hz rTMS for five consecutive days bilaterally over lobule VIII of the cerebellum appeared to have re-established the connectivity in the cerebello-thalamo-cortical network only, and this change in functional connectivity was accompanied by a significant improvement in symptoms. Another study that also used an rTMS/rs-fMRI protocol carried out a whole-brain connectivity analysis to unravel the effect of rTMS on functional connectivity and motor symptoms in patients with multiple system atrophy (Chou et al., 2015). 5 Hz rTMS was applied over the left M1 of such patients for 10 sessions over the course of two weeks. Only the active rTMS group showed a significant improvement in motor symptoms, and these improvements were correlated to the modulation of functional links connecting to the default mode, cerebellar, and limbic networks by high-frequency rTMS. These findings suggest that rTMS can be used to target specific brain networks as a therapy for patients with multiple system atrophy.

Predicting Susceptibility to rTMS Therapy

More recently, baseline functional connectivity was shown to be a potential predictor of response to rTMS treatment, for example, in Mal de Debarquement Syndrome, a neurological condition representing a persistent false perception of rocking and swaying following exposure to unfamiliar motion patterns (Yuan et al., 2017). Pre- and post-rTMS rs-fMRI were carried out to assess functional connectivity changes as a result of daily rTMS treatment to the DLPFC (1,200 pulses of 1 Hz rTMS over right DLPFC followed by 2000 pulses of 10 Hz rTMS to the left DLPFC) over five consecutive days. A significantly positive baseline functional connectivity between the right DLPFC and the right entorhinal cortex and between the left DLPFC and bilateral entorhinal cortex were identified in patients showing improvement in symptoms following treatment, but not in patients whose symptoms worsened or remained unchanged (**Figure 3A**). Improvement in symptom severity was correlated with a decrease in functional connectivity between the left entorhinal cortex and posterior DMN regions such as the contralateral entorhinal cortex, the right inferior parietal lobule, and the left precuneus (**Figure 3B**).

Functional connectivity analysis on pre-treatment fMRI has also been used to predict the response to rTMS treatment in depression. Drysdale et al. (2017) found two groups of functional connectivity features that were linked to specific combinations of clinical symptoms in patients with depression. Anhedonia and psychomotor retardation were primarily linked to frontostriatal and orbitofrontal connectivity features, while anxiety and insomnia were primarily linked to a different group of primarily limbic connectivity features involving the amygdala, ventral hippocampus, ventral striatum, subgenual cingulate, and lateral prefrontal control areas. Testing the abnormalities in these connectivity features, based on their rs-fMRI data, revealed that not all patients with depression had the same functional connectivity patterns. They could be categorized, with high sensitivity and specificity, into four biotypes based on the distinct patterns of dysfunctional connectivity in the frontostriatal and limbic networks, which were most homogeneous within the subtypes and most dissimilar between subtypes. Moreover, patients with these neurophysiological subtypes of depression had different susceptibility to rTMS therapy: after five weeks of high-frequency rTMS delivered to the dorsomedial prefrontal cortex, biotype 1 patients showed a significant response to rTMS therapy (82.5% of that group), and biotype 2 patients were the least responsive (25.0%). This study suggests that heterogeneous symptom profiles in depression could be caused by distinct patterns of dysfunctional connectivity and that categorizing patients into subtypes based on these patterns might enable the prediction of treatment response to rTMS. Two years earlier, Downar et al. (2015) found that the resting-state functional connectivity features of the DLPFC to the subgenual cingulate cortex in patients with major depressive disorder could predict response either to 10 Hz or iTBS rTMS therapy. The role of subgenual cingulate connectivity in patients with depression has been indicated in several other studies (Greicius et al., 2007; Fox et al., 2012a; Liston et al., 2014; Hopman et al., 2017). More recent studies have since confirmed that it is possible to predict the response to iTBS or 10 Hz rTMS using resting-state functional connectivity between ventral striatum and bilateral frontal pole, as well as between the left DLPFC and the left anterior cingulate cortex (Dunlop et al., 2017). Therefore, rs-fMRI potentially could be used to select optimal rTMS parameters for the treatment of patients with depression.

Other Outcomes

Combining fMRI and rTMS has proven useful for investigating a range of other neural functions, providing evidence supporting the following: the functional relevance of the parietal cortex for visuospatial functions (Sack et al., 2002); a link between neural activity in the left inferior prefrontal cortex and episodic memory formation (Köhler et al., 2004); the involvement of premotor cortical areas in speech perception (for review, see Iacoboni, 2008); the presence of functional asymmetry highlighting interhemispheric differences in the auditory network (Andoh et al., 2015); and enabled targeting of stimulation based on the individual's MRI anatomy, functional connectivity results or activated brain regions during specific tasks (e.g., Sack et al., 2002;

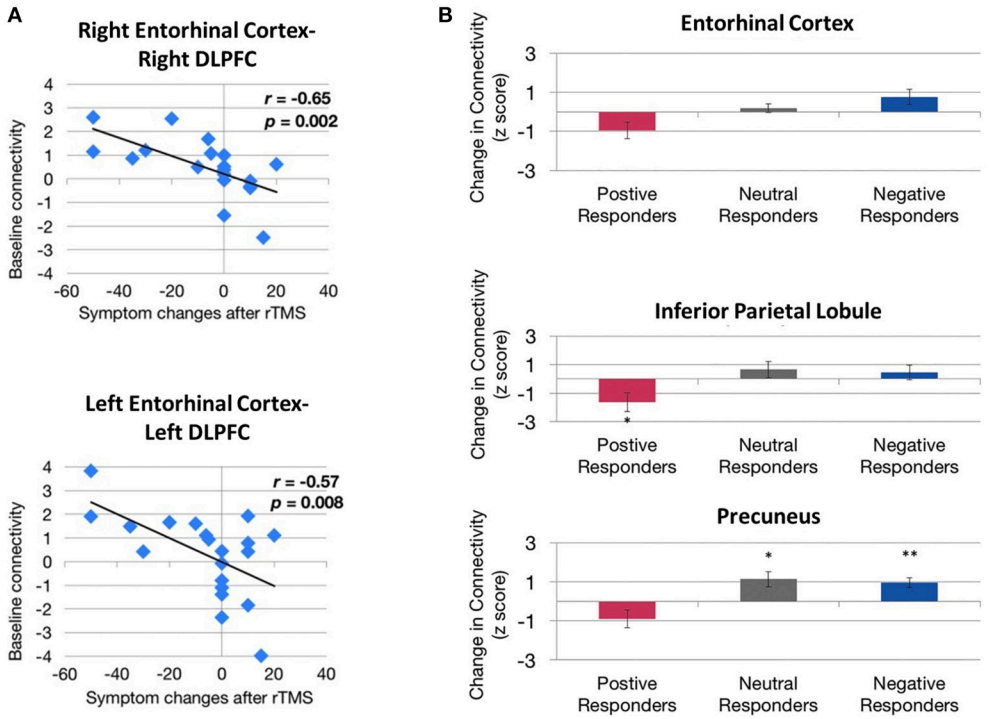

FIGURE 3 | Evidence of correlation between behavioral improvements and functional connectivity before and after rTMS treatment. **(A)** Correlation between baseline entorhinal cortex–dorsolateral prefrontal cortex (DLPFC) functional connectivity and treatment response. Higher baseline functional connectivity exhibited by both right entorhinal cortex–right DLPFC connectivity (top) and left entorhinal cortex–left DLPFC connectivity (bottom) is associated with a greater magnitude of symptom reduction (change < 0) after rTMS. **(B)** Directional effect of functional connectivity changes between the left entorhinal cortex and the right entorhinal cortex (top), right inferior parietal lobule (middle), and the left precuneus (bottom). Functional connectivity between these regions decreased in patients showing improvement in symptoms (positive responders) compared with patients whose symptoms remained unchanged (neutral responders) or worsened (negative responders). *,**Indicate significant changes for $p < 0.05$ and $p < 0.01$, respectively. Image from Yuan et al. (2017), an open access article distributed under the terms of the Creative Commons Attribution License, which permits unrestricted use, distribution, and reproduction in any medium, provided the original work is properly cited.

Fitzgerald et al., 2009; Eldaief et al., 2011; Binney and Lambon Ralph, 2015; Nierat et al., 2015; Valchev et al., 2015).

NEED FOR ANIMAL rTMS/fMRI STUDIES

The induction of plasticity as described in previous sections has been the driving force behind clinical studies of rTMS as a potential treatment of neurological and psychiatric conditions. However, even in neurologically normal subjects, the variability in response to rTMS is high (Maeda et al., 2000). Increasing evidence suggests that rTMS may not induce reliable and reproducible effects, therefore limiting the current therapeutic usefulness of this technology (for review, see Ridding and Ziemann, 2010). Animal models give us the opportunity to mitigate the confounding effects of variability in studies by controlling for gender, age, diet, drugs, genetic background, and the time at which experiments are carried out. The relative importance of these contributing factors can then be identified using animal studies (e.g., state-dependent variability explored in Pasley et al., 2009).

Interleaving rTMS and fMRI has opened doors to many possibilities in the clinical setting. However, there have been no reports of animal studies using those same techniques. fMRI in rodent research is becoming increasingly popular because of its high translatability. Moreover, rodent rs-fMRI studies have confirmed that rodents possess a DMN similar to humans despite the distinct evolutionary paths of rodent and primate brains (**Figure 4**; Lu et al., 2012). Because rodents are widely used as preclinical models of neuropsychiatric disease (e.g., Tan et al., 2013; Yang et al., 2014, 2015; Zhang et al., 2015; Kistsen et al., 2016), a thorough understanding of how rTMS affects the rodent neural networks is of particular importance for both interpreting rodent fMRI data and translating findings from humans to animals and back again.

Future Experiments: Linking Functional Connectivity Changes Post rTMS to Genetic/Molecular Changes

Animal models provide a unique opportunity to combine techniques: changes in functional connectivity between spatially separated brain regions caused by long-term modulation of network dynamics by rTMS, can be studied in parallel with changes in behavioral measures, and followed by invasive procedures to detect cellular and molecular changes, all within the same animal. As shown in human rTMS/fMRI studies, the

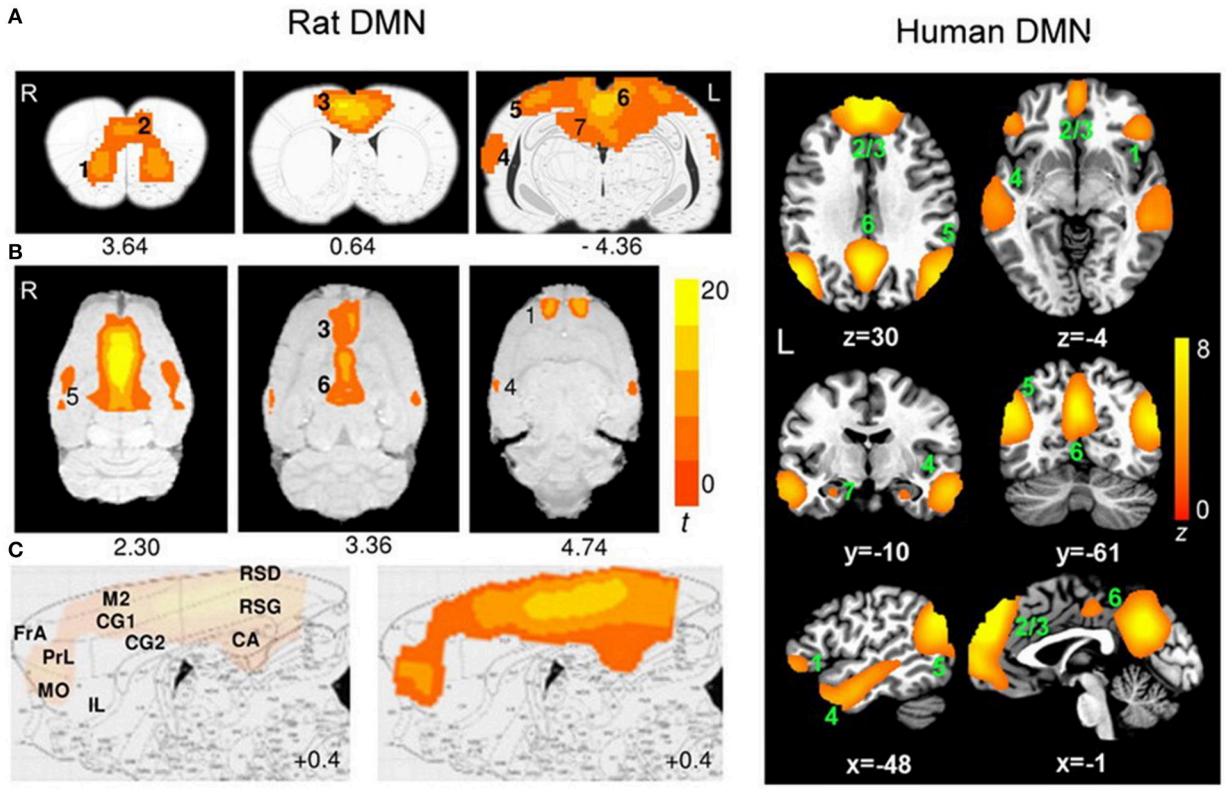

FIGURE 4 | Evidence of translatability of fMRI studies: similar brain regions forming part of the default mode network (DMN) in the rat (Paxino's atlas coordinates indicated) and human (Talairach coordinates indicated) brains. Connectivity maps are shown in the coronal **(A)**, axial **(B),** and sagittal **(C)** planes. Significant clusters for rat DMN (left) include: 1, orbital cortex; 2, prelimbic cortex (PrL); 3, cingulate cortex (CG1, CG2); 4, auditory/temporal association cortex (Au1, AuD, AuV, TeA); 5, posterior parietal cortex; 6, retrosplenial cortex (corresponding to the posterior cingulate cortex in humans); 7, hippocampus (CA1). The sagittal plane (medial–lateral: +0.4 mm) also shows: FrA, frontal association cortex; MO, medial orbital cortex; RSG/RSD, granular/dysgranular retrosplenial cortex. Color bar indicates t scores ($n = 16$, $t > 5.6$, corrected $p < 0.05$). Significant clusters for human DMN (right) include: 1, orbital frontal cortex; 2/3, medial prefrontal cortex/anterior cingulate cortex; 4, lateral temporal cortex; 5, inferior parietal lobe; 6, posterior cingulate cortex; 7, hippocampus/parahippocampal cortex. Color bar indicates z scores ($n = 39$, $z > 2.1$, corrected $p < 0.05$). Image adapted from Lu et al. (2012), an open access article under the creative commons license and can be republished without the need to apply for permission provided the material is cited correctly and is republished under the same license.

functional connectivity effects of rTMS are distributed across the whole brain (**Figure 1**). But, even when in-depth studies of the molecular mechanisms are carried out (e.g., quantification of gene expresssion in multiple brain regions using low-density PCR arrays by Ljubisavljevic et al., 2015), how these molecular changes from animal studies underpin functional connectivity changes described in humans remains unclear. Future studies should aim to identify brain regions affected by the stimulation in animals using fMRI and then rTMS mechanisms further elucidated in the same individuals, for example by measuring changes in gene expression in the corresponding brain regions postmortem. Such correlational approaches will provide a compelling view of how rTMS affects the brain at systems levels.

Future Experiments: Linking Functional Connectivity Changes Post rTMS to Structural Changes

The induction of brain plasticity has been the driving force behind clinical studies of rTMS as a potential treatment of neurological and psychiatric conditions. A more detailed understanding of how rTMS treatment leads to long-term modulation of network dynamics will be essential for the interpretation of neuropsychological and cognitive effects of rTMS in a clinical context. Combined rTMS/fMRI studies in animals can be used in longitudinal studies to investigate the long-term effects of rTMS. For example, fMRI can be used to measure cumulative effects of repeated rTMS delivery, following which fluorescent dye tracers can be injected into brain to anatomically label neuronal pathways of interest identified by fMRI. Conducting neuronal tract tracing after an fMRI study could elucidate whether long-term treatment with rTMS can eventually elicit changes in fiber tracts in the brain. Analyzing functional connectivity and anatomical connectivity within the same animals will provide information about how observed functional changes correlate with the structural changes detected at a cellular level. Although there is a general trend toward functional and structural connectivity being strongly associated, there are some mismatches within the DMN whereby regions showing high correlation have low fiber connectivity (Hsu et al.,

2016). Therefore, future studies to investigate whether the effect of rTMS on functional connectivity is related to fiber connectivity are warranted.

Future Experiments: Combined rTMS/fMRI Studies Using Animal Models

An important recent development in animal research has been the use of rs-fMRI for the characterization of models of neuropsychiatric disorders. Studies have revealed abnormal functional connectivity patterns in animal models due to pharmacological modulations or genetic manipulations which mimic connection abnormalities observed in corresponding human disorders (Jonckers et al., 2015; Gozzi and Schwarz, 2016; Gorges et al., 2017). These animal models represent a powerful tool to understand the neurobiological basis of the reported ability of rTMS to assist in remediating functional dysconnectivity observed in human disorders. First, fMRI can be used to identify the abnormal functional connectivity in an animal model specific to a neurological disorder. For example, the Wistar-Kyoto rat, an accepted model for depression which has shown resistance to acute antidepressant treatment (Lahmame et al., 1997; López-Rubalcava and Lucki, 2000), also shows functional connectivity anomalies between hippocampus, cortical, and sub-cortical regions (Williams et al., 2014), as has been observed in humans with major depressive disorder. Future studies can investigate the effects of rTMS on such animal models. Functional connectivity changes post-rTMS treatment can then be linked to improvement in symptoms (through behavioral tests such as the forced swim test commonly used in depression studies) as well as to any induced molecular and cellular changes (through postmortem analysis). Therefore, extending the use of combined rTMS/fMRI techniques in various types of neurological and psychiatric conditions using appropriate animal models is a promising avenue for understanding the fundamental properties of the functional re-organization in these conditions in a unique way.

While the use of combined rTMS/fMRI techniques in rodent research has great potential because of its high translatability, there are challenges as we review below.

CHALLENGES ASSOCIATED WITH rTMS/fMRI STUDIES IN ANIMALS

Choice of Animal Model and Development of rTMS Coils

A wide range of animal models have been used with the aim of understanding the underlying mechanisms and optimizing the therapeutic applications of rTMS: rats (Tan et al., 2013; Yang et al., 2015; Zhang et al., 2015), mice (Kistsen et al., 2016), guinea pigs (Mulders et al., 2016), rabbits (Guo et al., 2008), felines (Allen et al., 2007; Valero-Cabré et al., 2007), and in a very limited way, non-human primates (Valero-Cabre et al., 2012; Salinas et al., 2013; Mueller et al., 2014). These animal models have contributed considerably to our current understanding of the non-invasive neuromodulatory effects of rTMS (reviewed in Tang et al., 2015). However, the variation in brain structure and the smaller sized brains of non-human animals present a fundamental challenge in the application of rTMS and interpretation of its effects.

Non-human primates are clearly the closest to humans in terms of brain structure and size and have the advantage that they can be taught behavioral tasks similar to those used in human rTMS studies. However, the high cost of using non-human primates limit opportunities for invasive studies in large numbers of animals. Rodents, on the other hand, although they are the most commonly used laboratory animals, have important differences in brain structure compared to humans. Their smooth cortex possesses a very different geometry to the highly folded human cortex and this is an important consideration because the characteristics of the electric field induced by rTMS are predicted to be influenced by the orientation of the tissue relative to the coil (Opitz et al., 2011). In addition to differences in brain structure, the small size of the rodent brain presents a serious challenge. In humans, rTMS is most commonly delivered using a coil shaped like a "figure-of-eight" (**Figure 5**). This configuration provides a stimulation hotspot at the intersection of the loops that can be positioned over the target brain region to provide focal stimulation. Adjacent brain areas also receive stimulation but at much lower intensity. In most animal models, even the smallest commercially available rTMS coil results in a different ratio between head size and coil size from that in humans, reducing stimulation focality and efficiency (Rodger and Sherrard, 2015). For example, using a standard, human-sized "figure-of-eight" coil in mice stimulates the entire brain and often an appreciable portion of the body (**Figure 5**). The discrepancy in size, therefore, precludes easy interpretation and translation of animal results into clinical applications. Many rodent studies are therefore compromised by the use of large, human-scale coils to deliver rTMS (e.g., Yang et al., 2014, 2015; Zhang et al., 2015), and some groups have used miniaturized rTMS coils in order to more closely mimic focal human rTMS in rodents. For example, custom-made 8 mm diameter round coils have been used to stimulate one hemisphere in both mice and rats (Rodger et al., 2012; Makowiecki et al., 2014), with the induced current fully contained within the brain, increasing the efficiency of induction. However, there is a heat dissipation problem when using small round coils (Cohen and Cuffin, 1991; Wassermann and Zimmermann, 2012), limiting the intensity of the magnetic field to levels roughly 10–100 times lower than those commonly applied in humans (low-intensity; LI-rTMS) (Rodger and Sherrard, 2015).

Despite the existing inability to deliver the same magnetic field parameters in humans and in animals with small brains (Rodger and Sherrard, 2015), beneficial effects are seen in animal models of neurological disease using human rTMS coils (e.g., Tan et al., 2013; Yang et al., 2015; Zhang et al., 2015; Kistsen et al., 2016) and small LI-rTMS coils (Makowiecki et al., 2014; Clarke et al., 2017), suggesting that both approaches have therapeutic potential. Because fMRI can detect both high and low-intensity rTMS effects in the brain, this technique will be useful in establishing a direct comparison of different intensity magnetic field effects in human and animal brains. This information is imperative if we are to define the best clinical protocols for rTMS.

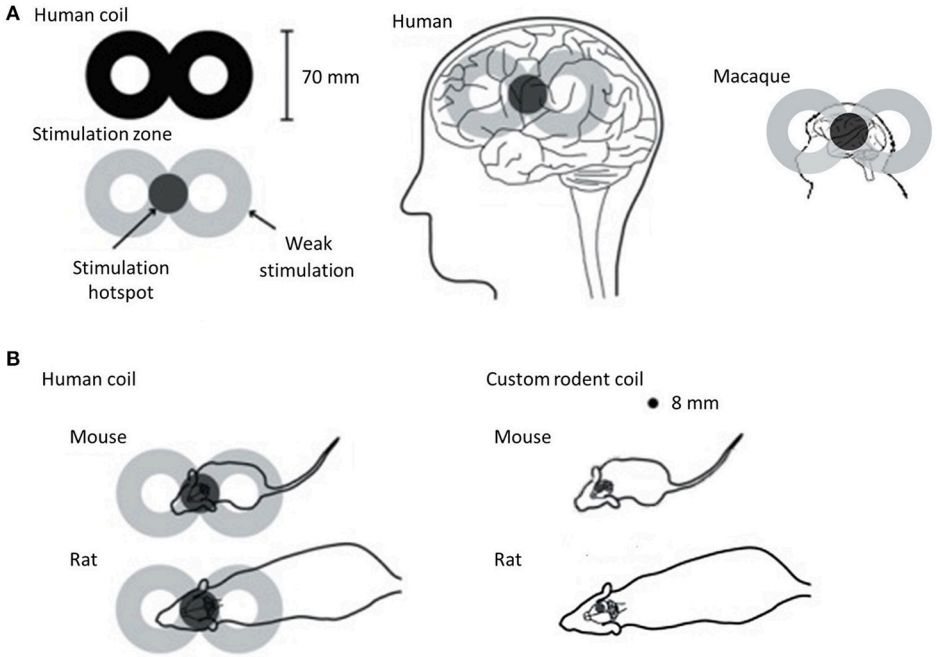

FIGURE 5 | rTMS coil size with respect to brain sizes of humans, macaque and rodents. For all panels, coils are shown in black and the approximate location of the induced current is in gray. **(A)** Typical human "figure of eight" coil with stimulation hotspot at the intersection of the loops in dark gray showing the "focal" stimulation in humans and macaques. When applied to the head, the hotspot is positioned over the target brain region, but the rest of the brain also receives stimulation, albeit at lower intensity. However, when this human coil is applied in rodents **(B)**, the hotspot is no longer focal relative to the target, but rather stimulates the entire head and an appreciable portion of the body (left). This reduces the efficiency of magnetic induction and changes the properties of the induced current. To address this problem, custom-made round coils (right) have been used to deliver focal stimulation in rodents (Rodger et al., 2012; Makowiecki et al., 2014; Tang et al., 2016). Although these deliver low intensity magnetic fields, the induced current is fully contained within the brain, increasing efficiency of induction. The coils are small enough to stimulate one hemisphere in both mice and rats. Image adapted from Rodger and Sherrard (2015), an open-access article distributed under the terms of the Creative Commons Attribution-Noncommercial-Share Alike 3.0 Unported, which permits unrestricted use, distribution, and reproduction in any medium, provided the original work is properly cited.

Use of Anesthetics in Animal fMRI Studies

Although fMRI can be performed on awake, normally behaving animals that have been extensively trained and habituated (Brydges et al., 2013; Kenkel et al., 2016), one advantage of rs-fMRI is that being a task-free technique, functional connectivity can be investigated in anesthetized animals without relying on, or being confounded by, behavior. In human studies, the physiological condition of the subject is assumed to be relatively constant throughout an fMRI scan session (Pan et al., 2015). On the other hand, in animal fMRI, the use of anesthesia is generally required to immobilize the animal and reduce stress (Vincent et al., 2007; Pan et al., 2015). Isoflurane is the anesthetic of choice for repeated long-term experiments because of its ease of use and control, and rapid reversibility (Masamoto and Kanno, 2012). However, anesthetics, including isoflurane, might confound the imaging results as they may cause alterations in neural activity, vascular reactivity, and neurovascular coupling. Isoflurane decreases excitatory and increases inhibitory transmission, causing an overall suppression of neural activity, most likely by modulating the intracellular concentration of calcium (Gomez and Guatimosim, 2003; Ouyang and Hemmings, 2005). As such, the ability of high-frequency rTMS to depolarise neurons is impaired in the presence of isoflurane (Gersner et al., 2011). Additionally, isoflurane, being a GABAergic anesthetic, induces vasodilation through the activation of ATP-sensitive potassium channels of smooth muscle cells in cerebral arteries (Ohata et al., 1999; Pan et al., 2015). Vasodilation leads to an increase in cerebral blood flow, which can be interpreted as an increase in activity. Moreover, the use of an isoflurane-only anesthetic regime has been reported to decrease inter-thalamic connectivity, thalamo–cortical connections, and DMN–thalamic network connections (Bukhari et al., 2017). These potential confounding effects of isoflurane should be taken into account when interpreting findings.

An alternative to general anesthesia is sedation, for example using medetomidine or its active enantiomer, dexmedetomidine. These drugs lack the dose-dependent vasodilation and neural suppression observed with isoflurane use. However, being α2-adrenergic agonists, they activate α2-adrenergic receptors and cause a decrease in cerebral blood flow, potentially because of increased vascular resistance via cerebral vasoconstriction (Prielipp et al., 2002). Moreover, there is a potential issue with prolonged studies because the dose of medetomidine needs to be increased after 2 h to maintain sedation (Pawela et al., 2009). Furthermore, the use of a medetomidine-only anesthetic regime produced decreased inter-cortical connectivity (Bukhari et al., 2017).

Interestingly, using a combination of low-dose isoflurane and medetomidine appears to mitigate some of these factors. This anesthetic combination not only allows stable sedation for over four hours (Lu et al., 2012) but also maintains strong inter-cortical and cortical-subcortical connectivity (Grandjean et al., 2014; Bukhari et al., 2017). The BOLD signal was determined to be maximally stable approximately 90 min after the initiation of medetomidine infusion, suggesting that fMRI data should be collected at this time (Lu et al., 2012). Moreover, data were reproducible from repeated fMRI experiments on the same animal one week apart (Lu et al., 2012). The high reproducibility and minimal impact on network connectivity of the medetomidine/isoflurane combination anesthesia make it a preferred anesthetic regime for prolonged and longitudinal rs-fMRI studies in rodents.

Rs-fMRI Studies in Rodents—Challenges in Data Analysis

As with human data, rodent rs-fMRI data need to undergo extensive pre-processing prior to analysis. Rodent studies have used a variety of software packages such as Statistical Parametric Mapping (SPM) (e.g., Jonckers et al., 2011), Analysis of Functional NeuroImages (AFNI) (e.g., Hsu et al., 2016), BrainVoyager (e.g., Hutchison et al., 2010), and Functional MRI of the Brain (FMRIB) Software Library (FSL) (e.g., Tambalo et al., 2015), which were designed for human fMRI data. Therefore, modifications to the data format and pre-processing steps are often necessary to undertake analysis of rodent brain data. For example, the field of view can be altered by up-scaling the voxel sizes by a factor of 10 to be closer to the size of a human brain (Tambalo et al., 2015). Likewise, because of the smaller size of the rodent brain, higher spatial smoothing may be required in animal fMRI data to increase the signal-to-noise ratio without reducing valid activation. Temporal band-pass filtering can also be used to reduce hardware noise, low-frequency signal drifts, and some artifacts caused by cardiac rhythm and respiration, as well as thermal noise (for review, see Pan et al., 2015). Recently, Zerbi et al. (2015) described the use of single-session independent component analysis (ICA) in the FSL for significantly improved artifact reduction in rs-fMRI rodent data. This method removes signals from common sources, for example breathing, which can be isolated into separate components and removed as noise from the data. Additionally, because of the difference in the shape of human and animal brains, skull-stripping—a fully-automated step in human fMRI data pre-processing required to prevent extra-brain matter from interfering with the results—is still largely performed through manual segmentation in animal studies (Sierakowiak et al., 2015; Zerbi et al., 2015). Before analysis, normalization to map functional networks onto a common space is necessary to allow for comparison across subjects or groups. However, because not all rodent strains have an available standard template or atlas for co-registration, some studies acquire and use high-resolution structural images or group-averaged images as a common space (Sierakowiak et al., 2015; Zerbi et al., 2015).

Two of the popular methods for rs-fMRI data are seed-based connectivity analysis (e.g., Hutchison et al., 2010; Sierakowiak et al., 2015; Huang et al., 2016) and ICA (e.g., Hutchison et al., 2010; Jonckers et al., 2011; Lu et al., 2012; Zerbi et al., 2015; Hsu et al., 2016). Seed-based correlation, used in the earliest functional connectivity studies, is a hypothesis-driven approach, which is particularly attractive for area-based hypotheses-driven rs-fMRI studies in rodents. The temporal correlation of all voxels within the brain is analyzed relative to user-defined seed voxel or small region of interest (Joel et al., 2011). However, seed-points can differ in their location between studies, which affects the connectivity patterns considerably and renders comparisons between studies difficult. In addition, this method is not suitable for exploratory analyses. In contrast, the use of data-driven ICA enables identification of networks of functional connectivity within the entire brain without *a priori* knowledge, and thus is a less biased approach (Cole et al., 2010). Moreover, this approach might improve reproducibility because there is no (arbitrary) seed selection (Rosazza et al., 2012). However, the results might depend on the number of components used. Despite the rodent DMN producing similar spatial patterns and being robust irrespective of the number of components (Lu et al., 2012), the number of components chosen can impact on the ease of analysis. For example, Jonckers et al. (2011) and Hsu et al. (2016) chose 15-components in ICA over ICAs repeated with a higher number of components to avoid splitting of the DMN or splitting of some brain regions into different components. Therefore, despite ICA becoming increasingly popular for the analysis of rodent rs-fMRI data, challenges remain as there is no set protocol for selecting the number of components.

SUMMARY

Considered together, the human studies discussed in this review demonstrate the broad relevance and significance of the results from combined rTMS/fMRI protocols. Results from human studies to date *inter alia* have permitted the characterization of corrupted networks in diseased states, as well as intriguing glimpses into how alterations in functional connectivity patterns after rTMS are correlated with improvements in symptoms. There is also exciting evidence that functional connectivity can be used to predict responses to rTMS treatment with high reliability.

Although methodological challenges remain in the use of brain imaging techniques in rodents, we anticipate that the use of fMRI to study rTMS in animal models will not only permit more detailed characterizations of how different rTMS protocols affect network dynamics and connectivity but will also elucidate how these changes reflect the manifestation of symptoms in preclinical models. Linking these functional changes to the molecular and cellular changes currently known in rodents will provide new insights into the fundamental mechanisms of brain plasticity and how to use rTMS therapeutically.

AUTHOR CONTRIBUTIONS

BJS: Wrote and edited the manuscript; SE: Provided feedback, structured and edited the manuscript; KWF: Provided feedback, structured and edited the manuscript; JR: Conceived the idea and approach of the review, structured and edited the manuscript.

ACKNOWLEDGMENTS

BJS is supported by a Forrest Research Foundation Scholarship, an International Postgraduate Research Scholarship, and a University Postgraduate Award. KWF is an Australian National Imaging Facility Fellow, a facility funded by the University, State, and Commonwealth Governments. JR was supported by an NHMRC Senior Research Fellowship.

REFERENCES

Allen, E. A., Pasley, B. N., Duong, T., and Freeman, R. D. (2007). Transcranial magnetic stimulation elicits coupled neural and hemodynamic consequences. *Science* 317, 1918–1921. doi: 10.1126/science.1146426

Andoh, J., Matsushita, R., Zatorre, R. J. (2015). Asymmetric interhemispheric transfer in the auditory network: evidence from TMS, resting-state fMRI, and diffusion imaging. *J. Neurosci.* 35, 14602–14611. doi: 10.1523/JNEUROSCI.2333-15.2015

Andoh, J., and Zatorre, R. J. (2012). Mapping the after-effects of theta burst stimulation on the human auditory cortex with functional imaging. *J. Vis. Exp.* 67:e3985. doi: 10.3791/3985

Arias-Carrión, O. (2008). Basic mechanisms of rTMS: implications in Parkinson's disease. *Int. Arch. Med.* 1:2. doi: 10.1186/1755-7682-1-2

Baeken, C., De Raedt, R., Van Schuerbeek, P., Vanderhasselt, M. A., De Mey, J., Bossuyt, A., et al. (2010). Right prefrontal HF-rTMS attenuates right amygdala processing of negatively valenced emotional stimuli in healthy females. *Behav. Brain Res.* 214, 450–455. doi: 10.1016/j.bbr.2010.06.029

Barker, A. T., and Freeston, I. (2007). Transcranial magnetic stimulation. *Scholarpedia J.* 2:2936. doi: 10.4249/scholarpedia.2936

Benali, A., Trippe, J., Weiler, E., Mix, A., Petrasch-Parwez, E., Girzalsky, W., et al. (2011). Theta-burst transcranial magnetic stimulation alters cortical inhibition. *J. Neurosci.* 31, 1193–1203. doi: 10.1523/JNEUROSCI.1379-10.2011

Bestmann, S., Baudewig, J., Siebner, H. R., Rothwell, J. C., and Frahm, J. (2004). Functional MRI of the immediate impact of transcranial magnetic stimulation on cortical and subcortical motor circuits. *Eur. J. Neurosci.* 19, 1950–1962. doi: 10.1111/j.1460-9568.2004.03277.x

Binney, R. J., and Ralph, M. A. (2015). Using a combination of fMRI and anterior temporal lobe rTMS to measure intrinsic and induced activation changes across the semantic cognition network. *Neuropsychologia* 76, 170–181. doi: 10.1016/j.neuropsychologia.2014.11.009

Biswal, B., Yetkin, F. Z., Haughton, V. M., and Hyde, J. S. (1995). Functional connectivity in the motor cortex of resting human brain using echo-planar MRI. *Magn. Reson. Med.* 34, 537–541. doi: 10.1002/mrm.1910340409

Bluhm, R. L., Miller, J., Lanius, R. A., Osuch, E. A., Boksman, K., Neufeld, R. W., et al. (2007). Spontaneous low-frequency fluctuations in the BOLD signal in Schizophrenic patients: anomalies in the default network. *Schizophr. Bull.* 33, 1004–1012. doi: 10.1093/schbul/sbm052

Bohning, D. E., Shastri, A., McConnell, K. A., Nahas, Z., Lorberbaum, J. P., Roberts, D. R., et al. (1999). A combined TMS/fMRI study of intensity-dependent TMS over motor cortex. *Biol. Psychiatry* 45, 385–394. doi: 10.1016/S0006-3223(98)00368-0

Bohning, D. E., Shastri, A., Nahas, Z., Lorberbaum, J. P., Andersen, S. W., Dannels, W. R., et al. (1998). Echoplanar BOLD fMRI of brain activation induced by concurrent transcranial magnetic stimulation. *Invest. Radiol.* 33, 336–340. doi: 10.1097/00004424-199806000-00004

Brusa, L., Ponzo, V., Mastropasqua, C., Picazio, S., Bonnì, S., Di Lorenzo, F., et al. (2014). Theta burst stimulation modulates cerebellar-cortical connectivity in patients with progressive supranuclear palsy. *Brain Stimul.* 7, 29–35. doi: 10.1016/j.brs.2013.07.003

Brydges, N. M., Whalley, H. C., Jansen, M. A., Merrifield, G. D., Wood, E. R., Lawrie, S. M., et al. (2013). Imaging conditioned fear circuitry using awake rodent fMRI. *PLoS ONE* 8:e54197. doi: 10.1371/journal.pone.0054197

Bukhari, Q., Schroeter, A., Cole, D. M., and Rudin, M. (2017). Resting state fMRI in mice reveals anesthesia specific signatures of brain functional networks and their interactions. *Front. Neural Circuits* 11:5. doi: 10.3389/fncir.2017.00005

Cárdenas-Morales, L., Nowak, D. A., Kammer, T., Wolf, R. C., and Schönfeldt-Lecuona, C. (2010). Mechanisms and applications of theta-burst rTMS on the human motor cortex. *Brain Topogr.* 22, 294–306. doi: 10.1007/s10548-009-0084-7

Cherkassky, V. L., Kana, R. K., Keller, T. A., and Just, M. A. (2006). Functional connectivity in a baseline resting-state network in autism. *Neuroreport* 17, 1687–1690. doi: 10.1097/01.wnr.0000239956.45448.4c

Cho, S. I., Nam, Y. S., Chu, L. Y., Lee, J. H., Bang, J. S., Kim, H. R., et al. (2012). Extremely low-frequency magnetic fields modulate nitric oxide signaling in rat brain. *Bioelectromagnetics* 33, 568–574. doi: 10.1002/bem.21715

Chou, Y. H., You, H., Wang, H., Zhao, Y. P., Hou, B., Chen, N. K., et al. (2015). Effect of repetitive transcranial magnetic stimulation on fMRI resting-state connectivity in multiple system atrophy. *Brain Connect.* 5, 451–459. doi: 10.1089/brain.2014.0325

Clark, C., Cole, J., Winter, C., Williams, K., and Grammer, G. (2015). A review of transcranial magnetic stimulation as a treatment for post-traumatic stress disorder. *Curr. Psychiatry Rep.* 17, 1–9. doi: 10.1007/s11920-015-0621-x

Clarke, D., Penrose, M. A., Harvey, A. R., Rodger, J., and Bates, K. A. (2017). Low intensity rTMS has sex-dependent effects on the local response of glia following a penetrating cortical stab injury. *Exp. Neurol.* 295, 233–242. doi: 10.1016/j.expneurol.2017.06.019

Cohen, D., and Cuffin, B. N. (1991). Developing a more focal magnetic stimulation. Part 1. Some basic principles. *J. Clin. Neurophysiol.* 8, 102–111. doi: 10.1097/00004691-199101000-00013

Cole, D. M., Smith, S. M., and Beckmann, C. F. (2010). Advances and pitfalls in the analysis and interpretation of resting-state fMRI data. *Front. Syst. Neurosci.* 4:8. doi: 10.3389/fnsys.2010.00008

Conchou, F., Loubinoux, I., Castel-Lacanal, E., Le Tinnier, A., Gerdelat-Mas, A., Faure-Marie, N., et al. (2009). Neural substrates of low-frequency repetitive transcranial magnetic stimulation during movement in healthy subjects and acute stroke patients. A PET study. *Hum. Brain Mapp.* 30, 2542–2557. doi: 10.1002/hbm.20690

Corti, M., Patten, C., and Triggs, W. (2012). Repetitive transcranial magnetic stimulation of motor cortex after stroke: a focused review. *Am. J. Phys. Med. Rehabil.* 91, 254–270. doi: 10.1097/PHM.0b013e318228bf0c

Davis, S. W., Dennis, N. A., Buchler, N. G., White, L. E., Madden, D. J., and Cabeza, R. (2009). Assessing the effects of age on long white matter tracts using diffusion tensor tractography. *Neuroimage* 46, 530–541. doi: 10.1016/j.neuroimage.2009.01.068

Dlabac-de Lange, J. J., Knegtering, R., and Aleman, A. (2010). Repetitive transcranial magnetic stimulation for negative symptoms of schizophrenia: review and meta-analysis. *J. Clin. Psychiatry* 71, 411–418. doi: 10.4088/JCP.08r04808yel

Downar, J., Dunlop, K., Schultze, L. L., Mansouri, F., Vila-Rodriguez, F., Giacobbe, P., et al. (2015). Resting-state functional connectivity to subgenual cingulate cortex differentially predicts treatment response for 10 Hz versus intermittent theta-burst rTMS in major depression. *Brain Stimul.* 8:396. doi: 10.1016/j.brs.2015.01.265

Drysdale, A. T., Grosenick, L., Downar, J., Dunlop, K., Mansouri, F., Meng, Y., et al. (2017). Resting-state connectivity biomarkers define neurophysiological subtypes of depression. *Nat. Med.* 23, 28–38. doi: 10.1038/nm.4246

Dunlop, K., Peters, S. K., Giacobbe, P., Daskalakis, Z. J., Lam, R. W., Kennedy, S. H., et al. (2017). Cortico-cortical and cortico-striatal resting-state functional connectivity differentially predicts response to 10 Hz rTMS and intermittent TBS to the DLPFC. *Brain Stimul.* 10:464. doi: 10.1016/j.brs.2017.01.360

Eldaief, M. C., Halko, M. A., Buckner, R. L., and Pascual-Leone, A. (2011). Transcranial magnetic stimulation modulates the brain's intrinsic activity in a frequency-dependent manner. *Proc. Natl. Acad. Sci. U.S.A.* 108, 21229–21234. doi: 10.1073/pnas.1113103109

Esslinger, C., Schüler, N., Sauer, C., Gass, D., Mier, D., Braun, U., et al. (2014). Induction and quantification of prefrontal cortical network plasticity using 5 Hz rTMS and fMRI. *Hum. Brain Mapp.* 35, 140–151. doi: 10.1002/hbm.22165

Fitzgerald, P. B., Hoy, K., McQueen, S., Maller, J. J., Herring, S., Segrave, R., et al. (2009). A randomized trial of rTMS targeted with MRI based neuro-navigation

in treatment-resistant depression. *Neuropsychopharmacology* 34, 1255–1262. doi: 10.1038/npp.2008.233

Fox, M. D., Buckner, R. L., White, M. P., Greicius, M. D., and Pascual-Leone, A. (2012a). Efficacy of TMS targets for depression is related to intrinsic functional connectivity with the subgenual cingulate. *Biol. Psychiatry* 72, 595–603. doi: 10.1016/j.biopsych.2012.04.028

Fox, M. D., Halko, M. A., Eldaief, M. C., and Pascual-Leone, A. (2012b). Measuring and manipulating brain connectivity with resting state functional connectivity magnetic resonance imaging (fcMRI) and transcranial magnetic stimulation (TMS). *Neuroimage* 62, 2232–2243. doi: 10.1016/j.neuroimage.2012.03.035

Galhardoni, R., Correia, G. S., Araujo, H., Yeng, L. T., Fernandes, D. T., Kaziyama, H. H., et al. (2015). Repetitive transcranial magnetic stimulation in chronic pain: a review of the literature. *Arch. Phys. Med. Rehabil.* 96, S156–S172. doi: 10.1016/j.apmr.2014.11.010

Gao, F., Wang, S., Guo, Y., Wang, J., Lou, M., Wu, J., et al. (2010). Protective effects of repetitive transcranial magnetic stimulation in a rat model of transient cerebral ischaemia: a microPET study. *Eur. J. Nucl. Med. Mol. Imaging* 37, 954–961. doi: 10.1007/s00259-009-1342-3

Gaynes, B. N., Lloyd, S. W., Lux, L., Gartlehner, G., Hansen, R. A., Brode, S., et al. (2014). Repetitive transcranial magnetic stimulation for treatment-resistant depression: a systematic review and meta-analysis. *J. Clin. Psychiatry* 75, 477–489. doi: 10.4088/JCP.13r08815

George, M. S., Wassermann, E. M., Williams, W. A., Callahan, A., Ketter, T. A., Basser, P., et al. (1995). Daily repetitive transcranial magnetic stimulation (rTMS) improves mood in depression. *Neuroreport* 6, 1853–1856. doi: 10.1097/00001756-199510020-00008

Gersner, R., Kravetz, E., Feil, J., Pell, G., and Zangen, A. (2011). Long-term effects of repetitive transcranial magnetic stimulation on markers for neuroplasticity: differential outcomes in anesthetized and awake animals. *J. Neurosci.* 31, 7521–7526. doi: 10.1523/JNEUROSCI.6751-10.2011

Glielmi, C. B., Butler, A. J., Niyazov, D. M., Darling, W. G., Epstein, C. M., Alberts, J. L., et al. (2014). Assessing low-frequency repetitive transcranial magnetic stimulation with functional magnetic resonance imaging: a case series. *Physiother. Res. Int.* 19, 117–125. doi: 10.1002/pri.518

Gomez, R. S., and Guatimosim, C. (2003). Mechanism of action of volatile anesthetics: involvement of intracellular calcium signaling. *Curr. Drug Targets CNS Neurol Disord.* 2, 123–129. doi: 10.2174/1568007033482940

González-García, N., Armony, J. L., Soto, J., Trejo, D., Alegria, M. A., and Drucker-Colin, R. (2011). Effects of rTMS on Parkinson's disease: a longitudinal fMRI study. *J. Neurol.* 258, 1268–1280. doi: 10.1007/s00415-011-5923-2

Gorges, M., Roselli, F., Müller, H. P., Ludolph, A. C., Rasche, V., and Kassubek, J. (2017). Functional connectivity mapping in the animal model: principles and applications of resting-state fMRI. *Front. Neurol.* 8:200. doi: 10.3389/fneur.2017.00200

Gozzi, A., and Schwarz, A. J. (2016). Large-scale functional connectivity networks in the rodent brain. *Neuroimage* 127, 496–509. doi: 10.1016/j.neuroimage.2015.12.017

Grandjean, J., Schroeter, A., Batata, I., and Rudin, M. (2014). Optimization of anesthesia protocol for resting-state fMRI in mice based on differential effects of anesthetics on functional connectivity patterns. *Neuroimage* 102, 838–847. doi: 10.1016/j.neuroimage.2014.08.043

Green, R. M., Pascual-Leone, A., and Wasserman, E. M. (1997). Ethical guidelines for rTMS research. *IRB Ethics Hum. Res.* 19, 1–7. doi: 10.2307/3563539

Grefkes, C., Nowak, D. A., Wang, L. E., Dafotakis, M., Eickhoff, S. B., Fink, G. R., et al. (2010). Modulating cortical connectivity in stroke patients by rTMS assessed with fMRI and dynamic causal modeling. *Neuroimage* 50, 233–242. doi: 10.1016/j.neuroimage.2009.12.029

Greicius, M. D., Flores, B. H., Menon, V., Glover, G. H., Solvason, H. B., Kenna, H., et al. (2007). Resting-state functional connectivity in major depression: abnormally increased contributions from subgenual cingulate cortex and thalamus. *Biol. Psychiatry* 62, 429–437. doi: 10.1016/j.biopsych.2006.09.020

Greicius, M. D., Srivastava, G., Reiss, A. L., and Menon, V. (2004). Default-mode network activity distinguishes Alzheimer's disease from healthy aging: evidence from functional MRI. *Proc. Natl. Acad. Sci. U.S.A.* 101, 4637–4642. doi: 10.1073/pnas.0308627101

Guo, T., Cao, X., and Xia, L. (2008). Repetitive transcranial magnetic stimulation causes significant changes of chemical substances in the brain of rabbits with experimental intracerebral hemorrhage. *Front. Med. China* 2, 406–409. doi: 10.1007/s11684-008-0078-y

Hampson, M., and Hoffman, R. E. (2010). Transcranial magnetic stimulation and connectivity mapping: tools for studying the neural bases of brain disorders. *Front. Syst. Neurosci.* 4:40. doi: 10.3389/fnsys.2010.00040

Hopman, H. J., Neggers, S. F. W., Lam, L. C. W., Mak, A. D., and Chan, S. S. M. (2017). Preliminary results: resting-state fMRI correlations between left dorsolateral prefrontal cortex and subgenual cingulate and the relationship with repetitive transcranial magnetic stimulation treatment response. *Brain Stimul.* 10:403. doi: 10.1016/j.brs.2017.01.197

Hsu, L. M., Liang, X., Gu, H., Brynildsen, J. K., Stark, J. A., Ash, J. A., et al. (2016). Constituents and functional implications of the rat default mode network. *Proc. Natl. Acad. Sci. U.S.A.* 113, e4541–e4547. doi: 10.1073/pnas.1601485113

Huang, S. M., Wu, Y. L., Peng, S. L., Peng, H. H., Huang, T. Y., Ho, K. C., et al. (2016). Inter-strain differences in default mode network: a resting state fMRI study on spontaneously hypertensive rat and Wistar Kyoto rat. *Sci. Rep.* 6:21697. doi: 10.1038/srep21697

Huang, Y. Z., Edwards, M. J., Rounis, E., Bhatia, K. P., and Rothwell, J. C. (2005). Theta burst stimulation of the human motor cortex. *Neuron* 45, 201–206. doi: 10.1016/j.neuron.2004.12.033

Hutchison, R. M., Mirsattari, S. M., Jones, C. K., Gati, J. S., and Leung, L. S. (2010). Functional networks in the anesthetized rat brain revealed by independent component analysis of resting-state fMRI. *J. Neurophysiol.* 103, 3398–3406. doi: 10.1152/jn.00141.2010

Iacoboni, M. (2008). The role of premotor cortex in speech perception: evidence from fMRI and rTMS. *J. Physiol.* 102, 31–34. doi: 10.1016/j.jphysparis.2008.03.003

Jaafari, N., Rachid, F., Rotge, J. Y., Polosan, M., El-Hage, W., Belin, D., et al. (2012). Safety and efficacy of repetitive transcranial magnetic stimulation in the treatment of obsessive-compulsive disorder: a review. *World J. Biol. Psychiatry* 13, 164–177. doi: 10.3109/15622975.2011.575177

Jacobs, J. (2014). Hippocampal theta oscillations are slower in humans than in rodents: implications for models of spatial navigation and memory. *Philos. Trans. R. Soc. B Biol. Sci.* 369:20130304. doi: 10.1098/rstb.2013.0304

Jansen, J. M., van Wingen, G., van den Brink, W., and Goudriaan, A. E. (2015). Resting state connectivity in alcohol dependent patients and the effect of repetitive transcranial magnetic stimulation. *Eur. Neuropsychopharmacol.* 25, 2230–2239. doi: 10.1016/j.euroneuro.2015.09.019

Joel, S. E., Caffo, B. S., van Zijl, P. C., and Pekar, J. J. (2011). On the relationship between seed-based and ICA-based measures of functional connectivity. *Magn. Reson. Med.* 66, 644–657. doi: 10.1002/mrm.22818

Jonckers, E., Shah, D., Hamaide, J., Verhoye, M., and Van der Linden, A. (2015). The power of using functional fMRI on small rodents to study brain pharmacology and disease. *Front. Pharmacol.* 6:231. doi: 10.3389/fphar.2015.00231

Jonckers, E., Van Audekerke, J., De Visscher, G., Van der Linden, A., and Verhoye, M. (2011). Functional connectivity fMRI of the rodent brain: comparison of functional connectivity networks in rat and mouse. *PLoS ONE* 6:e18876. doi: 10.1371/journal.pone.0018876

Kelly, A. M., Uddin, L. Q., Biswal, B. B., Castellanos, F. X., and Milham, M. P. (2008). Competition between functional brain networks mediates behavioral variability. *Neuroimage* 39, 527–537. doi: 10.1016/j.neuroimage.2007.08.008

Kenkel, W. M., Yee, J. R., Moore, K., Madularu, D., Kulkarni, P., Gamber, K., et al. (2016). Functional magnetic resonance imaging in awake transgenic fragile X rats: evidence of dysregulation in reward processing in the mesolimbic/habenular neural circuit. *Transl. Psychiatry* 6:e763. doi: 10.1038/tp.2016.15

Kennedy, D. P., Redcay, E., and Courchesne, E. (2006). Failing to deactivate: resting functional abnormalities in autism. *Proc. Natl. Acad. Sci. U.S.A.* 103, 8275–8280. doi: 10.1073/pnas.0600674103

Kimbrell, T. A., Little, J. T., Dunn, R. T., Frye, M. A., Greenberg, B. D., Wassermann, E. M., et al. (1999). Frequency dependence of antidepressant response to left prefrontal repetitive transcranial magnetic stimulation (rTMS) as a function of baseline cerebral glucose metabolism. *Biol. Psychiatry* 46, 1603–1613. doi: 10.1016/S0006-3223(99)00195-X

Kistsen, V., Evstigneev, V., Dubovik, B., and Ulashchik, V. (2016). The effects of repetitive transcranial magnetic stimulation on picrotoxin-induced convulsions in mice. *Adv. Clin. Exp. Med.* 25, 317–325. doi: 10.17219/acem/36597

Klomjai, W., Katz, R., and Lackmy-Vallée, A. (2015). Basic principles of transcranial magnetic stimulation (TMS) and repetitive TMS (rTMS). *Ann. Phys. Rehabil. Med.* 58, 208–213. doi: 10.1016/j.rehab.2015.05.005

Köhler, S., Paus, T., Buckner, R. L., and Milner, B. (2004). Effects of left inferior prefrontal stimulation on episodic memory formation: a two-stage fMRI—rTMS study. *J. Cogn. Neurosci.* 16, 178–188. doi: 10.1162/089892904322984490

Komssi, S., Kähkönen, S., and Ilmoniemi, R. J. (2004). The effect of stimulus intensity on brain responses evoked by transcranial magnetic stimulation. *Hum. Brain Mapp.* 21, 154–164. doi: 10.1002/hbm.10159

Kozel, F. A., Tian, F., Dhamne, S., Croarkin, P. E., McClintock, S. M., Elliott, A., et al. (2009). Using simultaneous repetitive transcranial magnetic stimulation/functional near infrared spectroscopy (rTMS/fNIRS) to measure brain activation and connectivity. *Neuroimage* 47, 1177–1184. doi: 10.1016/j.neuroimage.2009.05.016

Lahmame, A., del Arco, C., Pazos, A., Yritia, M., and Armario, A. (1997). Are Wistar-Kyoto rats a genetic animal model of depression resistant to antidepressants? *Eur. J. Pharmacol.* 337, 115–123. doi: 10.1016/S0014-2999(97)01276-4

Larson, J., Wong, D., and Lynch, G. (1986). Patterned stimulation at the theta frequency is optimal for the induction of hippocampal long-term potentiation. *Brain Res.* 368, 347–350. doi: 10.1016/0006-8993(86)90579-2

Lenz, M., and Vlachos, A. (2016). Releasing the cortical brake by non-invasive electromagnetic stimulation? rTMS induces LTD of GABAergic neurotransmission. *Front. Neural Circuits* 10:96. doi: 10.3389/fncir.2016.00096

Lerman, C., Gu, H., Loughead, J., Ruparel, K., Yang, Y., and Stein, E. A. (2014). Large-scale brain network coupling predicts acute nicotine abstinence effects on craving and cognitive function. *JAMA Psychiatry* 71, 523–530. doi: 10.1001/jamapsychiatry.2013.4091

Li, J., Zhang, X. W., Zuo, Z. T., Lu, J., Meng, C. L., Fang, H. Y., et al. (2016). Cerebral functional reorganization in ischemic stroke after repetitive transcranial magnetic stimulation: an fMRI study. *CNS Neurosci. Ther.* 22, 952–960. doi: 10.1111/cns.12593

Lipton, R. B., and Pearlman, S. H. (2010). Transcranial magnetic simulation in the treatment of migraine. *Neurotherapeutics* 7, 204–212. doi: 10.1016/j.nurt.2010.03.002

Liston, C., Chen, A. C., Zebley, B. D., Drysdale, A. T., Gordon, R., Leuchter, B., et al. (2014). Default mode network mechanisms of transcranial magnetic stimulation in depression. *Biol. Psychiatry* 76, 517–526. doi: 10.1016/j.biopsych.2014.01.023

Ljubisavljevic, M. R., Javid, A., Oommen, J., Parekh, K., Nagelkerke, N., Shehab, S., et al. (2015). The effects of different repetitive transcranial magnetic stimulation (rTMS) protocols on cortical gene expression in a rat model of cerebral ischemic-reperfusion injury. *PLoS ONE* 10:e0139892. doi: 10.1371/journal.pone.0139892

López-Rubalcava, C., and Lucki, I. (2000). Strain differences in the behavioral effects of antidepressant drugs in the rat forced swimming test. *Neuropsychopharmacology* 22, 191–199. doi: 10.1016/S0893-133X(99)00100-1

Lowe, M. J., Phillips, M. D., Lurito, J. T., Mattson, D., Dzemidzic, M., and Mathews, V. P. (2002). Multiple sclerosis: low-frequency temporal blood oxygen level-dependent fluctuations indicate reduced functional connectivity initial results. *Radiology* 224, 184–192. doi: 10.1148/radiol.2241011005

Lu, H., Zou, Q., Gu, H., Raichle, M. E., Stein, E. A., and Yang, Y. (2012). Rat brains also have a default mode network. *Proc. Natl. Acad. Sci. U.S.A.* 109, 3979–3984. doi: 10.1073/pnas.1200506109

Machado, S., Arias-Carrion, O., Paes, F., Uehara, E., Velasques, B., Teixeira, S., et al. (2011). Effects of repetitive transcranial magnetic stimulation on dystonia: an overview. *Am. J. Neurosci.* 2, 5–16. doi: 10.3844/amjnsp.2011.5.16

Maeda, F., Keenan, J. P., Tormos, J. M., Topka, H., and Pascual-Leone, A. (2000). Interindividual variability of the modulatory effects of repetitive transcranial magnetic stimulation on cortical excitability. *Exp. Brain Res.* 133, 425–430. doi: 10.1007/s002210000432

Makowiecki, K., Harvey, A. R., Sherrard, R. M., and Rodger, J. (2014). Low-intensity repetitive transcranial magnetic stimulation improves abnormal visual cortical circuit topography and upregulates BDNF in mice. *J. Neurosci.* 34, 10780–10792. doi: 10.1523/JNEUROSCI.0723-14.2014

Marcotte, K., Perlbarg, V., Marrelec, G., Benali, H., and Ansaldo, A. I. (2013). Default-mode network functional connectivity in aphasia: therapy-induced neuroplasticity. *Brain Lang.* 124, 45–55. doi: 10.1016/j.bandl.2012.11.004

Masamoto, K., and Kanno, I. (2012). Anesthesia and the quantitative evaluation of neurovascular coupling. *J. Cereb. Blood Flow Metab.* 32, 1233–1247. doi: 10.1038/jcbfm.2012.50

Mintun, M. A., Lundstrom, B. N., Snyder, A. Z., Vlassenko, A. G., Shulman, G. L., and Raichle, M. E. (2001). Blood flow and oxygen delivery to human brain during functional activity: Theoretical modeling and experimental data. *Proc. Natl. Acad. Sci. U.S.A.* 98, 6859–6864. doi: 10.1073/pnas.111164398

Mitaki, S., Onoda, K., Abe, S., Oguro, H., and Yamaguchi, S. (2016). The effectiveness of repetitive transcranial magnetic stimulation for poststroke apathy is associated with improved interhemispheric functional connectivity. *J. Stroke Cerebrovasc. Dis.* 25, e219–221. doi: 10.1016/j.jstrokecerebrovasdis.2016.05.014

Mueller, J. K., Grigsby, E. M., Prevosto, V., Petraglia, F. W. III, Rao, H., Deng, Z. D., et al. (2014). Simultaneous transcranial magnetic stimulation and single-neuron recording in alert non-human primates. *Nat. Neurosci.* 17, 1130–1136. doi: 10.1038/nn.3751

Mulders, W. H., Vooys, V., Makowiecki, K., Tang, A. D., and Rodger, J. (2016). The effects of repetitive transcranial magnetic stimulation in an animal model of tinnitus. *Sci. Rep.* 6:38234. doi: 10.1038/srep38234

Müller-Dahlhaus, F., and Vlachos, A. (2013). Unraveling the cellular and molecular mechanisms of repetitive magnetic stimulation. *Front. Mol. Neurosci.* 6:50. doi: 10.3389/fnmol.2013.00050

Nettekoven, C., Volz, L. J., Kutscha, M., Pool, E. M., Rehme, A. K., Eickhoff, S. B., et al. (2014). Dose-dependent effects of theta burst rTMS on cortical excitability and resting-state connectivity of the human motor system. *J. Neurosci.* 34, 6849–6859. doi: 10.1523/JNEUROSCI.4993-13.2014

Nierat, M. C., Hudson, A. L., Chaskalovic, J., Similowski, T., and Laviolette, L. (2015). Repetitive transcranial magnetic stimulation over the supplementary motor area modifies breathing pattern in response to inspiratory loading in normal humans. *Front. Physiol.* 6:273. doi: 10.3389/fphys.2015.00273

O'Reardon, J. P., Solvason, H. B., Janicak, P. G., Sampson, S., Isenberg, K. E., Nahas, Z., et al. (2007). Efficacy and safety of transcranial magnetic stimulation in the acute treatment of major depression: a multisite randomized controlled trial. *Biol. Psychiatry* 62, 1208–1216. doi: 10.1016/j.biopsych.2007.01.018

Ohata, H., Iida, H., Dohi, S., and Watanabe, Y. (1999). Intravenous dexmedetomidine inhibits cerebrovascular dilation induced by isoflurane and sevoflurane in dogs. *Anesth. Analg.* 89, 370–377. doi: 10.1213/00000539-199908000-00023

Opitz, A., Windhoff, M., Heidemann, R. M., Turner, R., and Thielscher, A. (2011). How the brain tissue shapes the electric field induced by transcranial magnetic stimulation. *Neuroimage* 58, 849–859. doi: 10.1016/j.neuroimage.2011.06.069

O'Shea, J., Johansen-Berg, H., Trief, D., Göbel, S., and Rushworth, M. F. S. (2007). Functionally specific reorganization in human premotor cortex. *Neuron* 54, 479–490. doi: 10.1016/j.neuron.2007.04.021

Ouyang, W., and Hemmings, H. C. (2005). Depression by isoflurane of the action potential and underlying voltage-gated ion currents in isolated rat neurohypophysial nerve terminals. *J. Pharmacol. Exp. Ther.* 312, 801–808. doi: 10.1124/jpet.104.074609

Pan, W. J., Billings, J. C. W., Grooms, J. K., Shakil, S., and Keilholz, S. D. (2015). Considerations for resting state functional MRI and functional connectivity studies in rodents. *Front. Neurosci.* 9:269. doi: 10.3389/fnins.2015.00269

Pasley, B. N., Allen, E. A., and Freeman, R. D. (2009). State-dependent variability of neuronal responses to transcranial magnetic stimulation of the visual cortex. *Neuron* 62, 291–303. doi: 10.1016/j.neuron.2009.03.012

Paus, T., Jech, R., Thompson, C. J., Comeau, R., Peters, T., and Evans, A. C. (1997). Transcranial magnetic stimulation during positron emission tomography: a new method for studying connectivity of the human cerebral cortex. *J. Neurosci.* 17, 3178–3184.

Pawela, C. P., Biswal, B. B., Hudetz, A. G., Schulte, M. L., Li, R., Jones, S. R., et al. (2009). A protocol for use of medetomidine anesthesia in rats for extended studies using task-induced BOLD contrast and resting-state functional connectivity. *Neuroimage* 46, 1137–1147. doi: 10.1016/j.neuroimage.2009.03.004

Pereira, L. S., Müller, V. T., da Mota Gomes, M., Rotenberg, A., and Fregni, F. (2016). Safety of repetitive transcranial magnetic stimulation in patients with epilepsy: a systematic review. *Epilepsy Behav.* 57(Pt A), 167–176. doi: 10.1016/j.yebeh.2016.01.015

Popa, T., Russo, M., Vidailhet, M., Roze, E., Lehéricy, S., Bonnet, C., et al. (2013). Cerebellar rTMS stimulation may induce prolonged clinical benefits in essential tremor, and subjacent changes in functional connectivity: an open label trial. *Brain Stimul.* 6, 175–179. doi: 10.1016/j.brs.2012.04.009

Prielipp, R. C., Wall, M. H., Tobin, J. R., Groban, L., Cannon, M. A., Fahey, F. H., et al. (2002). Dexmedetomidine-induced sedation in volunteers decreases regional and global cerebral blood flow. *Anesth. Analg.* 95, 1052–1059. doi: 10.1213/00000539-200210000-00048

Raichle, M. E., MacLeod, A. M., Snyder, A. Z., Powers, W. J., Gusnard, D. A., and Shulman, G. L. (2001). A default mode of brain function. *Proc. Natl. Acad. Sci. U.S.A.* 98, 676–682. doi: 10.1073/pnas.98.2.676

Ridding, M. C., and Ziemann, U. (2010). Determinants of the induction of cortical plasticity by non-invasive brain stimulation in healthy subjects. *J. Physiol.* 588, 2291–2304. doi: 10.1113/jphysiol.2010.190314

Rodger, J., Mo, C., Wilks, T., Dunlop, S. A., and Sherrard, R. M. (2012). Transcranial pulsed magnetic field stimulation facilitates reorganization of abnormal neural circuits and corrects behavioral deficits without disrupting normal connectivity. *FASEB J.* 26, 1593–1606. doi: 10.1096/fj.11-194878

Rodger, J., and Sherrard, R. M. (2015). Optimising repetitive transcranial magnetic stimulation for neural circuit repair following traumatic brain injury. *Neural. Regener. Res.* 10, 357–359. doi: 10.4103/1673-5374.153676

Rosazza, C., Minati, L., Ghielmetti, F., Mandelli, M. L., and Bruzzone, M. G. (2012). Functional connectivity during resting-state functional MR imaging: study of the correspondence between independent component analysis and region-of-interest-based methods. *Am. J. Neuroradiol.* 33, 180–187. doi: 10.3174/ajnr.A2733

Rotenberg, A., Muller, P. A., Vahabzadeh-Hagh, A. M., Navarro, X., López-Vales, R., Pascual-Leone, A., et al. (2010). Lateralization of forelimb motor evoked potentials by transcranial magnetic stimulation in rats. *Clin. Neurophysiol.* 121, 104–108. doi: 10.1016/j.clinph.2009.09.008

Sack, A. T., Hubl, D., Prvulovic, D., Formisano, E., Jandl, M., Zanella, F. E., et al. (2002). The experimental combination of rTMS and fMRI reveals the functional relevance of parietal cortex for visuospatial functions. *Cogn. Brain Res.* 13, 85–93. doi: 10.1016/S0926-6410(01)00087-8

Salinas, F. S., Narayana, S., Zhang, W., Fox, P. T., and Szabó, C. Á. (2013). Repetitive transcranial magnetic stimulation elicits rate-dependent brain network responses in non-human primates. *Brain Stimul.* 6, 777–787. doi: 10.1016/j.brs.2013.03.002

Sbardella, E., Petsas, N., Tona, F., and Pantano, P. (2015). Resting-state fMRI in MS: general concepts and brief overview of its application. *Biomed Res. Int.* 2015, 1–8. doi: 10.1155/2015/212693

Schneider, S. A., Pleger, B., Draganski, B., Cordivari, C., Rothwell, J. C., Bhatia, K. P., et al. (2010). Modulatory effects of 5Hz rTMS over the primary somatosensory cortex in focal dystonia—An fMRI-TMS study. *Mov. Disord.* 25, 76–83. doi: 10.1002/mds.22825

Seeley, W. W., Crawford, R. K., Zhou, J., Miller, B. L., and Greicius, M. D. (2009). Neurodegenerative diseases target large-scale human brain networks. *Neuron* 62, 42–52. doi: 10.1016/j.neuron.2009.03.024

Sierakowiak, A., Monnot, C., Aski, S. N., Uppman, M., Li, T. Q., Damberg, P., et al. (2015). Default mode network, motor network, dorsal and ventral basal ganglia networks in the rat brain: comparison to human networks using resting state-fMRI. *PLoS ONE* 10:e0120345. doi: 10.1371/journal.pone.0120345

Soleimani, R., Jalali, M. M., and Hasandokht, T. (2015). Therapeutic impact of repetitive transcranial magnetic stimulation (rTMS) on tinnitus: a systematic review and meta-analysis. *Eur. Arch. Oto Rhino Laryngol.* 273, 1663–1675. doi: 10.1007/s00405-015-3642-5

Speer, A. M., Kimbrell, T. A., Wassermann, E. M. D., Repella, J., Willis, M. W., Herscovitch, P., et al. (2000). Opposite effects of high and low frequency rTMS on regional brain activity in depressed patients. *Biol. Psychiatry* 48, 1133–1141. doi: 10.1016/S0006-3223(00)01065-9

Sutherland, M. T., McHugh, M. J., Pariyadath, V., and Stein, E. A. (2012). Resting state functional connectivity in addiction: lessons learned and a road ahead. *Neuroimage* 62, 2281–2295. doi: 10.1016/j.neuroimage.2012.01.117

Sykes, M., Matheson, N. A., Brownjohn, P. W., Tang, A. D., Rodger, J., Shemmell, J. B. H., et al. (2016). Differences in motor evoked potentials induced in rats by transcranial magnetic stimulation under two separate anesthetics: implications for plasticity studies. *Front. Neural Circuits* 10:80. doi: 10.3389/fncir.2016.00080

Tambalo, S., Peruzzotti-Jametti, L., Rigolio, R., Fiorini, S., Bontempi, P., Mallucci, G., et al. (2015). Functional magnetic resonance imaging of rats with experimental autoimmune encephalomyelitis reveals brain cortex remodeling. *J. Neurosci.* 35, 10088–10100. doi: 10.1523/JNEUROSCI.0540-15.2015

Tan, T., Xie, J., Liu, T., Chen, X., Zheng, X., Tong, Z., et al. (2013). Low-frequency (1Hz) repetitive transcranial magnetic stimulation (rTMS) reverses Aβ1–42-mediated memory deficits in rats. *Exp. Gerontol.* 48, 786–794. doi: 10.1016/j.exger.2013.05.001

Tang, A. D., Lowe, A. S., Garrett, A. R., Woodward, R., Bennett, W., Canty, A. J., et al. (2016). Construction and evaluation of rodent-specific rTMS coils. *Front. Neural Circuits* 10:47. doi: 10.3389/fncir.2016.00047

Tang, A., Thickbroom, G., and Rodger, J. (2015). Repetitive transcranial magnetic stimulation of the brain: mechanisms from animal and experimental models. *Neuroscientist* 23, 82–94. doi: 10.1177/1073858415618897

Valchev, N., Curčić-Blake, B., Renken, R. J., Avenanti, A., Keysers, C., Gazzola, V., et al. (2015). cTBS delivered to the left somatosensory cortex changes its functional connectivity during rest. *Neuroimage* 114, 386–397. doi: 10.1016/j.neuroimage.2015.04.017

Valero-Cabré, A., Payne, B., and Pascual-Leone, A. (2007). Opposite impact on 14 C-2-deoxyglucose brain metabolism following patterns of high and low frequency repetitive transcranial magnetic stimulation in the posterior parietal cortex. *Exper. Brain Res.* 176, 603–615. doi: 10.1007/s00221-006-0639-8

Valero-Cabre, A., Wattiez, N., Monfort, M., François, C., Rivaud-Péchoux, S., Gaymard, B., et al. (2012). Frontal non-invasive neurostimulation modulates antisaccade preparation in non-human primates. *PLoS ONE* 7:e38674. doi: 10.1371/journal.pone.0038674

van den Heuvel, M. P., and Hulshoff Pol, H. E. (2010). Exploring the brain network: a review on resting-state fMRI functional connectivity. *Eur. Neuropsychopharmacol.* 20, 519–534. doi: 10.1016/j.euroneuro.2010.03.008

van der Werf, Y. D., Sanz-Arigita, E. J., Menning, S., and van den Heuvel, O. A. (2010). Modulating spontaneous brain activity using repetitive transcranial magnetic stimulation. *BMC Neurosci.* 11:145. doi: 10.1186/1471-2202-11-145

Vincent, J. L., Patel, G. H., Fox, M. D., Snyder, A. Z., Baker, J. T., Van Essen, D. C., et al. (2007). Intrinsic functional architecture in the anaesthetized monkey brain. *Nature* 447, 83–86. doi: 10.1038/nature05758

Waites, A. B., Briellmann, R. S., Saling, M. M., Abbott, D. F., and Jackson, G. D. (2006). Functional connectivity networks are disrupted in left temporal lobe epilepsy. *Ann. Neurol.* 59, 335–343. doi: 10.1002/ana.20733

Walsh, V. (1998). Brain mapping: faradization of the mind. *Curr. Biol.* 8, R8–R11. doi: 10.1016/S0960-9822(98)70098-3

Wang, J. X., Rogers, L. M., Gross, E. Z., Ryals, A. J., Dokucu, M. E., Brandstatt, K. L., et al. (2014). Targeted enhancement of cortical-hippocampal brain networks and associative memory. *Science* 345, 1054–1057. doi: 10.1126/science.1252900

Wassermann, E. M., and Zimmermann, T. (2012). Transcranial magnetic brain stimulation: therapeutic promises and scientific gaps. *Pharmacol. Ther.* 133, 98–107. doi: 10.1016/j.pharmthera.2011.09.003

Watrous, A. J., Lee, D. J., Izadi, A., Gurkoff, G. G., Shahlaie, K., and Ekstrom, A. D. (2013). A comparative study of human and rat hippocampal low frequency oscillations during spatial navigation. *Hippocampus* 23, 656–661. doi: 10.1002/hipo.22124

Whitfield-Gabrieli, S., Thermenos, H. W., Milanovic, S., Tsuang, M. T., Faraone, S. V., McCarley, R. W., et al. (2009). Hyperactivity and hyperconnectivity of the default network in Schizophrenia and in first-degree relatives of persons with Schizophrenia. *Proc. Natl. Acad. Sci. U.S.A.* 106, 1279–1284. doi: 10.1073/pnas.0809141106

Williams, K. A., Mehta, N. S., Redei, E. E., Wang, L., and Procissi, D. (2014). Aberrant resting-state functional connectivity in a genetic rat model of depression. *Psychiatry Res.* 222, 111–113. doi: 10.1016/j.pscychresns.2014.02.001

Wilson, M. T., and St George, L. (2016). Repetitive transcranial magnetic stimulation: a call for better data. *Front. Neural Circuits* 10:57. doi: 10.3389/fncir.2016.00057

Xia, G., Gajwani, P., Muzina, D. J., Kemp, D. E., Gao, K., Ganocy, S. J., et al. (2008). Treatment-emergent mania in unipolar and bipolar depression: focus

on repetitive transcranial magnetic stimulation. *Int. J. Neuropsychopharmacol.* 11, 119–130. doi: 10.1017/S1461145707007699

Yang, H., Shi, O., Jin, Y., Henrich-Noack, P., Qiao, H., Cai, C., et al. (2014). Functional protection of learning and memory abilities in rats with vascular dementia. *Restor. Neurol. Neurosci.* 32, 689–700. doi: 10.3233/RNN-140409

Yang, H. Y., Liu, Y., Xie, J. C., Liu, N. N., and Tian, X. (2015). Effects of repetitive transcranial magnetic stimulation on synaptic plasticity and apoptosis in vascular dementia rats. *Behav. Brain Res.* 281, 149–155. doi: 10.1016/j.bbr.2014.12.037

Yuan, H., Shou, G., Gleghorn, D., Ding, L., and Cha, Y. H. (2017). Resting state functional connectivity signature of treatment effects of repetitive transcranial magnetic stimulation in mal de debarquement syndrome. *Brain Connect.* 7, 617–626. doi: 10.1089/brain.2017.0514

Zangen, A., and Hyodo, K. (2002). Transcranial magnetic stimulation induces increases in extracellular levels of dopamine and glutamate in the nucleus accumbens. *Neuroreport* 13, 2401–2405. doi: 10.1097/00001756-200212200-00005

Zerbi, V., Grandjean, J., Rudin, M., and Wenderoth, N. (2015). Mapping the mouse brain with rs-fMRI: an optimized pipeline for functional network identification. *Neuroimage* 123, 11–21. doi: 10.1016/j.neuroimage.2015.07.090

Zhang, N., Xing, M., Wang, Y., Tao, H., and Cheng, Y. (2015). Repetitive transcranial magnetic stimulation enhances spatial learning and synaptic plasticity via the VEGF and BDNF–NMDAR pathways in a rat model of vascular dementia. *Neuroscience* 311, 284–291. doi: 10.1016/j.neuroscience.2015.10.038

Conflict of Interest Statement: The authors declare that the research was conducted in the absence of any commercial or financial relationships that could be construed as a potential conflict of interest.

frontiers in Neuroscience

REVIEW
published: 09 November 2017
doi: 10.3389/fnins.2017.00627

Connectopathy in Autism Spectrum Disorders: A Review of Evidence from Visual Evoked Potentials and Diffusion Magnetic Resonance Imaging

Takao Yamasaki[1,2]*, *Toshihiko Maekawa*[1], *Takako Fujita*[3] and *Shozo Tobimatsu*[1]

[1] Department of Clinical Neurophysiology, Neurological Institute, Graduate School of Medical Sciences, Kyushu University, Fukuoka, Japan, [2] Department of Neurology, Minkodo Minohara Hospital, Fukuoka, Japan, [3] Department of Pediatrics, Fukuoka University School of Medicine, Fukuoka, Japan

Individuals with autism spectrum disorder (ASD) show superior performance in processing fine details; however, they often exhibit impairments of gestalt face, global motion perception, and visual attention as well as core social deficits. Increasing evidence has suggested that social deficits in ASD arise from abnormal functional and structural connectivities between and within distributed cortical networks that are recruited during social information processing. Because the human visual system is characterized by a set of parallel, hierarchical, multistage network systems, we hypothesized that the altered connectivity of visual networks contributes to social cognition impairment in ASD. In the present review, we focused on studies of altered connectivity of visual and attention networks in ASD using visual evoked potentials (VEPs), event-related potentials (ERPs), and diffusion tensor imaging (DTI). A series of VEP, ERP, and DTI studies conducted in our laboratory have demonstrated complex alterations (impairment and enhancement) of visual and attention networks in ASD. Recent data have suggested that the atypical visual perception observed in ASD is caused by altered connectivity within parallel visual pathways and attention networks, thereby contributing to the impaired social communication observed in ASD. Therefore, we conclude that the underlying pathophysiological mechanism of ASD constitutes a "connectopathy."

Keywords: autism spectrum disorder, connectopathy, visual perception, attention, visual evoked potentials, event-related potentials, diffusion tensor imaging, magnetic resonance imaging

OPEN ACCESS

Edited by:
Giancarlo Zito,
Ospedale San Giovanni Calibita Fatebenefratelli, Italy

Reviewed by:
Xiaoli Li,
Beijing Normal University, China
Waldemar Karwowski,
University of Central Florida, United States

***Correspondence:**
Takao Yamasaki
yamasa@neurophy.med.kyushu-u.ac.jp

Specialty section:
This article was submitted to Neural Technology, a section of the journal Frontiers in Neuroscience

Received: *10 June 2017*
Accepted: *26 October 2017*
Published: *09 November 2017*

Citation:
Yamasaki T, Maekawa T, Fujita T and Tobimatsu S (2017) Connectopathy in Autism Spectrum Disorders: A Review of Evidence from Visual Evoked Potentials and Diffusion Magnetic Resonance Imaging. Front. Neurosci. 11:627. doi: 10.3389/fnins.2017.00627

INTRODUCTION

Autism spectrum disorder (ASD) is a neurodevelopmental condition that is characterized by alterations in social communication and interaction; it co-occurs with restricted, repetitive patterns of behavior, interests, or activities (American Psychiatric Association, 2013). Recent neuroimaging studies have suggested that ASD is a disconnection syndrome that is associated with connectivity alterations between distributed brain areas recruited during social information processing, rather than local deficits in specific brain regions (Müller, 2008). Specifically, functional connectivity comprising long-range connections in the brain may be diminished in ASD; this is accompanied

by greater localized connectivity (Geschwind and Levitt, 2007; Anderson, 2014). However, precise mechanisms underlying such abnormalities in ASD remain largely unknown.

Besides core social deficits, ASD exhibits peculiar sensory processing (e.g., superior simple and lower-level perception, but poor complex and higher-level processing) during visual (Simmons et al., 2009) and auditory (O'Connor, 2012) behavioral tasks (Yamasaki et al., 2017). In the visual aspect, ASD displays superb performance in fine-form perception (i.e., perception of local structures; Jolliffe and Baron-Cohen, 1997; Happé and Frith, 2006). In contrast, ASD is characterized by poor performance in several aspects of face (Golarai et al., 2006; Simmons et al., 2009) and motion (Spencer et al., 2000; Milne et al., 2002; Bertone et al., 2003) perception (Yamasaki et al., 2014). Various levels of visual attention deficits have been noted in ASD (Pruett et al., 2011; Amso et al., 2014). Overall, these visual perception abnormalities may contribute to social cognition impairment in ASD (Dakin and Frith, 2005).

In humans, the distinctive feature of the visual system is a set of parallel, hierarchical, multistage systems, which contribute to the processing of different visual stimulus types. Two major parallel pathways are present: parvocellular (P or ventral) and magnocellular (M or dorsal) pathways (Yamasaki et al., 2013; **Figures 1A,B**). These streams comprise multiple visual cortical areas and are structurally connected by fiber tracts (**Figure 1C**). These pathways are functionally connected by feedforward, feedback, and lateral interactions (Tobimatsu and Celesia, 2006). Moreover, the following two attention networks have been described in the human brain: ventral (bottom-up) and dorsal (top-down) frontoparietal attention networks (Corbetta et al., 2008). Both include several key nodes and are structurally connected by the periventricular white matter fiber tracts (Doricchi et al., 2008; Umarova et al., 2010; **Figure 2**). Therefore, it is probable that atypical visual perception in ASD is caused by alterations to the local circuitry within the visual area and connectivity between distributed visual cortical areas as well as the connectivity of attention networks.

Visual evoked potentials (VEPs) and event-related potentials (ERPs) are objective, non-invasive methods to delineate subtle functional abnormalities in the human visual system. Both VEPs and ERPs offer a direct measure of neuronal activities with high temporal resolution, in the order of milliseconds (Tobimatsu and Celesia, 2006; Yamasaki and Tobimatsu, 2014). VEP and ERP abnormalities are closely correlated with white matter damage of parallel visual pathways (Yamasaki et al., 2004). Diffusion tensor imaging (DTI) is a powerful technique that measures the white matter microstructure *in vivo*; it enables us to compute the anatomical connectivity among the brain areas (Basser and Jones, 2002). Therefore, the combined use of electrophysiological measurements (VEP and ERP) and DTI is ideally suited to examine alterations to connectivities underlying atypical visual perception in ASD.

Based on a narrative review of a series of VEP, ERP, and DTI studies conducted in our laboratory (Noriuchi et al., 2010; Fujita et al., 2011, 2013; Maekawa et al., 2011; Yamasaki et al., 2011a,b, 2013, 2014, 2017), we propose that altered connectivities (hyperconnectivity and underconnectivity) of visual and attention networks contribute to social cognition impairment in ASD. Specifically, we propose that ASD can be conceptualized as a brain network disorder that might be best characterized as a "connectopathy."

CONCEPT OF PARALLEL VISUAL PATHWAYS

As previously mentioned, both P and M pathways are important for processing the detailed visual information (Livingstone and Hubel, 1988; Nealey and Maunsell, 1994; Tobimatsu and Celesia, 2006; Yamasaki and Tobimatsu, 2012; Yamasaki et al., 2014; **Figures 1A,B**). Both pathways begin in the retina and there are direct anatomical connection to the primary visual cortex (V1) via the lateral geniculate nucleus. The segregation of these two pathways is perpetuated in V1. The P pathway primarily terminates in layer 4Cβ of V1 and is further differentiated into the P-blob and P-interblob pathways. The former pathway projects to the thin stripes of V2 via cytochrome oxidase (CO)-rich blobs in V1, while the latter pathway projects to the interstripes of V2 via non-CO-rich interblobs in V1. The P-blob and P-interblob pathways project to V4, and visual information is consecutively sent to the inferior temporal cortex (ventral stream). The P-blob and P-interblob streams thus act in fully different and complementary manners. The P-blob cells are involved in color discrimination. In contrast, the P-interblob cells are not color selective and respond to a line or edge of the correct orientation (form) (Livingstone and Hubel, 1988).

The M pathway primarily terminates in layer 4Cα of V1 and travels to the thick stripes of V2 via layer 4B. Cells in layer 4B most strongly respond to lines of a particular orientation. Thus, they are most selective for the direction of movement. However, cells in layer 4B lack color selectivity. The M pathway further sends their output to the V5/middle temporal area (MT) and V6 and reaches in the posterior parietal cortex (dorsal stream). The M pathway is important to detect motion and process the global structure. The dorsal stream consists of two functional streams: dorso-dorsal (d-d) and ventro-dorsal (v-d) pathways. The d-d pathway includes V6 and the superior parietal lobule (SPL), while the v-d pathway includes V5/MT and the inferior parietal lobule (IPL) (Yamasaki et al., 2012a). The distinct functions of the P-blob (color), P-interblob (form), and M pathways depend on their specific physiological properties (Livingstone and Hubel, 1988; Tobimatsu and Celesia, 2006; **Table 1**).

In relation to the white matter bundle, the ventral stream constitutes the inferior longitudinal fasciculus (ILF: orange in **Figure 1C**) and inferior fronto-occipital fasciculus (IFOF: yellow in **Figure 1C**). The former connects the occipital and temporal lobes while the latter connects the occipitoparietal and frontal regions (ffytche et al., 2010; Kravitz et al., 2013; **Figure 1C**). In contrast, the dorsal stream involves the inferior and superior parietal brain regions and connects with the frontal lobes via a long-range white matter bundle called the superior longitudinal fasciculus (SLF: sky-blue in **Figure 1C**; ffytche et al., 2010; Kravitz et al., 2011).

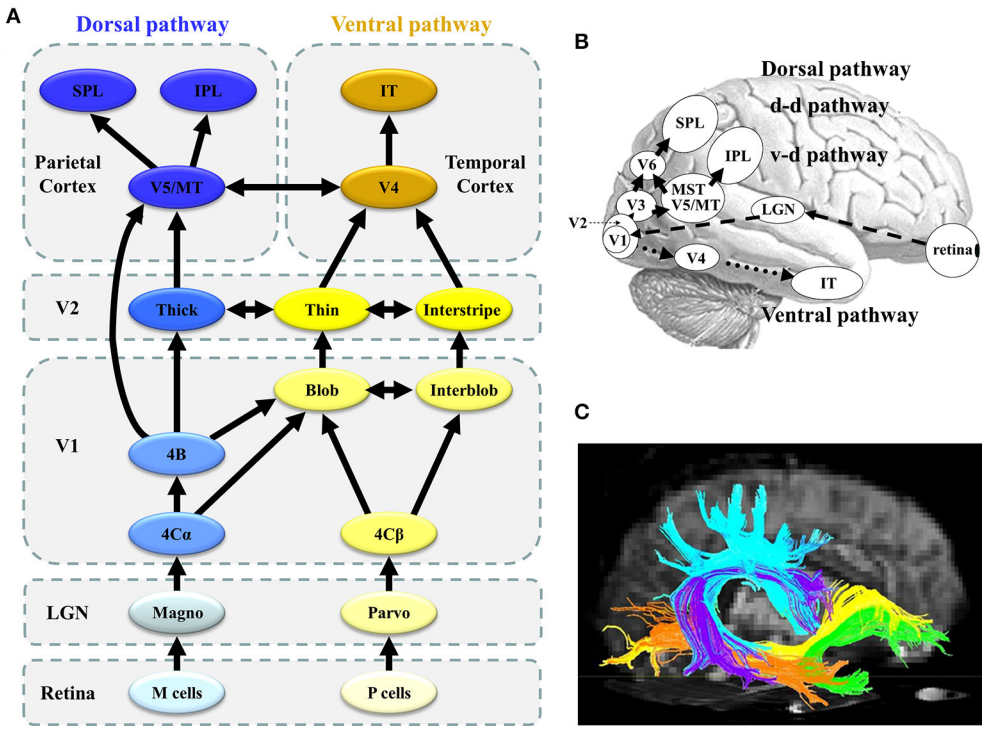

FIGURE 1 | Parallel visual pathways in humans. **(A)** The monkey visual system is characterized by a set of parallel, hierarchical, multistage systems. There are two major parallel streams: parvocellular (or ventral) and magnocellular (or dorsal) pathways (see section Concept of Parallel Visual Pathways for more detailed information). **(B)** The human visual system is analogous to that of the monkey. Two major parallel streams: parvocellular (or ventral) and magnocellular (or dorsal) pathways are present. **(C)** The ventral stream corresponds to the ILF (orange) and IFOF (yellow), while the dorsal stream is related to the SLF (sky-blue) ([C] Modified from Jang, 2013 with no permission was required to reproduce). d-d pathway, dorso-dorsal pathway; v-d pathway, ventro-dorsal pathway; LGN, lateral geniculate nucleus; MT, middle temporal area; MST, medial superior temporal area; IPL, inferior parietal lobule, SPL, superior parietal lobule; IT, inferior temporal cortex; SLF, superior longitudinal fasciculus, IFOF, inferior fronto-occipital fasciculus; ILF, inferior longitudinal fasciculus.

TABLE 1 | Physiological characteristics of the magnocellular, parvocellular-blob, and parvocellular-interblob pathways.

Physiology	Magnocellular	Parvocellular	
		Blob	Interblob
Spatial frequency selectivity	Low frequency	Medium frequency	**High frequency**
Color selectivity	No	**Yes**	No
Contrast sensitivity	**High**	Low	Low
Temporal resolution	**Fast**	Slow	Slow
Conduction velocity	**Fast**	Slow	Slow

The bold means the important characteristics.

VEP STUDIES IN ASD

Parvocellular and Magnocellular Functions at V1 in ASD

The functional characteristics of the P pathway are summarized as follows: high spatial frequency (SF) selectivity (P-interblob), color sensitivity (P-blob), low contrast sensitivity, poor temporal resolution, and slow conduction velocity (Livingstone and Hubel, 1988; Tobimatsu and Celesia, 2006; **Table 1**). Therefore, using red/green (RG) chromatic sinusoidal gratings with isoluminance of red and green are appropriate stimuli for the P pathway (P-blob [color] pathway; **Figure 3A**). This type of stimulus elicits the occipital N1 component (about 120 ms; Yamasaki and Tobimatsu, 2012; Yamasaki et al., 2014). The characteristics of the M pathway are summarized as follows: high contrast sensitivity, good temporal resolution, fast conduction velocity, color insensitivity, and low SF selectivity (**Table 1**). Accordingly, low contrast achromatic (black/white, BW) sinusoidal gratings with a frequency of 8 Hz (16 reversals/s) are appropriate stimuli (**Figure 3B**). This type of the stimulus evokes the occipital P1 component (about 120 ms), followed by steady-state responses (Yamasaki and Tobimatsu, 2012; Yamasaki et al., 2014).

The functions of lower-level P and M pathways at V1 were examined in adults with high-functioning ASD and typically developing (TD) adults (Fujita et al., 2011; Yamasaki et al., 2014). When testing the P pathway function, an unexpected finding was that the N1 latency for RG stimuli was more significantly delayed in ASD adults than in the TD controls (**Figure 3A**). RG stimuli could preferentially stimulate the P-blob but not the P-interblob pathway because the latter pathway responds better to stimuli with high SF and contrast (**Table 1**; Tobimatsu and Celesia, 2006). Thus, this finding suggests

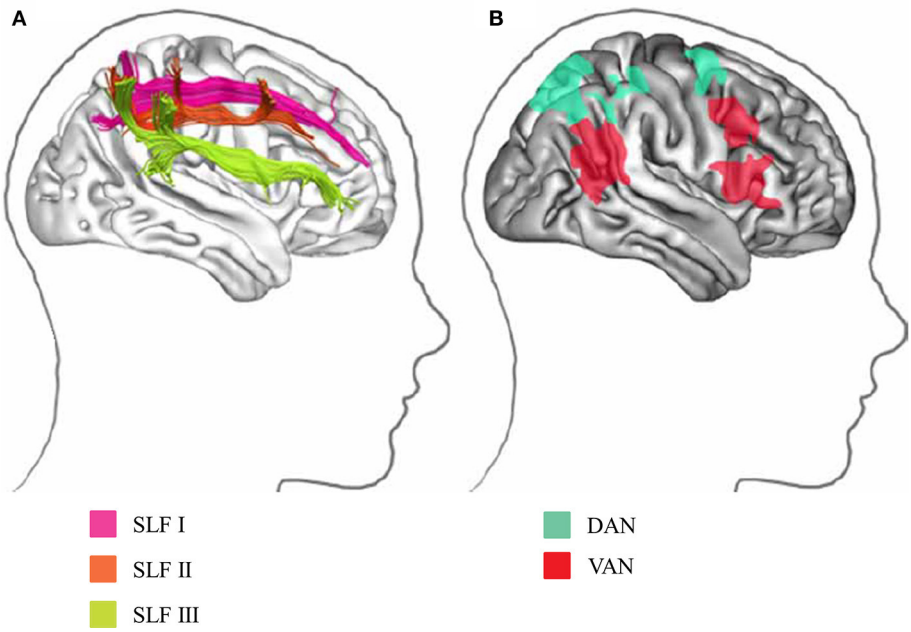

FIGURE 2 | Visual attention network in humans. **(A)** Parietal and frontal areas involved in spatial attention are linked by three distinct white matter tracts in the SLF. **(B)** Projection sites in the parietal and frontal cortices correspond to the division into the DAN and VAN. DAN, dorsal attention network; VAN, ventral attention network (Modified from Bartolomeo et al., 2012 with no permission was required to reproduce).

that the pathology of ASD implicates impairment of the P-blob pathway at a relatively low level (Fujita et al., 2011). Earlier psychophysical studies (Franklin et al., 2008, 2010) have tested color vision in ASD children and demonstrated altered color perception (color memory, color search, and chromatic discrimination) in ASD without color deficits determined by Ishihara color plates (Franklin et al., 2008, 2010; Fujita et al., 2011). Therefore, we proposed the likelihood of P-blob (color) dysfunction with compensatory P-interblob (form)-biased function (detailed form perception; Fujita et al., 2011). This interpretation was supported by adequate evidence of excellent fine form perception in ASD (Dakin and Frith, 2005). However, these studies did not assess the function of the P-interblob pathway.

Regarding the function of the M pathway, high-temporal frequency BW stimuli were used and both TD and ASD adults showed an occipital P1 with quasi-sinusoidal waveforms corresponding to the reversal frequency of BW. However, no significant difference was found in either P1 or steady-state responses between the two groups (**Figure 3B**; Fujita et al., 2011; Yamasaki et al., 2014). Accordingly, it appears that the function of lower-level M pathway is intact in ASD adults. Some psychological studies have reported abnormal function of the M pathway at the higher level (dorsal stream) in ASD adults, with preserved function of the M pathway at the lower level (Bertone et al., 2003; Pellicano et al., 2005), further supporting our VEP results (Fujita et al., 2011) that showed normal lower-level M pathway activity.

Ventral Stream Function in ASD

Based on the unexpected finding of P-blob pathway impairment in ASD (section Parvocellular and Magnocellular Functions at V1 in ASD), we further investigated the methods by which the P-interblob and P-blob pathways within the ventral stream at the lower (V1) and higher (V4) levels are functionally abnormal in high-functioning adults with ASD (Yamasaki et al., 2017).

We used three types of visual stimuli (**Figures 4A,B**). An isoluminant chromatic RG pattern with medium SF (2.0 cycles/degree, cpd) and high-contrast achromatic BW gratings with high SF (5.3 cpd) could preferentially stimulate the P-blob and P-interblob pathways at the V1 level, respectively. The occipital N1 is a major component of responses to both stimuli in **Figure 4A** (Tobimatsu et al., 1996; Yamasaki et al., 2017). In addition, face stimuli are helpful to sequentially evaluate the form pathway from V1 to V4. The right-lateralized occipital P1 (V1 origin) and occipito-temporal N170 (V4 origin) are the major components of face VEPs (**Figure 4B**; Goto et al., 2005; Deffke et al., 2007; Nakashima et al., 2008; Mitsudo et al., 2011). P1 reflects the low-level features of the visual stimuli including the contrast, luminance, and SF (Rossion and Jacques, 2008). The N170 component reflects the processing of facial features or facial identification within the fusiform face area (Bentin et al., 1996).

In a study measuring RG VEPs, ASD adults exhibited prolonged N1 latency compared with TD adults. This indicates that the function of the P-blob pathway at V1 is impaired in adults with ASD (**Figure 4A**; Yamasaki et al., 2017). These results exhibited vigorous reproducibility even though ASD participants in this study were completely different from those in

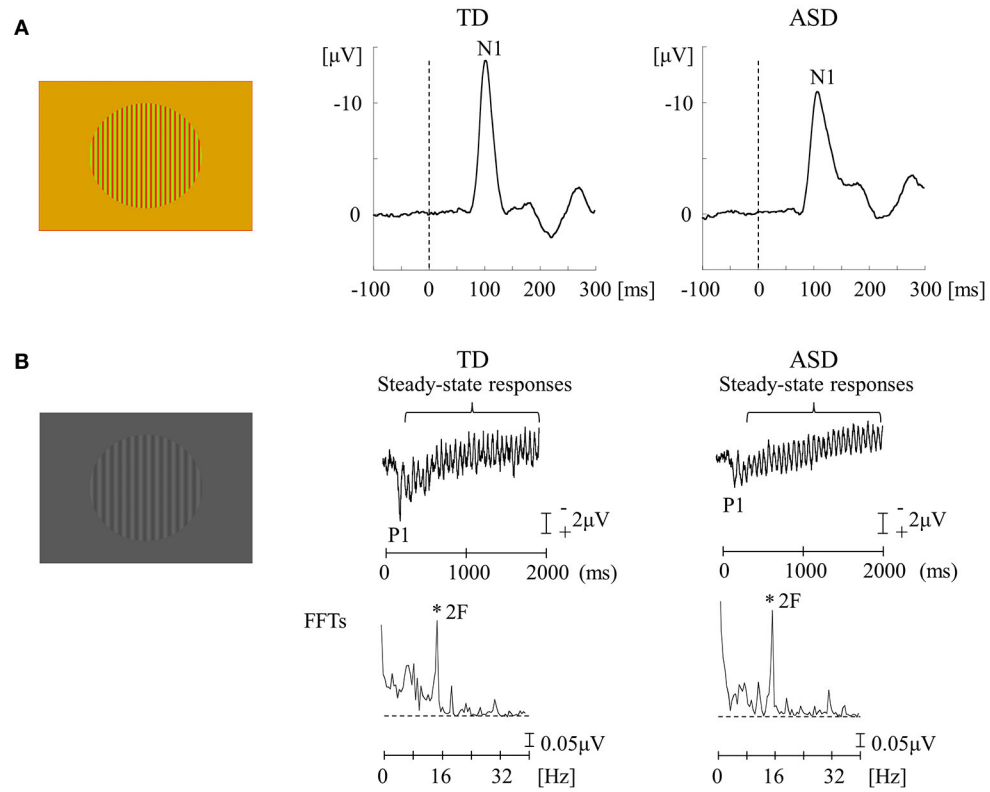

FIGURE 3 | VEPs in response to RG and BW stimuli in the TD and ASD groups. **(A)** For RG stimuli (isochromatic, SF: 2.0 cpd), the mean N1 latency in the ASD group was significantly longer than that in the TD group. **(B)** For BW stimuli [low-contrast (16.6%), SF: 1.0 cpd, 8 Hz (16 reversals/s)], there was no obvious difference in the distribution of P1 and steady-state responses between the two groups. VEPs, visual evoked potentials; RG, red/green; BW, black/white; TD, typically developing; ASD, autism spectrum disorder; cpd, cycles per degree; SF, spatial frequency; FFTs, fast Fourier transforms; 2F, second harmonic (Modified from Fujita et al., 2011 with permission).

our earlier VEP study (Fujita et al., 2011; section Parvocellular and Magnocellular Functions at V1 in ASD). In BW VEPs, a significantly shorter N1 latency was found in adults with ASD adults than in TD adults (**Figure 4A**), suggesting enhanced P-interblob pathway function in V1 in ASD (Yamasaki et al., 2017). As the BW stimulus used in our study (Yamasaki et al., 2017) comprised high SF information (5.3 cpd), a shorter N1 latency was thought to reflect superior fine-form (high SF) processing at V1 in ASD. These findings further support our prediction of P-blob (color) dysfunction with P-interblob (form)-biased function in ASD (section Parvocellular and Magnocellular Functions at V1 in ASD).

For face VEPs, ASD adults showed a significantly faster P1 latency (V1 origin) than TD adults (**Figure 4B**), which suggested enhanced V1 function (Yamasaki et al., 2017). Neuropsychological studies have reported that ASD individuals may be more biased in favor of high SF than low SF in face recognition (Deruelle et al., 2004, 2008). Moreover, a previous VEP study demonstrated that the emotional effect on P1 was significant for high SF, but not low SF, in an ASD group (Vlamings et al., 2010). As the face stimuli used in our study (Yamasaki et al., 2017) were composed of broadband SF, superior V1 function could reflect better fine-form perception related to the local high SF processing of faces in V1 in ASD adults. This finding is concordant with the results of study using BW VEPs (**Figure 4A**; Yamasaki et al., 2017).

Adults with ASD were also found to exhibit prolonged N170 latency in response to face stimuli (**Figure 4B**). In addition, a greater difference in latency between P1 and N170 and between N1 for BW and N170 (i.e., prolonged cortico-cortical conduction time between V1 and V4) was found in ASD adults. Therefore, we concluded that individuals with ASD exhibit impaired global face processing owing to deficits in integrating multiple local high SF facial information processing at V4 (Yamasaki et al., 2017).

Overall, adults with ASD exhibit enhanced P-interblob (form; local high SF) processing but impaired P-blob (color) processing in V1. Moreover, they show poor gestalt face processing due to insufficiencies in incorporating multiple sources of local high SF facial information at V4 (Yamasaki et al., 2017).

Dorsal Stream Function in ASD

Coherent motion stimuli using random dots are useful in the investigation of higher-level dorsal function (Yamasaki and Tobimatsu, 2012; Yamasaki et al., 2014). Radial optic flow (OF) and horizontal motion (HO) are the most commonly used in exploring global motion (**Figure 5**). The occipito-temporal N170

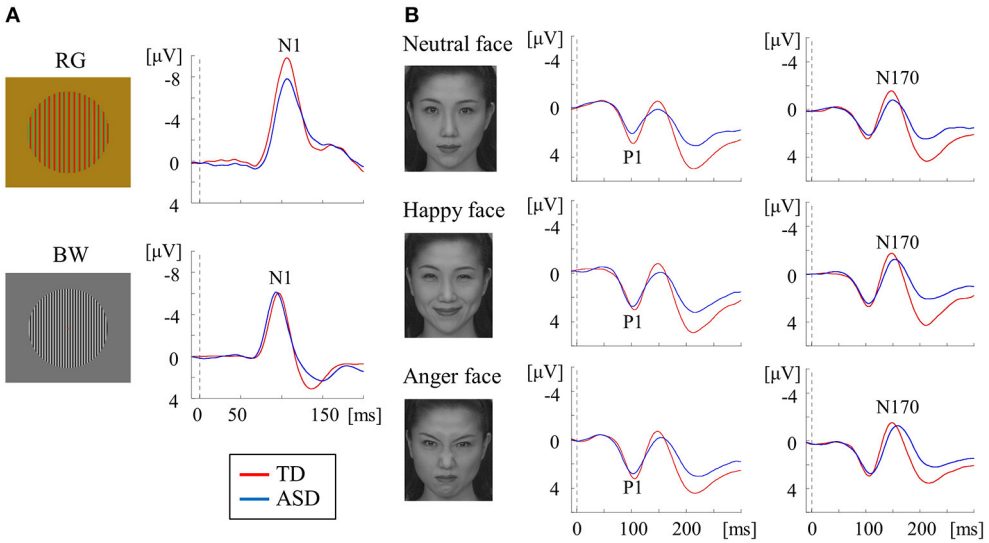

FIGURE 4 | VEPs in response to RG, BW, and face stimuli in the TD and ASD groups. **(A)** For RG stimuli (isochromatic, SF: 2.0 cpd), compared with the TD group, the mean N1 latency was significantly prolonged in the ASD group. In contrast, for BW stimuli [high-contrast (98.8%), SF: 5.3 cpd], the mean N1 latency was significantly shorter in the ASD group than in the TD group. **(B)** For face stimuli (neutral, happy, and angry faces), the mean P1 latency in the ASD group was significantly shorter than that in the TD group, regardless of facial expression, while the mean N170 latency was significantly longer in the ASD group than in the TD group (Modified from (Yamasaki et al., 2017) with no permission was required to reproduce).

(V5/MT origin) and parietal P200 (parietal lobe origin) are evoked by these stimuli in VEPs. We found that OF is largely handled by the v-d stream including IPL, whereas HO is mainly processed in the d-d stream including SPL in healthy subjects using functional magnetic resonance imaging (fMRI; Yamasaki et al., 2011a, 2012a,b).

A comparison of coherent OF and HO perception in adults with ASD and TD (Yamasaki et al., 2011b, 2014) showed comparable VEP responses and scalp maps between the two groups. Conversely, ASD exhibited the significant delayed latencies of N170 and P200 components in response to OF, but not HO, stimuli (**Figure 5**). These findings indicated the selective impairment of OF perception, which was associated with higher-level dorsal (the v-d pathway) function in ASD adults despite the fact that psychophysical thresholds were preserved (Yamasaki et al., 2014). OF is a type of complex motion characterized by multidirectional movement with depth, which is crucial for the navigation of self-movement (Gibson, 1950). OF information is also basis of action-related information including biological motion and facial expressions. Thus, OF processing is related to the dorsal stream (the v-d stream) function that is necessary to perceive the outer world, including other individuals. Consequently, the specific dysfunction of this pathway could underlie the social impairment observed in ASD. Furthermore, children with ASD demonstrated postural hyporeactivity to visually perceived environmental motion (visuo-postural tuning) compared with children with TD (Gepner and Mestre, 2002), which partially supports the notion that OF perception is specifically reduced in ASD individuals (Yamasaki et al., 2011b, 2014).

Subliminal Face Processing at V1 in ASD

Conscious perception of (supra-threshold) face evokes the occipital N1 (about 100 ms), P1 (about 120 ms), and the occipito-temporal N170 (about 170 ms). N1 and P1 components are originated in V1 while N170 generated from V4 (Bötzel et al., 1995; George et al., 1996; Fujita et al., 2013). If a supra-threshold face is presented upside down (the so-called "face inversion effect"), N170 reveals augmented amplitude and prolonged latency (Jacques et al., 2007). This phenomenon reflects the disrupted integration of features into a gestalt whole or holistic face representation (Young et al., 1987). We have previously described that in healthy subjects, the amplitudes of occipital P1 for unrecognizable (subliminal) faces are significantly greater than those for objects in the upright position (Mitsudo et al., 2011). In contrast, a significant reduction was found in P1 amplitudes for inverted faces compared with those of upright faces. This effect is quite opposite to the face inversion effect for supra-threshold stimuli and is called the "subliminal face effect (SFE)" (Fujita et al., 2013). Therefore, it is likely that faces and objects are processed in a different way at the V1 level, even when subjects are unaware of stimuli before face-specific processing occurs within the fusiform gyrus (V4). Overall, alterations of N1 or P1 in response to subliminal upright and inverted faces can offer insight into the neural mechanism of automatic face processing in high-functioning individuals with ASD (Fujita et al., 2013).

We recorded VEPs in response to visual stimuli with upright and inverted faces (fearful and neutral) and objects that were presented subliminally to ASD and TD adults using a backward-masking paradigm (Fujita et al., 2013; **Figure 6**). The TD adults exhibited a fearful-specific SFE in the upright condition.

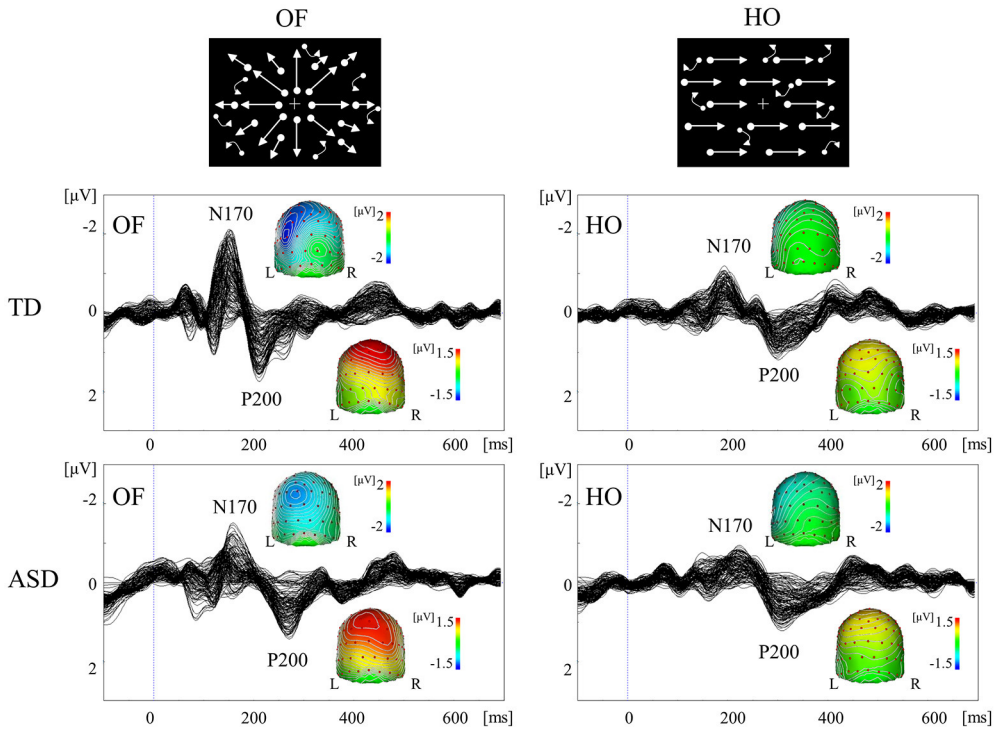

FIGURE 5 | VEPs in response to coherent OF and HO motion in the TD and ASD groups. The ASD group displayed significantly prolonged N170 and P200 latencies in response to OF, but not HO, stimuli, compared with the TD group. OF, optic flow; HO, horizontal motion (Modified from Yamasaki et al., 2011b with permission).

Conversely, adults with ASD displayed a lack of SFE, as shown by the unchanged N1 for stimuli of different types and orientations (**Figure 6**). The TD adults did not show upright SFE for neutral faces, which implies that at least emotional face information is altered in ASD adults. Therefore, ASD appear to exhibit different automatic visual processing for emotional faces in V1 level (Fujita et al., 2013). In TD adults, a fearful face-specific SFE can be based on the effect of low SF information on faces (Mitsudo et al., 2011), which is processed by the M pathway (Tobimatsu and Celesia, 2006). However, in our previous VEP study (section Parvocellular and Magnocellular Functions at V1 in ASD), the lower-level M pathway function was maintained in ASD adults during the perception of high-temporal frequency BW stimuli (Fujita et al., 2011). Thus, a lack of fearful face-specific SFE in ASD may reflect the impairment of the M pathway from layers 4Cα and 4B to the P-blob region within V1, but not from layer 4Cα to the thick stripes of V2 and V5/MT.

VISUAL ATTENTION IN ASD

Concept of Attention Networks

Selective attention is the cognitive process of focusing on a particular aspect of information. There exists two major mechanisms: bottom-up attention and top-down attention. Bottom-up attention is automatically produced or driven by the properties of stimuli. In contrast, top-down attention denotes the volitional attention, which focuses on a location and/or an object on the basis of current behavioral goals (Ciaramelli et al., 2008). These attention mechanisms can drive in parallel, although bottom-up attention arises more quickly than top-down attention (Treisman et al., 1992; Maekawa et al., 2011).

The following two attention networks have been described in the human brain: ventral attention network (VAN) and dorsal attention network (DAN) (Corbetta et al., 2008; Vuilleumier, 2013; Farrant and Uddin, 2016; **Figure 2B**). The VAN contains key nodes in the temporoparietal junction and ventral frontal cortices, which are related to bottom-up attention. In contrast, the DAN consists of key nodes in the bilateral intraparietal sulcus, SPL, and frontal eye fields, which are associated with top-down attention (Farrant and Uddin, 2016). The cortical projections of three branches of SLF overlap with VAN and DAN nodes (**Figure 2A**). The SLF I connects brain regions within the DAN. The SLF II connects the VAN's parietal regions of the VAN with the DAN's prefrontal regions, allowing these two networks to communicate. The SLF III connects regions within the VAN. The SLF III is larger on the right than the left, while the SLF I is symmetrical; the SLF II tends to be larger in the right hemisphere (Lunven and Bartolomeo, 2017).

ERP Study: Bottom-Up and Top-Down Attention in ASD

The ERP helps capture neural activity related to both sensory and cognitive process. Two specific ERP components, the visual mismatch negativity (MMN) and visual P300 (or P3), are

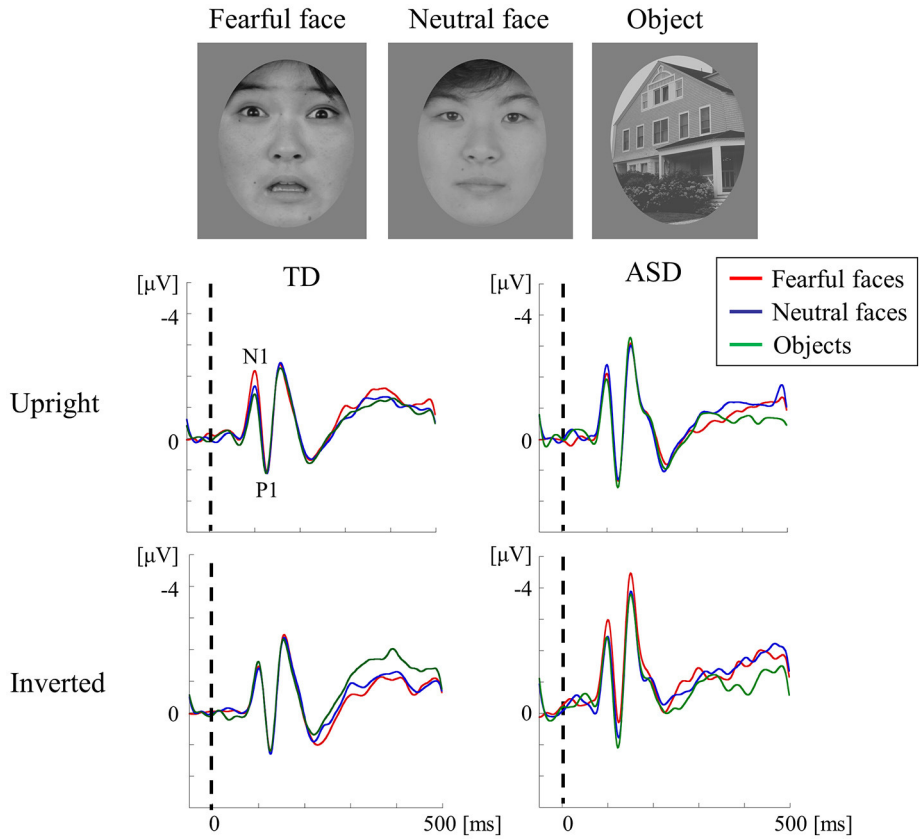

FIGURE 6 | VEPs in response to subliminal face stimuli using a backward-masking paradigm in the TD and ASD groups. Faces (neutral and fearful faces) and objects were randomly presented for 20 ms (sub-threshold duration) in an upright or inverted orientation, followed by a 1,000-ms pattern mask. The target appeared in 10% of the trials in each block and was presented for 600 ms to draw the participant's attention away from the experimental stimuli. In both groups, the stimuli (in both orientations) elicited a negative component at ∼100 ms (N1) and a following positive peak at ∼120 ms (P1) after stimulus onset. The TD group exhibited a fearful-specific SFE in the upright condition. In contrast, adults with ASD exhibited no signs of SFE, as reflected by the unaltered N1 for stimuli of different types and orientations. SFE, subliminal face effect (Modified from Fujita et al., 2013 with permission).

candidate biomarkers for bottom-up and top-down attention, respectively (Maekawa et al., 2011; Yamasaki et al., 2014). The visual MMN component reflects the pre-attentive, automatic processing of visual stimuli. It is obtained by subtracting waveforms elicited by frequently occurring, standard stimuli from infrequently occurring, deviant stimuli presented in an oddball paradigm. The visual MMN is defined as negativity measured at occipital electrodes between 150 and 350 ms after the onset of a deviant visual stimulus. The neural origin of the visual MMN has been considered to originate from the prestriate and prefrontal areas (Maekawa et al., 2012). The P300 response reflects higher-level attention and memory-related processing. It arises ∼300 ms after presenting a stimulus and is elicited when discriminating deviant and standard stimuli. The P300 response has two subcomponents that are related to either passive or active attention. The P3a component reflects the involuntary attention switching to stimuli. In contrast, the P3b component underlies the active response (active attention) to stimuli (Samson et al., 2006; Yamasaki et al., 2014).

We performed ERPs to examine the function of bottom-up (VAN) and top-down (DAN) visual attention systems in ASD and TD adults (Maekawa et al., 2011; Yamasaki et al., 2014). The oddball paradigm using windmill pattern stimuli (**Figure 7**) was applied to ERPs, which produced MMN (bottom-up attention), P300 (top-down attention), and P1 (lower level processing) components. Interestingly, ASD adults detected the target much faster than TD controls. Nevertheless, there was no significant difference in the MMN response between the two groups (**Figure 7C**). On the contrary, the reduction of the P1 and P300 amplitudes with the prolonged P300 latency were observed in ASD adults compared to TD adults (**Figures 7A,B**). Hence we concluded that intact bottom-up attention (MMN), which was related to the VAN, may contribute to the greater performance of simple task in ASD individuals though lower-level processing (P1) and top-down attention (P300) were impaired (Maekawa et al., 2011, 2012; Yamasaki et al., 2014).

DTI STUDIES IN ASD

DTI provides a measure of structural connectivity by measuring the diffusion of water molecules in the brain to reconstruct white matter tracts (Hernandez et al., 2015). The DTI indices

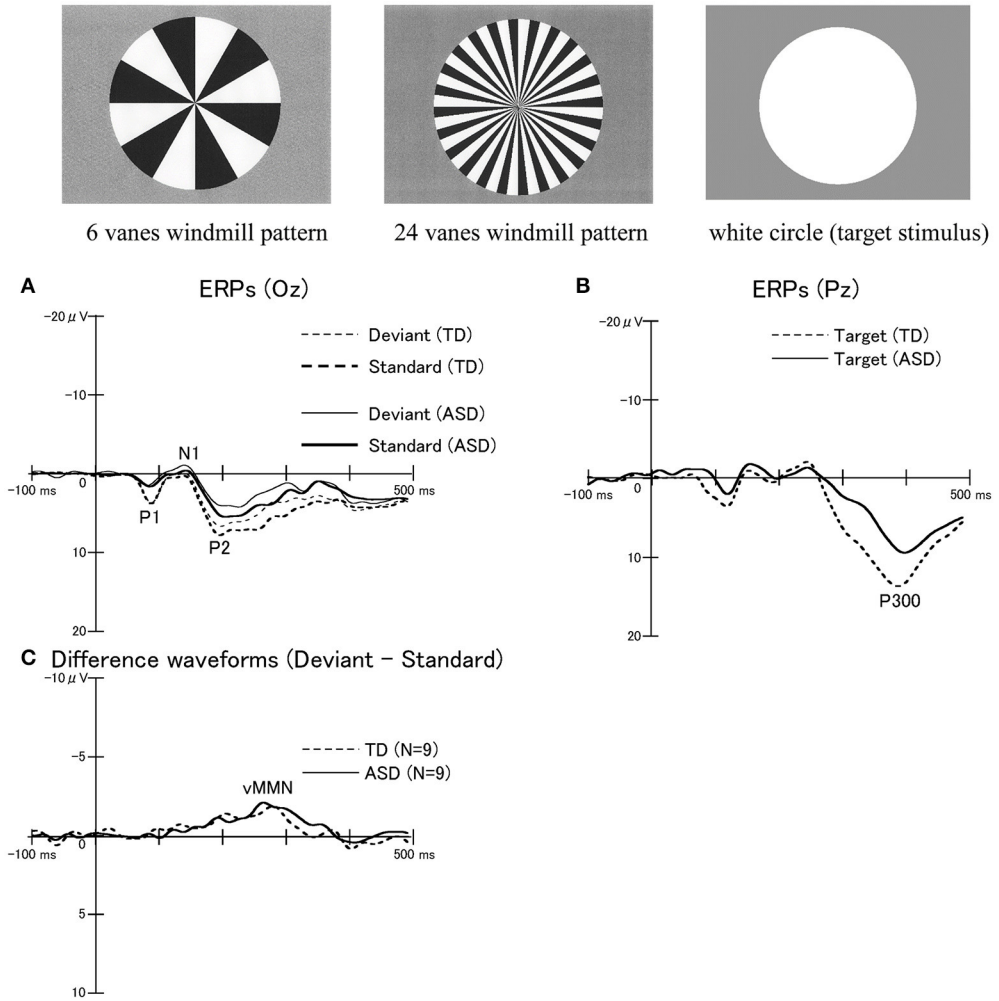

FIGURE 7 | ERPs in response to windmill pattern stimuli using an oddball paradigm in the TD and ASD groups. Three stimulus types were used to evoke ERPs using an oddball paradigm: circular black-white windmill pattern stimuli with 6 vanes and with 24 vanes and an unpatterned white circle stimulus. The two windmill pattern stimuli were adopted as standard or deviant stimuli (their probabilities changed between sessions). A white circle was always used as the target stimulus. Probabilities of standard, deviant, and target stimuli are 8:1:1, respectively. **(A)** Waveforms for standard stimuli (TD, thick dotted line; ASD, thick solid line) and for deviant stimuli (TD, thin dot line; ASD, thin solid line) at Oz. **(B)** Waveforms for target stimuli at Pz (TD, dotted line; ASD, solid line). While there were no significant differences in P300 latencies between the two groups, the P300 amplitudes in the ASD group were significantly smaller than those in the TD group. **(C)** Differences in waveforms from responses to standard stimuli relative to responses to deviant stimuli at Oz (TD, dotted line; ASD, solid line). There were no statistically significant differences in the mean peak latency and amplitude of visual MMN between the two groups. MMN, mismatch negativity (Modified from Yamasaki et al., 2014 with permission).

that are commonly reported include the following: (1) fractional anisotropy (FA) quantifies the degree of the directionality of water diffusion, ranging 0 (random) to 1 (unidirectional); (2) mean diffusivity (MD) represents average amount of water diffusion within a given voxel; and (3) axial (parallel), and (4) radial (perpendicular) diffusivity are indices of water molecule movement running parallel and perpendicular to the principle axis of diffusion, respectively (Ameis and Catani, 2015). These DTI indices provide us information about the integrity and architectural organization of the underlying white matter microstructure (Ameis and Catani, 2015). Lower FA and higher MD values usually imply damaged or impaired fiber integrity, which is attributable to increased diffusion and loss of coherence in the preferred movement direction (Soares et al., 2013). Reduced axial diffusivity values suggest a decline in axonal integrity, and decreased radial diffusivity values may provide a non-invasive surrogate marker of demyelination. These values reflect subtle structural abnormalities that cannot be detected by FA (Papadakis et al., 1999; Noriuchi et al., 2010).

We conducted DTI analysis in high-functioning children with ASD and TD controls (Noriuchi et al., 2010). DTI revealed the significant reduction of FA and axial diffusivity values in the several regions of white matter in the ASD subjects compared to TD controls. These regions included the white matter around the left dorsolateral prefrontal cortex (DLPFC), temporoparietal junction, right temporal pole, amygdala, SLF,

and IFOF, which were related to the parallel visual pathways and attentional networks. In the left DLPFC, a negative correlation was found between the FA value in this area and the degree of social impairment in children with ASD. The cerebellar vermis lobules showed higher axial diffusivity values in the ASD group. These DTI findings and their relationship with social impairment provide additional evidence of functional abnormalities in cerebral and cerebellar white matter in ASD (Noriuchi et al., 2010).

Our DTI findings are in accordance with numerous DTI studies from other research groups in children, adolescents, and adults with ASD (Travers et al., 2012; Ameis and Catani, 2015; Hernandez et al., 2015; Rane et al., 2015; Ismail et al., 2016; Li et al., 2017). These studies have documented multiple structural connectivity differences, mostly suggesting reduced white matter integrity (lower FA and/or higher MD values) in long-range anterior-posterior and interhemispheric fiber tracts. Notably, many specific fiber tracts reported to be altered in ASD serve as structural connections among the brain areas related to social cognition (Hernandez et al., 2015). The most commonly reported areas for decreased FA values are association fibers (the most common being the SLF, IFOF, uncinate fasciculus, ILF, and cingulum) and the corpus callosum. The SLF, corpus callosum, and corticospinal tract are the most commonly mentioned structures in reports of increased MD in ASD (Rane et al., 2015).

Few studies have directly studied the relationship between DTI and visual perception in ASD. One DTI study examined white matter pathways involved in face processing in adolescents and adults with ASD and TD controls (Conturo et al., 2008). Radial diffusivity values were increased in amygdala-fusiform connections bilaterally and hippocampus-fusiform connections in the left side in individuals with ASD. In contrast, hippocampus-fusiform connections in the right side showed reduced radial diffusivity in ASD, which correlated with lower face recognition scores. These findings suggested an early functionally significant pathological process in the right hippocampus-fusiform pathway in accordance with small-diameter axons (with corresponding slower neural transmission) and/or higher packing density (Conturo et al., 2008). Another DTI study has demonstrated the significant alterations in the microstructural organization of white matter in the right IFOF, which is associated with an inferior visuospatial processing performance in ASD. The authors concluded that structural brain abnormalities may influence atypical visuospatial processing in ASD (McGrath et al., 2013a,b). Accordingly, it is likely that white matter connectivity (in particular, SLF, IFOF, and ILF) that are associated with parallel visual pathways and visual attention networks are often disrupted in ASD.

ALTERED CONNECTOME FUNCTIONS IN ASD

In our series of VEP and ERP studies, we found that the following: (1) enhanced and impaired processing co-exists within the lower visual area (V1) (sections Parvocellular and Magnocellular Functions at V1 in ASD and Ventral Stream Function in ASD), (2) local information integration from lower visual areas (V1) is impaired in higher-level visual areas after V4 and V5/MT (sections Ventral Stream Function in ASD and Dorsal Stream Function in ASD), and (3) the DAN is impaired while the VAN is intact in ASD (section ERP Study: Bottom-Up and Top-Down Attention in ASD; **Figure 8**). These complex functional alterations in visual and attention networks support the possibility of altered connectivity within and between distributed brain regions, instead of local deficits in specific brain areas in ASD (Müller, 2008).

The most important finding in our VEP studies was the co-existence of enhanced P-interblob and impaired P-blob pathway processing with an intact M pathway in V1 in individuals with ASD. Many behavioral studies have reported a preference for local processing in ASD (Dakin and Frith, 2005). An fMRI study demonstrated atypical increment of local functional connectivity in ASD in posterior brain areas including V1 (Keown et al., 2013). Thus, our VEP finding of an enhanced P-interblob pathway in ASD partly supports these previous behavioral and neuroimaging findings. Conversely, to date,

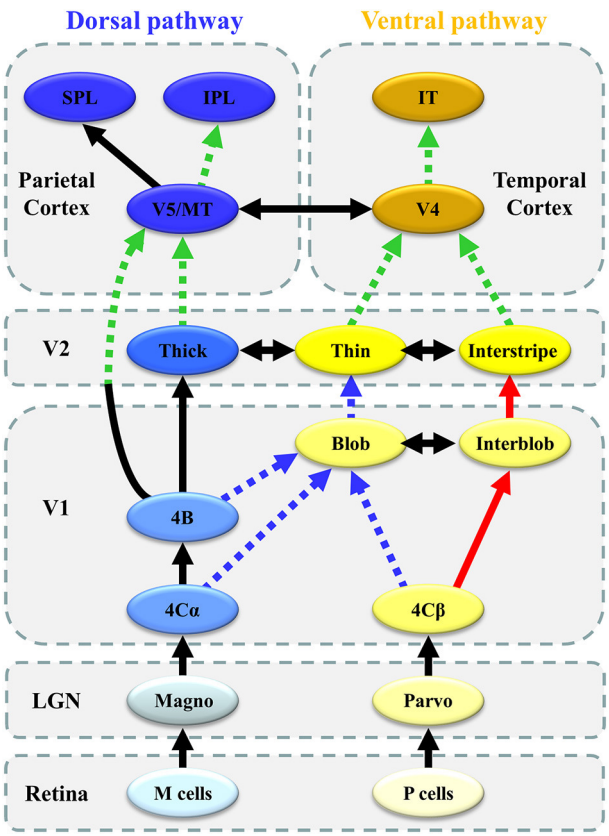

FIGURE 8 | Schematic representation of altered connectivity of visual networks in ASD. Red thick solid arrows indicate enhanced processing (or overconnectivity), whereas blue broken arrows suggest impaired processing (or underconnectivity) in the local circuitry within V1. Green broken arrows indicate impaired global integration of local information (or long-range underconnectivity) between lower-and higher-level visual areas.

no electrophysiological or neuroimaging studies have reported impaired P-blob function in V1 in ASD. Recent data have suggested that the alteration of connectivity within V1 is more complex than earlier suggestions of enhanced simple (local) processing in V1, thereby providing new insight into the neural circuit mechanisms underlying ASD.

At present, mechanisms underlying altered V1 connectivity in ASD remain unclear. We speculate that blob impairment is a key component of this mechanism. In V1, the P-blob stream is characterized by a higher mitochondrial CO concentration, whereas the P-interblob stream has a lower concentration of CO. CO is well-known to be the last enzyme in the respiratory chain of mitochondria that is related to oxidative metabolism and energy production (Liu and Wong-Riley, 1995; Bókkon and Vimal, 2010, 2013) and is closely coupled to neuronal functional activity (Liu and Wong-Riley, 1995). It is interesting to note that recent neuroimaging and postmortem studies have reported mitochondrial dysfunction in the brains of ASD individuals (Rossignol and Frye, 2012, 2014). Thus, deficits in the P-blob pathway in ASD may reflect mitochondrial dysfunction in the blob region of V1 (Yamasaki et al., 2017). This impairment in turn induces the compensatory enhancement of P-interblob function in ASD because the P-blob pathway anatomically interacts with the P-interblob pathway (Yabuta and Callaway, 1998). Further studies are needed to confirm this hypothesis using neuroimaging techniques that can separately evaluate the blob and interblob regions.

In contrast, behavioral studies have proposed that neuro-integrative processing at higher cortical levels in the ventral and dorsal pathways is impaired, while lower-level processing is spared (Bertone et al., 2003, 2005; Bertone and Faubert, 2006). Numerous fMRI studies have demonstrated that individuals with ASD had long-range underconnectivity with local overconnectivity (Courchesne and Pierce, 2005; Anderson et al., 2011; Keown et al., 2013). Many DTI studies, including ours (section DTI Studies in ASD), detected white matter alterations of the ventral (ILF and IFOF) and dorsal (SLF) streams in ASD (Rane et al., 2015). Therefore, our VEP findings of altered connectivity in parallel visual pathways between V1 and V4 or between V1 and V5/MT are consistent with the alterations of anatomical and functional connectivity of the ventral and dorsal streams revealed by DTI and fMRI studies in ASD.

Interestingly, our VEP studies using coherent motion revealed dissociative impairment within the dorsal stream along the SLF; the v-d stream (OF processing) was impaired with preserved d-d stream (HO processing) function in ASD (section Dorsal Stream Function in ASD). Furthermore, in our ERP study, the DAN (top-down) related to SLF I was impaired with an intact VAN (bottom-up) related to SLF III in ASD (section ERP Study: Bottom-Up and Top-Down Attention in ASD). Thus, connectivity impairment may be anatomically uneven within the SLF. Alternatively, SLF connectivity impairment may be exhibited in situations requiring more complex processing (OF processing vs. HO processing; top-down vs. bottom-up).

As mentioned above, this review suggests that altered functional connectivity within visual and attention networks exists in ASD. However, it remains unknown (1) how the strength and direction of functional connectivity within these networks differ between ASD and TD, and (2) how the altered networks influence the social cognition network in ASD. In the field of network neuroscience, a mathematical modeling approach (graph-theoretical approach) is used for whole-brain functional connectivity analysis on the basis of resting-state fMRI and magnetoencephalography data (Uehara et al., 2014; Bassett and Sporns, 2017). This approach can reveal the strength and direction of whole-brain functional connectivity in detail. From our VEP and ERP data, the different visual stimuli may induce differential effects on whole-brain functional network in ASD. Therefore, further studies using network neuroscience methods on functional connectomes in the ASD brain under visual task-related condition will be needed to understand the neural mechanisms of atypical visual perception and social impairment in ASD.

CONCLUSION

Recent data have revealed that unusual visual perception observed in ASD may result from alterations to the local circuitry within the visual area and connectivity between distributed visual cortical areas as well as the connectivity of attention networks. Therefore, we conclude that the altered connectivity of visual processing networks may contribute to impaired social communication exhibited in ASD. The underlying pathophysiological mechanism of ASD can be considered a "connectopathy."

AUTHOR CONTRIBUTIONS

Conceived and designed the experiments: TY, TM, TF, and ST. Performed the experiments: TY, TM, and TF. Analyzed the data: TY, TM, and TF. Wrote the paper: TY, TM, TF, and ST.

FUNDING

This study was partly supported by JSPS KAKENHI Grant Numbers JP23601010 and JP26350931 to TY and by a KAKENHI Grant-in-Aid for Scientific Research on Innovative Areas (No. 15H05875) from the Ministry of Education, Culture, Sports, Science, and Technology to ST. This work was also supported in part by a grant from the Center of Developmental Education and Research (CODER) to TY.

ACKNOWLEDGMENTS

We wish to thank Drs. Yoko Kamio and Madoka Noriuchi (Department of Child and Adolescent Mental Health, National Institute of Mental Health, National Center of Neurology and Psychiatry) for their research assistance.

REFERENCES

Ameis, S. H., and Catani, M. (2015). Altered white matter connectivity as a neural substrate for social impairment in autism spectrum disorder. *Cortex* 62, 158–181. doi: 10.1016/j.cortex.2014.10.014

American Psychiatric Association (2013). *Diagnostic and Statistical Manual of Mental Disorders, 5th Edn*. Washington, DC: APA.

Amso, D., Haas, S., Tenenbaum, E., Markant, J., and Sheinkopf, S. J. (2014). Bottom-up attention orienting in young children with autism. *J. Autism Dev. Disord.* 44, 664–673. doi: 10.1007/s10803-013-1925-5

Anderson, J. S. (2014). "Cortical underconnectivity hypothesis in autism: evidence from functional connectivity MRI," in *Comprehensive Guide to Autism*, eds V. B. Patel, V. R. Preedy, and C. R. Martin (New York, NY: Springer Science+Business Media), 1457–1471.

Anderson, J. S., Druzgal, T. J., Froehlich, A., DuBray, M. B., Lange, N., Alexander, A. L., et al. (2011). Decreased interhemispheric functional connectivity in autism. *Cereb. Cortex* 21, 1134–1146. doi: 10.1093/cercor/bhq190

Bartolomeo, P., Thiebaut de Schotten, M., and Chica, A. B. (2012). Brain networks of visuospatial attention and their disruption in visual neglect. *Front. Hum. Neurosci.* 6:110. doi: 10.3389/fnhum.2012.00110

Basser, P. J., and Jones, D. K. (2002). Diffusion-tensor MRI: theory, experimental design and data analysis - a technical review. *NMR Biomed.* 15, 456–467. doi: 10.1002/nbm.783

Bassett, D. S., and Sporns, O. (2017). Network neuroscience. *Nat. Neurosci*. 20, 353–364. doi: 10.1038/nn.4502

Bentin, S., Allison, T., Puce, A., Perez, E., and McCarthy, G. (1996). Electrophysiological studies of face perception in humans. *J. Cogn. Neurosci.* 8, 551–565. doi: 10.1162/jocn.1996.8.6.551

Bertone, A., and Faubert, J. (2006). Demonstrations of decreased sensitivity to complex motion information not enough to propose an autism-specific neural etiology. *J. Autism Dev. Disord.* 36, 55–64. doi: 10.1007/s10803-005-0042-5

Bertone, A., Mottron, L., Jelenic, P., and Faubert, J. (2003). Motion perception in autism: a "complex" issue. *J. Cogn. Neurosci.* 15, 218–225. doi: 10.1162/089892903321208150

Bertone, A., Mottron, L., Jelenic, P., and Faubert, J. (2005). Enhanced and diminished visuo-spatial information processing in autism depends on stimulus complexity. *Brain* 128, 2430–2441. doi: 10.1093/brain/awh561

Bókkon, I., and Vimal, R. L. (2010). Implications on visual apperception: energy, duration, structure and synchronization. *Biosystems* 101, 1–9. doi: 10.1016/j.biosystems.2010.04.008

Bókkon, I., and Vimal, R. L. (2013). Theoretical implications on visual (color) representation and cytochrome oxidase blobs. *Act. Nerv. Super*. 55, 15–37. doi: 10.1007/BF03379594

Bötzel, K., Schulze, S., and Stodieck, S. R. (1995). Scalp topography and analysis of intracranial sources of face-evoked potentials. *Exp. Brain Res.* 104, 134–143. doi: 10.1007/BF00229863

Ciaramelli, E., Grady, C. L., and Moscovitch, M. (2008). Top-down and bottom-up attention to memory: a hypothesis (AtoM) on the role of the posterior parietal cortex in memory retrieval. *Neuropsychologia* 46, 1828–1851. doi: 10.1016/j.neuropsychologia.2008.03.022

Conturo, T. E., Williams, D. L., Smith, C. D., Gultepe, E., Akbudak, E., and Minshew, N. J. (2008). Neuronal fiber pathway abnormalities in autism: an initial MRI diffusion tensor tracking study of hippocampo-fusiform and amygdalo-fusiform pathways. *J. Int. Neuropsychol. Soc*. 14, 933–946. doi: 10.1017/S1355617708081381

Corbetta, M., Patel, G., and Shulman, G. L. (2008). The reorienting system of the human brain: from environment to theory of mind. *Neuron* 58, 306–324. doi: 10.1016/j.neuron.2008.04.017

Courchesne, E., and Pierce, K. (2005). Why the frontal cortex in autism might be talking only to itself: local over-connectivity but long-distance disconnection. *Curr. Opin. Neurobiol.* 15, 225–230. doi: 10.1016/j.conb.2005.03.001

Dakin, S., and Frith, U. (2005). Vagaries of visual perception in autism. *Neuron* 48, 497–507. doi: 10.1016/j.neuron.2005.10.018

Deffke, I., Sander, T., Heidenreich, J., Sommer, W., Curio, G., Trahms, L., et al. (2007). MEG/EEG sources of the 170-ms response to face are co-localized in the fusiform gyrus. *Neuroimage* 35, 1495–1501. doi: 10.1016/j.neuroimage.2007.01.034

Deruelle, C., Rondan, C., Gepner, B., and Tardif, C. (2004). Spatial frequency and face processing in children with autism and Asperger syndrome. *J. Autism Dev. Disord.* 34, 199–210. doi: 10.1023/B:JADD.0000022610.09668.4c

Deruelle, C., Rondan, C., Salle-Collemiche, X., Bastard-Rosset, D., and Da Fonséca, D. (2008). Attention to low- and high-spatial frequencies in categorizing facial identities, emotions and gender in children with autism. *Brain Cogn.* 66, 115–123. doi: 10.1016/j.bandc.2007.06.001

Doricchi, F., Thiebaut de Schotten, M., Tomaiuolo, F., and Bartolomeo, P. (2008). White matter (dis)connections and gray matter (dys)functions in visual neglect: gaining insights into the brain networks of spatial awareness. *Cortex* 44, 983–995. doi: 10.1016/j.cortex.2008.03.006

Farrant, K., and Uddin, L. Q. (2016). Atypical developmental of dorsal and ventral attention networks in autism. *Dev. Sci.* 19, 550–563. doi: 10.1111/desc.12359

ffytche, D. H., Blom, J. D., and Catani, M. (2010). Disorders of visual perception. *J. Neurol. Neurosurg. Psychiatry* 81, 1280–1287. doi: 10.1136/jnnp.2008.171348

Franklin, A., Sowden, P., Burley, R., Notman, L., and Alder, E. (2008). Color perception in children with autism. *J. Autism Dev. Disord*. 38, 1837–1847. doi: 10.1007/s10803-008-0574-6

Franklin, A., Sowden, P., Notman, L., Gonzalez-Dixon, M., West, D., and Alexander, I. (2010). Reduced chromatic discrimination in children with autism spectrum disorders. *Dev. Sci.* 13, 188–200. doi: 10.1111/j.1467-7687.2009.00869.x

Fujita, T., Kamio, Y., Yamasaki, T., Yasumoto, S., Hirose, S., and Tobimatsu, S. (2013). Altered automatic face processing in individuals with high-functioning autism spectrum disorders: evidence from visual evoked potentials. *Res. Autism Spectr. Disord*. 7, 710–720. doi: 10.1016/j.rasd.2013.03.001

Fujita, T., Yamasaki, T., Kamio, Y., Hirose, S., and Tobimatsu, S. (2011). Parvocellular pathway impairment in autism spectrum disorder: evidence from visual evoked potentials. *Res. Autism Spectr. Disord.* 5, 277–285. doi: 10.1016/j.rasd.2010.04.009

George, N., Evans, J., Fiori, N., Davidoff, J., and Renault, B. (1996). Brain events related to normal and moderately scrambled faces. *Cogn. Brain Res*. 4, 65–76. doi: 10.1016/0926-6410(95)00045-3

Gepner, B., and Mestre, D. R. (2002). Brief report: postural reactivity to fast visual motion differentiates autistic from children with Asperger syndrome. *J. Autism Dev. Disord*. 32, 231–238. doi: 10.1023/A:1015410015859

Geschwind, D. H., and Levitt, P. (2007). Autism spectrum disorders: developmental disconnection syndromes. *Curr. Opin. Neurobiol.* 17, 103–111. doi: 10.1016/j.conb.2007.01.009

Gibson, J. J. (1950). *The Perception of the Visual World*. Boston, MA: Houghton Mifflin.

Golarai, G., Grill-Spector, K., and Reiss, A. L. (2006). Autism and the development of face processing. *Clin. Neurosci. Res*. 6, 145–160. doi: 10.1016/j.cnr.2006.08.001

Goto, Y., Kinoe, H., Nakashima, T., and Tobimatsu, S. (2005). Familiarity facilitates the corticocortical processing of face perception. *Neuroreport* 16, 1329–1334. doi: 10.1097/01.wnr.0000174404.86644.af

Happé, F., and Frith, U. (2006). The weak coherence account: detail-focused cognitive style in autism spectrum disorders. *J. Autism Dev. Disord*. 36, 5–25. doi: 10.1007/s10803-005-0039-0

Hernandez, L. M., Rudie, J. D., Green, S. A., Bookheimer, S., and Dapretto, M. (2015). Neural signatures of autism spectrum disorders: insights into brain network dynamics. *Neuropsychopharmacology* 40, 171–189. doi: 10.1038/npp.2014.172

Ismail, M. M., Keynton, R. S., Mostapha, M. M., El Tanboly, A. H., Casanova, M. F., Gimel'farb, G. L., et al. (2016). Studying autism spectrum disorder with structural and diffusion magnetic resonance imaging: a survey. *Front. Hum. Neurosci.* 10:211. doi: 10.3389/fnhum.2016.00211

Jacques, C., d'Arripe, O., and Rossion, B. (2007). The time course of the inversion effect during individual face discrimination. *J. Vis.* 7:3. doi: 10.1167/7.8.3

Jang, S. H. (2013). Diffusion tensor imaging studies on arcuate fasciculus in stroke patients: a review. *Front. Hum. Neurosci.* 7:749. doi: 10.3389/fnhum.2013.00749

Jolliffe, T., and Baron-Cohen, S. (1997). Are people with autism and Asperger syndrome faster than normal on the embedded figures test? *J. Child Psychol. Psychiatry* 38, 527–534. doi: 10.1111/j.1469-7610.1997.tb01539.x

Keown, C. L., Shih, P., Nair, A., Peterson, N., Mulvey, M. E., and Müller, R. A. (2013). Local functional overconnectivity in posterior brain regions is

associated with symptom severity in autism spectrum disorders. *Cell Rep.* 5, 567–572. doi: 10.1016/j.celrep.2013.10.003

Kravitz, D. J., Saleem, K. S., Baker, C. I., and Mishkin, M. (2011). A new neural framework for visuospatial processing. *Nat. Rev. Neurosci.* 12, 217–230. doi: 10.1038/nrn3008

Kravitz, D. J., Saleem, K. S., Baker, C. I., Ungerleider, L. G., and Mishkin, M. (2013). The ventral visual pathway: an expanded neural framework for the processing of object quality. *Trends Cogn. Sci.* 17, 26–49. doi: 10.1016/j.tics.2012.10.011

Li, D., Karnath, H. O., and Xu, X. (2017). Candidate biomarkers in children with autism spectrum disorder: a review of MRI studies. *Neurosci. Bull.* 33, 219–237. doi: 10.1007/s12264-017-0118-1

Liu, S., and Wong-Riley, M. (1995). Disproportionate regulation of nuclear- and mitochondrial-encoded cytochrome oxidase subunit proteins by functional activity in neurons. *Neuroscience* 67, 197–210. doi: 10.1016/0306-4522(95)00043-I

Livingstone, M., and Hubel, D. (1988). Segregation of form, color, movement, and depth: anatomy, physiology, and perception. *Science* 240, 740–749. doi: 10.1126/science.3283936

Lunven, M., and Bartolomeo, P. (2017). Attention and spatial cognition: neural and anatomical substrates of visual neglect. *Ann. Phys. Rehabil. Med.* 60, 124–129. doi: 10.1016/j.rehab.2016.01.004

Maekawa, T., Hirano, S., and Onitsuka, T. (2012). Auditory and visual mismatch negativity in psychiatric disorders: a review. *Curr. Psychiatry Rev.* 8, 97–105. doi: 10.2174/1573400511208020097

Maekawa, T., Tobimatsu, S., Inada, N., Oribe, N., Onitsuka, T., Kanba, S., et al. (2011). Top-down and bottom-up visual information processing of non-social stimuli in high-functioning autism spectrum disorder. *Res. Autism Spectr. Disord.* 5, 201–209. doi: 10.1016/j.rasd.2010.03.012

McGrath, J., Johnson, K., O'Hanlon, E., Garavan, H., Gallagher, L., and Leemans, A. (2013a). White matter and visuospatial processing in autism: a constrained spherical deconvolution tractography study. *Autism Res.* 6, 307–319. doi: 10.1002/aur.1290

McGrath, J., Johnson, K., O'Hanlon, E., Garavan, H., Leemans, A., and Gallagher, L. (2013b). Abnormal functional connectivity during visuospatial processing is associated with disrupted organization of white matte in autism. *Front. Hum. Neuroscei.* 7:434. doi: 10.3389/fnhum.2013.00434

Milne, E., Swettenham, J., Hansen, P., Campbell, R., Jeffries, H., and Plaisted, K. (2002). High motion coherence thresholds in children with autism. *J. Child Psychol. Psychiatry* 43, 255–263. doi: 10.1111/1469-7610.00018

Mitsudo, T., Kamio, Y., Goto, Y., Nakashima, T., and Tobimatsu, S. (2011). Neural responses in the occipital cortex to unrecognizable faces. *Clin. Neurophysiol.* 122, 708–718. doi: 10.1016/j.clinph.2010.10.004

Müller, R. A. (2008). From loci to networks and back again: anomalies in the study of autism. *Ann. N.Y. Acad. Sci.* 1145, 300–315. doi: 10.1196/annals.1416.014

Nakashima, T., Kaneko, K., Goto, Y., Abe, T., Mitsudo, T., Ogata, K., et al. (2008). Early ERP components differentially extract facial features: evidence for spatial frequency-and-contrast detectors. *Neurosci. Res.* 62, 225–235. doi: 10.1016/j.neures.2008.08.009

Nealey, T. A., and Maunsell, J. H. (1994). Magnocellular and parvocellular contributions to the responses of neurons in macaque striate cortex. *J. Neurosci.* 14, 2069–2079.

Noriuchi, M., Kikuchi, Y., Yoshiura, T., Kira, R., Shigeto, H., Hara, T., et al. (2010). Altered white matter fractional anisotropy and social impairment in children with autism spectrum disorder. *Brain Res.* 1362, 141–149. doi: 10.1016/j.brainres.2010.09.051

O'Connor, K. (2012). Auditory processing in autism spectrum disorder: a review. *Neurosci. Biobehav. Rev.* 36, 836–854. doi: 10.1016/j.neubiorev.2011.11.008

Papadakis, N. G., Xing, D., Houston, G. C., Smith, J. M., Smith, M. I., James, M. F., et al. (1999). A study of rotationally invariant and symmetric indices of diffusion anisotropy. *Magn. Reson. Imaging* 17, 881–892. doi: 10.1016/S0730-725X(99)00029-6

Pellicano, E., Gibson, L., Maybery, M., Durkin, K., and Badcock, D. R. (2005). Abnormal global processing along the dorsal visual pathway in autism: a possible mechanism for weak visuospatial coherence? *Neuropsychologia* 43, 1044–1053. doi: 10.1016/j.neuropsychologia.2004.10.003

Pruett, J. R. Jr., LaMacchia, A., Hoertel, S., Squire, E., McVey, K., Todd, R. D., et al. (2011). Social and non-social cueing of visuospatial attention in autism and typical development. *J. Autism Dev. Disord.* 41, 715–731. doi: 10.1007/s10803-010-1090-z

Rane, P., Cochran, D., Hodge, S. M., Haselgrove, C., Kennedy, D. N., and Frazier, J. A. (2015). Connectivity in autism: a review of MRI connectivity studies. *Harv. Rev. Psychiatry* 23, 223–244. doi: 10.1097/HRP.0000000000000072

Rossignol, D. A., and Frye, R. E. (2012). Mitochondrial dysfunction in autism spectrum disorders: a systematic review and meta-analysis. *Mol. Psychiatry* 17, 290–314. doi: 10.1038/mp.2010.136

Rossignol, D. A., and Frye, R. E. (2014). Evidence linking oxidative stress, mitochondrial dysfunction, and inflammation in the brain of individuals with autism. *Front. Physiol.* 5:150. doi: 10.3389/fphys.2014.00150

Rossion, B., and Jacques, C. (2008). Does physical interstimulus variance account for early electrophysiological face sensitive responses in the human brain? Ten lessons on the N170. *Neuroimage* 39, 1959–1979. doi: 10.1016/j.neuroimage.2007.10.011

Samson, F., Mottron, L., Jemel, B., Belin, P., and Ciocca, V. (2006). Can spectro-temporal complexity explain the autistic pattern of performance on auditory task? *J. Autism Dev. Disord.* 36, 65–76. doi: 10.1007/s10803-005-0043-4

Simmons, D. R., Robertson, A. E., McKay, L. S., Toal, E., McAleer, P., and Pollick, F. E. (2009). Vision in autism spectrum disorders. *Vis. Res.* 49, 2705–2739. doi: 10.1016/j.visres.2009.08.005

Soares, J. M., Marques, P., Alves, V., and Sousa, N. (2013). A hitchhiker's guide to diffusion tensor imaging. *Front. Neurosci.* 7:31. doi: 10.3389/fnins.2013.00031

Spencer, J., O'Brien, J., Riggs, K., Braddick, O., Atkinson, J., and Wattam-Bell, J. (2000). Motion processing in autism: evidence for a dorsal stream deficiency. *Neuroreport* 11, 2765–2767. doi: 10.1097/00001756-200008210-00031

Tobimatsu, S., and Celesia, G. G. (2006). Studies of human visual pathophysiology with visual evoked potentials. *Clin. Neurophysiol.* 117, 1414–1433. doi: 10.1016/j.clinph.2006.01.004

Tobimatsu, S., Tomoda, H., and Kato, M. (1996). Human VEPs to isoluminant chromatic and achromatic sinusoidal gratings: separation of parvocellular components. *Brain Topogr.* 8, 241–243. doi: 10.1007/BF01184777

Travers, B. G., Adluru, N., Ennis, C., Tromp do, D. M., Destiche, D., Doran, S., et al. (2012). Diffusion tensor imaging in autism spectrum disorder: a review. *Autism Res.* 5, 289–313. doi: 10.1002/aur.1243

Treisman, A., Vieira, A., and Hayes, A. (1992). Automaticity and preattentive processing. *Am. J. Psychol.* 105, 341–362. doi: 10.2307/1423032

Uehara, T., Yamasaki, T., Okamoto, T., Koike, T., Kan, S., Miyauchi, S., et al. (2014). Efficiency of a "small-world" brain network depends on consciousness level: a resting-state fMRI study. *Cereb. Cortex* 24, 1529–1539. doi: 10.1093/cercor/bht004

Umarova, R. M., Saur, D., Schnell, S., Kaller, C. P., Vry, M. S., Glauche, V., et al. (2010). Structural connectivity for visuospatial attention: significance of ventral pathways. *Cereb. Cortex* 20, 121–129. doi: 10.1093/cercor/bhp086

Vlamings, P. H., Jonkman, L. M., van Daalen, E., van der Gaag, R. J., and Kemner, C. (2010). Basic abnormalities in visual processing affect face processing at an early age in autism spectrum disorder. *Biol. Psychiatry* 68, 1107–1113. doi: 10.1016/j.biopsych.2010.06.024

Vuilleumier, P. (2013). Mapping the functional neuroanatomy of spatial neglect and human parietal lobe functions: progress and challenges. *Ann. N. Y. Acad. Sci.* 1296, 50–74. doi: 10.1111/nyas.12161

Yabuta, N. H., and Callaway, E. M. (1998). Functional streams and local connections of layer 4C neurons in primary visual cortex of the macaque monkey. *J. Neurosci.* 18, 9489–9499.

Yamasaki, T., Fujita, T., Kamio, Y., and Tobimatsu, S. (2011a). "Motion perception in autism spectrum disorder," in *Advances in Psychology Research*, *Vol. 82,* ed A. M. Columbus (New York, NY: Nova Science Publishers), 197–211.

Yamasaki, T., Fujita, T., Kamio, Y., and Tobimatsu, S. (2013). Electrophysiological assessment of visual function in autism spectrum disorders. *Neurosci. Biomed. Eng.* 1, 5–12. doi: 10.2174/2213385211301010003

Yamasaki, T., Fujita, T., Ogata, K., Goto, Y., Munetsuna, S., Kamio, Y., et al. (2011b). Electrophysiological evidence for selective impairment of optic flow perception in autism spectrum disorder. *Res. Autism Spectr. Disord.* 5, 400–407. doi: 10.1016/j.rasd.2010.06.002

Yamasaki, T., Goto, Y., Ohyagi, Y., Monji, A., Munetsuna, S., Minohara, M., et al. (2012a). "A deficit of dorsal stream function in patients with mild cognitive impairment and Alzheimer's disease," in *2012 IEEE/ICME International Conference on Complex Medical Engineering* (Kobe), 28–31.

Yamasaki, T., Horie, S., Muranaka, H., Kaseda, Y., Mimori, Y., and Tobimatsu, S. (2012b). Relevance of in vivo neurophysiological biomarkers for mild cognitive impairment and Alzheimer's disease. *J. Alzheimers Dis.* 31, S137–S154. doi: 10.3233/JAD-2012-112093

Yamasaki, T., Maekawa, T., Miyanaga, Y., Takahashi, K., Takamiya, N., Ogata, K., et al. (2017). Enhanced fine-form perception does not contribute to gestalt face perception in autism spectrum disorder. *PLoS ONE* 12:e0170239. doi: 10.1371/journal.pone.0170239

Yamasaki, T., Maekawa, T., Takahashi, H., Fujita, T., Kamio, Y., and Tobimatsu, S. (2014). "Electrophysiology of visual and auditory perception in autism spectrum disorders," in *Comprehensive Guide to Autism*, eds V. B. Patel, V. R. Preedy, and C. R. Martin (New York, NY: Springer Science+Business Media), 791–808.

Yamasaki, T., Taniwaki, T., Tobimatsu, S., Arakawa, K., Kuba, H., Maeda, Y., et al. (2004). Electrophysiological correlates of associative visual agnosia lesioned in the ventral pathway. *J. Neurol. Sci.* 221, 53–60. doi: 10.1016/j.jns.2004.03.024

Yamasaki, T., and Tobimatsu, S. (2012). "Electrophysiological assessment of the human visual system," in *Neuroscience Research Progress, Visual Cortex: Anatomy, Functions and Injuries*, eds J. M. Harris and J. Scott (New York, NY: Nova Science Publishers), 37–67.

Yamasaki, T., and Tobimatsu, S. (2014). Electrophysiological biomarkers for improved etiological diagnosis of cognitive impairment. *Curr. Biomark Find.* 4, 69–79. doi: 10.2147/CBF.S46067

Young, A. W., Hellawell, D., and Hay, D. C. (1987). Configurational information in face perception. *Perception* 16, 747–759. doi: 10.1068/p160747

Conflict of Interest Statement: The authors declare that the research was conducted in the absence of any commercial or financial relationships that could be construed as a potential conflict of interest.

frontiers in Neuroscience

ORIGINAL RESEARCH
published: 28 February 2018
doi: 10.3389/fnins.2018.00101

Galvanic Vestibular Stimulation (GVS) Augments Deficient Pedunculopontine Nucleus (PPN) Connectivity in Mild Parkinson's Disease: fMRI Effects of Different Stimuli

Jiayue Cai[1], Soojin Lee[2,3], Fang Ba[4], Saurabh Garg[3], Laura J. Kim[3], Aiping Liu[3,5], Diana Kim[6], Z. Jane Wang[1] and Martin J. McKeown[1,3,6]*

[1] Department of Electrical and Computer Engineering, University of British Columbia, Vancouver, BC, Canada, [2] School of Biomedical Engineering, University of British Columbia, Vancouver, BC, Canada, [3] Pacific Parkinson's Research Centre, Vancouver, BC, Canada, [4] Division of Neurology, Department of Medicine, University of Alberta, Edmonton, AB, Canada, [5] School of Electronics and Applied Physics, Hefei University of Technology, Hefei, China, [6] Department of Medicine (Neurology), University of British Columbia, Vancouver, BC, Canada

OPEN ACCESS

Edited by:
Takashi Hanakawa, National Center of Neurology and Psychiatry, Japan

Reviewed by:
Martijn Müller, University of Michigan, United States
Antonio Currà, Sapienza Università di Roma, Italy
Kazumi Iseki, Sakakibara Hakuho Hospital, Japan

***Correspondence:**
Aiping Liu
aipingl@ece.ubc.ca

Specialty section:
This article was submitted to Neural Technology, a section of the journal Frontiers in Neuroscience

Received: *16 October 2017*
Accepted: *09 February 2018*
Published: *28 February 2018*

Citation:
Cai J, Lee S, Ba F, Garg S, Kim LJ, Liu A, Kim D, Wang ZJ and McKeown MJ (2018) Galvanic Vestibular Stimulation (GVS) Augments Deficient Pedunculopontine Nucleus (PPN) Connectivity in Mild Parkinson's Disease: fMRI Effects of Different Stimuli. Front. Neurosci. 12:101. doi: 10.3389/fnins.2018.00101

Falls and balance difficulties remain a major source of morbidity in Parkinson's Disease (PD) and are stubbornly resistant to therapeutic interventions. The mechanisms of gait impairment in PD are incompletely understood but may involve changes in the Pedunculopontine Nucleus (PPN) and its associated connections. We utilized fMRI to explore the modulation of PPN connectivity by Galvanic Vestibular Stimulation (GVS) in healthy controls ($n = 12$) and PD subjects even without overt evidence of Freezing of Gait (FOG) while on medication ($n = 23$). We also investigated if the type of GVS stimuli (i.e., sinusoidal or stochastic) differentially affected connectivity. Approximate PPN regions were manually drawn on T1 weighted images and 58 other cortical and subcortical Regions of Interest (ROI) were obtained by automatic segmentation. All analyses were done in the native subject's space without spatial transformation to a common template. We first used Partial Least Squares (PLS) on a subject-by-subject basis to determine ROIs across subjects that covaried significantly with the voxels within the PPN ROI. We then performed functional connectivity analysis on the PPN-ROI connections. In control subjects, GVS did not have a significant effect on PPN connectivity. In PD subjects, baseline overall magnitude of PPN connectivity was negatively correlated with UPDRS scores ($p < 0.05$). Both noisy and sinusoidal GVS increased the overall magnitude of PPN connectivity ($p = 6 \times 10^{-5}$, 3×10^{-4}, respectively) in PD, and increased connectivity with the left inferior parietal region, but had opposite effects on amygdala connectivity. Noisy stimuli selectively decreased connectivity with basal ganglia and cerebellar regions.

Our results suggest that GVS can enhance deficient PPN connectivity seen in PD in a stimulus-dependent manner. This may provide a mechanism through which GVS assists balance in PD, and may provide a biomarker to develop individualized stimulus parameters.

Keywords: vestibular stimulation, pedunculopontine nucleus, functional connectivity, Parkinson's Disease, non-invasive neuromodulation, fMRI

INTRODUCTION

Falls in older adult populations are a significant cause of morbidity and mortality (Cameron et al., 2012) with non-fatal injuries initiating a vicious cycle leading to a fear of falling, social isolation, loss of independence, deconditioning, and a significantly greater use of health care services (Stevens et al., 2006; Williams et al., 2006).

In Parkinson's Disease (PD), gait disturbances such as decreased stride length and gait variability are associated with increased risk of falls. Balance and gait deficits in PD are frequently refractory to therapy (Azevedo Coste et al., 2014; Perez-Lloret et al., 2014) and may be actually worsened by pharmacological and surgical interventions (Bloem et al., 1996), making falls a significant source of morbidity in PD (Schaafsma et al., 2003). Freezing of gait (FOG) is a syndrome normally seen in advanced PD and can occur when subjects are either on or off medication. FOG may be partly due to a failure to adequately scale amplitudes for the intended movement (Chee et al., 2009) and/or defective motor programming setting by the Supplemental Motor Area (SMA) and its maintenance by the basal ganglia, leading to a mismatch between intention and automation (Chee et al., 2009).

Cognitive and motor function must be carefully integrated to execute gait. Dysfunction of the basal ganglia in PD results in impaired motor control of skilled voluntary movements (Magrinelli et al., 2016) and movements become excessively slow and underscaled in size (Benecke et al., 1987). Biochemically, imbalance in multiple neurotransmitters (including but not limited to dopamine, acetylcholine, and GABA) is seen not only in basal ganglia and motor structures, but also limbic circuitries (Ondo and Hunter, 2003; Perez-Lloret and Barrantes, 2016). Balance disturbance and falls in PD may be more related to disruption in cholinergic rather than dopaminergic neurotransmission (Bohnen et al., 2009).

A key part of the subcortical cholinergic system is the pedunculopontine nucleus (PPN), which appears critically involved in gait disturbances in PD (Mazzone et al., 2005; Androulidakis et al., 2008; Acar et al., 2011), as PPN neuronal loss is evident in PD (Rinne et al., 2008) (Note that although we refer to the "PPN" throughout this manuscript, at the resolution of the imaging used here, it would perhaps be more accurate to refer to this region as the "mesencephalic locomotor region" as it likely includes the cuneiform nucleus—however, we use PPN as this terminology is consistent with much prior literature (e.g., Mazzone et al., 2005; Androulidakis et al., 2008; Acar et al., 2011).

Connectivity to/from the PPN appears critical for FOG in PD (Fling et al., 2014). Structural deficits in connectivity are evident between basal ganglia-PPN and other tracts in FOG (Fling et al., 2014; Vercruysse et al., 2015). DTI tractography obtained with 3T MR imaging in PD patients with FOG has demonstrated asymmetrically decreased connectivity between the PPN and the SMA, compared to PD subjects without FOG (Fling et al., 2014). FOG is also associated with diffuse white matter damage involving major cortico-cortical, corticofugal motor, and several striatofrontal tracts with DTI (Vercruysse et al., 2015). In addition to structural/anatomical connectivity, advanced neuroimaging techniques have enabled the studies of functional connectivity, which refers to the statistical temporal dependences between anatomically separated brain regions, to reveal the functional communication in the brain. Functional imaging studies (e.g., fMRI) have reported increased activity or altered connectivity during gait visualization in the midbrain locomotion centers between FOG episodes (Hanakawa et al., 1999), possibly reflecting compensatory mechanisms which might be overwhelmed with stress by turning or multitasking (Shine et al., 2013). Moreover, resting state functional magnetic resonance imaging (rs-fMRI) has allowed the inference of functional connectivity by measuring the level of spontaneous co-activation between fMRI time courses of brain regions recorded during rest. *In vivo* functional connectivity studies with rs-fMRI suggest that FOG patients may have significantly altered connectivity between PPN-SMA (Fling et al., 2014), which might reflect a maladaptive compensatory mechanism.

While the PPN has most often been investigated in PD in the context of FOG, it is unclear if altered PPN activity is present in non-FOG PD patients. Surgical targeting of the PPN is usually reserved for people with FOG resulting in significant impairment. Yet, even in early stages of the disease, there are a number of ways in which Parkinsonian gait is different from controls. While mildly affected PD patients can usually perform simple straight-line walk tasks without difficulty, they experience difficulties with turning, and when performing simultaneous motor or cognitive tasks (dual tasks), and/or crossing obstacles (Camicioli et al., 1998; Bond and Morris, 2000). They may have an abnormal gait pattern characterized by a shortened stride length, increased stride variability, and reduced walking speed (Morris et al., 2001; Buckley et al., 2008).

Ways to modulate PPN activity and connectivity have proven elusive. Acetylcholinesterase inhibitors may affect the PPN but such effects are likely to be modest. PPN Deep Brain Stimulation (DBS) has been shown to (inconsistently) improve gait difficulties in PD (Mazzone et al., 2005; Peppe et al., 2010; Acar et al., 2011; Hamani et al., 2011; Tykocki et al., 2011; Wilcox et al., 2011). However, the PPN tends to be spatially diffuse and is

difficult to visualize on standard T1-weighted images, making electrode placement for DBS therapy difficult. Another potential way to modulate PPN is through the vestibular system, as PPN neurons tend to be highly vestibular-responsive (Aravamuthan and Angelaki, 2012). Galvanic vestibular stimulation (GVS) is a non-invasive technique that activates vestibular afferents to the thalamus and also the basal ganglia (Stiles and Smith, 2015) which in turn are directed to the PPN (Visser and Bloem, 2005), possibly explaining why GVS may positively impact posture/standing balance in PD (Kataoka et al., 2016). A few studies have demonstrated that noisy GVS improved postural and balance responses (Pal et al., 2009; Samoudi et al., 2015) as well as motor deficits in PD (Yamamoto et al., 2005; Pan et al., 2008; Lee et al., 2015a,b). These studies have speculated that noisy vestibular input may have improved information flow through the basal ganglia via *stochastic facilitation* (SF). SF is a phenomenon observed in a non-linear system where stochastic biological noise paradoxically increases sensitivity of a system to detect a weak stimulus possibly resulting in functional benefits (Mcdonnell and Ward, 2011). In addition to noisy stimuli, sinusoidal stimuli have been suggested as a means to activate steady-state, as opposed to transient balance responses that would be induced with pulsed stimuli (Latt et al., 2003). Sinusoidally oscillating stimuli may also activate irregular vestibular afferents (Gensberger et al., 2016) relying on voltage dependent K-channels (Eatock and Songer, 2011). While a couple of fMRI studies have shown sinusoidal GVS modulated activations in various brain regions (Della-Justina et al., 2014; Lee et al., 2016), GVS's influence on the PPN has not yet been investigated. A recent study in healthy older adults ($n = 20$) found that noisy GVS resulted in sustained reduction in Centre of Pressure (COP) parameters, such as velocity, and Root Mean Square (RMS) (Fujimoto et al., 2016). The mechanisms of this reduction was speculated to be on the basis of induced synaptic plasticity in the vestibular nuclei and the flocculus of the cerebellum, but effects on the PPN were not considered (Fujimoto et al., 2016).

Given the non-invasive, and potentially portable nature of GVS, we wished to determine if PPN connectivity could be modulated in mildly-affected PD subjects who may demonstrate reduced stride length for example, and thus may be at increased risk for falls, but did not exhibit FOG. Thus, in this study, we investigated whether or not functional connectivity between the PPN and other brain regions could be reliably assessed, whether or not these connections were significantly modulated by GVS, and if the connectivity was modulated in a stimulus-specific manner. Since *a priori* knowledge about functional connectivity to/from the PPN at the spatial and temporal resolution afforded by fMRI is unknown, this was essentially an exploratory approach. Careful care was taken to detect robust activation from PPN structures by analyzing the data in native space (without registration to a template) and utilizing subject-specific weightings of voxels within the PPN region. We demonstrated that PPN connectivity is sensitive to vestibular stimulation in PD in a stimulus-dependent manner.

METHODS

Subjects

Twenty three PD patients (see **Table 1** for the clinical information) and 12 age-matched healthy controls [5 females; age: 63.3 ± 10.4 (mean ± standard deviation)] participated in the study. The PD patients had mild to moderate PD (Hoehn and Yahr stage I–III) (see **Table 1**) and were scanned at the on-medication state. All participants were recruited from the Pacific Parkinson's Research Centre (PPRC) at the University of British Columbia (UBC) and provided written, informed consent prior to participation. All studies were approved by the UBC Ethics Review Board. The data were collected in two experiments: in the first group GVS was assessed both ON and OFF L-dopa medication and has been partially reported in a separate short report (Lee et al., 2016), and the second group were only assessed in the ON medication state. Only the ON medication studies from the first group are reported here. In the first group, UPDRS scores Part III were assessed in the OFF medication state, while in the second group UPDRS scores were assessed in the ON medication state. A regression model was used to control for these differences (described below).

GVS

Digital signals of the GVS stimuli were first generated on a PC with MATLAB (MathWorks, MA, USA) and were converted to analog signals via a NI USB-6221 BNC digital acquisition module (National Instruments, TX, USA). The analog command voltage signals were then subsequently passed to a bipolar, constant current stimulator (DS5 model, Digitimer Ltd., U.K.). The DS5 constant current stimulator was isolated in the console room with the output cable leading into the scanning room through a waveguide. Along the twisted coaxial output cable, four inductance capacity filters spaced 20 cm apart and tuned for the Larmor frequency (128 MHz) were custom-built. Near the subject, high-resistance radiotranslucent carbon-fiber leads (Biopac Inc., Montreal, Canada) were connected to pre-gelled Ag/AgCl electrodes that were MR-compatible (Biopac Inc., Montreal, Canada). For bilateral stimulation, an electrode was placed over the mastoid process behind each ear. Since the GVS stimuli are alternating current (AC), the anode and cathode are not fixed on one side (as for DC) but they are alternating.

TABLE 1 | Clinical information on PD patients.

Characteristics	Statistics (mean ± standard deviation)
Age	66.4 ± 7.0
Sex	17 males, 6 females
UPDRS motor score	22.3 ± 12.4
UPDRS assessed during on/off medication	13 on-medication, 10 off-medication
Hoehn and Yahr stage	1.9 ± 1.0
L-dopa equivalent daily dose (LEDD)	988.8 ± 798.9

The order of GVS condition was kept consistent to be rest, noisy GVS, and sinusoidal GVS across all the participants. The potential caveat of keeping the sequence the same is the case where there are any post-stimulation effects. To avoid such confounding effects, we allowed a 2-min break between the two GVS conditions. To the best of our knowledge, after-effects of GVS on cortical activation have not yet been investigated. However, we think that the break time was sufficient to avoid after effects based on literature on after-effects of transcranial alternating current stimulation (Strüber et al., 2015).

Since individuals have an inherently subjective perception of GVS, prior to scanning, we determined the individual sensory threshold level (cutaneous sensation at the electrode site) utilizing systematic procedures used in prior GVS studies (Hummel et al., 2005; Wilkinson et al., 2008; Utz et al., 2011). We delivered two different types of stimuli at 90% of the individual threshold level: noisy and sinusoidal. The noisy stimulus was zero-mean with 1/f-type power spectrum between 0.1 and 10 Hz and the sinusoidal stimulus was a 1 Hz sine wave.

MRI

Resting state data were collected on a 3 Tesla scanner (Philips Achieva 3.0T R3.2; Philips Medical Systems, Netherlands) equipped with a head-coil. During the scanning, all the subjects were instructed to be awake with eyes closed. Blood oxygenation level-dependent (BOLD) contrast echo-planar (EPI) T2*-weighted images were taken with the following specifications with a repetition time of 1,985 ms, echo time of 37 ms, flip angle 90°, field of view 240.00 mm, matrix size 128 × 128, and with pixel size 1.9 × 1.9 mm. The duration of each functional run was 8 min for rest condition and 5 min for GVS condition with noisy and sinusoidal stimulus, respectively. As stated above, the order of functional runs was rest, noisy GVS and sinusoidal GVS, and it was kept consistent across all subjects. We allowed 2 min gaps after the noisy stimulus to account for possible post-stimulation effects.

An ROI presumed to include the PPN and cuneiform nucleus was drawn manually on the T1 sequence at the level of the superior cerebellar decussation between medial lemniscus and superior cerebellar peduncle (Aravamuthan et al., 2007; Zrinzo et al., 2008) (**Figure 1**). T1 and the fMRI data were registered via FLIRT (with "Boundary-Based Registration" option) in FSL (Smith et al., 2004). The PPN voxels drawn on the T1 were then registered to the fMRI data by applying the inverse transformation calculated by registering the fMRI to the T1 weighted image. After registration, we included neighboring voxels around PPN voxels in our analysis to account for possible partial volume effects.

Resting State Functional MRI (rs-fMRI) Preprocessing

The acquired fMRI data were preprocessed using both AFNI and SPM8 software packages. On the whole brain, several preprocessing steps from the AFNI software package were performed. These included despiking, slice timing correction, and 3D isotropic correction (3 mm in each dimension). While the subjects were asked to keep the head still during the scanning session, some head movements occurred during the acquisition process. Motion correction using rigid body alignment was performed to correct for any major head motion during the scan. Besides the fMRI scans, we also collected a T1-weighted structural scan of each of the participants. FreeSurfer was performed on the T1-weighted scans to get the different ROI masks in the T1 space. Each of the subjects' structural scans was then registered to the fMRI scan using rigid registration. This registration step provided us with the FreeSurfer segmented ROI mask in the fMRI space. All analysis was done in the individual fMRI space rather than transforming all fMRI data to a common template. This was done to prevent introducing any unwanted distortions in the fMRI data by registering it to a common template. In the next step, several sources of variance such as head-motion parameters, their temporal derivatives and their squares, white-matter signal, CSF signal were removed using nuisance regression. The fMRI signal was then detrended, and any linear or quadratic trends in the fMRI signal were removed. The signal was then iteratively smoothed until it reached 6 FWHM of smoothness. Finally, bandpass filtering was performed to retain the signal between the recommended frequencies of interest (0.01–0.08 Hz).

Since the brainstem can move independently from the rest of the brain, motion correction on the whole brain motion estimates may not be ideal. Therefore, a separate motion correction of the brainstem was performed. First, the brainstem mask was generated using FreeSurfer on the T1-weighted image of the same subject. The mask was then transferred over to the fMRI using registration as mentioned before. The registered mask was then dilated using a spherical structuring element of radius 3 to incorporate for any errors in the segmentation and registration process. The motion within the brainstem was then corrected independently using the SPM toolbox.

Brain Region Selection

In this study, we included 58 ROIs automatically segmented by FreeSurfer as shown in **Table 2**. Two PPN ROIs were manually drawn on the T1-weighted images to include the PPN on each side, namely left PPN, and right PPN, respectively. When assessing the functional connectivity between PPN and other brain regions, we first utilized Partial Least Squares (PLS) to initially select candidate brain regions that significantly covaried with PPN voxels.

PLS is a statistical method that explores the predictive models between predictor variables and response variables (Wold, 1985). It constructs a linear regression model by projecting the predictor variables and response variables to a new set of latent variables the covariance of which is maximized. PLS is particularly useful when the predictor variables are highly collinear, or when the number of predictor variables is larger than that of observations, while classical multiple linear regression models will fail in these cases. PLS has been widely used in various fields of chemometrics, social science, bioinformatics, and neuroscience (e.g., Ziegler et al., 2013; Chen et al., 2016).

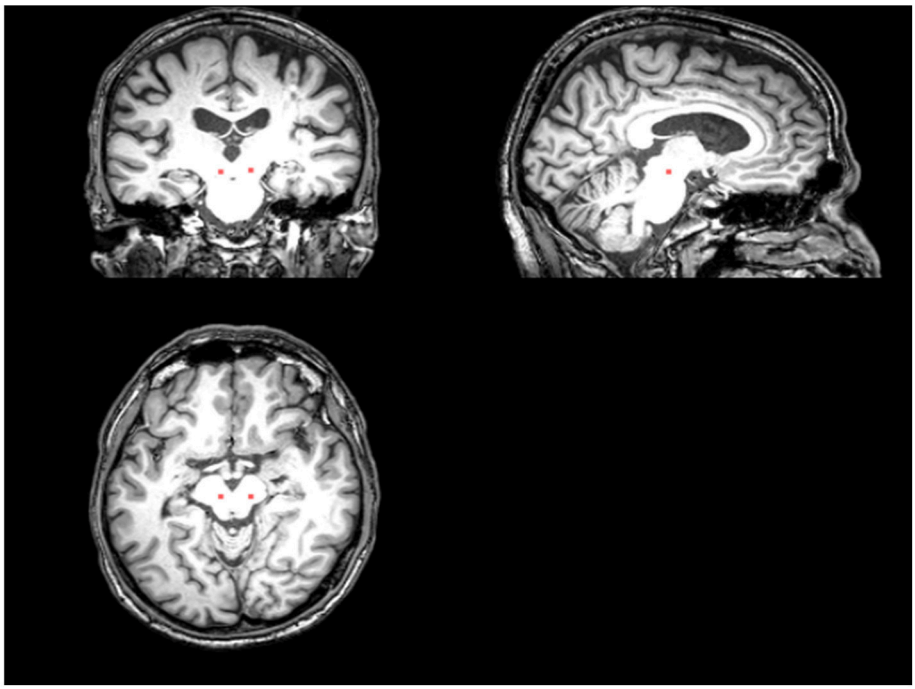

FIGURE 1 | The placement of the PPN VOI on the T1 sequence. The red area represents where the PPN VOI is placed.

When applying PLS, we used the 58-ROI dataset as predictor variables, X, and the PPN voxels as response variables, Y, and then tried to predict PPN activity from those 58-ROI time courses.

The general model for PLS is

$$X = TP^T + E \quad (1)$$

$$Y = UQ^T + F \quad (2)$$

where X is a t-by-m matrix of ROI data (predictor variables), with t corresponding to the number of time points, and m (= 58) representing the number of subject-independent (non-PPN) ROIs; Y is a t-by-n matrix of PPN voxel time courses (response variables), where n is the number of PPN voxels (which was subject-dependent); T and U are, respectively, t-by-c component matrices decomposed from X and Y (T and U are also called X Score and Y Score, respectively), where c is the number of components; P is an m-by-c loading matrix of ROI dataset, and Q is an n-by-c loading matrix of PPN voxels; and E, F are the t-by-m and t-by-n matrices, respectively, representing error terms. Essentially, PLS performs the decompositions of X and Y to maximize the covariance between T and U.

We then interrogated the loadings of the X components (i.e., the columns of P) to determine if they were significantly different from zero across subjects. The same procedure was conducted for both left PPN and right PPN, respectively, and then the union set of the selected regions from left PPN and right PPN was used as the final candidate set of brain regions. In addition, we used the first component of Y (i.e., the first column of Y Score) to represent the PPN signal in the subsequent functional connectivity analyses.

Functional Connectivity Analyses

We further performed functional connectivity analyses between the PPN and PLS-derived regions. Functional connectivity measures were obtained by computing the partial correlation coefficients between the represented PPN signal, which was obtained by the PLS analysis, and the averaged time courses of each PLS-derived region. We conducted the functional connectivity analyses on a subject-by-subject and task-by-task basis. Specifically, for each subject, functional connectivity was assessed for each of the three conditions, i.e., rest, noisy and sinusoidal GVS conditions, by taking the time courses for each condition time segment of interest from the PPN and PLS-derived regions and computing the partial correlation coefficients between them. For simplicity, we summed the absolute values of the significant connectivity coefficients from both left and right PPN to get an overall PPN connectivity.

To investigate whether or not functional connectivity between the PPN nuclei and PLS-derived regions was significantly affected by GVS, we calculated overall PPN connectivity differences between GVS on (i.e., noisy/sinusoidal GVS condition) and GVS off (i.e., rest condition). An independent one-sample t-test was then performed on the calculated connection coefficient *differences* across subjects, with the null hypothesis that the difference was zero, to determine if significant connectivity changes were induced by GVS.

TABLE 2 | The 58 ROIs (in addition to the 2 PPN ROIs) used in the analysis.

1	Left-Cerebellum-Cortex
2	Left-Thalamus-Proper
3	Left-Caudate
4	Left-Putamen
5	Left-Pallidum
6	Left-Hippocampus
7	Left-Amygdala
8	Left-Accumbens-area
9	ctx-lh-caudalanteriorcingulate
10	ctx-lh-caudalmiddlefrontal
11	ctx-lh-cuneus
12	ctx-lh-entorhinal
13	ctx-lh-inferiorparietal
14	ctx-lh-inferiortemporal
15	ctx-lh-lateralorbitofrontal
16	ctx-lh-medialorbitofrontal
17	ctx-lh-middletemporal
18	ctx-lh-parahippocampal
19	ctx-lh-paracentral
20	ctx-lh-postcentral
21	ctx-lh-posteriorcingulate
22	ctx-lh-precentral
23	ctx-lh-precuneus
24	ctx-lh-rostralanteriorcingulate
25	ctx-lh-rostralmiddlefrontal
26	ctx-lh-superiorfrontal
27	ctx-lh-superiorparietal
28	ctx-lh-superiortemporal
29	ctx-lh-insula
30	Right-Cerebellum-Cortex
31	Right-Thalamus-Proper
32	Right-Caudate
33	Right-Putamen
34	Right-Pallidum
35	Right-Hippocampus
36	Right-Amygdala
37	Right-Accumbens-area
38	ctx-rh-caudalanteriorcingulate
39	ctx-rh-caudalmiddlefrontal
40	ctx-rh-cuneus
41	ctx-rh-entorhinal
42	ctx-rh-inferiorparietal
43	ctx-rh-inferiortemporal
44	ctx-rh-lateralorbitofrontal
45	ctx-rh-medialorbitofrontal
46	ctx-rh-middletemporal
47	ctx-rh-parahippocampal
48	ctx-rh-paracentral
49	ctx-rh-postcentral
50	ctx-rh-posteriorcingulate
51	ctx-rh-precentral
52	ctx-rh-precuneus
53	ctx-rh-rostralanteriorcingulate
54	ctx-rh-rostralmiddlefrontal
55	ctx-rh-superiorfrontal
56	ctx-rh-superiorparietal
57	ctx-rh-superiortemporal
58	ctx-rh-insula

RESULTS

Brain Region Selection

The PLS analysis results found 10 ROIs in the PD group and 5 ROIs in the control group that significantly covaried with PPN voxels ($p < 0.05$). In the PD group, the ROIs included the cerebellum cortex, hippocampus, amygdala, inferior parietal, middle temporal, and precuneus regions on the left, and the pallidum, hippocampus, amygdala, and middle temporal on the right (**Figure 2**). In the control group, the caudate on the left, and the caudate, entorhinal cortex, inferior temporal, and parahippocampal regions on the right were associated with PPN activity (**Figure 3**).

Functional Connectivity Analyses

To determine the effect of the L-dopa equivalent daily dose (LEDD) on connectivity and to correct for the fact that some subjects had their UPDRS assessed off medication, we performed a regression analysis where connection strengths across subjects was the dependent variable, and LEDD, UPDRS score, whether or not the UPDRS was done on or off medication were independent variables. We then evaluated the regression coefficients for the LEDD to determine if it had a significant effect on overall PPN connectivity, which it did not ($p > 0.05$).

The functional analysis results demonstrated that GVS differently affected overall PPN connectivity in PD and control groups. In the control group, no significant differences in overall PPN connectivity were found between GVS on (i.e., noisy/sinusoidal GVS condition) and GVS off (i.e., rest condition). In the PD group, the overall magnitude of PPN connectivity correlated negatively with UPDRS scores ($r = -0.39$, $p = 0.035$, **Figure 4**). Both noisy and sinusoidal GVS increased the magnitude of overall PPN connectivity ($p = 6 \times 10^{-5}$ and 3×10^{-4}, respectively, **Figure 5**). Furthermore, in order to determine if overall connectivity of the PPN was particularly related to postural instability, we also compared the connectivity to the retropulsion test score from the UPDRS (**Figure 4**, inset). Since our emphasis was on early patients, we could not perform a statistical analysis, as there was only 1 subject with a score of 2 and 1 subject with a score of 4. However, as shown in **Figure 4**, and consistent with overall UPDRS scores, there was a trend toward decreased connectivity with higher retropulsion test scores.

Although both types of stimuli augmented overall PPN connectivity (both positive and negative connectivity as shown in **Figure 5**), in order to determine if there are differences between the types of stimuli, we performed a *post-hoc* analysis to determine which PPN connections were most influential in

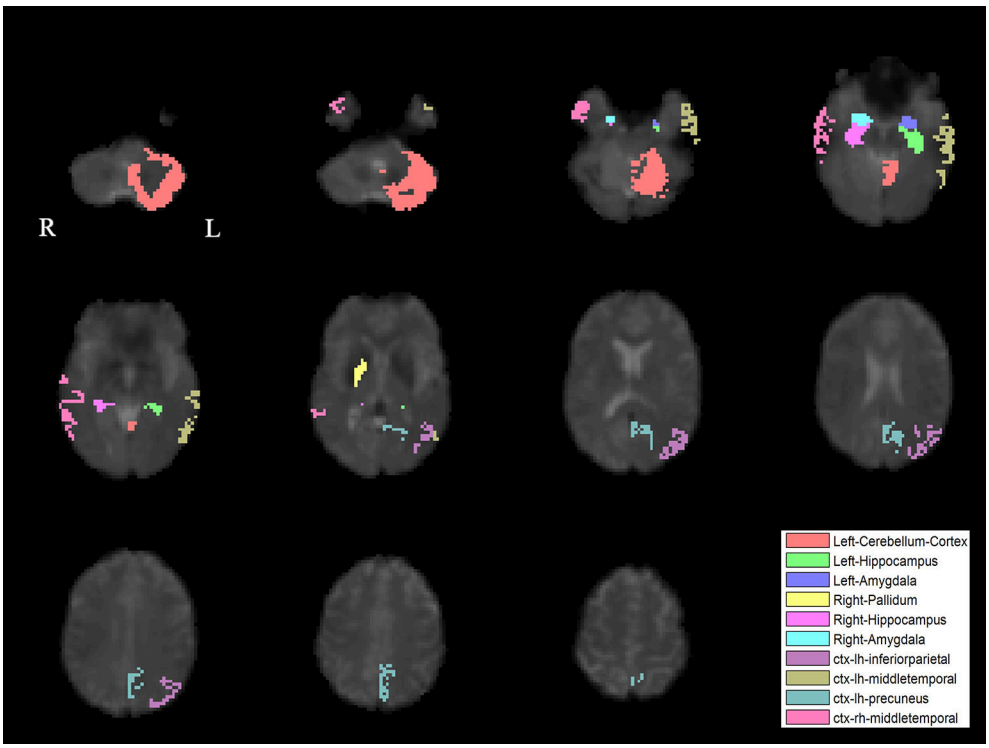

FIGURE 2 | PLS-derived ROIs in the PD group that significantly covaried with PPN voxels. The detected 10 regions, including cerebellum cortex, hippocampus, amygdala, inferior parietal, middle temporal, and precuneus regions on the left, and the pallidum, hippocampus, amygdala, and middle temporal on the right, are marked with different colors.

determining changes in overall connectivity. Specifically, we performed *t*-tests on each connection to determine if the different types of GVS stimuli increased or decreased connectivity between the PPN and other brain regions.

For the left PPN, noisy GVS decreased connectivity with the right pallidum and sinusoidal GVS increased connectivity with the left inferior parietal region (**Table 3** and **Figure 6**). For the right PPN, noisy GVS decreased connectivity with the left cerebellar cortex, increased connectivity with the right amygdala and increased connectivity with the left inferior parietal region; sinusoidal GVS decreased connectivity with the left amygdala (**Table 4** and **Figure 7**). Note that only the connection between left PPN and left inferior parietal region would survive multiple comparisons.

DISCUSSION

Balance impairment remains a vexing problem in PD and is associated with considerable morbidity. Pharmacological (particularly dopaminergic) and surgical interventions have had varying degrees of success. Development of novel therapies has also been challenging because the pathophysiology and neuropathological substrates underlying gait disturbances are incompletely known.

To the best of our knowledge, we have shown for the first time that is possible with GVS to non-invasively modulate the functional connectivity in PD subjects between cortical/subcortical ROIs and the PPN—a structure critical for normal supraspinal control of locomotion. This demonstrated alteration in functional connectivity complements previous work examining anatomic connectivity patterns. Anatomically, the PPN has been shown to have connections with various areas such as the vestibular nuclei (Aravamuthan and Angelaki, 2012), deep cerebellar nuclei (Hazrati and Parent, 1992), premotor, supplemental motor (SMA) and primary motor cortices (Aravamuthan et al., 2007), frontal eye fields (Matsumura et al., 2000), thalamic nuclei and basal ganglia nuclei (Charara et al., 1996). Widespread projections involving the PPN include direct glutamatergic inputs from the motor cortex, and GABAergic inputs from substantia nigra pars reticulata (SNr), globus pallidus internus (GPi), subthalamic nucleus (STN), and deep nuclei of cerebellum. Ascending efferent projections target GPi, substantia nigra pars compacta (SNc), and thalamus. Descending efferent projections connect to pontine, medullary reticular formation, and the spinal cord vital for control of muscle tone and locomotion. Additionally, the PPN appears to be important in the initiation, acceleration, deceleration, and termination of locomotion through connections to the basal ganglia and higher cortical regions (Lee et al., 2000).

Our results indicate significant differences in the PPN functional connectivity between PD subjects and controls. This is particularly relevant when noting that none of our PD subjects

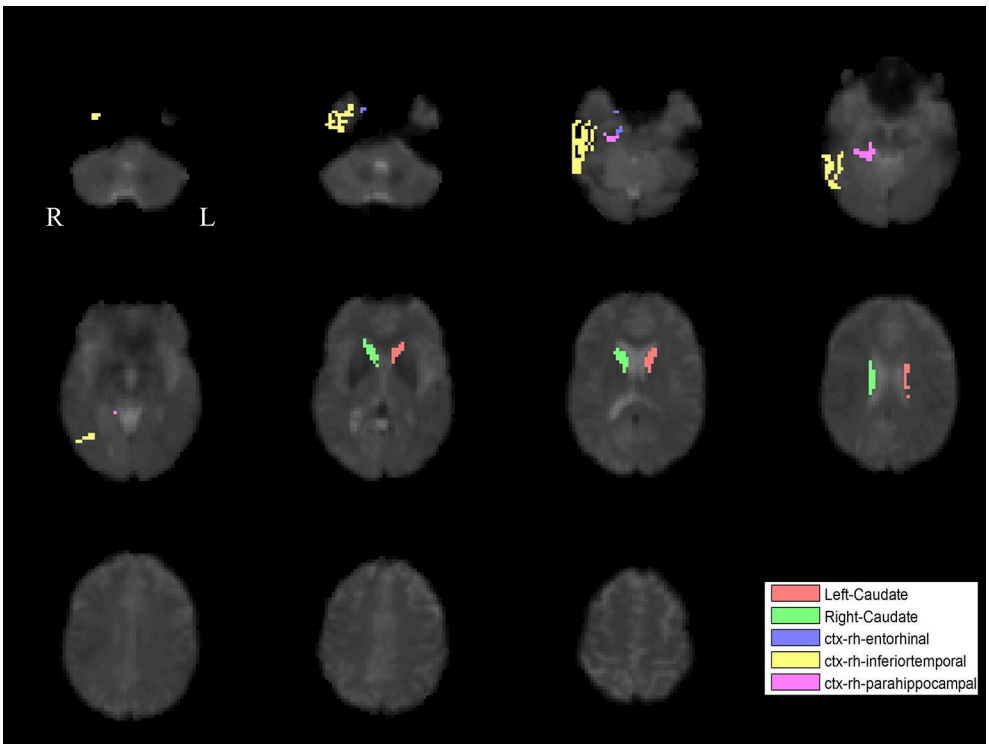

FIGURE 3 | PLS-derived ROIs in the control group that significantly covaried with PPN voxels. The detected five regions, including the caudate on the left, and the caudate, entorhinal cortex, inferior temporal, and parahippocampal regions on the right, are marked with different colors.

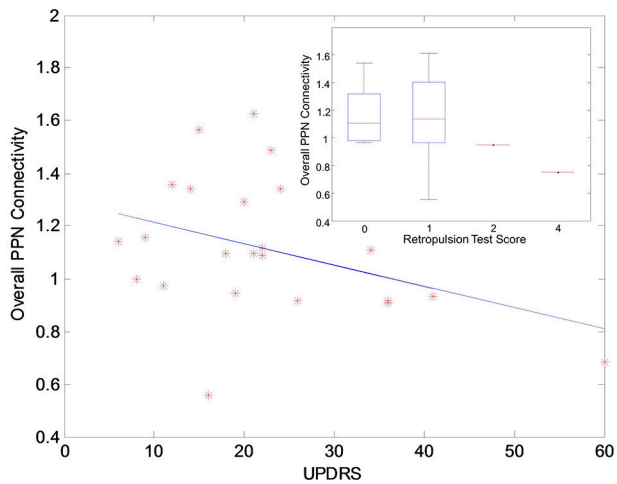

FIGURE 4 | The correlation relationship between the overall PPN connectivity and UPDRS scores in the PD group. The inset shows the relationship between the overall PPN connectivity and the retropulsion test scores from the UPDRS.

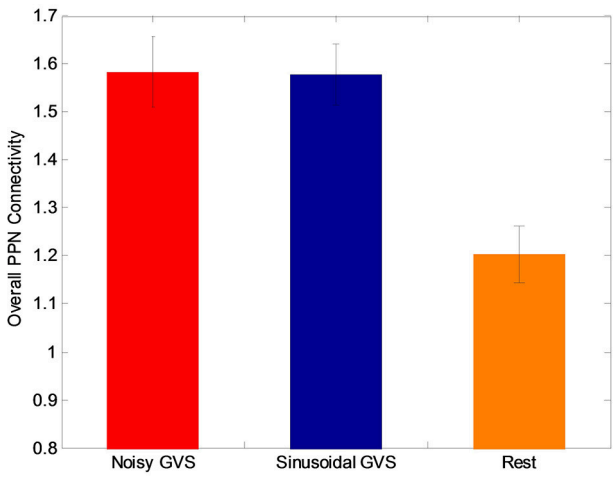

FIGURE 5 | The overall PPN connectivity differences between GVS on (i.e., noisy and sinusoidal GVS condition) and GVS off (i.e., rest condition) in the PD group.

had FOG, given their relatively mild disease. However, even mild disease is associated with altered gait and our results suggest that PPN functional connectivity patterns change even in the early stages of disease course.

We have shown that both GVS stimuli patterns (noisy and sinusoidal) augment overall deficient PPN connectivity in PD. Our results are consistent with previous studies demonstrating GVS activation of vestibular afferents to basal ganglia (Visser and Bloem, 2005; Stiles and Smith, 2015), which are also directed to the midbrain locomotion network (Peppe et al., 2010). PET studies in humans have also shown activation in the putamen in response to vestibular stimulation (Bottini et al., 1994).

We found differences in PPN network connectivity depending upon the type of stimulus used. Noisy GVS significantly decreased the functional connectivity between the left PPN and right-pallidum in PD. The PPN receives strong inhibitory, GABAergic inputs from the BG nuclei (GPi, STN, and SNr), which have disrupted connectivity in PD (Pahapill and Lozano, 2000). In particular, previous studies suggest that the PPN may be the principal target of pallidal outflow, since more than 80% GPi neurons were found to send axonal branches to both the PPN and thalamus in monkeys (Harnois and Filion, 1982). In PD, the inhibitory GABAergic synaptic activities from the GPi to the PPN is abnormally overactive, which may underlie the akinesia and the gait problems seen in the PD (Pahapill and Lozano, 2000). Taken together, these studies demonstrate the important role of the PPN and pallidal connectivity in motor and gait dysfunctions of PD. We demonstrated that noisy GVS significantly decreased connectivity between the left PPN and right-pallidum in PD (but not normal controls), which suggests that potential benefits of GVS on balance in PD may be partly mediated through attenuation of overactive pallidal inputs to the PPN.

Noisy GVS also decreased connectivity between the right PPN and the left cerebellar cortex. A DWI study found the connectivity of the PPN region with the cerebellum, thalamus, pallidum, and STN (Muthusamy et al., 2007). The cerebellum functions that help control of movement, coordination, and posture (Saab and Willis, 2003) are speculated to be associated with the existence of the pathway with the PPN (Muthusamy et al., 2007). The fact that prior studies have suggested a beneficial effect of noisy GVS (Fujimoto et al., 2016) may indicate that hyperactive PPN-cerebellar connections are partly "normalized" with GVS.

TABLE 3 | Statistics on significant left PPN connectivity changes induced by GVS stimuli in the PD group.

Connectivity	Type of Stimuli	*t*-value	*p*-value
Right pallidum	Noisy GVS	−2.32	0.015
Left inferior parietal	Sinusoidal GVS	2.81	0.005

TABLE 4 | Statistics on significant right PPN connectivity changes induced by GVS stimuli in the PD group.

Connectivity	Type of Stimuli	*t*-value	*p*-value
Left cerebellum cortex	Noisy GVS	−1.89	0.036
Right amygdala	Noisy GVS	1.90	0.035
Left inferior parietal	Noisy GVS	2.05	0.026
Left amygdala	Sinusoidal GVS	−2.09	0.024

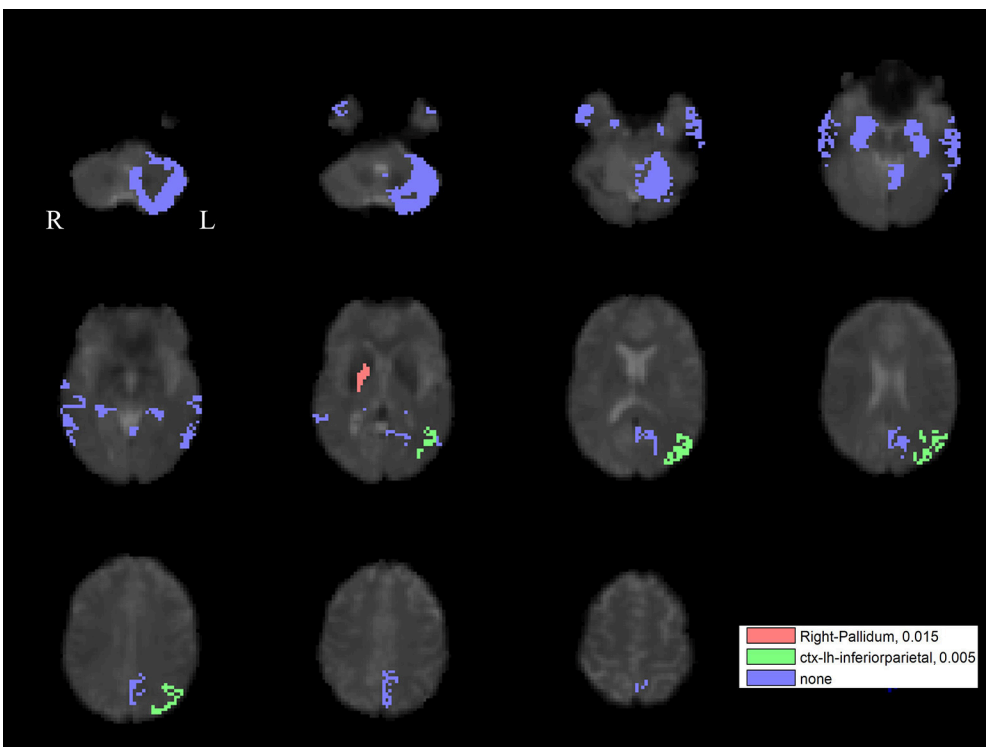

FIGURE 6 | The GVS impact on the connectivity between the left PPN and PLS-derived regions in the PD group. The red areas represent the regions significantly affected by noisy GVS. The green areas represent the regions significantly affected by sinusoidal GVS. The blue areas represent the regions with no significant changes. The corresponding ROI names and significance values are labeled in the figure.

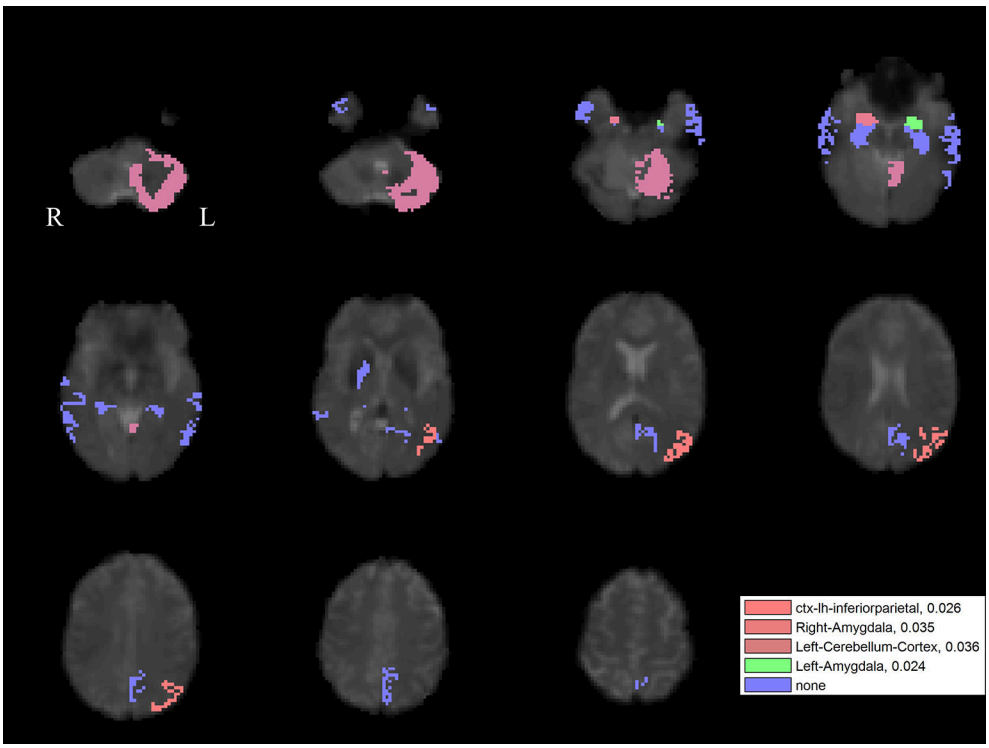

FIGURE 7 | The GVS impact on the connectivity between the right PPN and PLS-derived regions in the PD group. The red areas (with three different color levels indicating the different levels of significance values) represent the regions significantly affected by noisy GVS. The green areas represent the regions significantly affected by sinusoidal GVS. The blue areas represent the regions with no significant changes. The corresponding ROI names and significance values are labeled in the figure.

We also found that GVS increased the functional connectivity between the left inferior parietal cortex and the right PPN (with noisy stimuli) and left PPN (with sinusoidal stimuli). Previous studies in non-human primates examining cortical inputs to the pontine nuclei have supported the anatomical and functional relationships between the PPN and the inferior parietal cortex (May and Andersen, 1986; Martinez-Gonzalez et al., 2011). Like the PPN, the left inferior parietal cortex is involved in gait as well as visuospatial information processing, motor planning, and preparation (Caspers et al., 2012). Imagining normal gait activates the left inferior parietal lobule, in addition to the precuneus and bilateral dorsal premotor cortex, the left dorsolateral prefrontal cortex, and the right posterior cingulate cortex (Malouin et al., 2003). The left inferior parietal cortex appears to be especially related to FOG. Gray matter volume in the left inferior parietal region is significantly reduced in PD subjects with FOG patients compared to both PD subjects without FOG and healthy controls (Kostić et al., 2012). Thus, our result that noisy GVS increased the connectivity between the PPN and the left inferior parietal cortex might suggest GVS could improve gait difficulties in PD by augmenting the connectivity.

In the current study, one of the advantages is that we performed analyses keeping each subject's data in their original space without warping the data to a common template. We are frankly skeptical of fMRI studies suggesting robust activation from brainstem structures (e.g., PPN) when data are spatially transformed to a template, given the significant registration errors that can occur to small brainstem nuclei during whole-brain registration (Ng et al., 2009). In addition, we utilized PLS to find the combination of PPN voxels on a subject-by-subject basis that maximally corresponded with other ROIs. In effect, the first column of Q in Equation (2) represents a subject-specific spatial filter to "focus" the activity that maximally covaried with other ROIs.

It is interesting that many of the abnormal connectivities that we detected are lateralized, when balance might be considered a "midline" function. Balance control and gait are asymmetrical in patients with PD, and gait asymmetries have been linked to the pathophysiology of FOG (Boonstra et al., 2014). The symptoms of PD generally show an asymmetric onset and progression and it has been proposed that this may lead to a degree of "unbalanced" motor function, such that FOG is triggered by a breakdown in the bilateral co-ordination underlying the normal timing of gait (Plotnik et al., 2005).

There are a few limitations in our study. We examined a relatively small number of PD patients. However, by carefully selecting the PPN voxels via PLS on a subject-by-subject basis, we expect that we have significantly enhanced our effect size, and thus increasing our statistical power and thus increasing our statistical power. PLS is one of the most widely used blind

source separation (BSS) approaches which have largely benefited the neuroscience studies (Ziegler et al., 2013; Chen et al., 2016, 2018; Smith and Nichols, 2018). In the future studies, we are interested to further explore the effective voxel selections using such data-driven approaches. We have shown GVS induced changes in PPN connectivity in people with mild to moderate PD but not in healthy controls. We speculate an "inverted-U" shape of effectiveness of GVS as a function of disease severity: in controls, GVS had minimal effect, in early/moderate PD, it had some effect (shown here), and in severe disease, degeneration in the PPN itself may prevent modulation of its connectivity. Future work is required to further investigate the relationship between disease severity and PPN connectivity and determine the behavioral significance of this altered PPN connectivity. We do note that we found a negative correlation between UPDRS scores and overall PPN connectivity, yet still found robust modulation of connectivity across all of our subjects.

The relation between behavioral gait measures (e.g., gait variability) and ultimate falls risk—the most important issue for people with PD—is an active area of research. Conceivably, previously-described GVS improvements in balance may not ultimately translate into reduced fall risk but such determination would require a prospective trial in the future. We have focused on the PPN because of its possible therapeutic implications, but gait disturbances in PD likely involve several cortical and subcortical structures. For example, PD patients have decreased activity of the SMA during gait (Hanakawa et al., 1999), and PD individuals have diminished pre-movement electroencephalographic potentials originating from the SMA prior to step initiation (Smith et al., 2012). Future studies to assess connectivity changes modified by GVS in other supra-spinal locomotion centers including SMA/pre-SMA may help to guide the development of optimal stimuli on a subject-specific basis.

ETHICS STATEMENT

This study was carried out in accordance with the recommendations of TCPS2, UBC Clinical Research Ethics Board with written informed consent from all subjects. All subjects gave written informed consent in accordance with the Declaration of Helsinki. The protocol was approved by the UBC Clinical Research Ethics Board.

AUTHOR CONTRIBUTIONS

This study is ideated by MM. SL, LK, and DK conducted the experiment and data acquisition. SG and FB contributed to the data preprocessing. JC performed data analysis and manuscript writing. Interpretation of the results was performed by SL, JC, AL, FB, and MM. MM, ZW, and AL contributed to the project supervision and manuscript finalization. All authors have approved the final manuscript.

ACKNOWLEDGMENTS

This work was partly supported by the National Key R&D Program of China (2017YFB1300301), NSFC (61701158), PPRI/UBC Chair in Parkinson's Research (MM) and a generous grant from the Mottershead Foundation.

REFERENCES

Acar, F., Acar, G., Bir, L. S., Gedik, B., and Oguzhanoglu, A. (2011). Deep brain stimulation of the pedunculopontine nucleus in a patient with freezing of gait. *Stereotact. Funct. Neurosurg.* 89, 214–219. doi: 10.1159/000326617

Androulidakis, A. G., Mazzone, P., Litvak, V., Penny, W., Dileone, M., Gaynor, L. M., et al. (2008). Oscillatory activity in the pedunculopontine area of patients with Parkinson's disease. *Exp. Neurol.* 211, 59–66. doi: 10.1016/j.expneurol.2008.01.002

Aravamuthan, B., Muthusamy, K., Stein, J., Aziz, T., and Johansen-Berg, H. (2007). Topography of cortical and subcortical connections of the human pedunculopontine and subthalamic nuclei. *Neuroimage* 37, 694–705. doi: 10.1016/j.neuroimage.2007.05.050

Aravamuthan, B. R., and Angelaki, D. E. (2012). Vestibular responses in the macaque pedunculopontine nucleus and central mesencephalic reticular formation. *Neuroscience* 223, 183–199. doi: 10.1016/j.neuroscience.2012.07.054

Azevedo Coste, C., Sijobert, B., Pissard-Gibollet, R., Pasquier, M., Espiau, B., and Geny, C. (2014). Detection of freezing of gait in Parkinson disease: preliminary results. *Sensors* 14, 6819–6827. doi: 10.3390/s140406819

Benecke, R., Rothwell, J., Dick, J., Day, B., and Marsden, C. (1987). Disturbance of sequential movements in patients with Parkinson's disease. *Brain* 110:361. doi: 10.1093/brain/110.2.361

Bloem, B. R., Beckley, D. J., Van Dijk, J. G., Zwinderman, A. H., Remler, M. P., and Roos, R. A. (1996). Influence of dopaminergic medication on automatic postural responses and balance impairment in Parkinson's disease. *Mov. Disord.* 11, 509–521. doi: 10.1002/mds.870110506

Bohnen, N., Muller, M., Koeppe, R., Studenski, S., Kilbourn, M., Frey, K., et al. (2009). History of falls in Parkinson disease is associated with reduced cholinergic activity. *Neurology* 73, 1670–1676. doi: 10.1212/WNL.0b013e3181c1ded6

Bond, J. M., and Morris, M. (2000). Goal-directed secondary motor tasks: their effects on gait in subjects with Parkinson disease. *Arch. Phys. Med. Rehabil.* 81, 110–116. doi: 10.1016/S0003-9993(00)90230-2

Boonstra, T. A., van Vugt, J. P. P., van der Kooij, H., and Bloem, B. R. (2014). Balance asymmetry in Parkinson's disease and its contribution to freezing of gait. *PLoS ONE* 9:e102493. doi: 10.1371/journal.pone.0102493

Bottini, G., Sterzi, R., Paulesu, E., Vallar, G., Cappa, S. F., Erminio, F., et al. (1994). Identification of the central vestibular projections in man: a positron emission tomography activation study. *Exp. Brain Res.* 99, 164–169. doi: 10.1007/BF00241421

Buckley, T. A., Pitsikoulis, C., and Hass, C. J. (2008). Dynamic postural stability during sit-to-walk transitions in Parkinson disease patients. *Mov. Disord.* 23, 1274–1280. doi: 10.1002/mds.22079

Cameron, I. D., Gillespie, L. D., Robertson, M. C., Murray, G. R., Hill, K. D., Cumming, R. G., et al. (2012). Interventions for preventing falls in older people in care facilities and hospitals. *Cochrane Database Syst. Rev.* 12:CD005465. doi: 10.1002/14651858.CD005465.pub3

Camicioli, R., Howieson, D., Oken, B., Sexton, G., and Kaye, J. (1998). Motor slowing precedes cognitive impairment in the oldest old. *Neurology* 50, 1496–1498. doi: 10.1212/WNL.50.5.1496

Caspers, S., Schleicher, A., Bacha-Trams, M., Palomero-Gallagher, N., Amunts, K., and Zilles, K. (2012). Organization of the human inferior parietal lobule based on receptor architectonics. *Cerebral Cortex* 23, 615–628. doi: 10.1093/cercor/bhs048

Charara, A., Smith, Y., and Parent, A. (1996). Glutamatergic inputs from the pedunculopontine nucleus to midbrain dopaminergic neurons in primates: *Phaseolus vulgaris*-leucoagglutinin anterograde labeling combined with

postembedding glutamate and GABA immunohistochemistry. *J. Comp. Neurol.* 364, 254–266. doi: 10.1002/(SICI)1096-9861(19960108)364:2<254::AID-CNE5>3.0.CO;2-4

Chee, R., Murphy, A., Danoudis, M., Georgiou-Karistianis, N., and Iansek, R. (2009). Gait freezing in Parkinson's disease and the stride length sequence effect interaction. *Brain* 132, 2151–2160. doi: 10.1093/brain/awp053

Chen, X., Wang, Z. J., and Mckeown, M. (2016). Joint blind source separation for neurophysiological data analysis: Multiset and multimodal methods. *IEEE Signal Process. Mag.* 33, 86–107. doi: 10.1109/MSP.2016.2521870

Chen, X., Xu, X., Liu, A., McKeown, M. J., and Wang, Z. J. (2018). The use of multivariate EMD and CCA for denoising muscle artifacts from few-channel EEG recordings. *IEEE Trans. Instrum. Meas.* 67, 359–370. doi: 10.1109/TIM.2017.2759398

Della-Justina, H. M., Manczak, T., Winkler, A. M., de Araújo, D. B. D., de Souza, M. A., Amaro Junior, E., et al. (2014). Galvanic vestibular stimulator for fMRI studies. *Rev. Bras. Eng. Bioméd.* 30, 70–82. doi: 10.4322/rbeb.2013.046

Eatock, R. A., and Songer, J. E. (2011). Vestibular hair cells and afferents: two channels for head motion signals. *Annu. Rev. Neurosci.* 34, 501–534. doi: 10.1146/annurev-neuro-061010-113710

Fling, B. W., Cohen, R. G., Mancini, M., Carpenter, S. D., Fair, D. A., Nutt, J. G., et al. (2014). Functional reorganization of the locomotor network in Parkinson patients with freezing of gait. *PLoS ONE* 9:e100291. doi: 10.1371/journal.pone.0100291

Fujimoto, C., Yamamoto, Y., Kamogashira, T., Kinoshita, M., Egami, N., Uemura, Y., et al. (2016). Noisy galvanic vestibular stimulation induces a sustained improvement in body balance in elderly adults. *Sci. Rep.* 6:37575. doi: 10.1038/srep37575

Gensberger, K. D., Kaufmann, A.-K., Dietrich, H., Branoner, F., Banchi, R., Chagnaud, B. P., et al. (2016). Galvanic vestibular stimulation: cellular substrates and response patterns of neurons in the vestibulo-ocular network. *J. Neurosci.* 36, 9097–9110. doi: 10.1523/JNEUROSCI.4239-15.2016

Hamani, C., Moro, E., and Lozano, A. M. (2011). The pedunculopontine nucleus as a target for deep brain stimulation. *J. Neural Transm.* 118, 1461–1468. doi: 10.1007/s00702-010-0547-8

Hanakawa, T., Fukuyama, H., Katsumi, Y., Honda, M., and Shibasaki, H. (1999). Enhanced lateral premotor activity during paradoxical gait in Parkinson's disease. *Ann. Neurol.* 45, 329–336. doi: 10.1002/1531-8249(199903)45:3<329::AID-ANA8>3.0.CO;2-S

Harnois, C., and Filion, M. (1982). Pallidofugal projections to thalamus and midbrain: a quantitative antidromic activation study in monkeys and cats. *Exp. Brain Res.* 47, 277–285. doi: 10.1007/BF00239387

Hazrati, L.-N., and Parent, A. (1992). Projection from the deep cerebellar nuclei to the pedunculopontine nucleus in the squirrel monkey. *Brain Res.* 585, 267–271. doi: 10.1016/0006-8993(92)91216-2

Hummel, F., Celnik, P., Giraux, P., Floel, A., Wu, W.-H., Gerloff, C., et al. (2005). Effects of non-invasive cortical stimulation on skilled motor function in chronic stroke. *Brain* 128, 490–499. doi: 10.1093/brain/awh369

Kataoka, H., Okada, Y., Kiriyama, T., Kita, Y., Nakamura, J., Morioka, S., et al. (2016). Can postural instability respond to galvanic vestibular stimulation in patients with Parkinson's disease? *J. Mov. Disord.* 9, 40–43. doi: 10.14802/jmd.15030

Kostić, V., Agosta, F., Pievani, M., Stefanova, E., Ječmenica-Lukić, M., Scarale, A., et al. (2012). Pattern of brain tissue loss associated with freezing of gait in Parkinson disease. *Neurology* 78, 409–416. doi: 10.1212/WNL.0b013e318245d23c

Latt, L., Sparto, P., Furman, J., and Redfern, M. (2003). The steady-state postural response to continuous sinusoidal galvanic vestibular stimulation. *Gait Posture* 18, 64–72. doi: 10.1016/S0966-6362(02)00195-9

Lee, M. S., Rinne, J. O., and Marsden, C. D. (2000). The pedunculopontine nucleus: Its role in the genesis of movement. *Yonsei Med. J.* 41 167–184. doi: 10.3349/ymj.2000.41.2.167

Lee, S., Cai, J., Kim, D., Wang, Z., and Mckeown, M. (2016). "Differential effects of noisy and sinusoidal galvanic vestibular stimulation on resting state functional connectivity," in *4th Annual Minnesota Neuromodulation Symposium* (Minneapolis, MN).

Lee, S., Kim, D. J., Svenkeson, D., Parras, G., Oishi, M. M. K., and Mckeown, M. J. (2015a). Multifaceted effects of noisy galvanic vestibular stimulation on manual tracking behavior in Parkinson's disease. *Front. Syst. Neurosci.* 9:5. doi: 10.3389/fnsys.2015.00005

Lee, S., Kim, D., Svenkeson, D., Oishi, M. M. K., and Mckeown, M. J. (2015b). Synergistic effects of noisy galvanic vestibular stimulation and oral L-dopa in improving manual tracking performance in Parkinson's disease. *Brain Stimul.* 8:368. doi: 10.1016/j.brs.2015.01.184

Magrinelli, F., Picelli, A., Tocco, P., Federico, A., Roncari, L., Smania, N., et al. (2016). Pathophysiology of motor dysfunction in Parkinson's disease as the rationale for drug treatment and rehabilitation. *Parkinson Dis.* 2016:9832839. doi: 10.1155/2016/9832839

Malouin, F., Richards, C. L., Jackson, P. L., Dumas, F., and Doyon, J. (2003). Brain activations during motor imagery of locomotor-related tasks: a PET study. *Hum. Brain Mapp.* 19, 47–62. doi: 10.1002/hbm.10103

Martinez-Gonzalez, C., Bolam, J. P., and Mena-Segovia, J. (2011). Topographical organization of the pedunculopontine nucleus. *Front. Neuroanat.* 5:22. doi: 10.3389/fnana.2011.00022

Matsumura, M., Nambu, A., Yamaji, Y., Watanabe, K., Imai, H., Inase, M., et al. (2000). Organization of somatic motor inputs from the frontal lobe to the pedunculopontine tegmental nucleus in the macaque monkey. *Neuroscience* 98, 97–110. doi: 10.1016/S0306-4522(00)00099-3

May, J., and Andersen, R. (1986). Different patterns of corticopontine projections from separate cortical fields within the inferior parietal lobule and dorsal prelunate gyrus of the macaque. *Exp. Brain Res.* 63, 265–278. doi: 10.1007/BF00236844

Mazzone, P., Lozano, A., Stanzione, P., Galati, S., Scarnati, E., Peppe, A., et al. (2005). Implantation of human pedunculopontine nucleus: a safe and clinically relevant target in Parkinson's disease. *Neuroreport* 16, 1877–1881. doi: 10.1097/01.wnr.0000187629.38010.12

Mcdonnell, M. D., and Ward, L. M. (2011). The benefits of noise in neural systems: bridging theory and experiment. *Nat. Rev. Neurosci.* 12, 415–426. doi: 10.1038/nrn3061

Morris, S., Morris, M. E., and Iansek, R. (2001). Reliability of measurements obtained with the Timed "Up & Go" test in people with Parkinson disease. *Phys. Ther.* 81, 810–818. doi: 10.1093/ptj/81.2.810

Muthusamy, K., Aravamuthan, B., Kringelbach, M., Jenkinson, N., Voets, N., Johansen-Berg, H., et al. (2007). Connectivity of the human pedunculopontine nucleus region and diffusion tensor imaging in surgical targeting. *J. Neurosurg.* 107, 814–820. doi: 10.3171/JNS-07/10/0814

Ng, B., Abu-Gharbieh, R., and Mckeown, M. J. (2009). "Adverse effects of template-based warping on spatial fMRI analysis," in *SPIE Medical Imaging* (Lake Buena Vista, FL).

Ondo, W. G., and Hunter, C. (2003). Flumazenil, a GABA antagonist, may improve features of Parkinson's disease. *Mov. Disord.* 18, 683–685. doi: 10.1002/mds.10426

Pahapill, P. A., and Lozano, A. M. (2000). The pedunculopontine nucleus and Parkinson's disease. *Brain* 123, 1767–1783. doi: 10.1093/brain/123.9.1767

Pal, S., Rosengren, S. M., and Colebatch, J. G. (2009). Stochastic galvanic vestibular stimulation produces a small reduction in sway in Parkinson's disease. *J. Ves. Res.* 19, 137–142. doi: 10.3233/VES-2009-0360

Pan, W., Soma, R., Kwak, S., and Yamamoto, Y. (2008). Improvement of motor functions by noisy vestibular stimulation in central neurodegenerative disorders. *J. Neurol.* 255, 1657–1661. doi: 10.1007/s00415-008-0950-3

Peppe, A., Pierantozzi, M., Chiavalon, C., Marchetti, F., Caltagirone, C., Musicco, M., et al. (2010). Deep brain stimulation of the pedunculopontine tegmentum and subthalamic nucleus: effects on gait in Parkinson's disease. *Gait Posture* 32, 512–518. doi: 10.1016/j.gaitpost.2010.07.012

Perez-Lloret, S., and Barrantes, F. J. (2016). Deficits in cholinergic neurotransmission and their clinical correlates in Parkinson's disease. *NPJ Parkinson Dis.* 2:16001. doi: 10.1038/npjparkd.2016.1

Perez-Lloret, S., Negre-Pages, L., Damier, P., Delval, A., Derkinderen, P., Destée, A., et al. (2014). Prevalence, determinants, and effect on quality of life of freezing of gait in Parkinson disease. *JAMA Neurol.* 71, 884–890. doi: 10.1001/jamaneurol.2014.753

Plotnik, M., Giladi, N., Balash, Y., Peretz, C., and Hausdorff, J. M. (2005). Is freezing of gait in Parkinson's disease related to asymmetric motor function? *Ann. Neurol.* 57, 656–663. doi: 10.1002/ana.20452

Rinne, J. O., Ma, S. Y., Lee, M. S., Collan, Y., and Röyttä, M. (2008). Loss of cholinergic neurons in the pedunculopontine nucleus in Parkinson's disease is

related to disability of the patients. *Parkinsonism Relat. Disord.* 14, 553–557. doi: 10.1016/j.parkreldis.2008.01.006

Saab, C. Y., and Willis, W. D. (2003). The cerebellum: organization, functions and its role in nociception. *Brain Res. Rev.* 42, 85–95. doi: 10.1016/S0165-0173(03)00151-6

Samoudi, G., Jivegård, M., Mulavara, A. P., and Bergquist, F. (2015). Effects of stochastic vestibular galvanic stimulation and LDOPA on balance and motor symptoms in patients with Parkinson's disease. *Brain Stimul.* 8, 474–480. doi: 10.1016/j.brs.2014.11.019

Schaafsma, J., Balash, Y., Gurevich, T., Bartels, A., Hausdorff, J. M., and Giladi, N. (2003). Characterization of freezing of gait subtypes and the response of each to levodopa in Parkinson's disease. *Eur. J. Neurol.* 10, 391–398. doi: 10.1046/j.1468-1331.2003.00611.x

Shine, J. M., Matar, E., Ward, P. B., Bolitho, S. J., Gilat, M., Pearson, M., et al. (2013). Exploring the cortical and subcortical functional magnetic resonance imaging changes associated with freezing in Parkinson's disease. *Brain* 136, 1204–1215. doi: 10.1093/brain/awt049

Smith, B. A., Jacobs, J. V., and Horak, F. B. (2012). Effects of magnitude and magnitude predictability of postural perturbations on preparatory cortical activity in older adults with and without Parkinson's disease. *Exp. Brain Res.* 222, 455–470. doi: 10.1007/s00221-012-3232-3

Smith, S. M., and Nichols, T. E. (2018). Statistical challenges in "Big Data" human neuroimaging. *Neuron* 97, 263–268. doi: 10.1016/j.neuron.2017.12.018

Smith, S. M., Jenkinson, M., Woolrich, M. W., Beckmann, C. F., Behrens, T. E., Johansen-Berg, H., et al. (2004). Advances in functional and structural MR image analysis and implementation as FSL. *Neuroimage* 23, S208–S219. doi: 10.1016/j.neuroimage.2004.07.051

Stevens, J. A., Corso, P. S., Finkelstein, E. A., and Miller, T. R. (2006). The costs of fatal and non-fatal falls among older adults. *Inj. Prev.* 12, 290–295. doi: 10.1136/ip.2005.011015

Stiles, L., and Smith, P. F. (2015). The vestibular–basal ganglia connection: balancing motor control. *Brain Res.* 1597, 180–188. doi: 10.1016/j.brainres.2014.11.063

Strüber, D., Rach, S., Neuling, T., and Herrmann, C. S. (2015). On the possible role of stimulation duration for after-effects of transcranial alternating current stimulation. *Front. Cell. Neurosci.* 9:311. doi: 10.3389/fncel.2015.00311

Tykocki, T., Mandat, T., and Nauman, P. (2011). Pedunculopontine nucleus deep brain stimulation in Parkinson's disease. *Arch. Med. Sci.* 7, 555–564. doi: 10.5114/aoms.2011.24119

Utz, K. S., Korluss, K., Schmidt, L., Rosenthal, A., Oppenländer, K., Keller, I., et al. (2011). Minor adverse effects of galvanic vestibular stimulation in persons with stroke and healthy individuals. *Brain Inj.* 25, 1058–1069. doi: 10.3109/02699052.2011.607789

Vercruysse, S., Leunissen, I., Vervoort, G., Vandenberghe, W., Swinnen, S., and Nieuwboer, A. (2015). Microstructural changes in white matter associated with freezing of gait in Parkinson's disease. *Mov. Dis.* 30, 567–576. doi: 10.1002/mds.26130

Visser, J. E., and Bloem, B. R. (2005). Role of the basal ganglia in balance control. *Neural Plast.* 12, 161–174. doi: 10.1155/NP.2005.161

Wilcox, R. A., Cole, M. H., Wong, D., Coyne, T., Silburn, P., and Kerr, G. (2011). Pedunculopontine nucleus deep brain stimulation produces sustained improvement in primary progressive freezing of gait. *J. Neurol. Neurosurg. Psychiatry* 82, 1256–1259. doi: 10.1136/jnnp.2010.213462

Wilkinson, D., Nicholls, S., Pattenden, C., Kilduff, P., and Milberg, W. (2008). Galvanic vestibular stimulation speeds visual memory recall. *Exp. Brain Res.* 189, 243–248. doi: 10.1007/s00221-008-1463-0

Williams, D., Watt, H., and Lees, A. (2006). Predictors of falls and fractures in bradykinetic rigid syndromes: a retrospective study. *J. Neurol. Neurosurg. Psychiatry* 77, 468–473. doi: 10.1136/jnnp.2005.074070

Wold, H. (1985). *Partial Least Squares. Encyclopedia of Statistical Sciences*. New York, NY: John Wiley & Sons.

Yamamoto, Y., Struzik, Z., Soma, R., Ohashi, K., and Kwak, S. (2005). Noisy vestibular stimulation improves autonomic and motor responsiveness in central neurodegenerative disorders. *Ann. Neurol.* 58, 175–181. doi: 10.1002/ana.20574

Ziegler, G., Dahnke, R., Winkler, A., and Gaser, C. (2013). Partial least squares correlation of multivariate cognitive abilities and local brain structure in children and adolescents. *Neuroimage* 82, 284–294. doi: 10.1016/j.neuroimage.2013.05.088

Zrinzo, L., Zrinzo, L. V., Tisch, S., Limousin, P. D., Yousry, T. A., Afshar, F., et al. (2008). Stereotactic localization of the human pedunculopontine nucleus: atlas-based coordinates and validation of a magnetic resonance imaging protocol for direct localization. *Brain* 131, 1588–1598. doi: 10.1093/brain/awn075

Conflict of Interest Statement: The authors declare that the research was conducted in the absence of any commercial or financial relationships that could be construed as a potential conflict of interest.

frontiers in Neuroscience

ORIGINAL RESEARCH
published: 01 September 2017
doi: 10.3389/fnins.2017.00470

Interhemispheric Resting-State Functional Connectivity Predicts Severity of Idiopathic Normal Pressure Hydrocephalus

Yousuke Ogata[1,2,3], Akihiko Ozaki[4], Miho Ota[1,5], Yurie Oka[1], Namiko Nishida[6], Hayato Tabu[6], Noriko Sato[7,8] and Takashi Hanakawa[1,3]**

[1] Department of Advanced Neuroimaging, Integrative Brain Imaging Center, National Center of Neurology and Psychiatry, Kodaira, Japan, [2] Biointerfaces Unit, Institute of Innovative Research, Tokyo Institute of Technology, Yokohama, Japan, [3] Department of Functional Brain Research, National Institute of Neuroscience, National Center of Neurology and Psychiatry, Kodaira, Japan, [4] Social Welfare Organization Saiseikai Imperial Gift Foundation, Inc., Osaka Saiseikai Nakatsu Hospital, Osaka, Japan, [5] Department of Mental Disorder Research, National Institute of Neuroscience, National Center of Neurology and Psychiatry, Kodaira, Japan, [6] Kitano Hospital, Tazuke Kofukai Medical Research Institute, Osaka, Japan, [7] Department of Radiology, National Center of Neurology and Psychiatry Hospital, Kodaira, Japan, [8] Department of Clinical Neuroimaging, Integrative Brain Imaging Center, National Center of Neurology and Psychiatry, Kodaira, Japan

OPEN ACCESS

Edited by:
Manuel Fernando Casanova, University of Louisville, United States

Reviewed by:
Zsigmond Tamás Kincses, University of Szeged, Hungary
Zhong Yin, University of Shanghai for Science and Technology, China

***Correspondence:**
Yousuke Ogata
ogata@cns.pi.titech.ac.jp
Takashi Hanakawa
hanakawa@ncnp.go.jp

Specialty section:
This article was submitted to Neural Technology, a section of the journal Frontiers in Neuroscience

Received: *02 June 2017*
Accepted: *08 August 2017*
Published: *01 September 2017*

Citation:
Ogata Y, Ozaki A, Ota M, Oka Y, Nishida N, Tabu H, Sato N and Hanakawa T (2017) Interhemispheric Resting-State Functional Connectivity Predicts Severity of Idiopathic Normal Pressure Hydrocephalus. Front. Neurosci. 11:470. doi: 10.3389/fnins.2017.00470

Idiopathic normal pressure hydrocephalus (iNPH) is characterized by a clinical triad (gait disturbance, dementia, and urinary incontinence), and by radiological findings of enlarged ventricles reflecting disturbance of central spinal fluid circulation. A diagnosis of iNPH is sometimes challenging, and the pathophysiological mechanisms underlying the clinical symptoms of iNPH remain largely unknown. Here, we used an emerging MRI technique, resting-state functional connectivity MRI (rsfcMRI), to develop a subsidiary diagnostic technique and to explore the underlying pathophysiological mechanisms of iNPH. rsfcMRI data were obtained from 11 patients with iNPH and 11 age-matched healthy volunteers, yielding rsfcMRI-derived functional connectivity (FC) from both groups. A linear support vector machine classifier was trained to distinguish the patterns of FCs of the patients with iNPH from those of the healthy volunteers. After dimensional reduction, the support vector machine successfully classified the two groups with an accuracy of 80%. Moreover, we found that rsfcMRI-derived FC carried information to predict the severity of the triad in iNPH. FCs relevant to the classification of severity were mainly based on interhemispheric connectivity, suggesting that disruption of the corpus callosum fibers due to ventricular enlargement may explain the triad of iNPH. The present results support the usefulness of rsfcMRI as a tool to understand pathophysiology of iNPH, and also to help with its clinical diagnosis.

Keywords: resting-state functional connectivity MRI, idiopathic normal pressure hydrocephalus, functional connectivity, supervised machine learning, support-vector machine, interhemispheric connectivity

INTRODUCTION

Idiopathic normal pressure hydrocephalus (iNPH) is a cryptogenic disorder characterized clinically by a triad (gait disturbance, cognitive impairment and urinary incontinence), and radiologically by enlarged cerebral ventricles because of non-obstructive disturbance of cerebrospinal fluid (CSF) circulation (Ishikawa, 2004). The diagnosis of iNPH is important, because it is one of the few

treatable dementias; namely, the clinical symptoms can be often relieved by a shunt operation. Although typical iNPH shows characteristic neuroradiological findings (Kitagaki et al., 1998; Ishikawa et al., 2008; Mori et al., 2012), the diagnosis of iNPH remains challenging in atypical cases, because no functional biomarkers of iNPH have been established (Leinonen et al., 2011; Jingami et al., 2015). The clinical guidelines of iNPH in Japan recommend a "tap test" involving the drainage of a small amount of CSF (30–50 ml) by a lumbar puncture to predict the effectiveness of a shunt operation. However, the tap test has limitations: it is an invasive procedure and carries some risks of adverse events, such as headache. Additionally, although a positive tap test result has a high predictive value for shunt operation outcomes, a negative result has a low predictive value because of a high false negative rate (Sakakibara et al., 2012). Thus, it is important to develop non-invasive and reliable diagnostic methods for iNPH. In particular, a functional neuroimaging method would not only help with a diagnosis of iNPH, but would also provide insight into the pathophysiological mechanisms of iNPH.

Recently, resting-state functional connectivity MRI (rsfcMRI) has drawn attention as a tool to help with a clinical diagnosis and the evaluation of neuropsychiatric disease. For rsfcMRI, participants are not required to perform demanding cognitive tasks, instead they only have to lie quietly in an MRI scanner. This property is advantageous for the application of rsfcMRI to patients with dementia, who might have difficulty in performing cognitive tasks. In fact, rsfcMRI has recently been applied to neuropsychiatric disorders (Greicius et al., 2004; Damoiseaux et al., 2006; Zhang et al., 2010; Khoo et al., 2015; Takamura and Hanakawa, 2017). In particular, Khoo et al. reported that resting-state functional connectivity (RSFC) was reduced in the default mode network (DMN) in iNPH patients, and that the reduction of the RSFC in DMN was positively correlated with symptoms of iNPH (Khoo et al., 2015). This pioneering study indicates that RSFCs may provide a useful biomarker for the assessment of iNPH. However, an alteration of RSFCs other than DMN remains unclear, because the analysis was limited to the DMN. Thus, it is important to test the contribution of multiple large-scale brain networks to the diagnosis of patients with iNPH. In this regard, an emerging method for a multivariate RSFC analysis is the application of machine-learning classification algorithms (Craddock et al., 2009; Arbabshirani et al., 2013). For example, Craddock and colleagues successfully applied support-vector machine (SVM) classification to identifying a pattern of RSFCs representing major depressive disorder (Craddock et al., 2009). A previous study (Arbabshirani et al., 2013) demonstrated that SVM with RSFC features could classify more accurately patients with neuropsychiatric disease than other linear classification methods. In addition, the SVM is particularly suitable to deal with the classification task with limited number of the training instances, and high feature dimensionality. This availability of SVM is suitable to clinical neuroimaging studies where typically just a limited number of dataset is available.

Recently, several researchers used SVM to examine the diagnostic, and prognostic potential of structural MRI, functional MRI, and rsfcMRI in various areas of neurological, and psychiatric disorders, including mild cognitive impairment, probable dementia of Alzheimer type, major depression, bipolar disorder, and schizophrenia (Chen et al., 2011; Costafreda et al., 2011; Orru et al., 2012; Wee et al., 2012; Zeng et al., 2012).

However, to our knowledge, machine-learning classification has not been applied to iNPH. A supervised machine-learning classification algorithm uses multivariate datasets such as whole-brain RSFC, and is able to classify the data into predetermined categories (i.e., iNPH and healthy). Moreover, a multivariate pattern analysis on RSFC has the potential to classify the severity of disease, like the iNPH grading scale (iNPH-GS).

In this study, we applied SVM to rsfcMRI data to test the hypothesis that differences in RSFCs might differentiate between iNPH patients, and healthy volunteers, and might also discriminate across the severity stages of iNPH symptoms.

METHODS

Participants

Eleven patients with iNPH (iNPH group; 5 male, 6 female; average age $\pm$ *SD*: 78.2 $\pm$ 6.8 years) and 11 age-matched healthy controls (HC group; 4 male, 7 female; average age $\pm$ *SD*: 69.8 $\pm$ 13.6) participated in the study. The two groups did not significantly differ in terms of age (two-sample *t*-test, $p = 0.07$) or sex (chi-square test, $p = 0.53$). Nine out of 11 patients fulfilled the criteria for probable iNPH (Ishikawa, 2004; Yamashita et al., 2014): (1) age of 60 years or older; (2) presence of at least one of the classic triad (gait disturbance, cognitive impairment, and urinary incontinence); (3) ventricular dilation with Evans' index >.3; (4) normal CSF pressure and content; (5) exclusion of other neurological or non-neurological disorder; and (6) a positive CSF tap test. Two patients were diagnosed as possible iNPH because the result of a CSF tap test was equivocal. The general clinical status of the iNPH patients was assessed with the iNPH grading scale (iNPH-GS) (Kubo et al., 2008). The iNPH-GS grades the severity of three main categories of symptoms (cognitive impairment, gait disturbance, and urinary disturbance) with five levels ranging from 0 (normal) to 4 (severe). Additionally, cognitive impairment was assessed with the Mini-Mental State Examination (MMSE), and the Frontal Assessment Battery (FAB). From the HC group, only the MMSE was available. The score of the MMSE showed significant differences between the iNPH group (22.8 ± 4.3, mean $\pm$ *SD*) and the HC group (28.9 ± 1.0) [$T_{(20)} = 3.93$, $p < 0.001$]. The profiles and clinical information of the iNPH patients are summarized in **Table 1**.

The iNPH patients were enrolled at the Kitano Hospital and the healthy participants were enrolled at the National Center of Neurology and Psychiatry. All participants gave their informed consent prior to their inclusion in the study according to the study protocol approved by the institutional ethics committee.

rsfcMRI Acquisition

For rsfcMRI, the participants were scanned for 7 min with a 3T-MRI system (Achieva 3.0TX, Philips Medical Systems, Best, The Netherlands). The participants were asked to stay relaxed and to close their eyes, but not to fall asleep, in a comfortable position

TABLE 1 | Profiles of the iNPH patients and healthy controls.

	Age group	MMSE	FAB	iNPH-GS gait	iNPH-GS cognition	iNPH-GS urinary	CSF tap test
iNPH1	80–85	17	10	3	3	0	Positive
iNPH2	80–85	25	11	2	1	1	Positive
iNPH3	70–75	22	10	2	2	0	Positive
iNPH4	70–75	16	9	3	3	3	Positive
iNPH5	76–80	19	6	3	2	2	Positive
iNPH6	70–75	28	13	2	2	2	Positive
iNPH7	80–85	25	6	2	2	0	Positive
iNPH8	66–70	29	13	1	2	0	Negative
iNPH9	76–80	25	17	1	1	0	Negative
iNPH10	76–80	25	16	2	2	4	Positive
iNPH11	86–90	20	12	2	3	2	Positive
iNPH (mean ± *SD*)	78.2 ± 6.8	22.8 ± 4.3	11.2 ± 3.5	2.1 ± 0.7	2.1 ± 0.7	1.3 ± 1.4	
Control (mean ± *SD*)	69.8 ± 13.6	28.9 ± 1.0	NA	NA	NA	NA	NA

MMSE, Mini-Mental State Examination; FAB, Frontal Assessment Battery; iNPH-GS, idiopathic normal pressure hydrocephalus grading scale; NA, not available.

within the scanner. They were also instructed not to think about anything in particular, and not to imagine specific figures or scenes. RsfcMRI data were acquired with a T_2*-weighted echo-planer imaging (EPI) sequence using the following parameters: repetition time (TR) = 3,000 ms, echo time (TE) = 30 ms, flip angle (FA) = 90°, 3-mm slice thickness with a 1-mm gap, voxel size = 1.875 × 1.875 × 3 mm, and 34 slices (descending order). In total, 120 volumes were acquired, and the first 4 volumes were discarded to exclude signal changes arising from T1 saturation effects.

Extracting Functional Connectivity

Preprocessing of the rsfcMRI data was conducted with Statistical Parametric Mapping 8 (SPM8, Well-come Department of Imaging Neuroscience, London, UK) implemented on MATLAB (MATHWORKS, Inc., MA, USA). After slice-timing correction was applied to the EPI images, the images were realigned to the first image, using a rigid-body transformation for correcting head motion. Then, the images were spatially normalized to the EPI image template conforming to the Montreal Neurological Institute (MNI) space, using the SPM normalization algorithm. These normalized images were resampled to a 3 × 3 × 3-mm^3 voxel size. The normalized EPI images were then spatially smoothed with an isotropic Gaussian kernel of 6-mm full width at half maximum. In addition, we computed gray matter, white matter and cerebrospinal fluid (CSF) images as binary masks for later use. High-quality three-dimensional anatomical images were available for the healthy controls, but not for the iNPH patients due to the limitation of scanning time. To avoid introducing a bias to the WM/CSF mask images between the groups, we directly segmented the normalized EPI images into GM, WM, and CSF images in both groups, by using a segmentation algorithm implemented in SPM8. The purpose of the segmentation here was to create masks for WM and CSF to compute signals to be regressed out from the data (denoising). This is recommended for the analysis of rsfMRI since signals from CSF and WM produce pseudo-correlations, resulting in non-zero mean and large standard deviations of the functional connectivity data (Whitfield-Gabrieli and Nieto-Castanon, 2012) For the quality check of our de-noising procedure using the EPI-derived WM, and CSF masks, we computed the degree to which false correlation was corrected by removing the signal from WM, and CSF. The QC results showed that the distribution of correlation coefficients was reasonably corrected to nearby zero mean and small standard deviation (before removal; average of mean = 0.18, average of standard deviation = 0.40, after removal; average of mean = 0.09, average of standard deviation = 0.21). Judging from this QC result, we believe that segmentation procedure has provided WM/CSF signals of reasonable quality to reduce the pseudo-correlation.

After these preprocessing steps, the CONN toolbox (Whitfield-Gabrieli and Nieto-Castanon, 2012) was used for conducting a region-of-interest (ROI)-to-ROI analysis to compute RSFC, indexing the degree of correlation between MRI signal time-courses in each pair of ROIs. For defining ROIs, 90 ROIs were defined according to the automated anatomical labeling (AAL) template implemented in the WFU Pickatlas (Tzourio-Mazoyer et al., 2002; Maldjian et al., 2003). First, we used standard AAL ROIs to compute FC. However, in this procedure, some ROIs overlapped the enlarged ventricles only in the iNPH group. To reduce the effects of the ventricle enlargement onto signals from ROIs, we next created modified AAL ROIs, by removing the intersection of the AAL, and the iNPH ventricle template. The iNPH ventricle template represented a map of voxels affected by enlarged ventricle in a group of iNPH patients compared with a group of healthy elderly subjects (Yamashita et al., 2010). We applied the same set of the modified AAL ROIs to the iNPH patients and healthy subjects. Because the results of SVM classification were essentially the same between the standard and modified AAL versions, we only described the results from the modified AAL approach for simplicity. For the removal of signals of no interest, signals correlated with six motion parameters from the realignment procedure and signals derived from the entire WM and CSF

mask were regressed out in each participant, by using a general linear model-based multiple regression.

After that, a signal time-series averaged across voxels was extracted from each ROI. Next, all of the confound-removed time course data underwent band-pass filtering of 0.001–0.1 Hz. Then, the correlation coefficient of the BOLD signal time-course was computed between all the pairs of ROIs, and Fisher's z-transform was applied for each coefficient, yielding an FC matrix including all the ROI pairs in each participant.

Classification Analysis Using Support-Vector Machine

We tested whether RSFC information could classify each participant into the iNPH group or the HC group. To do so, we used a linear SVM, a machine-learning algorithm implemented in the e1071 machine-learning package of R version 3.1.3. SVM is a method for classifying data consisting of multi-dimensional features. SVM labels each data input by computing a hyperplane that best classifies the data in the feature space. Under the context of supervised machine learning, SVM identifies the closest data to a hyperplane as sample (or representative) data, and reconfigures the hyperplane to maximize the distance between the sample data with different labels. We used a z-transformed FC between each ROI pair as a feature and computed weights on the FC for successful classification of the iNPH and HC groups. We also tested if RSFC was able to predict the severity of iNPH patients (i.e., iNPH-GS). For the prediction of iNPH-GS, multi-class SVM with a one-against-all classification method was used. Because the iNPH-GS score of iNPH participants in the present cohort varied from 0 to 3 in the gait assessment, from 0 to 3 in the cognitive assessment, from 0 to 4 in the urinary assessment, these scores were set as a label for classification. Because of the limited number of participants, we included data from healthy volunteers for the training of SVM. Because iNPH-GS assessment was not available for the HC group, the label of these data was assumed to be 0 (normal). First, all the FC pairs were fed in to the SVM algorithm in both analyses as feature quantity. All of the features were scaled internally to zero mean and unit variance. The SVM model was constructed with parameters as follows: linear kernel function, C-classification algorithm, and cost factor = 1. Also, to avoid a bias arising from the asymmetry of labels, we defined class the weight vector as 1 divided by number of each labels (Chang and Lin, 2011). Second, we used a feature selection method with a *t*-test filter to reduce the feature dimension in view of the excess of features against the number of data samples (Craddock et al., 2009). For the *t*-test filter, we applied a two-sample *t*-test on the FC comparing between iNPH and HC, and then employed FC with a difference (p-value threshold = 0.05). To validate the SVM model for predicting a new data set, we employed a leave-one-out cross validation (LOOCV) procedure. In the LOOCV analysis, an SVM was trained with FC from a randomly selected 21 out of the 22 participants. After learning, the performance of the SVM classifier was tested to classify the remaining participant. After this procedure was repeated until the FC from every participant had become the test data, we calculated the classification accuracy as the number of correct labels divided by the number of LOOCV tests. To evaluate the specificity of classification accuracy for iNPH patients, we limited the LOOCV test round to the data derived from the iNPH patients in the iNPH-GS classification. A binomial test was used to determine the significance of the classification accuracy.

RESULTS

Classification between iNPH and HC

When the SVM was trained with all 4,005 pairs of the FC (no feature selection), the classifier was able to distinguish iNPH from HC with an accuracy of 63% (**Figure 1**), which was not significantly different from chance level (binominal test, 14 of 22 LOOCV tests, $p = 0.28$). However, when the SVM was trained with 476 features after the feature selection (*t*-test filtering), classification accuracy was 81% (**Figure 1**), which was significantly above chance level (18 of 22 tests, $p < 0.01$).

To clarify which FC was important for the classification, we assessed SVM weights, representing the degree of contribution of each FC to the classification. We found that relatively high weights were placed onto the FC between the left superior temporal pole and left inferior frontal operculum, the bilateral insula, the left middle temporal pole, and right hippocampus, the right superior medial frontal cortex, and left superior orbitofrontal cortex, and the left paracentral lobule, and left medial frontal cortex. Interhemispheric connectivity accounted for more than half (56%) of the FCs that contributed to the classification after the *t*-test filtering. **Figure 2**, **Table 2** show the top 20 FC with high-level weights. These 20 weights accounted for 15.6% of the total weights.

Prediction of iNPH-GS

We next tested whether the RSFCs contained information about the severity of iNPH-related symptoms. Specifically, we applied SVM with LOOCV to FCs to predict the level of gait disturbance,

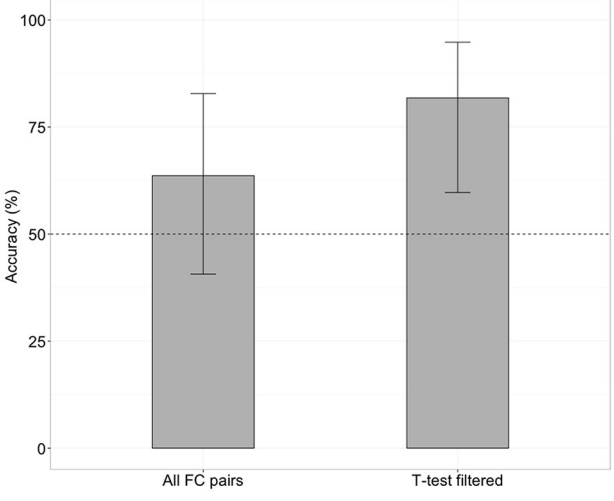

FIGURE 1 | Classification accuracy without **(left)** and with **(right)** future selection. Error bars mean 95% confidence interval from a binomial test.

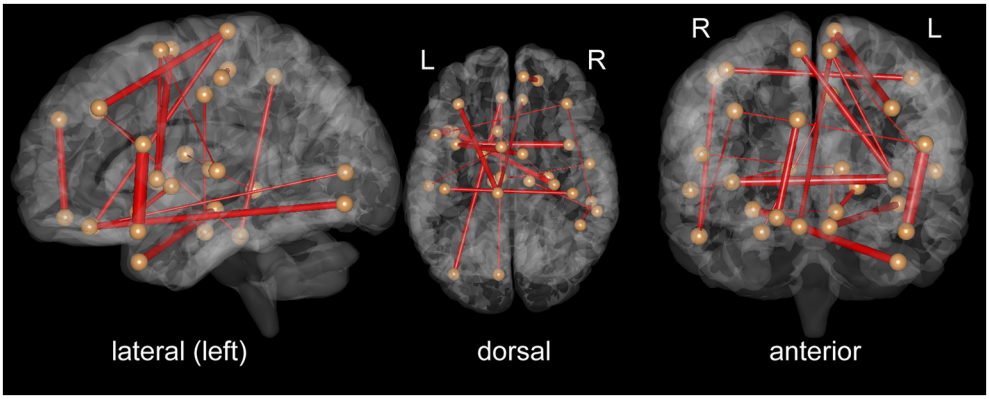

FIGURE 2 | Top 20 functional connectivity pairs contributing to the classification between iNPH and HC groups in the views from the left **(left)**, top **(middle)**, front **(right)**. The spheres represent the barycenter of ROIs, and the lines connecting spheres stand for edges with high SVM weights listed in **Table 2**. The thickness of the lines represents relative SVM weights.

TABLE 2 | SVM weights contributing to the classification of iNPH and HC.

Functional connectivity	Weight of SVM
L superior temporal pole–L inferior frontal operculum	0.0072
R insula–L insula	0.0064
L middle temporal pole–R hippocampus	0.0061
R superior frontal gyrus, medial orbital–L superior frontal gyrus, orbital part	0.0059
L paracentral lobule–L medial frontal cortex	0.0059
L inferior occipital gyrus–L gyrus rectus	0.0058
L insula–R supplementary motor area	0.0058
R postcentral gyrus–L postcentral gyrus	0.0055
R inferior temporal gyrus–R inferior parietal gyrus	0.0054
L paracentral lobule–R gyrus rectus	0.0053
L pallidum–L olfactory cortex	0.0052
L insula–L supplementary motor area	0.0049
L calcarine fissure–L gyrus rectus	0.0048
R parahippocampal gyrus–L median cingulate gyrus	0.0047
R inferior temporal gyrus–R middle frontal gyrus	0.0046
R middle temporal gyrus–R thalamus	0.0046
L superior temporal gyrus–L supplementary motor area	0.0045
L inferior frontal gyrus, opercular part–R middle frontal gyrus	0.0045
L thalamus–R rolandic operculum	0.0044
R hippocampus–L olfactory cortex	0.0043

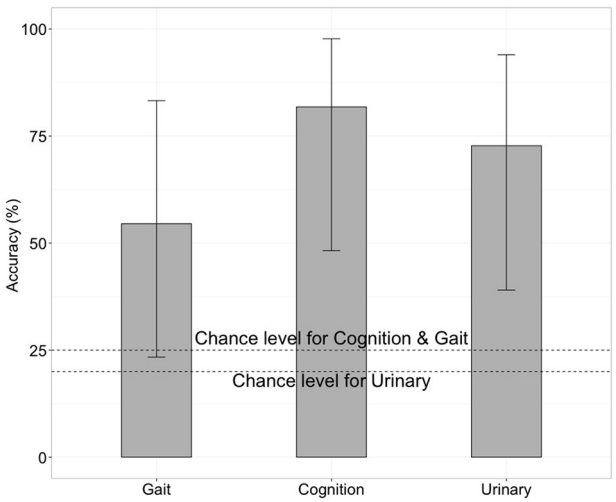

FIGURE 3 | Classification accuracy for severity of iNPH symptoms when we limited the test round to the data derived from the iNPH patients, using functional connectivity as the classification feature. Error bars mean 95% confidence interval of binomial test.

cognitive impairment and urinary incontinence as indexed by iNPH-GS. This was done after the feature selection by applying *t*-test filtering comparing the two groups as described above. We found that FC contained significant information concerning the severity of iNPH (**Figure 3**). Classification accuracy was significantly higher than chance when we limited the test round to the data derived from the iNPH patients: 81% for the iNPH-GS cognition (9 out of 11 tests, $p < 0.05$ by a binominal test), 55% for the iNPH-GS gait (6 out of 11 tests, $p < 0.001$), and 72% for the iNPH-GS urinary score (8 tests of 11 tests, $p < 1.0 \times 10^{-7}$).

For all the three symptoms, the assessment of SVM weights indicated the importance of inter-hemispheric functional connectivity. The top 30 FCs with high contributions to classification are shown in **Tables 3–5**; **Figure 4**. The sum of these top 30 weights accounts for 16.9% of the total weights for iNPH-GS gait, 16.4% for iNPH-GS cognition, and 15.0% for iNPH-GS urinary incontinence.

To confirm the significance of inter-hemispheric FC for classification, we calculated the sum of weights of inter-hemispheric FC and that of intra-hemispheric FC, all of which contributed to the prediction of iNPH-GS (**Table 6**).

The results showed greater contribution of the inter-hemispheric FC than that of the intra-hemispheric FC significantly for gait ($p = 0.02$, Wilcoxon rank-sum test),

TABLE 3 | SVM weight for classification with iNPH grading scale for gait disturbance.

Functional connectivity	Weight of SVM
iNPH-GS gait	
R postcentral gyrus–L postcentral gyrus	0.048
R paracentral lobule–L paracentral lobule	0.047
R median cingulate gyri–L median cingulate gyri	0.047
R superior frontal gyrus, medial orbital–L superior frontal gyrus, medial orbital	0.046
R cuneus–R calcarine fissure	0.046
R superior frontal gyrus, medial orbital–R superior frontal gyrus, dorsolateral	0.042
R cuneus–L calcarine fissure	0.041
L superior occipital gyrus–L calcarine fissure	0.039
R paracentral lobule–R supplementary motor area	0.038
R inferior frontal gyrus, orbital part–L inferior frontal gyrus, orbital part	0.036
R supplementary motor area–R precentral gyrus	0.036
L paracentral lobule–R supplementary motor area	0.036
L paracentral lobule–R postcentral gyrus	0.036
R angular gyrus–R middle frontal gyrus, orbital part	0.035
L supplementary motor area–L precentral gyrus	0.034
R supplementary motor area–L precentral gyrus	0.033
R inferior temporal gyrus–L inferior temporal gyrus	0.032
R postcentral gyrus–R supplementary motor area	0.032
L paracentral lobule–R precentral gyrus	0.031
L superior frontal gyrus, medial orbital–R superior frontal gyrus, dorsolateral	0.030
R rolandic operculum–L rolandic operculum	0.030
R inferior frontal gyrus, opercular part–R middle frontal gyrus	0.030
R insula–L insula	0.030
R middle temporal gyrus–L superior temporal gyrus	0.030
R precuneus–R superior frontal gyrus, dorsolateral	0.028
R superior frontal gyrus, medial orbital–R middle frontal gyrus	0.028
R hippocampus–L hippocampus	0.028
L middle frontal gyrus, orbital part–L superior frontal gyrus, orbital part	0.028
R inferior frontal gyrus, opercular part–L inferior frontal gyrus, opercular part	0.028
L inferior frontal gyrus, orbital part–L superior frontal gyrus, orbital part	0.028

Bold fonts indicate interhemispheric connectivity.

TABLE 4 | SVM weight for classification with iNPH grading scale for cognitive impairment.

Functional connectivity	Weight of SVM
iNPH-GS cognition	
R superior frontal gyrus, medial orbital–L superior frontal gyrus, medial orbital	0.053
R superior frontal gyrus, medial orbital–R superior frontal gyrus, dorsolateral	0.050
R median cingulate gyri–L median cingulate gyri	0.049
R postcentral gyrus–L postcentral gyrus	0.047
R paracentral lobule–L paracentral lobule	0.046
R cuneus–R calcarine fissure	0.045
R cuneus–L calcarine fissure	0.041
R insular cortex–L insular cortex	0.041
L superior occipital gyrus–L calcarine fissure	0.038
L supplementary motor area–L precentral gyrus	0.038
R supplementary motor area–R precentral gyrus	0.036
R precuneus–R angular gyrus	0.036
R inferior frontal gyrus, orbital part–L inferior frontal gyrus, orbital part	0.036
R angular gyrus–R middle frontal gyrus, orbital part	0.035
L paracentral lobule–R supplementary motor area	0.035
R paracentral lobule–R supplementary motor area	0.034
R angular gyrus–R posterior cingulate gyrus	0.034
R hippocampus–L hippocampus	0.033
L paracentral lobule–R postcentral gyrus	0.033
R rolandic operculum–L rolandic operculum	0.033
R inferior frontal gyrus, opercular part–R middle frontal gyrus	0.033
R superior frontal gyrus, medial orbital–R middle frontal gyrus	0.033
L middle frontal gyrus, orbital part–L superior frontal gyrus, orbital part	0.032
L superior frontal gyrus, medial orbital–R superior frontal gyrus, dorsolateral	0.032
R precuneus–R superior frontal gyrus, dorsolateral	0.032
R postcentral gyrus–R supplementary motor area	0.032
R inferior frontal gyrus, opercular part–L inferior frontal gyrus, opercular part	0.031
R middle temporal gyrus–R precuneus	0.031
R supplementary motor area–L precentral gyrus	0.030
L precuneus–R superior frontal gyrus, dorsolateral	0.029

Bold font indicates interhemispheric connectivity.

cognition ($p = 0.002$), and marginally for urinary symptoms ($p = 0.07$).

DISCUSSION

The SVM classifier, combined with feature selection, was able to learn differences in high-dimensional FCs between the iNPH patients, and the healthy controls, thereby successfully classifying each participant with an accuracy of 80%. Considering the importance, and difficulty of a clinical diagnosis of iNPH, rsfcMRI is promising as a tool for providing a biomarker for the diagnosis of iNPH. Furthermore, the assessment of the spatial distribution of FC contributing to classification has shed light on the pathophysiology of iNPH.

FCs having relevance to the classification of iNPH included the superior temporal pole, middle temporal pole, insula, orbitofrontal cortex, and medial frontal cortex. Almost all of these areas were located near the enlarged cerebral sulci (i.e., increased CSF space) in iNPH patients as shown in a previous voxel-based morphometry study (Yamashita et al., 2010, 2014). In a study by Lenfeldt et al. (2008), the left dorsal premotor cortex and bilateral supplementary motor areas (SMA) showed enhanced activation during hand motor task performance after a three-day continuous CSF drainage in iNPH patients (Lenfeldt et al., 2008). In the present study, FC between insula and SMA, and between bilateral postcentral gyri showed relatively high

TABLE 5 | SVM weight for classification with iNPH grading scale for urinary incontinence.

Functional connectivity	Weight of SVM
iNPH-GS urinary	
R superior frontal gyrus, medial orbital–L superior frontal gyrus, medial orbital	0.047
R median cingulate gyri–L median cingulate gyri	0.043
R superior frontal gyrus, medial orbita–R superior frontal gyrus, dorsolateral	0.042
R postcentral gyrus–L postcentral gyrus	0.036
R paracentral lobule–L paracentral lobule	0.035
R superior frontal gyrus, medial orbital–R middle frontal gyrus	0.034
R cuneus–R calcarine fissure	0.034
R cuneus–L calcarine fissure	0.034
R hippocampus–L hippocampus	0.032
R insular cortex–L insular cortex	0.032
R inferior frontal gyrus, orbital part–L inferior frontal gyrus, orbital part	0.032
R precuneus–R superior frontal gyrus, dorsolateral	0.032
R inferior frontal gyrus, opercular part–R middle frontal gyrus	0.031
L superior frontal gyrus, medial orbital–R superior frontal gyrus, dorsolateral	0.031
L supplementary motor area–L precentral gyrus	0.030
R angular gyrus–R middle frontal gyrus, orbital part	0.030
L precuneus–R superior frontal gyrus, dorsolateral	0.029
R supplementary motor area–R precentral gyrus	0.029
L superior occipital gyrus–L calcarine fissure	0.028
R inferior frontal gyrus, opercular part–L inferior frontal gyrus, opercular part	0.028
L paracentral lobule–R supplementary motor area	0.028
L inferior frontal gyrus, orbital part–L superior frontal gyrus, orbital part	0.028
L inferior frontal gyrus, opercular part–L middle frontal gyrus	0.028
L paracentral lobule–R postcentral gyrus	0.027
R middle temporal gyrus–R superior frontal gyrus, dorsolateral	0.027
R rolandic operculum–L rolandic operculum	0.027
R angular gyrus–R posterior cingulate gyrus	0.027
L paracentral lobule–R precentral gyrus	0.026
R postcentral gyrus–R supplementary motor area	0.026
L postcentral gyrus–R supplementary motor area	0.026

Bold font indicates interhemispheric connectivity.

contribution to the classification of iNPH, and HC as indexed by the SVM weights. Additionally, it is suggested that that the effectiveness of CSF drainage possibly results from the reversal of subcortical chronic ischemia, especially in the periventricular zones (Momjian et al., 2004; Malm and Eklund, 2006; Lenfeldt et al., 2008). Our results suggest that the contribution of periventricular areas to the iNPH-HC classification may indicate the abnormality of these FCs because of the compression of fiber connections by enlarged ventricles.

Moreover, the prediction of iNPH-GS indicated the relevance of inter-hemispheric connectivity to the discrimination of the triad: gait disturbance, cognitive impairment, and urinary incontinence. This finding is consistent with the idea that damage to the inter-hemispheric connections via the corpus callosum may underlie the pathophysiology of iNPH. A majority of previous diffusion tensor imaging studies have observed lower fractional anisotropy (FA) values in the corpus callosum in iNPH patients than in normal controls. For instance, Koyama et al. showed that there was a conspicuous decline in FA values in the corpus callosum in iNPH patients, and that the degree of FA reduction was associated with the severity of gait disturbance, which is the most frequent clinical manifestation of iNPH (Koyama et al., 2012, 2013). Consistent with this result, the reduction of FA in the corpus callosum is correlated with gait disturbance and cognitive decline in patients with age-related white matter changes (Iseki et al., 2015). In this study, the corpus callosum connections are suggested to mediate information relevant to gait planning.

Previous imaging studies suggest that the micturition center is located in the pons, and that SMA is involved in the inhibitory control of the micturition reflex (Fukuyama et al., 1996; Zhang et al., 2005). Because we did not include the pons in the ROI set, the results of the present study would mainly reflect the decline of functional connections to and from the SMA related to the inhibitory control of micturition. The insular cortex and cingulate cortex are thought to be involved in the regulation of the bladder filling sensation and void control (Fowler et al., 2008; de Groat et al., 2015). In our results, the interhemispheric connectivity of cingulate cortex, and insular cortex showed respectively high weights for iNPH-GS urinary classification (see **Table 5**).

To account for cognitive impairment in iNPH, the present finding of inter-hemispheric disconnectivity in iNPH is consistent with the findings that the severity of Alzheimer's disease is correlated with the reduction of volume and FA in the corpus callosum (Chaim et al., 2007; Tomaiuolo et al., 2007). Additionally, Khoo and coworkers have demonstrated that the reduction of RSFC in the DMN was positively correlated with iNPH-GS cognition and urinary incontinence in the iNPH patients (Khoo et al., 2015). Consistent with this result, the present study showed that interhemispheric connectivity in the medial orbital part of the superior frontal gyrus, a part of the DMN, had high weight for all symptoms for iNPH-GS classification. Several researchers reported that white matter alterations in NPH include not only the reduction of FA, but also the alteration of mean diffusivity (MD) and radial diffusivity (RD) (Hattingen et al., 2010; Kanno et al., 2011). In addition, a recent study by Horinek et al. demonstrated reduced FA in the corpus callosum and increased FA, MD, and RD in the cortico-fugal fibers in NPH patients (Horinek et al., 2016). It is possible that the alteration of interhemispheric FC in the iNPH patients shown here is founded on the structural changes of the white matter indexed by those diffusion measures. In sum, the present study suggests the importance of interhemispheric functional connectivity in accounting for the triad of iNPH. For the treatment of iNPH, it is well-recognized that the symptoms are relievable by a shunt operation. The improvement of iNPH triads by CSF drainage can be explained by the idea that a shunt operation releases the compression of the corpus callosum and restores the inter-hemispheric functional connectivity. In a study

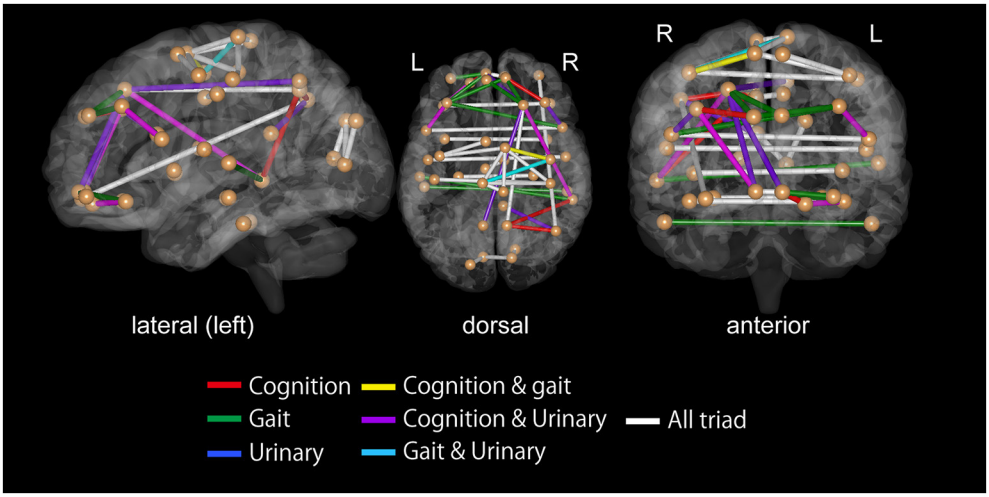

FIGURE 4 | Top 30 functional connectivity with higher SVM weights in classification for iNPH grading scale as viewed from the left **(left)**, top **(middle)**, and front **(right)**. Spheres represent the barycenter of each ROI, and lines between spheres stand for connections that showed higher SVM weights listed in **Tables 3**–**5**.

TABLE 6 | Sum of SVM weights from inter-hemispheric and intra-hemispheric connectivity contributing to prediction of iNPH-GS.

	iNPH-GS gait	iNPH-GS cognition	iNPH-GS urinary
Inter-hemispheric connectivity	3.361	3.568	4.057
Intra-hemispheric connectivity	2.873	3.190	3.441

by Scheel et al. (2012), abnormality of the corpus callosum FA in iNPH patients showed a trend toward normalization following shunt surgery. It is likely that the enlarged ventricles compressed the corpus callosum, affecting inter-hemispheric functional connectivity. The present findings also suggest that the degree of such compression and the resulting functional disconnectivity are correlated with the severity of iNPH symptoms.

This study has several limitations. First, the present data are derived from a relatively small number of participants. Moreover, we acquired data with the same MRI aperture and EPI sequences, but in different hospital sites. This was for a purely practical reason; scanning of the healthy population was not possible in one hospital, and iNPH patients were not available in the other hospital. It is possible that differences in the sites affected the characteristics of the MRI data, because between-site reliability might be relatively low compared with test-retest reliability (Friedman et al., 2008). However, Turner and collages carried out a multi-site rsfcMRI study on schizophrenia patients, and suggested that critical RSFC information important for disease classification was preserved when the scanner model, and scanning parameters were the same. In the present study, we used the same MRI model, and scanning parameters. Therefore, we believe that the difference in site did not critically impair the RSFC information important for the disease/severity classification.

Second, we were not able to associate the present findings with the information regarding treatment of iNPH, such as responsiveness to a CSF tap test. Aoki et al. (2013, 2015) found that responders to a shunt operation showed higher variance in the power of beta-frequency electroencephalography oscillations in the right fronto-temporo-occipital region than non-responders. Because a CSF tapping test is an invasive procedure and carries some risks of adverse events, we agree that predicting the responsiveness to a CSF tap test beforehand is of clinical benefit. However, we only had two negative responders to a tap test, precluding further analysis between responders, and non-responders. The question of whether rsfcMRI-derived functional connectivity can predict the responsiveness to CSF drainage should be tested in the future.

Finally, it may be possible to enhance classification accuracy by improving the machine-learning algorithm. Recently, many methods have been proposed such as linear discrimination analysis, random forest, and sparse logistic regression (Yamashita et al., 2008). We used SVM for the machine-learning classifier, because SVM does not need many samples under the condition that the number of feature dimensions is optimally reduced (Hua et al., 2005). Moreover, classification accuracy may be further improved by optimizing the cost function, kernel type, and classification algorithm. However, considering the computational cost, the exploration of the huge parameter space is beyond the scope of the present study. Future challenges include the improvement of classification accuracy by optimizing the classifiers and feature selection methods. Future challenges include the improvement of classification accuracy by optimizing the classifiers and feature selection methods.

CONCLUSION

In conclusion, a machine-learning algorithm combined with rsfcMRI data was able to discriminate between patients with iNPH and elderly controls. This result indicates

that iNPH patients have abnormalities in the RSFC, especially in inter-hemispheric functional connectivity, which contributed to the classification of clinical stages. RsfcMRI may have the potential to discriminate iNPH from other neurological diseases, contributing to a differential diagnosis of iNPH.

AUTHOR CONTRIBUTIONS

YOg designed the study, performed analyses and literature review, and drafted the manuscript. AO, MO, NN, HT, NS recruited healthy volunteers and iNPH patients and performed experiments. YOk developed experimental and analytic programs. TH designed the study and supervised the research and revised the manuscript. All the authors read and approved the final manuscript.

ACKNOWLEDGMENTS

This study was in part supported by the Strategic Research Program for Brain Science of BMI Technologies for Clinical Application carried out under the Strategic Research Program for Brain Sciences and Brain Mapping by Integrated Neurotechnologies for Disease Studies (Brain/MINDS), Health Labor Science Research Grants from Japan Agency for Medical Research and development (AMED) and KAKENHI (26120008 and 16H03306) from MEXT, the Research Grant from Saiseikai, and the Intramural Research Grant for Neurological and Psychiatric Disorders of National Center of Neurology and Psychiatry, Japan, to TH. This study was partially supported by JSPS KAKENHI Grant Number 15K16080 to YOg. This study was also in part supported by JSPS KAKENHI Grant Number 15K10378 to NN.

REFERENCES

Aoki, Y., Kazui, H., Tanaka, T., Ishii, R., Wada, T., Ikeda, S., et al. (2015). Noninvasive prediction of shunt operation outcome in idiopathic normal pressure hydrocephalus. *Sci. Rep.* 5:775. doi: 10.1038/srep07775

Aoki, Y., Kazui, H., Tanaka, T., Ishii, R., Wada, T., Ikeda, S., et al. (2013). EEG and neuronal activity topography analysis can predict effectiveness of shunt operation in idiopathic normal pressure hydrocephalus patients. *NeuroImage* 3, 522–530. doi: 10.1016/j.nicl.2013.10.009

Arbabshirani, M. R., Kiehl, K. A., Pearlson, G. D., and Calhoun, V. D. (2013). Classification of schizophrenia patients based on resting-state functional network connectivity. *Front. Neurosci.* 7:133. doi: 10.3389/fnins.2013.00133

Chaim, T. M., Duran, F. L., Uchida, R. R., Perico, C. A., de Castro, C. C., and Busatto, G. F. (2007). Volumetric reduction of the corpus callosum in Alzheimer's disease *in vivo* as assessed with voxel-based morphometry. *Psychiatry Res.* 154, 59–68. doi: 10.1016/j.pscychresns.2006.04.003

Chang, C. C., and Lin, C. J. (2011). LIBSVM: a library for support vector machines. *Acm Trans. Intell. Syst. Technol.* 2:27. doi: 10.1145/1961189.1961199

Chen, G., Ward, B. D., Xie, C., Li, W., Wu, Z., Jones, J. L., et al. (2011). Classification of Alzheimer disease, mild cognitive impairment, and normal cognitive status with large-scale network analysis based on resting-state functional MR imaging. *Radiology* 259, 213–221. doi: 10.1148/radiol.10100734

Costafreda, S. G., Fu, C. H. Y., Picchioni, M., Toulopoulou, T., McDonald, C., Kravariti, E., et al. (2011). Pattern of neural responses to verbal fluency shows diagnostic specificity for schizophrenia and bipolar disorder. *BMC Psychiatry* 11:18. doi: 10.1186/1471-244X-11-18

Craddock, R. C., Holtzheimer, P. E. III, Hu, X. P., and Mayberg, H. S. (2009). Disease state prediction from resting state functional connectivity. *Magn. Reson. Med.* 62, 1619–1628. doi: 10.1002/mrm.22159

Damoiseaux, J. S., Rombouts, S., Barkhof, F., Scheltens, P., Stam, C. J., Smith, S. M., et al. (2006). Consistent resting-state networks across healthy subjects. *Proc. Natl. Acad. Sci. U.S.A.* 103, 13848–13853. doi: 10.1073/pnas.0601417103

de Groat, W. C., Griffiths, D., and Yoshimura, N. (2015). Neural control of the lower urinary tract. *Compr. Physiol.* 5, 327–396. doi: 10.1002/cphy.c130056

Fowler, C. J., Griffiths, D., and de Groat, W. C. (2008). The neural control of micturition. *Nat. Rev. Neurosci.* 9, 453–466. doi: 10.1038/nrn2401

Friedman, L., Stern, H., Brown, G. G., Mathalon, D. H., Turner, J., Glover, G. H., et al. (2008). Test–retest and between-site reliability in a multicenter fMRI study. *Hum. Brain Mapp.* 29, 958–972. doi: 10.1002/hbm.20440

Fukuyama, H., Matsuzaki, S., Ouchi, Y., Yamauchi, H., Nagahama, Y., Kimura, J., et al. (1996). Neural control of micturition in man examined with single photon emission computed tomography using 99mTc-HMPAO. *Neuroreport* 7, 3009–3012. doi: 10.1097/00001756-199611250-00042

Greicius, M. D., Srivastava, G., Reiss, A. L., and Menon, V. (2004). Default-mode network activity distinguishes Alzheimer's disease from healthy aging: evidence from functional MRI. *Proc. Natl. Acad. Sci. U.S.A.* 101, 4637–4642. doi: 10.1073/pnas.0308627101

Hattingen, E., Jurcoane, A., Melber, J., Blasel, S., Zanella, F. E., Neumann-Haefelin, T., et al. (2010). Diffusion tensor imaging in patients with adult chronic idiopathic hydrocephalus. *Neurosurgery* 66, 917–924. doi: 10.1227/01.NEU.0000367801.35654.EC

Horinek, D., Stepan-Buksakowska, I., Szabo, N., Erickson, B. J., Toth, E., Sulc, V., et al. (2016). Difference in white matter microstructure in differential diagnosis of normal pressure hydrocephalus and Alzheimer's disease. *Clin. Neurol. Neurosurg.* 140, 52–59. doi: 10.1016/j.clineuro.2015.11.010

Hua, J., Xiong, Z., Lowey, J., Suh, E., and Dougherty, E. R. (2005). Optimal number of features as a function of sample size for various classification rules. *Bioinformatics* 21, 1509–1515. doi: 10.1093/bioinformatics/bti171

Iseki, K., Fukuyama, H., Oishi, N., Tomimoto, H., Otsuka, Y., Nankaku, M., et al. (2015). Freezing of gait and white matter changes: a tract-based spatial statistics study. *J. Clin. Mov. Disord.* 2:1. doi: 10.1186/s40734-014-0011-2

Ishikawa, M. (2004). Clinical guidelines for idiopathic normal pressure hydrocephalus. *Neurol. Med. Chir.* 44, 222–223. doi: 10.2176/nmc.44.222

Ishikawa, M., Hashimoto, M., Kuwana, N., Mori, E., Miyake, H., Wachi, A., et al. (2008). Guidelines for management of idiopathic normal pressure hydrocephalus. *Neurol. Med. Chir.* 48, S1–S23. doi: 10.2176/nmc.48.S1

Jingami, N., Asada-Utsugi, M., Uemura, K., Noto, R., Takahashi, M., Ozaki, A., et al. (2015). Idiopathic normal pressure hydrocephalus has a different cerebrospinal fluid biomarker profile from Alzheimer's disease. *J. Alzheimers. Dis.* 45, 109–115. doi: 10.3233/JAD-142622

Kanno, S., Abe, N., Saito, M., Takagi, M., Nishio, Y., Hayashi, A., et al. (2011). White matter involvement in idiopathic normal pressure hydrocephalus: a voxel-based diffusion tensor imaging study. *J. Neurol.* 258, 1949–1957. doi: 10.1007/s00415-011-6038-5

Khoo, H. M., Kishima, H., Tani, N., Oshino, S., Maruo, T., Hosomi, K., et al. (2015). Default mode network connectivity in patients with idiopathic normal pressure hydrocephalus. *J. Neurosurg.* 124, 350–358. doi: 10.3171/2015.1.JNS141633

Kitagaki, H., Mori, E., Ishii, K., Yamaji, S., Hirono, N., and Imamura, T. (1998). CSF spaces in idiopathic normal pressure hydrocephalus: morphology and volumetry. *Am. J. Neuroradiol.* 19, 1277–1284.

Koyama, T., Marumoto, K., Domen, K., and Miyake, H. (2013). White matter characteristics of idiopathic normal pressure hydrocephalus: a diffusion tensor tract-based spatial statistic study. *Neurol. Med. Chir.* 53, 601–608. doi: 10.2176/nmc.oa2012-0307

Koyama, T., Marumoto, K., Domen, K., Ohmura, T., and Miyake, H. (2012). Diffusion tensor imaging of idiopathic normal pressure hydrocephalus: a voxel-based fractional anisotropy study. *Neurol. Med. Chir.* 52, 68–74. doi: 10.2176/nmc.52.68

Kubo, Y., Kazui, H., Yoshida, T., Kito, Y., Kimura, N., Tokunaga, H., et al. (2008). Validation of grading scale for evaluating symptoms of idiopathic

normal-pressure hydrocephalus. *Dement. Geriatr. Cogn. Disord.* 25, 37–45. doi: 10.1159/000111149

Leinonen, V., Menon, L. G., Carroll, R. S., Dello Iacono, D., Grevet, J., Jaaskelainen, J. E., et al. (2011). Cerebrospinal fluid biomarkers in idiopathic normal pressure hydrocephalus. *Int. J. Alzheimers. Dis.* 2011:312526. doi: 10.4061/2011/312526

Lenfeldt, N., Larsson, A., Nyberg, L., Andersson, M., Birgander, R., Eklund, A., et al. (2008). Idiopathic normal pressure hydrocephalus: increased supplementary motor activity accounts for improvement after CSF drainage. *Brain* 131, 2904–2912. doi: 10.1093/brain/awn232

Maldjian, J. A., Laurienti, P. J., Kraft, R. A., and Burdette, J. H. (2003). An automated method for neuroanatomic and cytoarchitectonic atlas-based interrogation of fMRI data sets. *Neuroimage* 19, 1233–1239. doi: 10.1016/S1053-8119(03)00169-1

Malm, J., and Eklund, A. (2006). Idiopathic normal pressure hydrocephalus. *Pract. Neurol.* 6, 14–27. doi: 10.1136/jnnp.2006.088351

Momjian, S., Owler, B. K., Czosnyka, Z., Czosnyka, M., Pena, A., and Pickard, J. D. (2004). Pattern of white matter regional cerebral blood flow and autoregulation in normal pressure hydrocephalus. *Brain* 127, 965–972. doi: 10.1093/brain/awh131

Mori, E., Ishikawa, M., Kato, T., Kazui, H., Miyake, H., Miyajima, M., et al. (2012). Guidelines for management of idiopathic normal pressure hydrocephalus: second edition. *Neurol. Med. Chir.* 52, 775–809. doi: 10.2176/nmc.52.775

Orru, G., Pettersson-Yeo, W., Marquand, A. F., Sartori, G., and Mechelli, A. (2012). Using support vector machine to identify imaging biomarkers of neurological and psychiatric disease: a critical review. *Neurosci. Biobehav. Rev.* 36, 1140–1152. doi: 10.1016/j.neubiorev.2012.01.004

Sakakibara, R., Uchida, Y., Ishii, K., Kazui, H., Hashimoto, M., Ishikawa, M., et al. (2012). Correlation of right frontal hypoperfusion and urinary dysfunction in iNPH: A SPECT study. *Neurourol. Urodyn.* 31, 50–55. doi: 10.1002/nau.21222

Scheel, M., Diekhoff, T., Sprung, C., and Hoffmann, K.-T. (2012). Diffusion tensor imaging in hydrocephalus-findings before and after shunt surgery. *Acta Neurochir.* 154, 1699–1706. doi: 10.1007/s00701-012-1377-2

Takamura, T., and Hanakawa, T. (2017). Clinical utility of resting-state functional connectivity magnetic resonance imaging for mood and cognitive disorders. *J. Neural Transm.* 124, 821–839. doi: 10.1007/s00702-017-1710-2

Tomaiuolo, F., Scapin, M., Di Paola, M., Le Nezet, P., Fadda, L., Musicco, M., et al. (2007). Gross anatomy of the corpus callosum in Alzheimer's disease: regions of degeneration and their neuropsychological correlates. *Dement. Geriatr. Cogn. Disord.* 23, 96–103. doi: 10.1159/000097371

Tzourio-Mazoyer, N., Landeau, B., Papathanassiou, D., Crivello, F., Etard, O., Delcroix, N., et al. (2002). Automated anatomical labeling of activations in SPM using a macroscopic anatomical parcellation of the MNI MRI single-subject brain. *Neuroimage* 15, 273–289. doi: 10.1006/nimg.2001.0978

Wee, C. Y., Yap, P. T., Zhang, D. Q., Denny, K., Browndyke, J. N., Potter, G. G., et al. (2012). Identification of MCI individuals using structural and functional connectivity networks. *Neuroimage* 59, 2045–2056. doi: 10.1016/j.neuroimage.2011.10.015

Whitfield-Gabrieli, S., and Nieto-Castanon, A. (2012). Conn: a functional connectivity toolbox for correlated and anticorrelated brain networks. *Brain Connect.* 2, 125–141. doi: 10.1089/brain.2012.0073

Yamashita, F., Sasaki, M., Saito, M., Mori, E., Kawaguchi, A., Kudo, K., et al. (2014). Voxel-based morphometry of disproportionate cerebrospinal fluid space distribution for the differential diagnosis of idiopathic normal pressure hydrocephalus. *J. Neuroimaging* 24, 359–365. doi: 10.1111/jon.12049

Yamashita, F., Sasaki, M., Takahashi, S., Matsuda, H., Kudo, K., Narumi, S., et al. (2010). Detection of changes in cerebrospinal fluid space in idiopathic normal pressure hydrocephalus using voxel-based morphometry. *Neuroradiology* 52, 381–386. doi: 10.1007/s00234-009-0610-z

Yamashita, O., Sato, M., Yoshioka, T., Tong, F., and Kamitani, Y. (2008). Sparse estimation automatically selects voxels relevant for the decoding of fMRI activity patterns. *Neuroimage* 42, 1414–1429. doi: 10.1016/j.neuroimage.2008.05.050

Zeng, L. L., Shen, H., Liu, L., Wang, L. B., Li, B. J., Fang, P., et al. (2012). Identifying major depression using whole-brain functional connectivity: a multivariate pattern analysis. *Brain* 135, 1498–1507. doi: 10.1093/brain/aws059

Zhang, H., Reitz, A., Kollias, S., Summers, P., Curt, A., and Schurch, B. (2005). An fMRI study of the role of suprapontine brain structures in the voluntary voiding control induced by pelvic floor contraction. *Neuroimage* 24, 174–180. doi: 10.1016/j.neuroimage.2004.08.027

Zhang, H.-Y., Wang, S.-J., Liu, B., Ma, Z.-L., Yang, M., Zhang, Z.-J., et al. (2010). Resting brain connectivity: changes during the progress of Alzheimer disease. *Radiology* 256, 598–606. doi: 10.1148/radiol.10091701

Conflict of Interest Statement: The authors declare that the research was conducted in the absence of any commercial or financial relationships that could be construed as a potential conflict of interest.

frontiers in Neuroscience

ORIGINAL RESEARCH
published: 03 August 2017
doi: 10.3389/fnins.2017.00444

Impairment of Long-Term Plasticity of Cerebellar Purkinje Cells Eliminates the Effect of Anodal Direct Current Stimulation on Vestibulo-Ocular Reflex Habituation

*Suman Das[1,2,3], Marcella Spoor[2], Tafadzwa M. Sibindi[2], Peter Holland[1,2], Martijn Schonewille[2], Chris I. De Zeeuw[2,4], Maarten A. Frens[2,5] and Opher Donchin[1,2]**

[1] Department of Biomedical Engineering and Zlotowski Center for Neuroscience, Ben Gurion University of the Negev, Be'er Sheva, Israel, [2] Department of Neuroscience, Erasmus Medical Center, Rotterdam, Netherlands, [3] Department of Integrative Neurophysiology, Center for Neurogenomics and Cognitive Research, Vrije Universiteit Amsterdam, Amsterdam, Netherlands, [4] Netherlands Institute for Neuroscience, Amsterdam, Netherlands, [5] Faculty of Social and Behavioral Sciences, Erasmus University College, Erasmus University, Rotterdam, Netherlands

OPEN ACCESS

Edited by:
Luca Berdondini, Fondazione Istituto Italiano di Technologia, Italy

Reviewed by:
Stefano Vassanelli, University of Padua, Italy
Enrique Claverol, Universitat Politecnica de Catalunya, Spain

***Correspondence:**
Opher Donchin
donchin@bgu.ac.il

Specialty section:
This article was submitted to Neural Technology, a section of the journal Frontiers in Neuroscience

Received: *12 February 2017*
Accepted: *20 July 2017*
Published: *03 August 2017*

Citation:
Das S, Spoor M, Sibindi TM, Holland P, Schonewille M, De Zeeuw CI, Frens MA and Donchin O (2017) Impairment of Long-Term Plasticity of Cerebellar Purkinje Cells Eliminates the Effect of Anodal Direct Current Stimulation on Vestibulo-Ocular Reflex Habituation. Front. Neurosci. 11:444. doi: 10.3389/fnins.2017.00444

Anodal direct current stimulation (DCS) of the cerebellum facilitates adaptation tasks, but the mechanism underlying this effect is poorly understood. We have evaluated whether the effects of DCS effects depend on plasticity of cerebellar Purkinje cells (PCs). Here, we have successfully developed a mouse model of cerebellar DCS, allowing us to present the first demonstration of cerebellar DCS driven behavioral changes in rodents. We have utilized a simple gain down vestibulo-ocular reflex (VOR) adaptation paradigm, that stabilizes a visual image on the retina during brief head movements, as behavioral tool. Our results provide evidence that anodal stimulation has an acute post-stimulation effect on baseline gain reduction of VOR (VOR gain in sham, anodal and cathodal groups are 0.75 ± 0.12, 0.68 ± 0.1, and 0.78 ± 0.05, respectively). Moreover, this anodal induced decrease in VOR gain is directly dependent on the PP2B medicated synaptic long-term potentiation (LTP) and intrinsic plasticity pathways of PCs.

Keywords: tDCS, LTP, purkinje cell, vor, cerebellum

INTRODUCTION

Transcranial direct current stimulation (tDCS) modulates cerebellar dependent motor learning tasks (Jayaram et al., 2012; Hardwick and Celnik, 2014; Herzfeld et al., 2014; Avila et al., 2015) by applying a weak constant electrical current (amplitude <2 mA) through scalp electrodes. This technique allows us to stimulate the target region by the positive (anodal) or negative (cathodal) current (Das et al., 2016). Data collected in humans suggests that polarity specific effects of tDCS may be obtained by changing cerebellar cortical excitability (Galea et al., 2009). However, the mechanism behind tDCS dependent modulation of motor learning is unclear (Das et al., 2016). To optimally use tDCS in various cerebellar dependent motor learning disorders, a better understanding of mechanisms is vital (Ivry and Spencer, 2004; Xu-Wilson et al., 2009; Bastian, 2011; Hardwick and Celnik, 2014; Benussi et al., 2015).

Various animal models of DCS (direct current stimulation that is not transcranial) serve in exploration of the mechanism of tDCS (Creutzfeldt et al., 1962; Bindman et al., 1964; Purpura and Mcmurtry, 1965). In these models, a small part of the skull is removed at the site of stimulation in order to reduce the inter-subject variability of transcranial-conductance.

Our current study aims to explore the mechanism of action of DCS on cerebellar learning. To probe polarity specific effects of DCS on cerebellar learning, we employed a gain-down vestibulo-ocular reflex (VOR) adaptation task. The VOR aims to compensate for head movement by making an eye movement in the opposite direction, in order to stabilize the image on the retina (Probst et al., 1986). This compensatory eye movement can be adapted based on mismatched visual input, a process that requires the cerebellum (Kawato and Gomi, 1992). Here we presented a sinusoidal optokinetic stimulation by using a 360° virtual environment and vestibular stimulus by using a turntable in phase, resulting in a decrease of the response to the same vestibular stimulus in the dark (Tempia et al., 1991). The turntable mimics the head movement while the movement direction of the virtual environment demands orientation specific compensation of the eye movement (similar to the natural environment).

The gain-down adaptation of the VOR (Tiliket et al., 1993) may depend partly on both the cerebellar flocculus and the downstream vestibular nuclei (VN) (Lisberger and Fuchs, 1974; Ito, 1982). To test the importance of Purkinje cell (PC) plasticity in polarity-specific DCS modulation, we investigated L7-PP2B mice, lacking postsynaptic and intrinsic plasticity of PC (Schonewille et al., 2010). Our prediction is that at least some DCS effects (caused either by anodal or cathodal stimulation) would be compromised in this mutant because DCS has an extensive modulatory role on PC dendrites (Chan and Nicholson, 1986; Chan et al., 1988).

A rodent model of DCS has been validated in cortical spreading depression (Liebetanz et al., 2006a) and epilepsy (Liebetanz et al., 2006b). Anodal stimulation of frontal cortex enhances the Blood-oxygen-level dependent (BOLD) signal, an indication of higher neuronal activity (Takano et al., 2011). Furthermore, DCS alters neocortical plasticity not only by altering pre-synaptic sensitivity (Márquez-Ruiz et al., 2012) but also by promoting brain-derived neurotrophic factor (BDNF) dependent long-term potentiation (LTP) (Fritsch et al., 2010). As the plasticity mechanisms of the cerebellar cortex are different from those in neocortex (Hansel, 2005; Lamont and Weber, 2012) there is ample justification for an animal model of cerebellar DCS. Moreover, the cerebellum is ideal to identify the mechanism(s) of DCS because—(i) the structure of rodent cerebellum is clear and accessible, (ii) the plasticity mechanisms are well studied, and (iii) there is a wide range of mutant mouse models available to test which pathways are functionally relevant (De Zeeuw et al., 2011). Therefore, the present study focuses not only on developing an animal model of cerebellar DCS but also utilizes one of the most important mutant mouse models to unravel the role of PC plasticity in mediating DCS effects on VOR adaptation.

METHODS

Summary of Methodology

C57BL/6 (wild type, $N = 24$) and L7-PP2B (LTP deficient mutants, $N = 22$) mice were implanted with a DCS-implant for administration of DCS over the cerebellum. DCS was applied to separate groups of mice as anodal, cathodal or sham-stimulation. Eye movements were recorded using an infrared-sensitive CCD camera during horizontal VOR gain-down adaptation learning. In testing sessions, the eye response to vestibular stimulation, i.e., the motion of the table, (amplitude of 5° at 1 Hz frequency) in the dark was recorded. In training sessions, vestibular and visual stimulation (amplitude of 5° at 1 Hz frequency) were coupled so as to cause reduction of the VOR gain. Two baseline test sessions were followed by 10 min of DC stimulation and then by an additional baseline test session. There were then 5 training sessions of 5 min each, each followed by a test session. We subsequently compared the reduction of VOR gain in the different stimulation groups and across strains.

Experimental Paradigm

Mice were habituated to the experimental apparatus for a minimum of 2 days to reduce the novelty-induced anxiety and restrain-stress after they recovered from the surgery.

Each experiment consisted of 8 test (T) and 5 training (Tr) sessions. The duration of each test session was 1 min, and the duration of each training session was 5 min. In test sessions, a sinusoidal vestibular stimulation which was generated by moving the table with a 5° amplitude at 1 Hz frequency, was applied in the dark. Eye movements were recorded simultaneously. In training sessions, in phase vestibular and optokinetic sinusoidal stimuli (5° amplitude at 1 Hz frequency) were given (**Figure 1A**), in order to reduce the VOR gain. Eye movements were continuously recorded.

Every experiment was initiated by two baseline measurements of VOR (T1 and T2). Then the mice were randomly divided into 3 groups, and received anodal, cathodal or sham DC stimulation. The current amplitude was ramped up over 30 s to 113.2 μA and kept constant for 10 min (positive polarity for the anodal group, negative polarity for the cathodal group). For the sham group, amplitude was then immediately ramped down (over 30 s) while for the anodal and cathodal groups current was maintained for 10 min of stimulation. After the stimulation, another session of testing (T3) was conducted and then gain-down adaptation learning training was initiated. A testing session was conducted to calculate the learning rate after every training session (**Figure 1A**).

Experimental Procedure

Animals

C57BL/6 ($N = 24$) mice were acquired from Charles River laboratories, Inc. (Wilmington, MA, USA). L7-PP2B mutants ($N = 22$) were bred in Erasmus MC, Rotterdam. Mouse lines used in this study have been described previously (Schonewille et al., 2010). Three to four mice were caged together in temperature-regulated (22 ± 1°C) housing with a 12:12 light-day

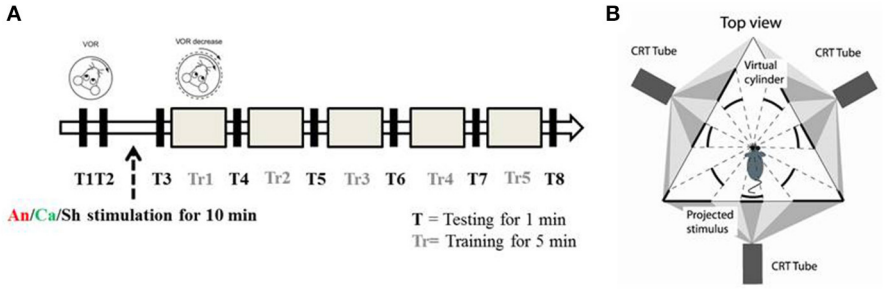

FIGURE 1 | Experimental paradigm and set up **(A)** Schematic diagram of the experimental paradigm. *T* represents a testing session during which the animal is exposed to VOR in the dark by moving the turntable in a sinusoidal manner (5° amplitude at 1 Hz). *Tr* represents the training session during which the animal is presented with a sinusoidal visual cue which is in phase with the table movement. After two testing sessions (*T1* and *T2*) the animals were randomly assigned to the anodal (*An*), cathodal (*Ca*) or sham (*Sh*) stimulation group. **(B)** Schematic diagram of the experimental apparatus. Top down view describes the position of the mouse in relation to the virtual environment created by three projectors.

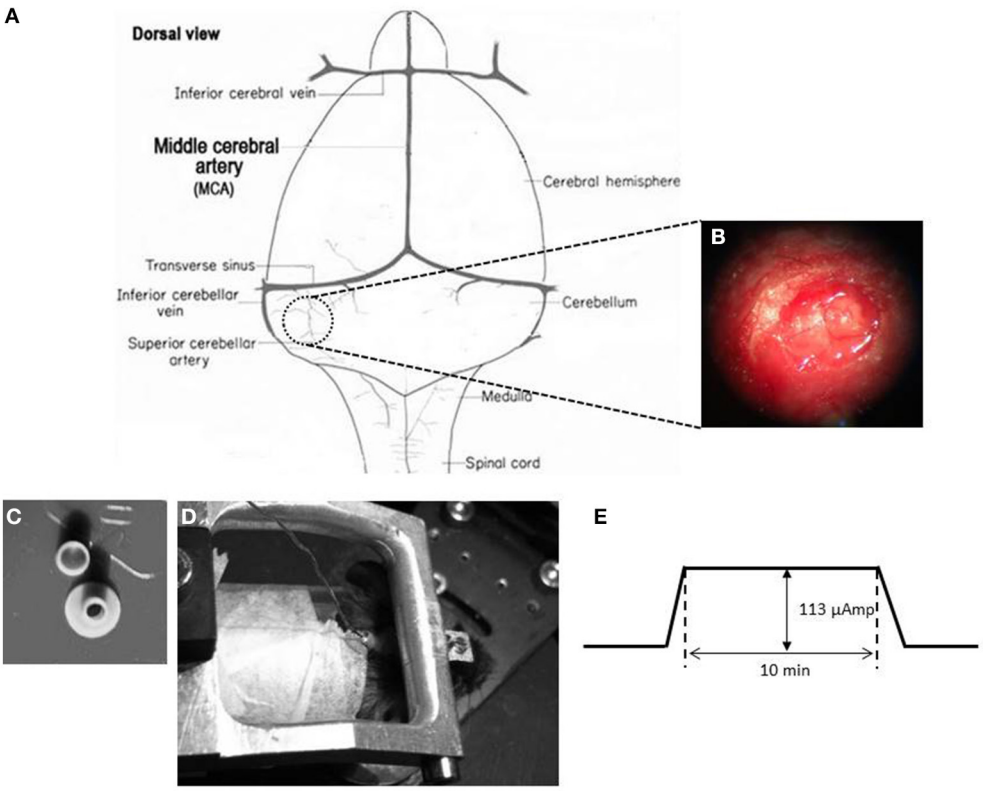

FIGURE 2 | DCS location and procedure **(A)** Schematic representation of craniotomy for placement of implant over the cerebellum of a mouse brain. **(B)** Craniotomy. Anatomical location for the DCS-implant placement. **(C)** DCS implant. The DCS chamber serves as a bridge between the stimulating electrode and the brain. Above the chamber is the cap that serves to protect the brain from infection. **(D)** Stimulating the mouse cerebellum. The DCS chamber is filled with saline (0.9% NaCl) solution. A silver wire that touches the saline solution but not the dura directly is connected to the current generator (SUI-91, Isolated current source). During stimulation the mouse is awake but head restrained. **(E)** Stimulation paradigm. DCS is ramped up to 113 µAmp. The current is maintained at its peak value for 10 min. After the stimulation the current is ramped down.

cycle. Behavioral experiments were performed in the light cycle. Food and water was provided *ad libitum*. All experiments were reviewed and approved by the Erasmus animal ethics committee and conducted in accordance with Animal Welfare Committee of the Erasmus University and the European Communities Council Directive (86/609/EEC).

Surgery

Mice, aged 10–12 weeks, were handled for 2 days before the surgery to reduce the effect of handling-induced stress. The surgical procedure was performed under sterile conditions. Isoflurane (5% induction, 1.5% in 0.5 L/min O_2, and 0.2 L/min air) was administered as an anesthetic drug while body

temperature was regulated around 36.5 ± 0.5° via a feedback-controlled heating pad. Breathing profile was continuously monitored. After shaving the head, a 1 cm long mid-sagittal incision was given. The bone was etched (37.5% phosphoric acid, Kerr, CA, USA) and a primer (Optibond, Kerr, CA, USA) was applied. To immobilize the animal during eye tracking, a pedestal containing two M1.4 nuts was glued to the skull using dental acrylic (Charisma, Flowline, Hereaus Kulzer GmBH, Germany).

In order to place a DCS implant, a circular craniectomy (approximately 2 mm in diameter) on the left occipital bone was performed after careful removal of the neck-muscles (vertical and horizontal) (**Figures 2A,B**). The placement was on the center of the left parietal bone (by keeping the superior cerebellar artery at the center of the implant). A lubricating ointment (Duratears, Alcon Nederland BV, NL) was applied epidurally to protect the exposed area of brain from drying. The DCS implant (**Figure 2C**) was placed identically in all animals using an anatomical marker (**Figures 2A,B**) and then glued to the skull using cyanoacrylate gel (Plastic One Inc., VA, USA).

The mice were given an analgesic (0.1 ml/mg of body weight Buprenorphine/Temgesic) and placed under an infrared heating lamp until the animals started to move. Mice were allowed at least 4–5 days to recover before recordings were performed.

Apparatus

Visual and Vestibular Stimulation

Mice were head-fixed in a restrainer, which was fixed onto the center of a turntable, placed at the center of an isolateral triangle made by three projector-screens. A panoramic virtual reality display with 360° field of view was created by projecting monochrome green dots on to those screens (**Figure 1B**). Horizontal rotation of the turntable was driven by a servomotor (Mavilor-DC motor 80, Infranor, Spain). Visual stimuli and movement of the turntable were under control of in-house software written in C++. Training and testing sessions were evoked by rotating the dots and/or the turntable sinusoidally. During each session, stimuli were ramped up to their peak velocity in 5 s for a smooth transition from static to dynamic state. They were also ramped down at the end.

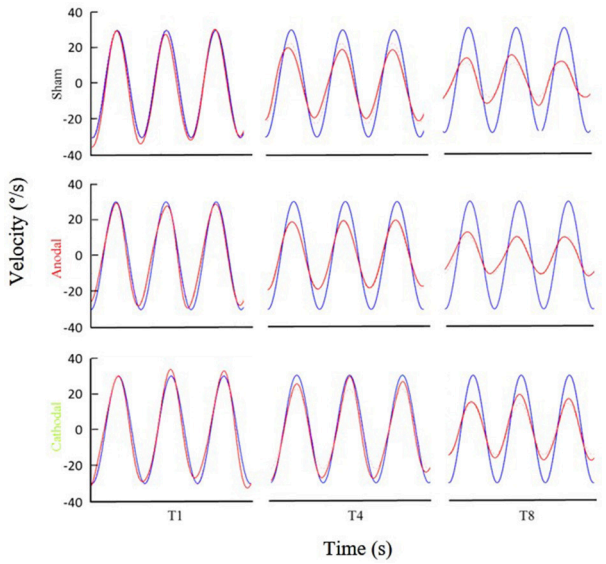

FIGURE 3 | Examples of eye movement in different stimulation conditions. Examples of filtered eye velocity illustrate results from mice that exhibited a decrease in the VOR after training with sham (top panels), anodal (middle panels) and cathodal (bottom panels) stimulation. Blue is vestibular stimulus and red is eye amplitude (solid red line is filtered eye-velocity, dotted red line fitted sine wave). Eye-trace of each stimulus condition has been presented during pre-training (T1), after first-training (T4) and after final-training (T8) in the left, middle and right panels, respectively.

Eye Movement Recordings

Eye movements were recorded with an infrared video system (ETL-200 with marker tracking modifications; ISCAN, Burlington, MA). The camera and lens were mounted under the table surface to reduce hindrance of the mouse vision. A hot mirror which was transparent to visible light and reflective to infrared light was used. The eye was illuminated with three infrared LEDs. The camera, mirror and LEDs were all mounted on an arm that could rotate about the vertical axis over a range of 26.12° (peak to peak). Eye movement recordings and calibration procedures were similar to those described by Stahl et al. (2000). Images of the eye were captured at 120 Hz with an infrared-sensitive CCD camera. The eye image contained a bright corneal reflection and a dark pupil reflection. The image was focused by manipulating the offset and the gain of the detectors through the ISCAN software. From this image, x and y positions of each of the three markers were recorded in real time giving their location on a 512 × 256-pixel grid, with a resolution of one-third pixel horizontally and one-tenth pixel vertically (van Alphen et al., 2010). These x and y translational positions of eye on the grid were converted into the angular rotation of the eyeball by the ISCAN system (resolution of 0.2° over a ±25° horizontal and ±20° vertical range using the pupil/corneal reflection difference). The horizontal and vertical pupil position data from the ISCAN were output as ±5 VDC signals. A delay of 30 ms in the eye movement signal was introduced by the video system. Furthermore, this output signal was low-pass filtered with a cutoff frequency of 300 Hz (Cyberamp 380; Axon Instruments, CA, USA), sampled at 1 kHz and stored for offline analysis.

Direct Current Stimulation

A low amplitude (113 μA) of continuous DCS was applied using a constant current stimulator (SUI-91, Isolated current source, Cygnus Technology Inc., NC, USA; range = 0.1 μA—10 mA). This intensity corresponded to a current density of 3.6 mA/cm^2 (Liebetanz et al., 2009). Currents were applied to the epidural surface of the cerebellar cortex through a circular DCS implant with a defined contact area (2 mm inner diameter). Prior to stimulation, the electrode was filled with saline solution (0.9% NaCl). A silver wire electrode connected to the stimulation device was attached to the DCS implant such that the tip of the silver wire touched the top level of the saline solution but did not touch the

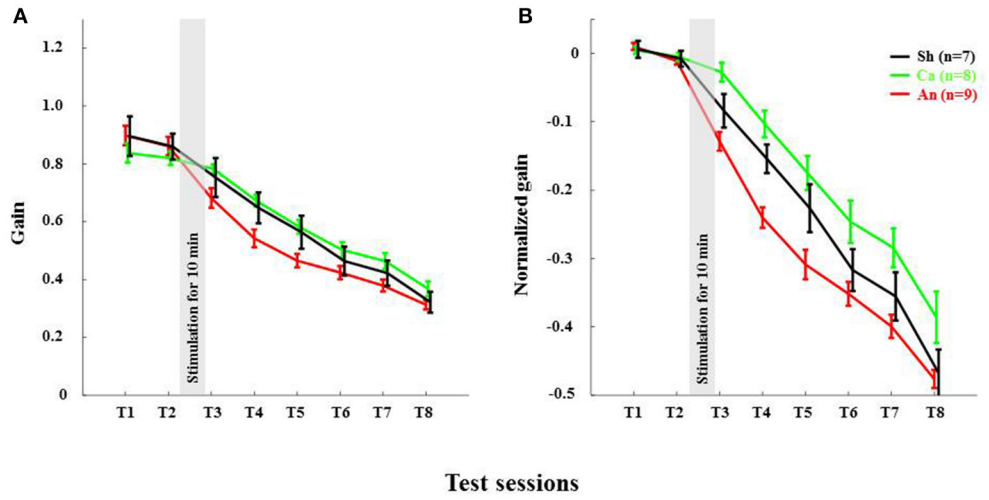

FIGURE 4 | Anodal stimulation reduces VOR gain acutely in wild type C57BL/6 mice. **(A)** Time course of gain reduction due to adaptation: Changes in mean VOR gain during VOR-decrease training. The VOR was tested pre- and post-training by measuring the eye movement response to the vestibular stimulus. **(B)** Time course of normalized gain reduction due to adaptation: Trial-to-trial changes in mean normalized VOR gain during VOR-decrease training. Black, Green and Red lines are for sham, cathodal and anodal stimulation conditions, respectively. The gray bar indicates the stimulation period. Error bars represent SEM.

brain directly. This circular active electrode (**Figure 2C**) was chosen to create a symmetric current density without any edge effects (Ambrus et al., 2011). A disposable foam electrode (Kendall Medi-Trace mini resting ECG electrode, Davis medical products Inc., CA, USA), was placed onto the ventral thorax of the animal to complete the circuit. The entire circuit was connected through a multimeter to check online current amplitude. Mice were awake during DCS to prevent possible interactions between DCS effects and anesthetic drugs. In addition, mice were introduced to the adaptation task right after the stimulation to quantify acute effects of stimulation. To avoid stimulation break effects (Liebetanz et al., 2009), the current intensity was ramped up and down gradually over 30 s.

Data Analysis

Custom routines written in MATLAB (The MathWorks Inc., Natick, MA, USA) were designed and employed for automated offline data analysis. The position signal was shifted 30 ms back in time to correct for the camera delay. A median filter (width 50 ms) with a low-pass cutoff of 10 Hz was applied to smooth the position data before transforming to velocity domain by a Savitski-Golay differentiating filter (frequency 50 Hz with a 3° polynomial). Rapid eye movements were detected and removed via a velocity threshold (150°/s). Then a 3 Hz FIR Butterworth low pass filter of 50 ms width was applied.

The processed data was divided into non-overlapping epochs of 2 s (corresponding to two cycles of the stimulus). Amplitude data was obtained by fitting sine waves to the eye movement data in custom-made Matlab curve fitting routines using the least-squares method. Median amplitude values of the eye movement were calculated from the fitted sine waves. Gain was calculated for,

$$G_T = \frac{E_{Tn}}{S} \qquad \begin{array}{l} \boldsymbol{E} = \text{fit eye amplitude of a testing session, } n = 1 \\ \quad \text{through 8,} \\ \boldsymbol{S} = \text{stimulus amplitude,} \end{array} \tag{1}$$

each testing session as the ratio between the fit eye velocity amplitude and stimulus velocity amplitude ($\boldsymbol{S}$).

Mice were excluded when the absolute difference between baseline gains (G_{T1}–G_{T2}) was > 0.2. The baseline gain ($\boldsymbol{G}_B$) was set as the mean of gains in G_{T1} and G_{T2}. Normalized gain ($\boldsymbol{G}_N$) was also calculated for every test session.

$$G_N = \frac{G_B - G}{G_B + G} \tag{2}$$

Statistical Analysis

Statistical analysis of the data was performed using SPSS 20.0 (SPSS, Chicago, IL). A three way mixed-ANOVA with repeated measures was used to compare interaction and group effects, as the data showed a normal distribution. Significance levels were set to 0.05. Later on, a Bonferroni corrected *post-hoc* analysis was applied to find intra-/inter-group interactions. Values are represented here as mean ± SEM.

RESULTS

Degree of Adaptation at the End of Training Session

The VOR gain-down adaptation paradigm caused a gradual reduction in VOR-amplitude in all mice (**Figures 3**–**6**). Initially, the amplitude of the eye movement was similar to the stimulus amplitude; i.e., the gain at T1 for C57BL/6 and L7-PP2B mice was 0.88 ± 0.03 and 1.03 ± 0.03, respectively (**Figures 4**, **6**). The

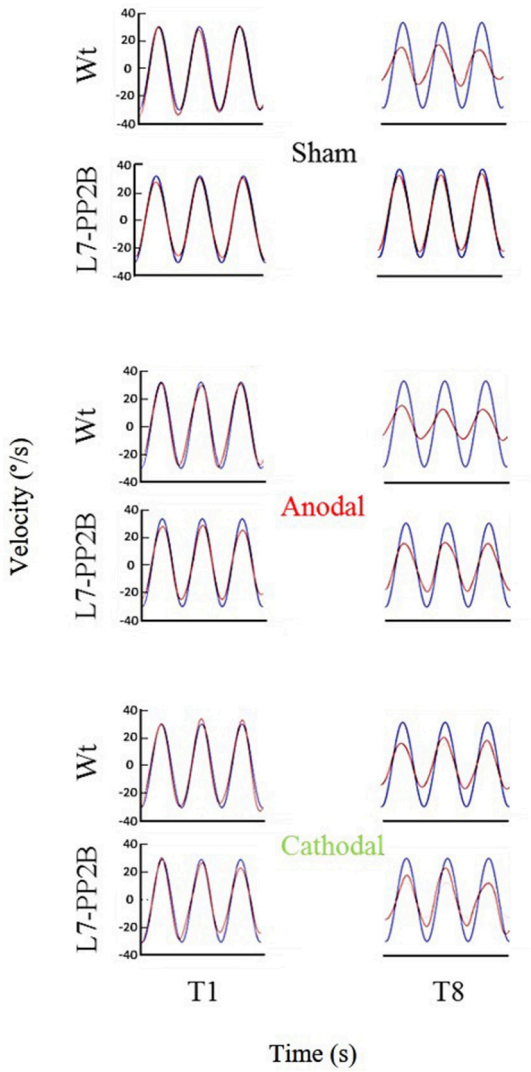

FIGURE 5 | Eye amplitude show clear deficit in learning of L7-PP2B mice in all three stimulus conditions. Example filtered eye velocity traces illustrate typical results from mice of both genetic backgrounds before (T1) and after (T8) adaptation. Blue is vestibular stimulus and red is eye velocity (solid red line is filtered eye-signal, dotted red line is the fitted sine wave). Eye amplitude decreases from pre- to post-training sessions (T1 and T8, respectively) in wild type mice. In contrast, L7-PP2B undergoes little change between T1 and T8 sessions.

baseline VOR gain in L7-PP2B of more than 1 indicated that the eye amplitude overshot the head amplitude in these mice. After being subjected for 25 min to the gain-down training, the amplitude of VOR at T8 was reduced for both C57BL/6 (raw T8 gain = 0.33 ± 0.03) and L7-PP2B (raw T8 gain = 0.70 ± 0.03) group. In our multivariate ANOVA on the non-normalized data, the main effect of training over the time course was highly significant, $F_{(7, 34)} = 46.20$, $p < 0.001$. However, comparison of the sham stimulation data showed that the degree of adaptation was significantly higher in C57BL/6 than L7-PP2B mice, $F_{(5, 40)} = 14.94$, $p < 0.001$.

Reduction of Gain in C57BL/6 and L7-PP2B Mice

The reduction in gain made across the eight test sessions was strongly dependent upon the genetic composition of mice, $F_{(7, 38)} = 4.98$, $p < 0.001$. We sought to find out at which steps the gain was maximally reduced between C57BL/6 and L7-PP2B mice. To do that, we checked the gain difference between two successive test sessions and then compared that across the mouse types. The tests of within-subjects contrasts illustrated that the gain reduction from T5 to T6 [$F_{(5, 40)} = 2.48$, $p < 0.05$] and from T7 to T8 [$F_{(5, 40)} = 2.66$, $p < 0.05$] was significantly greater for C57BL mice compared to the L7-PP2B mice.

Effects of DCS on VOR Adaptation

ANOVA further indicated that DCS polarity had a significant modulatory role on the gain reduction, $F_{(14, 70)} = 2.07$, $p < 0.05$, suggesting that the amplitude of gain decrease across the eight tests (from T1 to T8) was dependent upon stimulus polarity. Moreover, the gain decrease across eight test sessions yielded a significant interaction between stimulus polarity and genetic background of the mice (C57BL/6 and L7-PP2B mice, [$F_{(7, 35)} = 2.52$, $p < 0.05$]. In the following sections, we discuss how the modulatory role of DCS was altered depending on the mouse type.

Anodal Stimulation Reduced VOR Gain in C57BL/6 Acutely

The anodal stimulation triggered faster initial VOR gain reduction compared to the cathodal stimulation [$F_{(2, 21)} = 9.56$, $p < 0.001$, **Figure 4A**] in wild type mice. There was a significant post-stimulation reduction of gain at T3 (pre-training reduction of gain) in the anodal group compared to the cathodal group. The contrast analysis, T2 vs. T3, comparing the raw gain at T2 with that made in T3, was statistically significant [$F_{(2, 21)} = 6.01$, $p < 0.01$]. Interestingly, the anodal, sham and cathodal groups finished at the same degree of adaptation (T8), although the anodal group showed significant initial reduction in VOR gain.

Next, we normalized the gain of every mouse to its own baseline to provide a comparable measure of gain for all animals. Normalized gain (**Figure 4B**) depicted a clear polarity-dependent divergence. The initial post-stimulation period showed that the cathodal stimulation significantly decelerated gain reduction compared to the anodal stimulation. The reduction of gain in the sham condition—as expected—remained between the rate in the anodal and the cathodal conditions (**Figure 4B**).

Deletion of PP2B in PC Abolished Anodal Effect

Anodal stimulation lost its modulatory role when potentiation was eliminated from PCs (**Figures 6A,B**). Anodal stimulation failed to improve learning in L7-PP2B mice (T8 gain = 0.74 ± 0.04), compared to the sham group (T8 gain = 0.65 ± 0.08; **Figure 5**). Moreover, anodal stimulation could not reduce the baseline gain in these mutants (T2 gain = 1.06 ± 0.04, T3 gain = 0.99 ± 0.04). The large error bars in the sham condition is due to low sampling

numbers ($N = 3$). Moreover, we think that chronic mutation (deletion of LTP in PCs) leads to the adoption of various adaptation mechanisms in the network. Therefore, when an external current stimulus was applied the network showed varied responses to cope with the situation. This could be the cause for finding a large variability in the stimulation groups.

An hour long sinusoidal oscillatory stimulus led to decrease in VOR gain (approximately to 28%) across various species (Tempia et al., 1991; Dow and Anastasio, 1998; Clément et al., 2002). The cause of this VOR gain reduction in rodents has been pointed out as habituation rather than learning (Tempia et al., 1991). Therefore, we think that the gain reduction (27 ± 2%) in L7-PP2B mice (similar to Schonewille et al., 2010) across all three stimulation-conditions is due to the habituation.

DISCUSSION

Our study demonstrates three major findings of the polarity specific effects of DCS on VOR gain-down adaptation. First, anodal stimulation of cerebellar cortex decreases VOR gain acutely compared to the cathodal stimulation condition in C57BL/6 control mice. Second, despite differences in initial post-stimulation reduction in gain amplitude, the final gain reduction is similar in the anodal and the cathodal stimulation groups of C57BL/6 control mice. Third, our data, remarkably, shows when potentiation of the PCs is genetically ablated in L7-PP2B mice, anodal stimulation no longer led to VOR gain reduction. Hence, our interpretation is that anodal stimulation driven VOR gain reduction depends on a PP2B-dependent PC potentiation pathway, either at the upstream dendritic level or at the downstream axonal level where PCs innervate VN neurons (Schonewille et al., 2010).

We found that anodal stimulation of the cerebellum decreases VOR gain acutely (**Figures 4A,B**), though we don't see an effect on adaptation-rate like in other studies (Jayaram et al., 2012; Herzfeld et al., 2014; Zuchowski et al., 2014; Avila et al., 2015). We see that VOR gain is reduced prior to the training. Perhaps anodal stimulation induced an acute increase in inhibition by enhancing PC activity. Indeed, others have also reported that artificial activation of PCs may contribute to the induction of VOR gain-down adaptation (Nguyen-Vu et al., 2013). Moreover, a low amplitude external electric field (EEF) is sufficient to modulate PC activity (Chan and Nicholson, 1986; Chan et al., 1988). Together these results suggest that anodal DCS may induce higher PC activity, which in turn could lead to inhibition of its downstream structures.

The possibility that the effects of DCS on plasticity are in part secondary effects on downstream structures comports with there being at least two sites of VOR plasticity (Hansel, 2005): one in the floccular region of cerebellar cortex and one in the VN (Gao et al., 2012). Physiological studies would be necessary to elucidate the relative effects, and these studies would need to include direct measurements from both regions.

We also found that the total gain reduction was similar in the anodal and the cathodal stimulation conditions although the gain reduction at the early phase is clearly different (**Figure 4A**). In our study, training and testing are assessed post DCS, whereas most of the reports available today are based on stimulation applied during learning. For instance, anodal stimulation facilitates learning in locomotor (Jayaram et al., 2012), force field (Herzfeld et al., 2014), and saccade (Avila et al., 2015) adaptation as well as eye-blink conditioning tasks (Zuchowski et al., 2014), while cathodal stimulation hinders

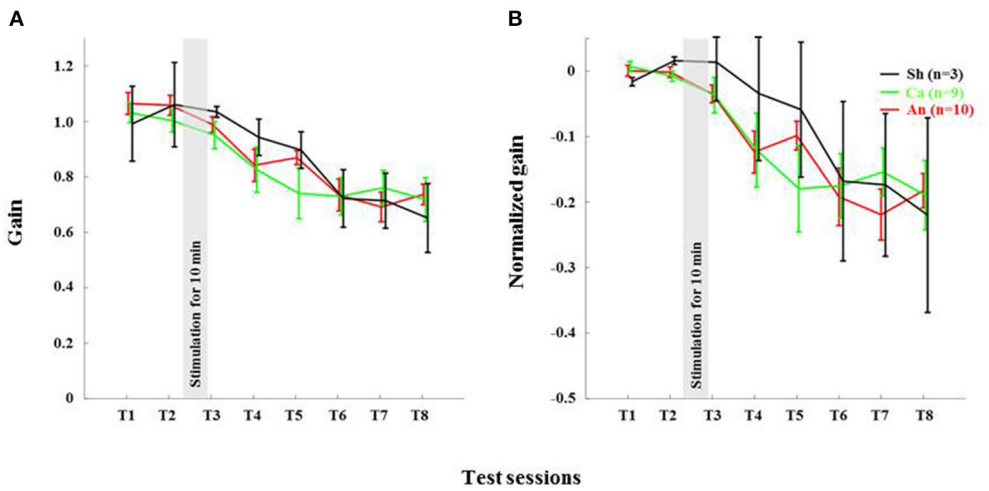

FIGURE 6 | Genetic ablation of PC plasticity in L7-PP2B mice abolishes effects of anodal stimulation on gain-down adaptation. **(A)** Plot of gain during gain-down adaptation: Changes in VOR gain during VOR-decrease training in L7-PP2B mice. The VOR was tested pre- and post-training by measuring the eye movement response to the vestibular stimulus. **(B)** Plot of normalized gain throughout the course of the behavioral paradigm: Changes in VOR gain during VOR-decrease training. Black, Green and Red lines are for sham, cathodal and anodal stimulation conditions, respectively. The gray bar indicates the stimulation period. Error bars represent SEM, because of large SEM we do not find any significant difference between the groups.

leaning in all these tasks. Surprisingly, the post-stimulation deadaptation curve (Jayaram et al., 2012; Herzfeld et al., 2014) or extinction rate (Zuchowski et al., 2014) shows no difference across various stimulation groups. The later finding is notable because irrespective of altered rate and total amount of learning, polarity has no effect on post-stimulation de-adaptation/ learning processes. In our study, we find that DCS has no post-stimulation effect on the learning phase. Therefore, our study clearly depicts both anodal and cathodal stimulation have short-lasting effects on the habituation phase of the gain-down VOR adaptation task. The de-adaptation experiment (like other studies) is redundant, as we have done all the adaptation training sessions in the post-stimulation period. To discover the actual cause, similar experiments should be performed with a gain increase VOR adaptation paradigm (Gao et al., 2012).

L7-PP2B mice often showed more than one gain during baseline measurements (**Figure 6A**). Possibly, the eye overshoots the head-position as we have used higher sinusoidal velocity (amplitude of 5° at 1 Hz frequency). We think that sensory signals coming from the parallel fibers fail to excite PC sharply, as there is no LTP in L7-PP2B mice. Therefore, when the high velocity head-movement stops, PCs could not generate sharp inhibition on the VN to stop the eye-movement. A sub-optimal PC inhibition may have caused facilitation of the eye movement in the absence of the head-movement.

We propose three, non-exclusive, possibilities that may explain reduced sensitivity to anodal stimulation in the L7-PP2B mutants: (i) PCs in the mutants may receive more background inhibition; (ii) plasticity at the PC-VN synapses may be essential for VOR gain-down adaptation (De Zeeuw and Ten Brinke, 2015; See CSHP book by Kandel); and/or (iii) plasticity of synapses on PCs in mutants may be saturated, preventing adaptation. The first point reflects the possibility that anodal stimulation may cause inhibition rather than excitation of PCs when there is no LTP or intrinsic plasticity at PCs. Anodal stimulation driven subthreshold depolarization may augment GABA release from molecular layer interneurons (MLI) (Christie et al., 2011; Stagg and Nitsche, 2011) and thereby increase inhibition onto PCs. The second possibility is that anodal DCS has a direct impact on PC-VN plasticity and thereby directly regulates the adaptation process. Loss of PC LTP may retard the effects of anodal stimulation on these synapses. The third reason could be that loss of LTP makes the circuit unresponsive to the pairing of the sensory stimulus with the motor response, as intrinsic plasticity of PCs is also erratic in these mutants (Schonewille et al., 2010). The PP2B transgene may disrupt normal signaling through the PCs or the homeostasis of the network (Lamont and Weber, 2012). This can corrupt the instructive signals sent by PCs to downstream sites like the VN.

Cathodal stimulation induced inhibition of adaptation in L7-PP2B mutants is significantly stronger compared to C57BL/6 mice but similar to the sham group of L7-PP2B mice (**Figures 5**, **6B**). It is evident that this cathodal suppression is a by-product of the mutation of potentiation at the PCs, as these mice fail to learn cerebellar tasks (Schonewille et al., 2010). In addition, we need to examine to what extent long-term depression (LTD) at PF-PC pathway plays a role following cathodal stimulation.

In conclusion, we have successfully developed a mouse model of cerebellar DCS, allowing us to present the first demonstration of cerebellar DCS driven behavioral changes in rodents. We used this model in combination with the popular paradigm of VOR adaptation to test the effect of current stimulation on motor adaptation. The results presented here provide evidence that anodal DCS reduces VOR gain acutely, an effect that is disrupted by ablation of PP2B in PCs. This study, also finds support for recent claims that anodal and cathodal stimulation modulate cerebellar dependent adaptation acutely through distinct pathways. Future research must address the neuronal activity following cerebellar stimulation to understand the spatiotemporal aspects of DCS effects.

AUTHOR CONTRIBUTIONS

SD, MSp, MF, and OD conceived and designed the experiments. SD performed the experiments. SD and PH analyzed the data. TS helped in building the experimental set-up. SD, OD, MF, MSc, and CD interpreted the data. SD drafted the manuscript. OD, MSc, MF, TS, and PH performed a critical review of the manuscript. CD and MSc were responsible for mutant verification. All the authors read and approved the final version of the manuscript.

FUNDING

This work was supported by Marie-Curie ITN C7 fellowship, EU Interreg grant TC2N, ERC-POC (Brainframe) and Ben-Gurion University Post-Doctoral Fellowship.

REFERENCES

Ambrus, G. G., Antal, A., and Paulus, W. (2011). Comparing cutaneous perception induced by electrical stimulation using rectangular and round shaped electrodes. *Clin. Neurophysiol.* 122, 803–807. doi: 10.1016/j.clinph.2010.08.023

Avila, E., van der Geest, J. N., Kengne Kamga, S., Verhage, M. C., Donchin, O., and Frens, M. A. (2015). Cerebellar transcranial direct current stimulation effects on saccade adaptation. *Neural Plast.* 2015:968970. doi: 10.1155/2015/968970

Bastian, A. J. (2011). Moving, sensing and learning with cerebellar damage. *Curr. Opin. Neurobiol.* 21, 596–601. doi: 10.1016/j.conb.2011.06.007

Benussi, A., Koch, G., Cotelli, M., Padovani, A., and Borroni, B. (2015). Cerebellar transcranial direct current stimulation in patients with ataxia: a double-blind, randomized, sham-controlled study. *Mov. Disord.* 30, 1701–1705. doi: 10.1002/mds.26356

Bindman, L. J., Lippold, O. C. J., and Redfearn, J. W. T. (1964). The action of brief polarizing currents on the cerebral cortex of the rat (1) during current flow and (2) in the production of long-lasting after-effects. *J. Physiol.* 172, 369–382. doi: 10.1113/jphysiol.1964.sp007425

Chan, C. Y., Hounsgaard, J., and Nicholson, C. (1988). Effects of electric fields on transmembrane potential and excitability of turtle cerebellar Purkinje cells *in vitro*. *J. Physiol.* 402, 751–771. doi: 10.1113/jphysiol.1988.sp017232

Chan, C. Y., and Nicholson, C. (1986). Modulation by applied electric fields of Purkinje and stellate cell activity in the isolated turtle cerebellum. *J. Physiol.* 371, 89–114. doi: 10.1113/jphysiol.1986.sp015963

Christie, J. M., Chiu, D. N., and Jahr, C. E. (2011). Ca^{2+}-dependent enhancement of release by subthreshold somatic depolarization. *Nat. Neurosci.* 14, 62–68. doi: 10.1038/nn.2718

Clément, G., Flandrin, J.-M., and Courjon, J.-H. (2002). Comparison between habituation of the cat vestibulo-ocular reflex by velocity steps and sinusoidal vestibular stimulation in the dark. *Exp. Brain Res.* 142, 259–267. doi: 10.1007/s00221-001-0930-7

Creutzfeldt, O. D., Fromm, G. H., and Kapp, H. (1962). Influence of transcortical d-c currents on cortical neuronal activity. *Exp. Neurol.* 5, 436–452. doi: 10.1016/0014-4886(62)90056-0

Das, S., Holland, P., Frens, M. A., and Donchin, O. (2016). Impact of transcranial direct current stimulation (tDCS) on neuronal functions. *Front. Neurosci.* 10:550. doi: 10.3389/fnins.2016.00550

De Zeeuw, C. I., Hoebeek, F. E., Bosman, L. W. J., Schonewille, M., Witter, L., and Koekkoek, S. K. (2011). Spatiotemporal firing patterns in the cerebellum. *Nat. Rev. Neurosci.* 12, 327–344. doi: 10.1038/nrn3011

De Zeeuw, C. I., and Ten Brinke, M. M. (2015). Motor learning and the cerebellum. *Cold Spring Harb. Perspect. Biol.* 7:a021683. doi: 10.1101/cshperspect.a021683

Dow, E. R., and Anastasio, T. J. (1998). Analysis and neural network modeling of the nonlinear correlates of habituation in the vestibulo-ocular reflex. *J. Comput. Neurosci.* 5, 171–190. doi: 10.1023/A:1008818016900

Fritsch, B., Reis, J., Martinowich, K., Schambra, H. M., Ji, Y., Cohen, L. G., et al. (2010). Direct current stimulation promotes BDNF-dependent synaptic plasticity: potential implications for motor learning. *Neuron* 66, 198–204. doi: 10.1016/j.neuron.2010.03.035

Galea, J. M., Jayaram, G., Ajagbe, L., and Celnik, P. (2009). Modulation of cerebellar excitability by polarity-specific noninvasive direct current stimulation. *J. Neurosci.* 29, 9115–9122. doi: 10.1523/JNEUROSCI.2184-09.2009

Gao, Z., van Beugen, B. J., and De Zeeuw, C. I. (2012). Distributed synergistic plasticity and cerebellar learning. *Nat. Rev. Neurosci.* 13, 619–635. doi: 10.1038/nrn3312

Hansel, C. (2005). When the B-team runs plasticity: GluR2 receptor trafficking in cerebellar long-term potentiation. *Proc. Natl. Acad. Sci. U.S.A.* 102, 18245–18246. doi: 10.1073/pnas.0509686102

Hardwick, R. M., and Celnik, P. A. (2014). Cerebellar direct current stimulation enhances motor learning in older adults. *Neurobiol. Aging* 35, 2217–2221. doi: 10.1016/j.neurobiolaging.2014.03.030

Herzfeld, D. J., Pastor, D., Haith, A. M., Rossetti, Y., Shadmehr, R., and O'Shea, J. (2014). Contributions of the cerebellum and the motor cortex to acquisition and retention of motor memories. *Neuroimage* 98, 147–158. doi: 10.1016/j.neuroimage.2014.04.076

Ito, M. (1982). Cerebellar control of the vestibulo-ocular reflex–around the flocculus hypothesis. *Annu. Rev. Neurosci.* 5, 275–296. doi: 10.1146/annurev.ne.05.030182.001423

Ivry, R. B., and Spencer, R. M. C. (2004). The neural representation of time. *Curr. Opin. Neurobiol.* 14, 225–232. doi: 10.1016/j.conb.2004.03.013

Jayaram, G., Tang, B., Pallegadda, R., Vasudevan, E. V. L., Celnik, P., and Bastian, A. (2012). Modulating locomotor adaptation with cerebellar stimulation. *J. Neurophysiol.* 107, 2950–2957. doi: 10.1152/jn.00645.2011

Kawato, M., and Gomi, H. (1992). The cerebellum and VOR/OKR learning models. *Trends Neurosci.* 15, 445–453. doi: 10.1016/0166-2236(92)90008-V

Lamont, M. G., and Weber, J. T. (2012). The role of calcium in synaptic plasticity and motor learning in the cerebellar cortex. *Neurosci. Biobehav. Rev.* 36, 1153–1162. doi: 10.1016/j.neubiorev.2012.01.005

Liebetanz, D., Fregni, F., Monte-Silva, K. K., Oliveira, M. B., Amâncio-dos-Santos, A., Nitsche, M. A., et al. (2006a). After-effects of transcranial direct current stimulation (tDCS) on cortical spreading depression. *Neurosci. Lett.* 398, 85–90. doi: 10.1016/j.neulet.2005.12.058

Liebetanz, D., Klinker, F., Hering, D., Koch, R., Nitsche, M. A., Potschka, H., et al. (2006b). Anticonvulsant effects of transcranial direct-current stimulation (tDCS) in the rat cortical ramp model of focal epilepsy. *Epilepsia* 47, 1216–1224. doi: 10.1111/j.1528-1167.2006.00539.x

Liebetanz, D., Koch, R., Mayenfels, S., König, F., Paulus, W., and Nitsche, M. A. (2009). Safety limits of cathodal transcranial direct current stimulation in rats. *Clin. Neurophysiol.* 120, 1161–1167. doi: 10.1016/j.clinph.2009.01.022

Lisberger, S. G., and Fuchs, A. F. (1974). Response of flocculus Purkinje cells to adequate vestibular stimulation in the alert monkey: fixation vs. compensatory eye movements. *Brain Res.* 69, 347–353. doi: 10.1016/0006-8993(74)90013-4

Márquez-Ruiz, J., Leal-Campanario, R., Sánchez-Campusano, R., Molaee-Ardekani, B., Wendling, F., Miranda, P. C., et al. (2012). Transcranial direct-current stimulation modulates synaptic mechanisms involved in associative learning in behaving rabbits. *Proc. Natl. Acad. Sci. U.S.A.* 109, 6710–6715. doi: 10.1073/pnas.1121147109

Nguyen-Vu, T. D. B., Kimpo, R. R., Rinaldi, J. M., Kohli, A., Zeng, H., Deisseroth, K., et al. (2013). Cerebellar Purkinje cell activity drives motor learning. *Nat. Neurosci.* 16, 1734–1736. doi: 10.1038/nn.3576

Probst, T., Brandt, T., and Degner, D. (1986). Object-motion detection affected by concurrent self-motion perception: psychophysics of a new phenomenon. *Behav. Brain Res.* 22, 1–11. doi: 10.1016/0166-4328(86)90076-8

Purpura, D. P., and Mcmurtry, J. G. (1965). Intracellular activities and evoked potential changes during polarization of motor cortex. *J. Neurophysiol.* 28, 166–185.

Schonewille, M., Belmeguenai, A., Koekkoek, S. K., Houtman, S. H., Boele, H. J., van Beugen, B. J., et al. (2010). Purkinje cell-specific knockout of the protein phosphatase PP2B impairs potentiation and cerebellar motor learning. *Neuron* 67, 618–628. doi: 10.1016/j.neuron.2010.07.009

Stagg, C. J., and Nitsche, M. A. (2011). Physiological basis of transcranial direct current stimulation. *Neuroscientist* 17, 37–53. doi: 10.1177/1073858410386614

Stahl, J. S., van Alphen, A. M., and De Zeeuw, C. I. (2000). A comparison of video and magnetic search coil recordings of mouse eye movements. *J. Neurosci. Methods* 99, 101–110. doi: 10.1016/S0165-0270(00)00218-1

Takano, Y., Yokawa, T., Masuda, A., Niimi, J., Tanaka, S., and Hironaka, N. (2011). A rat model for measuring the effectiveness of transcranial direct current stimulation using fMRI. *Neurosci. Lett.* 491, 40–43. doi: 10.1016/j.neulet.2011.01.004

Tempia, F., Dieringer, N., and Strata, P. (1991). Adaptation and habituation of the vestibulo-ocular reflex in intact and inferior olive-lesioned rats. *Exp. Brain Res.* 86, 568–578. doi: 10.1007/BF00230530

Tiliket, C., Shelhamer, M., Tan, H. S., and Zee, D. S. (1993). Adaptation of the vestibulo-ocular reflex with the head in different orientations and positions relative to the axis of body rotation. *J. Vestib. Res.* 3, 181–195.

van Alphen, B., Winkelman, B. H. J., and Frens, M. A. (2010). Three-dimensional optokinetic eye movements in the C57BL/6J mouse. *Invest. Ophthalmol. Vis. Sci.* 51, 623–630. doi: 10.1167/iovs.09-4072

Xu-Wilson, M., Chen-Harris, H., Zee, D. S., and Shadmehr, R. (2009). Cerebellar contributions to adaptive control of saccades in humans. *J. Neurosci.* 29, 12930–12939. doi: 10.1523/JNEUROSCI.3115-09.2009

Zuchowski, M. L., Timmann, D., and Gerwig, M. (2014). Acquisition of conditioned eyeblink responses is modulated by cerebellar tDCS. *Brain Stimul.* 7, 525–531. doi: 10.1016/j.brs.2014.03.010

Conflict of Interest Statement: The authors declare that the research was conducted in the absence of any commercial or financial relationships that could be construed as a potential conflict of interest.

frontiers in Neuroscience

ORIGINAL RESEARCH
published: 27 September 2017
doi: 10.3389/fnins.2017.00526

Effect of Error Augmentation on Brain Activation and Motor Learning of a Complex Locomotor Task

Laura Marchal-Crespo[1,2], Lars Michels[3,4], Lukas Jaeger[1,3], Jorge López-Olóriz[1] and Robert Riener[1,2]*

[1] Sensory-Motor Systems Lab, Department of Health Sciences and Technology, Institute of Robotics and Intelligent Systems, ETH Zurich, Zurich, Switzerland, [2] Reharobotics Group, Spinal Cord Injury Center, Balgrist University Hospital, Medical Faculty, University of Zurich, Zurich, Switzerland, [3] Clinic of Neuroradiology, University Hospital Zurich, Zurich, Switzerland, [4] MR-Center, University Children's Hospital Zurich, Zurich, Switzerland

Up to date, the functional gains obtained after robot-aided gait rehabilitation training are limited. Error augmenting strategies have a great potential to enhance motor learning of simple motor tasks. However, little is known about the effect of these error modulating strategies on complex tasks, such as relearning to walk after a neurologic accident. Additionally, neuroimaging evaluation of brain regions involved in learning processes could provide valuable information on behavioral outcomes. We investigated the effect of robotic training strategies that augment errors—error amplification and random force disturbance—and training without perturbations on brain activation and motor learning of a complex locomotor task. Thirty-four healthy subjects performed the experiment with a robotic stepper (MARCOS) in a 1.5 T MR scanner. The task consisted in tracking a Lissajous figure presented on a display by coordinating the legs in a gait-like movement pattern. Behavioral results showed that training without perturbations enhanced motor learning in initially less skilled subjects, while error amplification benefited better-skilled subjects. Training with error amplification, however, hampered transfer of learning. Randomly disturbing forces induced learning and promoted transfer in all subjects, probably because the unexpected forces increased subjects' attention. Functional MRI revealed main effects of training strategy and skill level during training. A main effect of training strategy was seen in brain regions typically associated with motor control and learning, such as, the basal ganglia, cerebellum, intraparietal sulcus, and angular gyrus. Especially, random disturbance and no perturbation lead to stronger brain activation in similar brain regions than error amplification. Skill-level related effects were observed in the IPS, in parts of the superior parietal lobe (SPL), i.e., precuneus, and temporal cortex. These neuroimaging findings indicate that gait-like motor learning depends on interplay between subcortical, cerebellar, and fronto-parietal brain regions. An interesting observation was the low activation observed in the brain's reward system after training with error amplification compared to training without perturbations. Our results suggest that to enhance learning of a locomotor task, errors should be augmented based on subjects' skill level. The impacts of these strategies on motor learning, brain activation, and motivation in neurological patients need further investigation.

Keywords: motor learning, error augmentation, random disturbance, error amplification, gait rehabilitation, rehabilitation robotics, MR-compatible robotics, fMRI

OPEN ACCESS

Edited by:
Lorenzo Masia, Nanyang Technological University, Singapore

Reviewed by:
Marco Bove, Università di Genova, Italy
Ryan McKendrick, Northrop Grumman, United States

****Correspondence:***
Laura Marchal-Crespo
laura.marchal@hest.ethz.ch

Specialty section:
This article was submitted to Neural Technology, a section of the journal Frontiers in Neuroscience

Received: *05 May 2017*
Accepted: *08 September 2017*
Published: *27 September 2017*

Citation:
Marchal-Crespo L, Michels L, Jaeger L, López-Olóriz J and Riener R (2017) Effect of Error Augmentation on Brain Activation and Motor Learning of a Complex Locomotor Task. Front. Neurosci. 11:526. doi: 10.3389/fnins.2017.00526

INTRODUCTION

Robot-aided gait rehabilitation was developed to improve rehabilitation in patients with severe gait impairments (Behrman and Harkema, 2000; Riener et al., 2005). During robotic gait training, patients are provided with body weight support while a gait orthosis moves their legs into a correct kinematic gait pattern. It is thought that by moving the limb in ways that patients are otherwise not able to move would provide novel somatosensory stimulation that helps induce brain plasticity (Poon, 2004; Rossini and Dal Forno, 2004). Furthermore, robotic guidance might motivate repetitive and intensive practice in a safe environment (Reinkensmeyer and Housman, 2007). However, robotic guidance also appears to decrease physical effort during training (Israel et al., 2006), suggesting that robotic rehabilitation could potentially decrease recovery if it encourages patient's slacking, i.e., a decrease in effort, energy consumption, or attention during repeated movements when movement errors are small (Scheidt et al., 2000; Reinkensmeyer et al., 2009).

In fact, up to date, the functional gains obtained after robotic gait training are still limited (Dobkin and Duncan, 2012). There have been several clinical studies that have compared robotic gait training to conventional therapy—see (Pennycott et al., 2012) for a review. Results from these studies suggest that robotic-aided gait rehabilitation is especially suitable in the stroke acute phase, when patients can benefit from the higher degree of support from the robotic device. In general, the best results were found when the robot was employed in combination with conventional therapy (Husemann et al., 2007; Schwartz et al., 2009). In fact, a recent report suggested that robotic therapy combined with conventional therapy was more effective than conventional therapy alone in subacute stroke patients with greater motor impairment (Morone et al., 2011). Thereby, current rehabilitation robots might be working with suboptimal training strategies—only using a fraction of the rehabilitation potential—by not considering the subjects' individual needs.

Active subject participation is vital in order to provoke motor plasticity (Lotze et al., 2003), and is therefore, an important feature of gait training, especially in patients with lower motor impairments. In order to promote higher levels of subject participation and challenge, "challenge-based" controllers have been proposed, i.e., controllers that, unlike guiding controllers, make movement tasks more challenging or difficult (Marchal-Crespo and Reinkensmeyer, 2009). Research on motor learning has emphasized that errors are needed in order to drive motor adaptation (Emken and Reinkensmeyer, 2005; Reisman et al., 2013). Experimental evidence with healthy subjects has demonstrated that adaptive processes can be accelerated when trajectory errors are amplified using robotic forces during walking (Emken and Reinkensmeyer, 2005). In post-stroke patients, increasing subjects' legs phasing error (i.e., walking asymmetry) through a split-belt treadmill that moved each leg at a different speed resulted in a long term increase in walking symmetry (Reisman et al., 2013). Error amplification training also induced more robust aftereffects after locomotion training as compared to assistive training (Yen et al., 2012). However, augmenting errors did not always benefit motor learning. In a recent experiment with healthy subjects, training a golf putting task with augmented velocity errors had no effect on task performance and resulted in a decrease in motivation that lasted even after the error augmentation was retired (Duarte and Reinkensmeyer, 2015). A possible rationale for these inconsistent results is that the motivation decrease associated with error amplification might hamper learning.

Movement errors can also be induced using unexpected randomly-varying robotic forces that disturb subjects' movements during training. Recent research has stated that motor variability exhibited before training predicts motor learning ability (i.e., subjects with more variable movements showed faster adaptation; Wu et al., 2014). Unexpected randomly-varying feedforward forces might increase movement variability, and therefore, create an excellent framework to boost motor learning. Furthermore, error exploration is an important element to enhance learning, especially during the first stages of learning (Huberdeau et al., 2015). Unexpected forces might push subjects away from their "comfort zone," and therefore, encourage them to explore and investigate the new motor tasks. In a motor learning experiment with healthy subjects, training with randomly-varying robotic forces resulted in better tracking skills than training without robotic assistance or training with repulsive forces proportional to errors (Lee and Choi, 2010). Furthermore, we found that adding random disturbing forces during training improved motor learning of a simple locomotion task, probably because the addition of unforeseen forces increased subjects' effort (muscle activation) and attention (Marchal-Crespo et al., 2014a,b).

A well-known motor learning theory, the Challenge Point Theory states that learning is maximized when the task difficulty is appropriate for the individual skill level of the performer (Guadagnoli and Lee, 2004). This is line with recent studies that found that robotic guidance seems to be especially helpful to train subjects with initial lower skill level (Marchal-Crespo et al., 2010, 2013), while error amplification was found to be more beneficial to train more skilled participants (Milot et al., 2010; Duarte and Reinkensmeyer, 2015). Additionally, error-augmenting strategies might be more suitable to enhance learning of especially simple tasks, i.e., tasks that can be learned in only one training session, since it might increase subjects' concentration (Marchal-Crespo et al., 2014b). On the other hand, in more challenging tasks, augmenting errors might decrease feelings of perceived satisfaction and competence and result in a decrease in motivation that might limit the effectiveness of error amplification on motor learning (Duarte and Reinkensmeyer, 2015).

Only few motor learning studies have compared the effectiveness of different robotic training strategies, and their relative benefits compared to unassisted practice, on motor learning. Most of these studies were performed with the upper limbs and/or using simple tasks, i.e., artificial tasks that have only one degree of freedom and can be learned in only one training session (Wulf and Shea, 2002). However, it has been shown that "*principles derived from the study of simple skills do not always generalize to complex skill learning,*" such as, relearning how to walk after a neurologic accident (Wulf and Shea, 2002). The goal

of robotic therapy is to develop robotic devices that promote motor recovery, i.e., that provoke participant's motor plasticity. Currently, however, there is not a solid scientific understanding of how this goal can best be achieved. Recent work has highlighted the relevance of motor learning principles in stroke recovery and neurorehabilitation (Krakauer, 2006; Shumway-Cook and Woollacott, 2007). In fact, it has been proposed that recovery after a brain injury is a form of motor learning or relearning (Dietz and Ward, 2015). Therefore, understanding the underlying mechanisms of motor learning might suggest novel training strategies to improve neurorehabilitation. Neuroimaging evaluation of brain areas involved in learning under different robotic training strategies can provide valuable insights on the observed behavioral outcomes. Furthermore, evaluation of brain areas involved in learning might also allow tailoring the best motor training strategies to the different patterns of brain damage (Burke and Cramer, 2013).

In this study, we present results of a motor learning experiment performed with thirty-four healthy subjects to evaluate the impact of three different training strategies on motor learning of a complex locomotor task: No perturbation, error amplification, and random force disturbance. The experiment was conducted while performing functional Magnetic Resonance Imaging (fMRI) employing an MRI-compatible robotic device (MARCOS). We hypothesized that training with the challenge-based strategies would result in better motor learning in initially more skilled subjects. We also expected that training with challenge-based strategies would hamper motor learning in initially less skilled subjects. To our knowledge, no studies have evaluated the brain regions activated during entire gait-like movements. Therefore, our hypothesis related to brain activation derives from studies that investigated isolated movements of ankle and knee joints (Luft et al., 2002) or imagination of walking (Miyai et al., 2003; Jahn et al., 2004; la Fougère et al., 2010). We hypothesize to find activity in somatosensory/motor related areas (S1/M1) and supplementary and pre-supplementary motor areas (SMA/pSMA). Hypothetically, during training with the challenge-based strategies, we expect more activity within all somatosensory/motor related areas, as well as in brain areas involved in error processing, such as, the anterior cingulate cortex (Mars et al., 2005), posterior medial frontal cortex (Hester et al., 2008), and cerebellum (Tseng et al., 2007; Grafton et al., 2008). Activation in the brainstem is also expected, based on animal studies.

METHODS

MARCOS

MARCOS was employed to conduct the experiment. MARCOS is an MRI-compatible robotic device pneumatically actuated and with one degree-of-freedom per leg (Hollnagel et al., 2011; **Figure 1**, left). MARCOS was built by the SMS-lab at ETH Zurich with low magnetic susceptibility materials to allow the assessment of brain activation using fMRI during gait-like stepping movements (Jaeger et al., 2014). The robot is actuated by two pneumatic cylinders (per leg), one attached to the subject's knee through a knee orthosis that can move the knee up and down, and a second one attached to the subject's foot sole using a special shoe, which can render forces that mimic ground reaction forces. The device allows hip, knee, and ankle flexion and extension movements in the sagittal plane that resemble on-the-spot stepping. The robot incorporates force sensors mounted at the orthoses-human contact points to measure the interaction forces between human and robot. The position of each cylinder piston is measured redundantly by optical encoders with a ceramic scale and a foil potentiometer. For more detailed information about the robot design, the reader is referred to (Hollnagel et al., 2011).

The Complex Locomotor Task

The experimental task consisted in tracking a white dot that moved on top of a Lissajous figure presented on a visual display (**Figure 1**, right) by coordinating the legs in a predefined gait-like pattern. The knees vertical displacements were mapped into the movement of a green dot on the visual display: The green dot moved up and down when the left leg moved up and down, and moved right and left when the right leg moved up and down. The predefined gait-like pattern to be learned consisted of moving the knees up and down following sinusoidal movements of equal frequency (0.5 Hz), but different amplitudes (left leg: 0.16 m; right leg: 0.08 m, i.e., axis ratio of 2) and with a phase difference between legs of 60°. This task was selected because it was challenging enough to observe learning in most of the subjects (Marchal-Crespo et al., 2014b). This task is also appealing because it resembles the abnormal gait pattern observed in stroke survivors with a paretic lower limb: An asymmetric pattern with the paretic leg performing shorter and faster steps.

Training Strategies

Subjects trained the gait-like task with one of three different training strategies: (i) No perturbation (NP): no disturbances were presented, (ii) Error amplification (EA): errors were amplified with repulsive forces proportional to errors, and (iii) Random force disturbance (RD): errors were induced with unexpected randomly-varying force disturbances. The design and evaluation of the training strategies was described in detail in (Marchal-Crespo et al., 2014b). Here, only a brief summary is given for completeness.

No Perturbation

When training with no perturbation, subjects are free to move without feeling any disturbance or assistance force from the robot. The control approach for the no perturbation strategy is a closed-loop zero force controller that minimizes the measured interaction forces between subjects and robot. The controller includes the compensation of the weight of the knee orthosis and the dependency of pressure build-up on chamber volume (Hollnagel et al., 2013; Marchal-Crespo et al., 2014b).

Error Amplification

In order to amplify the tracking errors (i.e., the differences between the desired and measured knee positions) created when trying to track the Lissajous figure, a proportional controller with

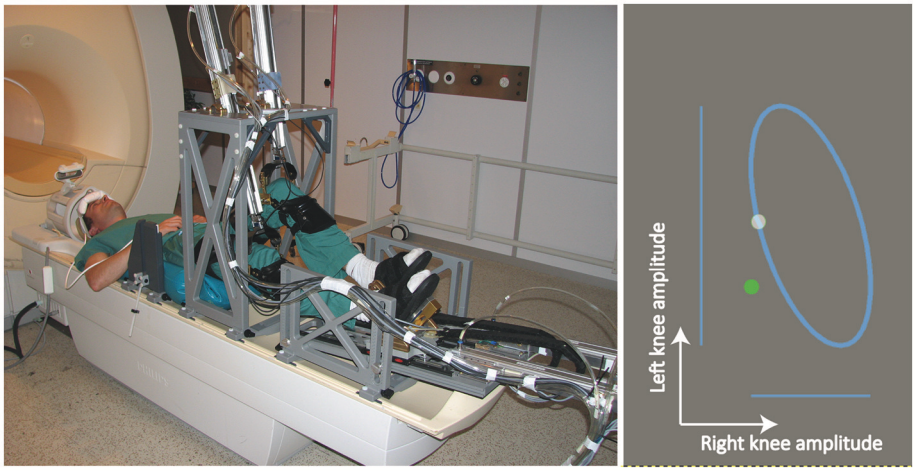

FIGURE 1 | (Left) The MRI-compatible robotic stepping actuator MARCOS in the 1.5 Tesla MR scanner (Hollnagel et al., 2011). The participant in this figure consented to the publication of his image. **(Right)** The Lissajous figure visually presented to participants. Subjects were requested to track a white dot that moved on top of a Lissajous figure by coordinating the legs in a predefined gait-like pattern. Subjects tracked the white dot with a green dot that moved up and down when the left leg moved up and down, and moved right and left when the right leg moved up and down.

negative impedance gain was developed. Therefore, the repulsive force applied by the knee cylinder is proportional to the tracking error, i.e., the force is smaller as smaller is the tracking error and increases proportional to the error. The forces from the error amplification controller were fed into a close-loop force controller. We saturated the magnitude of the error-amplification forces to guarantee the subjects' safety and to limit the difficulty of the task (Marchal-Crespo et al., 2014b).

Random Force Disturbance

The idea behind the random force disturbance strategy is to push subjects away from their "comfort zone," by forcing them to experience errors/movements that would otherwise not been created. The controller applies unpredictable random perturbing forces using the knee cylinder while subjects train the tracking task. The knee cylinder applies a disturbing force that last for 0.1 s with a random magnitude between $\pm$ 100 N, every 0.5 s. The random force disturbance controller works on top of a closed-loop force controller, therefore, the subjects are always in charge of the movement generation (Marchal-Crespo et al., 2014b).

Experimental Protocol

The study was approved by the local ethical committee (Kantonale Ethikkommission Zürich, Application Number: EK-856) and conducted in compliance with the Declaration of Helsinki. Thirty-four healthy subjects (23 male), 26.6 $\pm$ 3.5 years old, gave written consent to participate. All subjects were right footed (evaluated with the Waterloo Handedness Questionnaire, (Bryden, 1977). FMRI was recorded in the MR-Center of the University of Zurich and ETH Zurich, on a Philips Achieva (Philips Medical System, Best, The Netherlands) 1.5 T MR system equipped with an 8-channel head coil.

Subjects were supine positioned with their knees fixed to the MARCOS knee orthosis, while the feet were placed in special shoes and fixed with Velcro fasteners (**Figure 1**, left). Head motion was minimized through several solutions, such as, custom made hip-fixations and shoulder belts, a vacuum pillow at the participants' back, and an inflatable headgear (Crania, www.pearltec.ch; Hollnagel et al., 2011). The video display of the game was projected onto a screen placed in front of the scanner and viewed by the subjects through a mirror mounted on the MRI head coil (**Figure 1**, left).

A parallel design was used in order to evaluate the effects of training with the three different training strategies (**Figure 2**). The first 23 subjects were randomly assigned to one of the three training groups: No perturbation (NP), error amplification (EA), random disturbance (RD). After a preliminary evaluation of the data, we found that the tracking errors created during baseline (i.e., before training) had a significant effect on the benefits of practicing with the different training strategies (Marchal-Crespo et al., 2014b). Although it is expected that by randomizing subjects into the different training groups would result in a balanced level of tracking error across groups, it is still possible—especially in relative small sampling sizes—to end up with imbalanced groups that could bias our results. Therefore, we decided to allocate the remainder 11 subjects to one of the three training groups using adaptive randomization methods. The idea was to yield training groups whose subjects' initial errors followed normal distributions with similar means and standard distributions. To accomplish this goal, we assigned new subjects to one of the three training groups based in the visualization of the histograms of the errors created by the subjects evaluated till the moment and the error performed by the new subjects during baseline. Eleven subjects ended in the no-perturbation group, eleven in the error-amplification group, and twelve in the random-disturbance group.

In order to instruct subjects about the task to be performed, they were presented with a video, outside the scanner room,

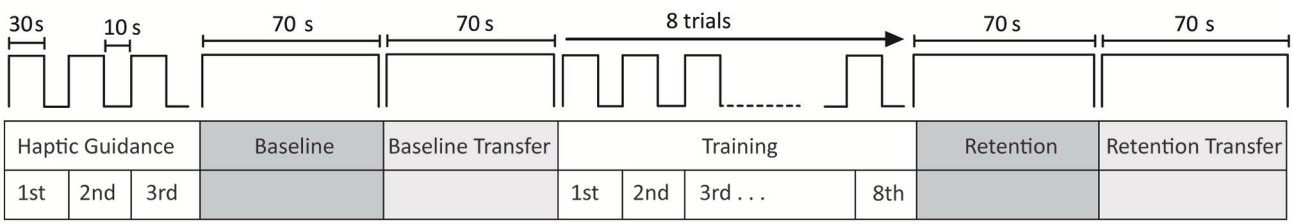

FIGURE 2 | Experimental protocol. Haptic guidance was employed to help subjects to understand the locomotor task. Three trials of 30 s with the robot passively moving the subjects' legs were employed to present the locomotor task. During baseline, subjects actively tracked the Lissajous figure during 70 s in no perturbation mode. Subjects performed a second baseline test (baseline-transfer), where they tracked a similar figure but with the left leg with the smallest amplitude. During training, subjects played with no perturbation, error amplification or random force disturbance, depending on their training group. Each training session consisted of eight trials of 30 s of movement with 10 s rest between trials. The short-term retention and transfer tests followed the same structure and order as baseline and baseline-transfer tests. Subjects were scanned by the fMRI during all phases.

that showed a subject in MARCOS moving alternatively his legs up and down and how these knee movements controlled the movement of a green dot on a screen. They were not informed about the training group they were assigned to, but were informed that during practice the robot could disturb them. The experiment started with a haptic demonstration phase, where the robot passively guided the subjects' legs in the desired gait-like pattern during three trials of 30 s, with 10 s of rest between trials in order to help subjects to understand the task to be performed (Hollnagel et al., 2013). During the haptic-guidance condition, subjects were instructed to relax and keep both legs passive while they observed the white and green dot moving on top of the Lissajous figure on the screen. After the haptic demonstration of the locomotor task, subjects performed the baseline test during 70 s. They were instructed to coordinate their legs in order to track the white dot that moved on top of the Lissajous figure in no perturbation mode. Transfer of learning, i.e., the capacity to apply an acquired skill on a task to another very similar task (Schmidt and Lee, 2010) is a crucial aspect of motor learning. Therefore, after baseline, subjects performed a second baseline test during 70 s (baseline-transfer), where they followed a similar Lissajous figure but with the left leg moving with the smallest amplitude (left leg: 0.08 m; right leg: 0.16 m). During training, subjects played without perturbation, error amplification or random force disturbance, depending on their training strategy group. Each training session consisted of eight trials of 30 s of movement with 10 s rest between trials. The challenge-based training strategies were applied to the left leg only, while the right leg was controlled in no perturbation mode in order to limit the task difficulty. The short-term retention and short-term retention transfer tests were 70 s long each and were performed in no perturbation mode. Overall, the experiment was <1 h. Subjects were actively scanned by the fMRI through the duration of the experiment.

Data Processing and Statistical Analysis

Behavioral Data

For each protocol test and training trial, we calculated the mean tracking error for each leg as the mean of the absolute value of the difference between the measured and target knee positions. We evaluated whether the challenge-based training strategies worked as expected (i.e., they increased the error during training): We compared the error of the left leg in the first training trial to the error during baseline using a repeated measures ANOVA with training strategy as a between subjects factor. To determine whether subjects increased the left leg error when training started, a paired t-test between baseline and the first training trial was performed per each training group. We further compared the tracking error during the eight training trials between training groups using ANOVAs. In order to determine whether subjects adapted to the challenged-based strategies during training—i.e., they reduced the error of the left leg during training—we performed a paired t-test between the left leg tracking error created at the first and last (eighth) training trials.

The absolute tracking error during baseline was employed as a qualitative measure of initial skill level (i.e. the larger the error during baseline, the initially less skilled a subject was). We used K-means cluster analysis to divide subjects into two skill-based groups, based on the tracking error created during baseline. Thirteen subjects who performed systematically worse during baseline (cluster center = 0.065 m) were assigned into the novice group (5 NP, 4 RD, 4 EA), and the remainder 21 subjects were classified (cluster center = 0.041 m) as skilled (6 NP, 8 RD, 7 EA). An ANOVA was used to evaluate whether the skill groups performed differently during baseline. We used repeated measures ANOVA to test the effect that training strategies [no perturbation (NP), error amplification (EA), and random force disturbance (RD) as fixed effect], initial skill level (novice and skilled as fixed effects) and their interaction had on the tracking error reduction from baseline to retention. In order to determine whether subjects learned the complex locomotor task, a paired t-test between baseline and retention was performed. To determine whether subjects in each training strategy group and skill level subgroup learned the task, a Wilcoxon test between the tracking error at baseline and retention was performed. We compared the error reduction between training groups in each skill level subgroup using Kruskal-Wallis tests. Four subjects in the skilled group (2 RD, 2 EA) who performed remarkably well during baseline (error < 0.032 m) were not considered in these Wilcoxon tests in order to avoid the negative effect of learning ceiling. To test the correlation between error reduction after the different training strategies and initial skill level, Pearson's correlation tests were performed.

We used a second performance variable in order to evaluate whether subjects learned the desired phase between legs. The period between legs at each step was calculated as the difference between the time at which the left leg is at its maximum high and the time when the right leg reaches its highest position during a step. The phase was calculated as 360° over this period. For each protocol test, the absolute mean phase error (calculated as the difference between the calculated phase and the desired one of 60°) across all steps was calculated. Data from one subject in the no-perturbation group during baseline was removed from statistical analysis, since the error reached its maximum. In order to test whether subjects learned the desired phase, a paired *t*-test between baseline and retention was performed. We used repeated measures ANOVA to test the effect that the training strategies, initial skill level and their interaction had on the phase error reduction from baseline to retention.

Transfer could not be evaluated in four subjects (1 NP, 2 RD, 1 EA), because data was not correctly recorded during baseline-transfer. Transfer was evaluated using repeated measures ANOVA to test the effect of the training strategy (NP, EA, and RD as fixed effects), initial skill level (novice and skilled) and their interaction on the tracking error reduction from baseline—transfer to retention-transfer. Paired *t*-tests between the tracking error created during baseline-transfer and retention-transfer were performed in order to evaluate whether subjects in each training group transferred the learned motor skills.

Normal distribution was checked visually using Q–Q plots. Post-hoc comparisons were performed with Tukey correction. The significance value was set to $\alpha = 0.05$. Statistical analyses were performed using IBM® SPSS® Software (version 23, Chicago, IL).

Functional MR Data

FMRI of the brain was acquired using a T2*-weighted, single-shot, echo planar imaging sequence (echo time = 50 ms, repetition time = 3.025 s, flip angle = 90°, SENSE factor = 1.6). A total of 35 interleaved, angulated, transversal slices covering the whole brain were acquired in each volume (FOV = 220 × 220 mm, acquisition voxel size: 2.75 × 2.8 × 3.8 mm, resliced to 1.72 × 1.72 × 3.8 mm).

FMRI data were analyzed using SPM8 (Wellcome Department of Cognitive Neurology, London, UK). Images were realigned to the mean image and normalized to standard MNI space using the EPI template provided by the Montreal Neurological Institute (MNI brain) and smoothed using an 8 mm full-width at half-maximum Gaussian kernel. The estimated realignment parameter data were filtered using the discrete cosine transform matrix filter incorporated in SPM8, to remove any linear drift. In order to avoid movement artifacts, FMRI data sets that after filtering showed a total head displacement above half voxel size in each dimension were excluded from the 1st-level statistical analysis. Contrast images of the motor task performed at different time points in the MR scanner (period: baseline, training, and retention) vs. an implicit rest (no movements) condition were calculated. FMRI data sets from 10 subjects during training, and data from one subject during the retention test were excluded from further analysis because the measured head motions were above the threshold. FMRI data from a total of 24 subjects (9 NP, 7 EA, and 8 RD) during training, and 33 (10 NP, 11 EA, 12 RD) during baseline and retention were employed at 2nd-level analysis. The 1st-level contrast images were then subject to a 2nd-level full factorial group analysis (2-way ANOVA). Here we computed main effects of initial skill level and training strategy for the contrasts: Training—rest, and retention—baseline. In case of significant main effect of strategy, we compared by *post-hoc* *t*-tests the following contrasts:

1. Error amplification vs. no perturbation (and vice versa)
2. Error amplification vs. random force disturbance (and vice versa)
3. No perturbation vs. random force disturbance (and vice versa)

In case of a significant main effect of skill level, we compared by unpaired *t*-tests skilled vs. novice participants (across all training strategies). We also computed strategy × initial skill-level interaction effects. However, we did not perform *post-hoc* tests on the interaction, as we had not enough subjects ($n < 10$) and, thus, lacking statistical power.

All statistical tests were thresholded at $p \leq 0.001$ (uncorrected) and were cluster-corrected ($k_E = 27$ voxels) to achieve $p < 0.05$ corrected. This cluster threshold was based on a Monte-Carlo simulation approach using a script to estimate the average size of the random clusters that can occur in our data given a $p \leq 0.001$ (Slotnick et al., 2003).

RESULTS

Behavioral Data

Performance during Training

The different training groups responded differently when training started, as suggested by a significant difference between training groups in the tracking error change from baseline to the first training trial [**Figure 3**, $F_{(2, 31)} = 9.84$, $p < 0.001$]. Subjects trained with error amplification significantly increased the error from baseline to the first training trial ($p = 0.002$), while subjects trained without perturbations and with random-disturbance did not changed the errors significantly. Subjects in the error-amplification group performed systematically worse than subjects in the random-disturbance and no-perturbation groups during the first training trials, as observed in a significant greater tracking error during the first, second and fourth training trials [**Figure 3**, Trial 2, $F_{(2, 31)} = 6.62$, $p = 0.004$; Trial 3, $F_{(2, 31)} = 4.17$, $p = 0.025$; Trial 4, $F_{(2, 31)} = 2.40$, $p = 0.107$; Trial 5, $F_{(2, 31)} = 4.17$, $p = 0.025$]. The differences between groups were non-significant during the last training trials. This is due to the fact that subjects in the error-amplification group adapted to the error amplification disturbance, suggested by the significant error reduction from the first to the last (eighth) training trials (paired *t*-test, $p = 0.004$). This adaptation was not observed in the no-perturbation and random-disturbance groups. Both groups reduced the error from the first to the last training trials, although not significantly. The random-disturbance and no-perturbation groups performed similarly through the duration of the training.

Effect of Training Strategies and Skill Level on Learning

The performance during baseline was significantly different between skill groups. They showed significant differences in the tracking error during baseline [$F_{(1, 32)} = 52.14$, $p < 0.001$]. We examined the effect of the subjects' skill level (i.e., the tracking error during baseline) on the effectiveness of the different training strategies. We found a non-significant linear correlation between initial skill level and the error reduction from baseline to retention after training without perturbations (**Figure 4** left, Pearson's correlation, $R = 0.544$, $p = 0.083$). We also found a quadratic relationship between the initial skill level and the error reduction from baseline to retention after training with error amplification (**Figure 4** left, $R = 0.716$, $p = 0.057$).

We used repeated measures ANOVA to test the effect that different training strategies [no perturbation (NP), error amplification (EA), random disturbance (RD)], initial skill level (novice, skilled), and their interaction had on the tracking error reduction from baseline to retention. We found that all subjects reduced the tracking error after training [$F_{(1, 28)} = 27.30$, $p < 0.001$]. Subjects in all training strategies learned the task (NP: $p = 0.011$; RD: $p = 0.016$; EA: $p = 0.022$). The main effect of initial skill level on the error reduction was non-significant. The main effect of training strategy was also non-significant. However, we found an interaction between the initial skill level and the training strategy that approached statistical significance [$F_{(2, 28)} = 3.22$, $p = 0.055$]. Novices only reduced the error significantly when trained without perturbation (**Figure 4** right, Wilcoxon, $p = 0.043$). In fact, novices tended to reduce the errors to a greater amount when trained without perturbation in comparison with the other training strategies (Kruskal-Wallis $p = 0.063$). The skilled group only reduced significantly the error after training with challenge-based strategies (**Figure 4** right, Wilcoxon, EA: $p = 0.043$, RD: $p = 0.075$).

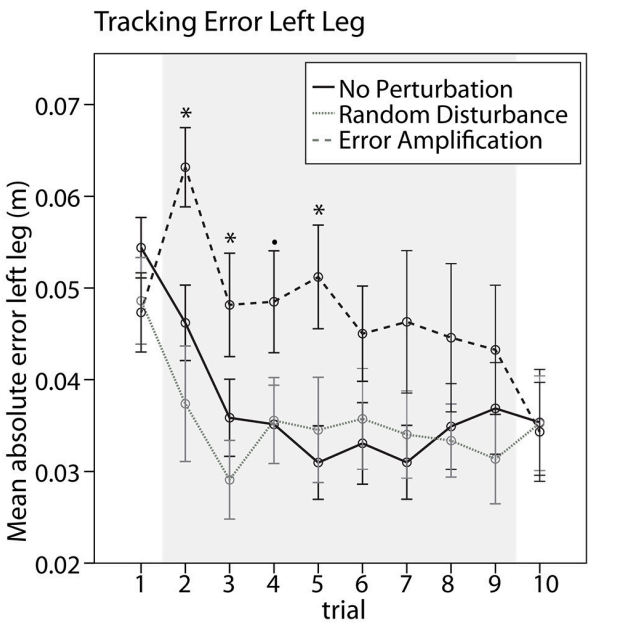

FIGURE 3 | Performance during training. Mean absolute tracking error created with the left leg during baseline (trial 1), training with the different strategies (trials 2–9, shaded area), and retention (trial 10). Error bars show ± 1 CI. *$p < 0.05$, •$p < 0.1$.

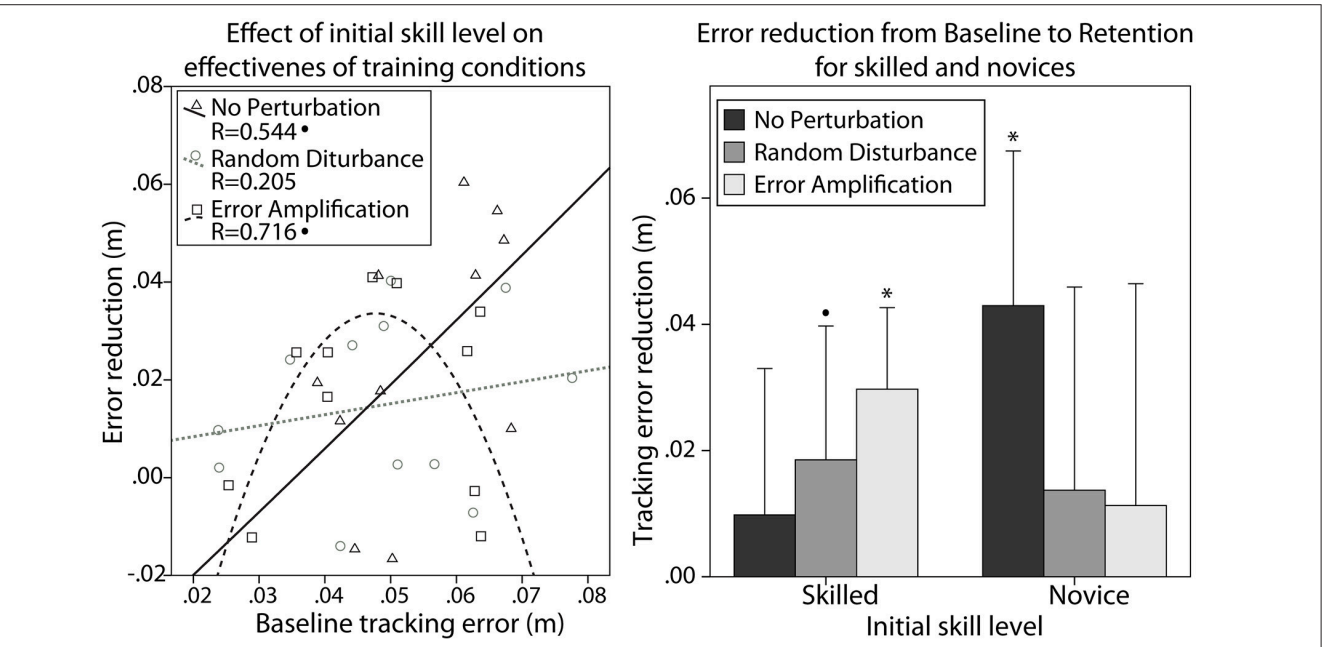

FIGURE 4 | (Left) Effect of initial skill level (i.e., tracking error during baseline) on the error reduction from baseline to retention with the different training strategies. **(Right)** Error reduction after training with the different training strategies, in the skilled and novice groups. Error bars show ± 1 CI. *$p < 0.05$, •$p < 0.1$.

In general, all subjects reduced the absolute phase error from baseline to retention [$F_{(1, 28)} = 7.50$, $p = 0.011$]. The effect of the training strategy on the phase error reduction was one-sided significant [$F_{(2, 28)} = 2.82$, $p = 0.076$]. In particular, the EA group reduced the error in a smaller amount than the NP group (**Figure 5**, $p = 0.077$). We did not find a significant effect of skill level in the error reduction, neither an interaction effect of the training strategy and the initial skill level.

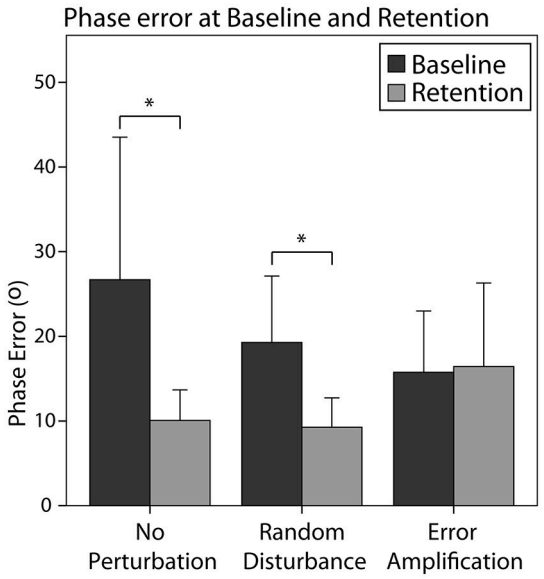

FIGURE 5 | Absolute phase error for the different training groups during baseline and retention. Error bars show ± 1 CI. *$p < 0.05$.

Effect of Training Strategy on Transfer

Subjects generalized the learning to the untrained task, i.e., they significantly reduced the errors from baseline-transfer to retention-transfer [$F_{(1, 24)} = 9.59$, $p = 0.005$]. In particular, subjects trained without perturbation reduced significantly the tracking error (**Figure 6** left, $p = 0.016$). Subjects trained with random disturbance also reduced the tracking errors significantly (**Figure 6** left, $p = 0.007$). However, subjects trained with error amplification did not reduce the error from baseline-transfer to retention-transfer. The main effect of training strategy was, however, non-significant [$F_{(2, 24)} = 1.58$, $p = 0.228$]. The main effect of initial skill level was also non-significant. The interaction effect of the skill level and training strategy did not reach significance [$F_{(2, 24)} = 2.64$, $p = 0.092$].

Subjects did not significantly reduce the phase error from baseline-transfer to retention-transfer (**Figure 6** right). The effect of the training strategy on the phase error reduction in the transfer task did not reach significance [$F_{(2, 24)} = 2.97$, $p = 0.070$]. As observed in **Figure 6** right, subjects trained without perturbation and with random disturbance reduced the errors (although not significantly), while subjects in the error-amplification group tended to increase the errors after training. The main effect of initial skill level was non-significant. The interaction effect of the skill level and training strategy almost reached significance [$F_{(2, 24)} = 3.25$, $p = 0.055$].

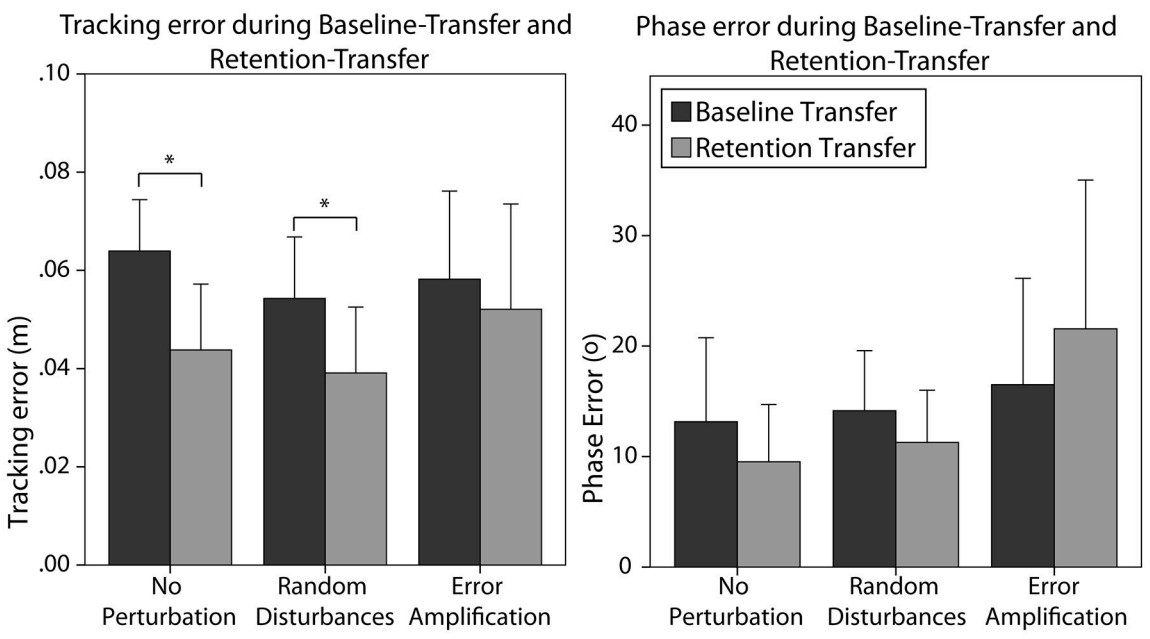

FIGURE 6 | Tracking error **(Left)** and phase error **(Right)** created by the different training groups during baseline-transfer and retention-transfer tests. Error bars show ± 1 CI. *$p < 0.05$.

Functional MRI Data

Training Period

We first visualized the general activation for the three different strategies (NP, EA, and RD) during the training period. As it can be observed in **Figure 7**, all strategies lead to significant bilateral activation ($p < 0.001$, uncorrected) in the area 4a (leg area). The activation map was most widespread for NP and activation for this strategy lead also to activation in other brain regions (results not reported).

Strategy-related main effects were seen in the basal ganglia (putamen, caudate nucleus, and pallidum), thalamus as well as in different parts of the cerebellum (**Table 1A**). In addition, fMRI signal responses were seen in the parietal cortex such as, the intraparietal sulcus (IPS)—which represented largest cluster in the activation map—the posterior cingulate cortex (PCC) and in different regions of the visual and frontal cortex.

We then asked which training strategies differed in brain activation strength (**Table 2**). Error amplification did not lead to stronger fMRI signal responses relative to no perturbation or random disturbance. On the contrary, the contrast "no perturbations vs. error amplification" revealed numerous brain activations, which are—for simplicity—reported on $p < 0.05$ (FWE-corrected, $t > 7.1$; **Table 2A**). In a similar vein, the comparison "no perturbations vs. random disturbance" showed several activated clusters ($p < 0.001$, $t > 3.6$, **Table 2B**). The contrast "random disturbance vs. error amplification" demonstrated few significant clusters ($p < 0.001$, $t > 3.6$, **Table 2C**).

Main effects of initial skill level were seen dominantly in right temporal and parietal regions, including the IPS (**Table 1B**). *Post-hoc t*-test analysis revealed that skilled subjects showed stronger activation compared to novices in the right IPS, SPL (precuneus), medial temporal lobe, and inferior temporal gyrus (**Table 3**). At the same threshold but with lower cluster-size cut-off ($k_E > 15$ voxels) we additionally observed activation in the brainstem and left cerebellum.

Similar to the main effect of training strategy, strategy × initial skill-level interaction effects were most pronounced (i.e., largest activation cluster) in the IPS (**Table 1C**). Apart from activation in frontal and visual brain regions, we noticed further activation of the basal ganglia, primary motor cortex (M1) and somatosensory regions (e.g., SMA) as well as the cerebellum.

Retention—Baseline Period

As summarized in **Table 4**, a main effect of strategy was seen in the subgenual and anterior cingulate cortex and in M1. No main effect of initial skill level was seen (also not when bi-directionally comparing skilled vs. non-skilled subjects by *t*-tests) nor a strategy × initial skill-level interaction. Post-hoc analysis on the main effect of strategy revealed significant differences for the contrasts "no perturbation vs. error amplification" and "random disturbance vs. error amplification" (see **Table 5**). The first contrast demonstrated primarily activation in the frontal cortex. Both contrasts revealed activation in orbitofrontal regions (**Figure 8**).

DISCUSSION

We evaluated the impact of three error-modulation robotic training strategies on brain activation and motor learning of a complex locomotor task: No perturbation, error amplification, and random force disturbance. The experimental task consisted in learning a complex locomotor task: Coordinating the legs in a particular gait–like pattern in order to track a Lissajous figure presented on a visual display. The MRI-compatible one degree-of-freedom steeper robot (MARCOS) developed in our institution was employed to conduct the experiment, while performing fMRI in a 1.5 Tesla MR scanner. Even though none of fMRI results survives a voxel threshold of $p < 0.05$ using familywise error correction, all fMRI results are presented at a widely accepted cluster-corrected *p*-value of $p < 0.05$.

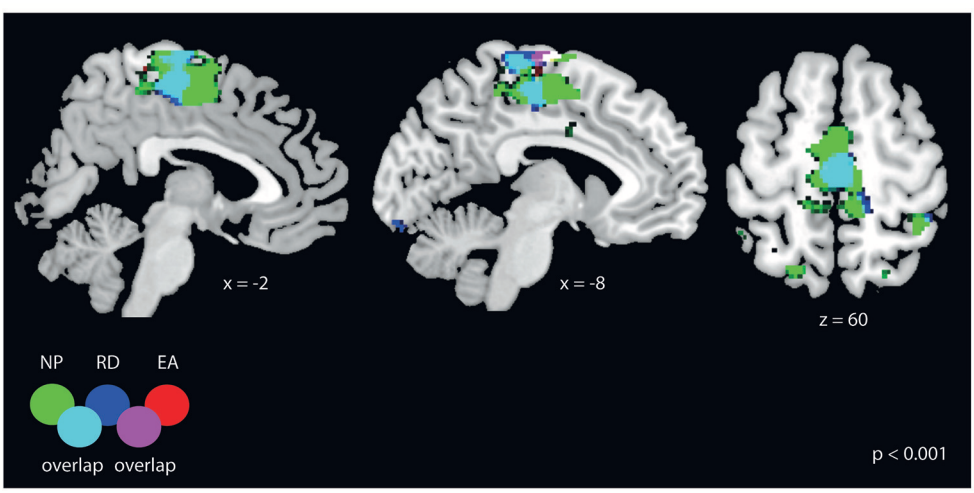

FIGURE 7 | General fMRI activation for the three training strategies: NP, RD, and EA. All results are displayed at $p < 0.001$ (uncorrected, $t > 3.6$) with a cluster-extend threshold of $k_E > 27$ voxels. The activation overlaps for all three training strategies at the somatosensory cortex (at the leg area).

TABLE 1 | Summary of brain activation during training for the main effect of training strategy, initial skill level, and its interaction in the training model.

Region	Hemisphere	MNI			Cluster-size
(A) MAIN EFFECT OF TRAINING STRATEGY					
Putamen	Left	−22	13	0	122
Middle orbital	Left	−35	47	0	225
Pallidum	Right	22	−4	0	82
Thalamus	Left	−13	−24	0	33
	Right	12	−6	12	28
Cerebellum (lobule VI)	Right	35	−41	−30	27
	Left	−20	−55	−8	52
Intraparietal sulcus (IPS)	Right	45	−55	38	934
	Left	−42	−57	39	153
Posterior cingulate cortex (PCC)	Right	1	−38	35	283
Inferior frontal gyrus (BA 44/45)	Left	−48	−13	34	326
	Right	48	23	28	45
Middle frontal gyrus	Left	−28	31	34	139
Cuneus	Right	18	−70	27	90
Amygdala	Left	−30	0	−19	61
Hippocampus	Right	40	−16	−14	59
Fusiform gyrus	Right	25	−61	5	55
(B) MAIN EFFECT OF INITIAL SKILL					
Medial temporal gyrus	Left	−40	14	−32	75
SPL (precuneus)	Right	−2	−66	60	56
IPS	Right	42	−49	36	64
Inferior temporal gyrus	Right	64	−38	−12	20
Rolandic operculum	Right	50	−1	13	16
(C) INTERACTION STRATEGY × INITIAL SKILL					
IPS	Right	42	−48	36	1595
	Left	−40	−57	39	320
Lingual/fusiform	Left	−20	−62	−6	226
Fusiform gyrus	Left	−37	−78	−12	28
Supplemtary motor area (SMA)	Right	2	−15	56	173
PCC	Right	4	−48	40	133
Primary motor cortex (area 4a/4p)	Right	28	−28	58	118
Middle frontal gyrus	Right	36	18	56	116
Postcental gyrus (area 1/2)	Right	24	−48	66	49
	Right	50	−40	58	109
Caudate nucleus	Right	18	12	10	108
Cerebellum (lobule VI)	Right	28	−36	−26	80
hOC3v	Left	−14	−92	2	70
Insula	Left	−26	19	0	56
Medial temporal gyrus	Right	56	−48	0	53
Superior orbital gyrus	Right	14	38	−14	47
Temporal pole	Left	−24	2	−28	44
Thalamus	Right	8	−2	12	41
Putamen	Right	16	8	4	107

All results are reported at $p < 0.001$ (uncorrected, $t > 3.6$), F-contrast, $k_E > 27$.

TABLE 2 | Summary of *post-hoc t*-tests on the main effect of training strategy during training.

Region	Hemisphere	MNI			Cluster-size
(A) NP—EA*					
IPS	Right	43	−50	37	72
Inferior parietal lobe	Right	42	−68	39	32
Inferior frontal gyrus	Left	−57	8	31	15
Middle orbital gyrus	Left	−36	48	0	4
(B) NP—RD**					
Angular gyrus	Right	42	−60	30	1262
Fusiform gyrus	Left	−22	−52	−8	217
	Left	−27	−77	−5	136
Thalamus	Left	−31	−27	1	161
	Right	15	−6	12	33
Superior frontal gyrus	Left	−21	18	38	92
Ant.insula/ant. putamen	Left	−28	16	1	73
Cerebellum (lobule VI)	Left	−26	−30	−26	72
Cerebellum (dentate nucleus)	Left	−22	−52	−32	32
PCC	Right	12	−50	32	68
Lingual gyrus	Right	26	−63	4	62
Pallidum	Right	17	1	6	59
Inferior frontal gyrus	Right	47	21	27	54
Caudate nucleus	Left	−14	6	9	50
Hippocampus	Right	37	−16	−14	40
Precentral gyrus	Right	64	−3	28	36
(C) RD—EA**					
IPS	Right	47	−56	39	587
Inferior frontal gyrus (BA 44/45)	Left	−54	10	34	111
Superior orbital gyrus	Left	−37	52	1	37
Calcarine gyrus (V1/V2)	Right	1	−99	9	35
Superior frontal gyrus	Left	−13	53	40	34

**$p < 0.05$ (FWE corrected, $t > 7.1$).*
***$p < 0.001$ (uncorrected, $t > 3.6$).*
The following training strategies were compared: NP—EA, NP—RD, RD—EA. For readability, results for NP—EA are shown at $p < 0.05$ (family-wise error corrected). All other contrasts are reported at $p < 0.001$ (uncorrected, $t > 3.6$), $k_E > 27$.

TABLE 3 | Brain activation differences for "skilled vs. non-skilled" participants averaged across all learning strategies during training.

Region	Hemisphere	MNI			Cluster-size
SKILLED vs. NON-SKILLED					
SPL (precuneus)	Midline	0	−68	57	94
Medial temporal pole	Left	−40	14	−32	114
IPS	Right	42	−48	36	96
Inferior temporal gyrus	Right	64	−38	−12	35

All results are reported at $p < 0.001$ (uncorrected, $t > 3.6$), F-contrast, kE > 27.

Effects of Training Strategies on Performance during Training

The error amplification training strategy worked as expected, i.e., it significantly increased the tracking error when firstly introduced. Training with error amplification resulted in larger tracking errors during the firsts training trials compared to training with random force disturbance and no perturbation, suggesting that error amplification was the most difficult training strategy. We did not find significant differences in subjects'

TABLE 4 | Summary of brain activation for the main effect of learning strategy for the contrast "retention—baseline".

Region	Hemisphere	MNI			Cluster-size
MAIN EFFECT OF STRATEGY					
Subgenual cingulate (BA 25)	Right	2	0	13	101
	Left	−8	−2	−12	88
Anterior cingulate cortex (BA 24/32)	Left	−13	16	−8	42
Primary motor cortex (area 4p)	Right	37	−16	38	29

Results are displayed at $p < 0.001$ (uncorrected, $t > 3.6$) with a cluster-extend threshold of $k_E > 27$ voxels. There was no significant main effect of initial skill level or an interaction effect (learning strategy × initial skill level) visible.

TABLE 5 | Summary of *post-hoc t*-tests on the main effect of learning strategy for the contrast "retention—baseline".

Region	Hemisphere	MNI			Cluster-size
(A) NP—EA					
Inferior temporal gyrus	Right	62	−42	−10	41
Frontal operculum	Right	6	0	−12	617
Superior orbital gyrus	Left	−12	16	−8	
	Right	14	2	−14	
Primary motor cortex (area 3a/4p)	Right	36	−16	38	95
	Right	48	−14	38	
Anterior temporal lobe	Left	−48	10	−16	147
	Left	−54	2	−16	
	Left	−48	−6	−16	
Middle orbital gyrus	Right	22	34	−4	34
	Right	32	36	−4	
Inferior frontal gyurs/Middle orbital gyrus	Right	34	26	−16	98
	Right	44	48	−14	
	Right	32	40	−8	
Precentral gyrus (BA 44/45)	Right	56	4	36	31
Frontal operculum (fo1)	Right	4	44	−14	29
Frontal operculum (fo3)	Left	−26	36	−2	27
(B) RD—EA					
Superior orbital gyrus	Left	−8	−2	−12	53
Superior orbital gyrus/BA 24 and BA 25	Right	6	−2	−12	33
Middle occipital gyrus (area hOC4lp)	Right	36	−86	16	34
Inferior temporal gyrus	Left	−40	−28	18	69
Supramarginal gyrus (IPL/IPS)	Left	−48	−42	34	64
OP2	Right	30	−24	22	39
OP1 (S2)	Left	−56	−30	24	58
IPL (PFm/PGa)	Left	−52	−64	42	39
	Left	−52	−54	44	
Thalamus	Right	4	−20	20	27
	Left	−4	−22	18	

Results are displayed at $p < 0.001$ (uncorrected $t > 3.6$) with a cluster-extend threshold of $k_E > 27$ voxels. NP and RD showed stronger fMRI signal changes compared to EA.

performance when training with random disturbance and no perturbation. The forces applied during random disturbance created short and fast change in the trajectory smoothness (Marchal-Crespo et al., 2011) and thereby, maybe the overall mean tracking error was not significantly affected. This is in line with a previous study we conducted using MARCOS to train a simple locomotor task with random force disturbance: The introduction of force disturbances did not increase the mean tracking error, but increased the muscle activation, suggesting that training with random disturbances was more physically demanding (Marchal-Crespo et al., 2014b). In fact, this higher muscular activity may explain why the tracking error during training with force disturbances did not differ from the mean error created when training without perturbations: Maybe subjects were able to cancel the tracking errors using muscular effort.

Subjects adapted to the error-amplification strategy during training. This is in line with previous research on motor learning that suggested that training with error-amplification promote the formation of an internal model (Emken and Reinkensmeyer, 2005). Subjects did not significantly reduce the tracking error when training with random disturbances, probably because the disturbing forces were unpredictably applied and the formation of an internal model was not possible.

The Training Strategy that Enhances Learning Depends on Subjects' Skill Level

We expected better motor learning when training with the challenge-based strategies in initially more skilled subjects. We also hypothesized that training with challenge-based strategies would hamper motor learning in initially less skilled subjects. Behavioral results confirmed our hypothesis: The training strategy that enhances learning depended on subjects' initial skill level. Training without perturbations benefited learning in novices, while amplifying tracking errors during training enhanced learning in initially more skilled subjects. This is in line with previous experiments that showed that error amplification seemed to be specifically beneficial for skilled subjects (Milot et al., 2010; Duarte and Reinkensmeyer, 2015). This can be explained by the Challenge Point Theory, which states that learning is maximized when the task difficulty is appropriate for the individual subject's level of expertise (Guadagnoli and Lee, 2004). Error amplification, on the other hand, hampered learning in initially less skilled subjects, maybe because it made the task to be learned too difficult and frustrating (Duarte and Reinkensmeyer, 2015). Indeed, our fMRI data showed an involvement of the brain reward system in the error-amplification group for the contrast NP—EA, which could support this theory.

In a previous experiment performed with MARCOS and similar error-challenging robotic strategies, we found contradictory results (Marchal-Crespo et al., 2014b). Training with error amplification was most suitable for initially less skilled subjects. This contradiction might be explained by the differences in the motor task to be learned. In the previous experiment, the task consisted in trying to synchronize the non-dominant leg with the dominant leg, passively moved by the robot. Therefore, it was a simple one degree-of-freedom locomotor task, compared to the complex two degree-of-freedom bipedal

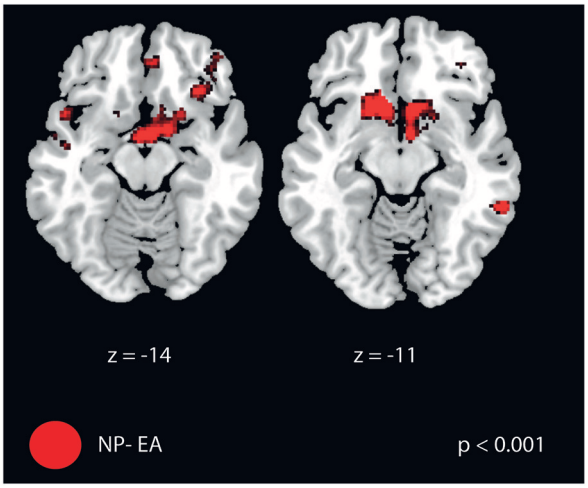

FIGURE 8 | Brain activation difference between "retention—baseline" for the contrast no perturbation—error amplification. FMRI signal changes were most pronounced in the frontal cortex including the orbitofrontal cortex (for a full list of activation see **Table 5**).

locomotor task employed in the current experiment. This is in line with previous research that found that "*principles derived from the study of simple skills do not always generalize to complex skill learning*" (Wulf and Shea, 2002). For less skilled subjects, error augmenting strategies might be more suitable to enhance learning of especially simple tasks, but might hamper learning of more complex tasks. Therefore, matching the training strategy to the relative trainee's skill level to perform a specific task, may provide the greatest opportunity for learning (Marchal-Crespo et al., 2015).

Interestingly, we found that for the error-amplification group, the relationship between error reduction after training and initial skill level was quadratic. Initially proficient subjects—i.e., subjects who performed particularly well during baseline—did not benefit from error amplification. This can be explained by the behavior of the controller. The perturbations of the error-amplification strategy depend on the subjects' performance—i.e., only existing errors are amplified, with higher amplification for larger errors. Thereby, proficient subjects may not have been sufficiently challenged during training, since they were making systematically small errors and thereby, error amplification failed to have a significant impact on their performance during training.

Random force disturbances seemed to benefit motor learning in all subjects, independently of their initial skill level. It is interesting to note that the random force disturbance did not increase the mean tracking error during training. The goal of the random force disturbance strategy is to push subjects away from their "comfort zone," so they are encouraged to examine and investigate new solutions to fulfill the motor tasks by themselves. Therefore, maybe the lack of anticipation of the random disturbing forces motivated subjects to be more concentrated and attentive during training. The random-disturbance strategy was independent of the subjects' performance, thus it might increase subjects' attention during training, even if proficient subjects created very small errors. Our fMRI data support this idea, since we found stronger activation in brain areas associated with attentional control (Shulman et al., 2003; Luks et al., 2007; such as, SPL and IPS) when training with random disturbance, compared to training with error amplification. However, we did not observe differences in brain activation between training with random force disturbances and without perturbations. This might be due to some overlapping activity in the frontal cortex (see **Tables 2A,B**) when we compare to error amplification. Alternatively, maybe the difference in the behavioral results was due to a change in the limbs' stiffness. Training in unstable environments tend to alter the effective stiffness of the limbs through co-contraction of muscles (Franklin et al., 2007; Marchal-Crespo et al., 2014b). However, this stiffness difference did not lead do detectable brain activation differences, maybe because the muscle co-contraction was not strong enough (Marchal-Crespo et al., 2014b).

Error Amplification Hampered Transfer of Learning

We confirmed our hypothesis that the training strategy that enhances learning of a complex locomotor task depends on subjects' initial skill level. However, we also found that training with error amplification limited transfer of learning, while training with no perturbation and random disturbance seemed to transfer the learning gains to a similar task. Although there was no statistical proof that the transfer was greater after training without perturbation and random noise relative to error amplification, our results suggest evidence for transfer in these conditions only. The lack of transfer observed in the error-amplification group contradicts motor learning research that found a positive effect of error amplification on transfer (Milot et al., 2010).

A possible rationale for the differences observed in transfer between the challenge-based training strategies is that subjects trained with error amplification focused mainly in reducing the tracking errors to reduce the perturbing forces, and failed to interiorized or consciously understand the desired gait-like pattern. This idea is supported by the fact that subjects trained with error amplification failed to learn the correct phase difference between legs also in the trained task, while subjects trained without perturbation and random disturbance did learn the correct diphase. Therefore, the good performance of subjects after training with error amplification might have resulted from implicit learning, i.e., subjects learned without awareness of what has been learned. On the other hand, subjects trained with random force disturbance (and without perturbation) might have experienced explicit learning, i.e. they actively searched for the gait-like pattern to correctly track the presented figure. Several studies have shown that implicit learning shows negative transfer of the acquired motor skills, whereas explicit learning showed strong positive transfer (Lee and Vakoch, 1996). Therefore, based on the transfer and phase error results, we hypothesized that for the specific complex locomotion task presented in this paper, error amplification

might have promoted implicit motor learning, while random force disturbance promoted explicit motor learning. Results from fMRI data support this hypothesis, since training with random disturbance revealed stronger activation in brain areas associated with explicit learning (such as, precuneus) when compared to training with error amplification (Yang and Li, 2012).

Effects of Training Strategies and Initial Skill Level on Brain Activation during Training

During the training period, strategy and skill-level dependent effects were observed in the IPS. Human fMRI studies support a decrease in activation in pre-SMA and dorsolateral prefrontal cortex (DLPFC), but an increase in activation in the parietal lobe (especially in the IPS) as visuomotor sequence learning progresses (Hikosaka et al., 1998; Sakai et al., 1998). Grafton et al. (1998) reported that activation in the parietal lobe progressively increased with learning, whereas other groups (Seitz et al., 1990; Jenkins et al., 1994; van Mier et al., 1998) demonstrated stronger parietal activation during learning of a novel motor sequence compared to performance on a pre-learned sequence.

Our study revealed stronger activation of the SPL (precuneus) and the IPS in skilled subjects (across all training strategies) during a motor task using leg movements. Less skilled subjects did not show any significant ($p < 0.001$) activation at the pre-selected voxel-threshold relative to skilled participants. In fact, the no-perturbation and random-disturbance strategies lead stronger activation in these (but also other frontal, visual, and temporal) regions than error amplification. This could suggest that attentional control is an important factor for motor learning but in different ways. During an easy condition such as no perturbation, a high level of attention is required to maintain subjects focused on the task. In contrast, during random disturbance, subjects are disturbed in an unexpected manner (in contrast to error amplification) to perform the task and hence attentional control is required to minimize tracking errors during training.

We found main effects of strategy as well as strategy × initial skill interaction effects in different parts of the cerebellum. Some authors demonstrated a particular link between cerebellum activation and skill level (Jenkins et al., 1994; Seitz et al., 1994). For example, Toni and colleagues (Toni et al., 1998) showed a decrease in left cerebellar activation (but also in other brain regions) during a prolonged period of trial and error motor sequence learning. The right anterior cerebellum, however, showed greater activation during later learning than during initial learning. In addition, in our experiment, skilled participants showed stronger activation of the cerebellum (and brainstem) compared to novices but this was only seen at $p < 0.001$ with $k_E > 15$ voxels instead of $k_E > 27$ voxels, indicating an association between the strength of the activation in the cerebellum and the success of learning. The only region—again at $p < 0.001$ and $k_E > 15$ voxels—showing greater activation in untrained participants was the right rolandic operculum.

The basal ganglia are involved in the regulation of non-motor as well as motor sequences, and motor sequence learning (Vakil et al., 2000; Exner et al., 2002; Tzvi et al., 2014, 2015, 2016; Fermin et al., 2016). Although the activation of the basal ganglia for the training period in our study might reflect on-line learning processes, we cannot distinguish activation linked to attentional demands and on-line error correction (adaptation). The activation of the basal ganglia was evident for the contrast "no perturbation (NP)—random disturbance (RD)." This was a bit surprising, as we did not expect a particular involvement of the basal ganglia in a very simple task such as no perturbation compared to random disturbance and error-amplification strategies. We conclude that basal ganglia are rather involved in the learning of non-challenging task, in which the sequence of motor movements is not disturbed by noise or by any error amplification.

Effects of Training Strategies on Brain Activation during Learning

The contrast "retention—baseline" revealed activation within the frontal cortex but also in sensorimotor regions (e.g., M1, parietal opercular regions, i.e., OP1 and OP2, Young et al., 2004). This activation could reflect learning (as the error rates drop during retention relative to baseline) but it is difficult to differentiate between mechanisms related to attention and error correction. One interesting observation was the involvement of orbitofrontal regions during no perturbation relative to error amplification (**Table 5**, **Figure 8**). In fact, practicing with error amplification is related to a persistent lower self-reported level of enjoyment (Duarte and Reinkensmeyer, 2015). The systematic large errors experienced during training with error amplification, which made the task more challenging, resulted in unconventionally low activation of the reward system. We computed several contrasts in order to further evaluate the effect of the skill level as we found differences comparing NP—EA in the reward system: (NP—EA skilled) > (NP—EA non-skilled) and vice versa,. We also performed the contrasts "EA skilled vs. EA non-skilled" and "NP skilled vs. NP non-skilled." Yet, we did not observe any activation differences for these contrasts (at $p < 0.001$, uncorrected), suggesting that the reward system was not differently activated between skill groups. However, when we used an unconventionally low threshold of $p < 0.01$ (uncorrected), we found some differences in the reward system between skilled and non-skilled subjects comparing conditions. Of course, this needs to be examined in future studies on the role of affective components during motor learning. However, it is evident from other studies that affective control (resulting in high motivation) is an important factor during complicated motor learning tasks (McAuley et al., 1989; Duarte and Reinkensmeyer, 2015).

Implications for Robot-Aided Gait Rehabilitation

Recovery after a brain injury has been proposed to be a form of motor learning or relearning (Dietz and Ward, 2015). However, we cannot guarantee that the impact on motor learning of the

training strategies here investigated do not differ in neurological patients. Patients probably have a lower initial skill level and therefore, their optimal challenge point (i.e., where subjects show the best motor learning) may be at a different level. Hypothetically, the haptic guidance mode may be especially suitable for more disabled patients, as suggested in Klamroth-Marganska et al. (2014).

Based on the results presented in this paper, we are developing new training strategies to improve rehabilitation outcomes using the Lokomat (Hocoma, Switzerland)—a commercially available robotic gait trainer that comprises two actuated leg orthoses (Riener et al., 2005). We developed a novel error-modulating robotic strategy that limits large errors that can be dangerous and frustrating with haptic guidance, while amplifies task relevant small errors. We also developed a random disturbance controller that can work together with the error-modulating controller (Rüdt et al., 2016). We hypothesize that an optimal framework for motor learning and neurorehabilitation would consist on a combination of all these strategies: Random force disturbance would increase subjects' concentration on the task, error amplification would increase subjects' active participation and awareness of small task relevant errors, and haptic guidance would limit dangerous and/or discouraging errors.

We plan to perform motor learning experiments with neurological patients employing the different controllers presented here, and the novel controllers derived from the actual findings. Results from the motor learning experiments performed with neurological patients will provide an insight into motor learning in the impaired motor system and may suggest new neurorehabilitation therapies and novel ways to use robots in rehabilitation. It has been hypothesized that in order to enhance recovery after a neurologic insult it is crucial to increase the dose and intensity of therapy (Dietz and Ward, 2015). We believe that employing a training strategy that optimizes learning based on patients' specific impairments and specific motor task to be performed would be a more effective approach than just increasing dose and intensity of raw therapy.

CONCLUSIONS

We investigated the effect of robotic training strategies that augment errors–error amplification and random force disturbance—on brain activation and learning of a complex locomotor task. We found that the most effective training strategy depends on subjects' initial skill level. Training without perturbations was especially suitable to enhance motor learning in initially less skilled subjects, while more skilled subjects benefited from error amplification. However, training with error amplification limited transfer of learning. Random disturbing forces induced learning and promoted transfer in all subjects, probably because they increased subjects' attention. A possible rationale for the differences in transfer between the challenge-based strategies is that for the specific complex locomotion task presented in this paper, error amplification might have promoted implicit motor learning, while random force disturbance promoted explicit motor learning.

FMRI analysis revealed main effects of strategy and skill level during training. These neuroimaging findings indicate that gait-like motor learning depends on interplay between subcortical, cerebellar, and fronto-parietal brain regions. An interesting observation was the low activation seen in the brain reward system after training with error amplification compared to training without perturbations.

Our results suggest that learning a complex locomotor task can be enhanced when errors are augmented based on subjects' initial skill level. The impacts of these strategies on motor learning, brain activation and motivation in neurological patients need further investigation.

AUTHOR CONTRIBUTIONS

LMC, LJ, and RR contributed to the experimental design and project supervision. LMC, LJ, and JL participated in the study design and data acquisition. LM, LJ, and JL performed the fMRI data analysis. Interpretation of the fMRI results was performed by LM. LMC performed the behavioral data analysis and interpretation of results. LMC and LM prepared the manuscript. All authors read and approved the final manuscript.

FUNDING

This work was supported partially by the Marie Curie International Income Fellowship PIIF-GA-2010-272289 hold by LMC and the Swiss National Science Foundation (SNF) through the grant number PMPDP2_151319.

ACKNOWLEDGMENTS

The authors would like to thank the Institute for Biomedical Engineering at ETH Zurich for the allocation of scanner time. The authors gratefully acknowledge the contributions of Spyros Kollias, Peter Wolf, Christoph Hollnagel, Mike Brügger, and Andre Fisher.

REFERENCES

Behrman, A. L., and Harkema, S. J. (2000). Locomotor training after human spinal cord injury: a series of case studies. *Phys. Ther.* 80, 688–700. doi: 10.1093/ptj/80.7.688

Bryden, M. P. (1977). Measuring handedness with questionnaires. *Neuropsychologia* 15, 617–624. doi: 10.1016/0028-3932(77)90067-7

Burke, E., and Cramer, S. C. (2013). Biomarkers and predictors of restorative therapy effects after stroke. *Curr. Neurol. Neurosci. Rep.* 13:329. doi: 10.1007/s11910-012-0329-9

Dietz, V., and Ward, N. (Eds) (2015). "The applicability of motor learning to neurorehabilitation," in *Oxford Textbook of Neurorehabilitation* (Oxford University Press), 55–64. Available online at: http://www.oxfordmedicine.com/view/10.1093/med/9780199673711.001.0001/med-9780199673711-chapter-7 (Accessed September 16, 2016).

Dobkin, B. H., and Duncan, P. W. (2012). Should body weight–supported treadmill training and robotic-assistive steppers for locomotor training trot back to the starting gate? *Neurorehabil. Neural Repair* 26, 308–317. doi: 10.1177/1545968312439687

Duarte, J. E., and Reinkensmeyer, D. J. (2015). Effects of robotically modulating kinematic variability on motor skill learning and motivation. *J. Neurophysiol.* 113, 2682–2691. doi: 10.1152/jn.00163.2014

Emken, J. L., and Reinkensmeyer, D. J. (2005). Robot-enhanced motor learning: accelerating internal model formation during locomotion by transient dynamic amplification. *IEEE Trans. Neural Syst. Rehabil. Eng.* 13, 33–39. doi: 10.1109/TNSRE.2004.843173

Exner, C., Koschack, J., and Irle, E. (2002). The differential role of premotor frontal cortex and basal ganglia in motor sequence learning: evidence from focal basal ganglia lesions. *Learn. Mem.* 9, 376–386. doi: 10.1101/lm.48402

Fermin, A. S. R., Yoshida, T., Yoshimoto, J., Ito, M., Tanaka, S. C., and Doya, K. (2016). Model-based action planning involves cortico-cerebellar and basal ganglia networks. *Sci. Rep.* 6:31378. doi: 10.1038/srep31378

Franklin, D. W., Liaw, G., Milner, T. E., Osu, R., Burdet, E., and Kawato, M. (2007). Endpoint stiffness of the arm is directionally tuned to instability in the environment. *J. Neurosci.* 27, 7705–7716. doi: 10.1523/JNEUROSCI.0968-07.2007

Grafton, S. T., Hazeltine, E., and Ivry, R. B. (1998). Abstract and effector-specific representations of motor sequences identified with PET. *J. Neurosci.* 18, 9420–9428.

Grafton, S. T., Schmitt, P., Van Horn, J., and Diedrichsen, J. (2008). Neural substrates of visuomotor learning based on improved feedback control and prediction. *Neuroimage* 39, 1383–1395. doi: 10.1016/j.neuroimage.2007.09.062

Guadagnoli, M. A., and Lee, T. D. (2004). Challenge point: a framework for conceptualizing the effects of various practice conditions in motor learning. *J. Mot. Behav.* 36, 212–224. doi: 10.3200/JMBR.36.2.212-224

Hester, R., Barre, N., Murphy, K., Silk, T. J., and Mattingley, J. B. (2008). Human medial frontal cortex activity predicts learning from errors. *Cereb. Cortex N. Y.* 18, 1933–1940. doi: 10.1093/cercor/bhm219

Hikosaka, O., Miyashita, K., Miyachi, S., Sakai, K., and Lu, X. (1998). Differential roles of the frontal cortex, basal ganglia, and cerebellum in visuomotor sequence learning. *Neurobiol. Learn. Mem.* 70, 137–149. doi: 10.1006/nlme.1998.3844

Hollnagel, C., Brügger, M., Vallery, H., Wolf, P., Dietz, V., Kollias, S., et al. (2011). Brain activity during stepping: a novel MRI-compatible device. *J. Neurosci. Methods* 201, 124–130. doi: 10.1016/j.jneumeth.2011.07.022

Hollnagel, C., Vallery, H., Schädler, R., López, I. G.-L., Jaeger, L., Wolf, P., et al. (2013). Non-linear adaptive controllers for an over-actuated pneumatic MR-compatible stepper. *Med. Biol. Eng. Comput.* 51, 799–809. doi: 10.1007/s11517-013-1050-9

Huberdeau, D. M., Krakauer, J. W., and Haith, A. M. (2015). Dual-process decomposition in human sensorimotor adaptation. *Curr. Opin. Neurobiol.* 33, 71–77. doi: 10.1016/j.conb.2015.03.003

Husemann, B., Müller, F., Krewer, C., Heller, S., and Koenig, E. (2007). Effects of locomotion training with assistance of a robot-driven gait orthosis in hemiparetic patients after stroke: a randomized controlled pilot study. *Stroke* 38, 349–354. doi: 10.1161/01.STR.0000254607.48765.cb

Israel, J. F., Campbell, D. D., Kahn, J. H., and Hornby, T. G. (2006). Metabolic costs and muscle activity patterns during robotic- and therapist-assisted treadmill walking in individuals with incomplete spinal cord injury. *Phys. Ther.* 86, 1466–1478. doi: 10.2522/ptj.20050266

Jaeger, L., Marchal-Crespo, L., Wolf, P., Riener, R., Michels, L., and Kollias, S. (2014). Brain activation associated with active and passive lower limb stepping. *Front. Hum. Neurosci.* 8:828. doi: 10.3389/fnhum.2014.00828

Jahn, K., Deutschländer, A., Stephan, T., Strupp, M., Wiesmann, M., and Brandt, T. (2004). Brain activation patterns during imagined stance and locomotion in functional magnetic resonance imaging. *Neuroimage* 22, 1722–1731. doi: 10.1016/j.neuroimage.2004.05.017

Jenkins, I. H., Brooks, D. J., Nixon, P. D., Frackowiak, R. S., and Passingham, R. E. (1994). Motor sequence learning: a study with positron emission tomography. *J. Neurosci.* 14, 3775–3790.

Klamroth-Marganska, V., Blanco, J., Campen, K., Curt, A., Dietz, V., Ettlin, T., et al. (2014). Three-dimensional, task-specific robot therapy of the arm after stroke: a multicentre, parallel-group randomised trial. *Lancet Neurol.* 13, 159–166. doi: 10.1016/S1474-4422(13)70305-3

Krakauer, J. W. (2006). Motor learning: its relevance to stroke recovery and neurorehabilitation. *Curr. Opin. Neurol.* 19, 84–90. doi: 10.1097/01.wco.0000200544.29915.cc

la Fougère, C., Zwergal, A., Rominger, A., Förster, S., Fesl, G., Dieterich, M., et al. (2010). Real versus imagined locomotion: a [18F]-FDG PET-fMRI comparison. *Neuroimage* 50, 1589–1598. doi: 10.1016/j.neuroimage.2009.12.060

Lee, J., and Choi, S. (2010). "Effects of haptic guidance and disturbance on motor learning: potential advantage of haptic disturbance," in *2010 IEEE Haptics Symposium* (Waltham, MA), 335–342.

Lee, Y., and Vakoch, D. A. (1996). Transfer and retention of implicit and explicit learning. *Br. J. Psychol.* 87, 637–651. doi: 10.1111/j.2044-8295.1996.tb02613.x

Lotze, M., Braun, C., Birbaumer, N., Anders, S., and Cohen, L. G. (2003). Motor learning elicited by voluntary drive. *Brain J. Neurol.* 126, 866–872. doi: 10.1093/brain/awg079

Luft, A. R., Smith, G. V., Forrester, L., Whitall, J., Macko, R. F., Hauser, T.-K., et al. (2002). Comparing brain activation associated with isolated upper and lower limb movement across corresponding joints. *Hum. Brain Mapp.* 17, 131–140. doi: 10.1002/hbm.10058

Luks, T. L., Simpson, G. V., Dale, C. L., and Hough, M. G. (2007). Preparatory allocation of attention and adjustments in conflict processing. *Neuroimage* 35, 949–958. doi: 10.1016/j.neuroimage.2006.11.041

Marchal-Crespo, L., Hollnagel, C., Brügger, M., Kollias, S., and Riener, R. (2011). An fMRI pilot study to evaluate brain activation associated with locomotion adaptation. *IEEE Int. Conf. Rehabil. Robot. Proc.* 2011:5975371. doi: 10.1109/ICORR.2011.5975371

Marchal-Crespo, L., López-Olóriz, J., Jaeger, L., and Riener, R. (2014a). Optimizing learning of a locomotor task: amplifying errors as needed. *Conf. Proc. Annu. Int. Conf. IEEE Eng. Med. Biol. Soc.* 2014, 5304–5307. doi: 10.1109/EMBC.2014.6944823

Marchal-Crespo, L., McHughen, S., Cramer, S. C., and Reinkensmeyer, D. J. (2010). The effect of haptic guidance, aging, and initial skill level on motor learning of a steering task. *Exp. Brain Res.* 201, 209–220. doi: 10.1007/s00221-009-2026-8

Marchal-Crespo, L., and Reinkensmeyer, D. J. (2009). Review of control strategies for robotic movement training after neurologic injury. *J. Neuroeng. Rehabil.* 6:20. doi: 10.1186/1743-0003-6-20

Marchal-Crespo, L., Schneider, J., Jaeger, L., and Riener, R. (2014b). Learning a locomotor task: with or without errors? *J. Neuroeng. Rehabil.* 11:25. doi: 10.1186/1743-0003-11-25

Marchal-Crespo, L., van Raai, M., Rauter, G., Wolf, P., and Riener, R. (2013). The effect of haptic guidance and visual feedback on learning a complex tennis task. *Exp. Brain Res.* 231, 277–291. doi: 10.1007/s00221-013-3690-2

Marchal-Crespo, L., Wolf, P., Gerig, N., Rauter, G., Jaeger, L., Vallery, H., et al. (2015). "The role of skill level and motor task characteristics on the effectiveness of robotic training: first results," in *2015 IEEE International Conference on Rehabilitation Robotics (ICORR)* (Singapore), 151–156.

Mars, R. B., Coles, M. G. H., Grol, M. J., Holroyd, C. B., Nieuwenhuis, S., Hulstijn, W., et al. (2005). Neural dynamics of error processing in medial frontal cortex. *Neuroimage* 28, 1007–1013. doi: 10.1016/j.neuroimage.2005.06.041

McAuley, E., Duncan, T., and Tammen, V. V. (1989). Psychometric properties of the intrinsic motivation inventory in a competitive sport setting: a confirmatory factor analysis. *Res. Q. Exerc. Sport* 60, 48–58. doi: 10.1080/02701367.1989.10607413

Milot, M.-H., Marchal-Crespo, L., Green, C. S., Cramer, S. C., and Reinkensmeyer, D. J. (2010). Comparison of error-amplification and haptic-guidance training techniques for learning of a timing-based motor task by healthy individuals. *Exp. Brain Res.* 201, 119–131. doi: 10.1007/s00221-009-2014-z

Miyai, I., Yagura, H., Hatakenaka, M., Oda, I., Konishi, I., and Kubota, K. (2003). Longitudinal optical imaging study for locomotor recovery after stroke. *Stroke J. Cereb. Circ.* 34, 2866–2870. doi: 10.1161/01.STR.0000100166.81077.8A

Morone, G., Bragoni, M., Iosa, M., De Angelis, D., Venturiero, V., Coiro, P., et al. (2011). Who may benefit from robotic-assisted gait training? A randomized clinical trial in patients with subacute stroke. *Neurorehabil. Neural Repair* 25, 636–644. doi: 10.1177/1545968311401034

Pennycott, A., Wyss, D., Vallery, H., Klamroth-Marganska, V., and Riener, R. (2012). Towards more effective robotic gait training for stroke rehabilitation: a review. *J. Neuroeng. Rehabil.* 9:65. doi: 10.1186/1743-0003-9-65

Poon, C.-S. (2004). Sensorimotor learning and information processing by Bayesian internal models. *Conf. Proc. Annu. Int. Conf. IEEE Eng. Med. Biol. Soc.* 6, 4481–4482. doi: 10.1109/IEMBS.2004.1404245

Reinkensmeyer, D. J., Akoner, O., Ferris, D. P., and Gordon, K. E. (2009). Slacking by the human motor system: computational models and implications for robotic orthoses. *Conf. Proc. Annu. Int. Conf. IEEE Eng. Med. Biol. Soc.* 2009, 2129–2132. doi: 10.1109/IEMBS.2009.5333978

Reinkensmeyer, D. J., and Housman, S. J. (2007). "If I can't do it once, why do it a hundred times? connecting volition to movement success in a virtual environment motivates people to exercise the arm after stroke," in *2007 Virtual Rehabilitation* (Venice), 44–48.

Reisman, D. S., McLean, H., Keller, J., Danks, K. A., and Bastian, A. J. (2013). Repeated split-belt treadmill training improves poststroke step length asymmetry. *Neurorehabil. Neural Repair* 27, 460–468. doi: 10.1177/1545968312474118

Riener, R., Lünenburger, L., Jezernik, S., Anderschitz, M., Colombo, G., and Dietz, V. (2005). Patient-cooperative strategies for robot-aided treadmill training: first experimental results. *IEEE Trans. Neural Syst. Rehabil. Eng.* 13, 380–394. doi: 10.1109/TNSRE.2005.848628

Rossini, P. M., and Dal Forno, G. (2004). Integrated technology for evaluation of brain function and neural plasticity. *Phys. Med. Rehabil. Clin. N. Am.* 15, 263–306. doi: 10.1016/S1047-9651(03)00124-4

Rüdt, S., Moos, M., Seppey, S., Riener, R., and Marchal-Crespo, L. (2016). "Towards more efficient robotic gait training: A novel controller to modulate movement errors," in *2016 6th IEEE International Conference on Biomedical Robotics and Biomechatronics (BioRob)* (Singapore), 876–881.

Sakai, K., Hikosaka, O., Miyauchi, S., Takino, R., Sasaki, Y., and Pütz, B. (1998). Transition of brain activation from frontal to parietal areas in visuomotor sequence learning. *J. Neurosci.* 18, 1827–1840.

Scheidt, R. A., Reinkensmeyer, D. J., Conditt, M. A., Rymer, W. Z., and Mussa-Ivaldi, F. A. (2000). Persistence of motor adaptation during constrained, multi-joint, arm movements. *J. Neurophysiol.* 84, 853–862.

Schmidt, R., and Lee, T. (2010). *Motor Control and Learning: A Behavioral Emphasis*. Champaign, IL: Human Kinetics Publishers.

Schwartz, I., Sajin, A., Fisher, I., Neeb, M., Shochina, M., Katz-Leurer, M., et al. (2009). The effectiveness of locomotor therapy using robotic-assisted gait training in subacute stroke patients: a randomized controlled trial. *PM R* 1, 516–523. doi: 10.1016/j.pmrj.2009.03.009

Seitz, R. J., Canavan, A. G., Yágüez, L., Herzog, H., Tellmann, L., Knorr, U., et al. (1994). Successive roles of the cerebellum and premotor cortices in trajectorial learning. *Neuroreport* 5, 2541–2544. doi: 10.1097/00001756-199412000-00034

Seitz, R. J., Roland, E., Bohm, C., Greitz, T., and Stone-Elander, S. (1990). Motor learning in man: a positron emission tomographic study. *Neuroreport* 1, 57–60. doi: 10.1097/00001756-199009000-00016

Shulman, G. L., McAvoy, M. P., Cowan, M. C., Astafiev, S. V., Tansy, A. P., d'Avossa, G., et al. (2003). Quantitative analysis of attention and detection signals during visual search. *J. Neurophysiol.* 90, 3384–3397. doi: 10.1152/jn.00343.2003

Shumway-Cook, A., and Woollacott, M. H. (2007). *Motor Control: Translating Research Into Clinical Practice*. Lippincott Williams & Wilkins.

Slotnick, S. D., Moo, L. R., Segal, J. B., and Hart, J. (2003). Distinct prefrontal cortex activity associated with item memory and source memory for visual shapes. *Brain Res. Cogn. Brain Res.* 17, 75–82. doi: 10.1016/S0926-6410(03)00082-X

Toni, I., Krams, M., Turner, R., and Passingham, R. E. (1998). The time course of changes during motor sequence learning: a whole-brain fMRI study. *Neuroimage* 8, 50–61. doi: 10.1006/nimg.1998.0349

Tseng, Y.-W., Diedrichsen, J., Krakauer, J. W., Shadmehr, R., and Bastian, A. J. (2007). Sensory prediction errors drive cerebellum-dependent adaptation of reaching. *J. Neurophysiol.* 98, 54–62. doi: 10.1152/jn.00266.2007

Tzvi, E., Münte, T. F., and Krämer, U. M. (2014). Delineating the cortico-striatal-cerebellar network in implicit motor sequence learning. *Neuroimage* 94, 222–230. doi: 10.1016/j.neuroimage.2014.03.004

Tzvi, E., Stoldt, A., Witt, K., and Krämer, U. M. (2015). Striatal-cerebellar networks mediate consolidation in a motor sequence learning task: an fMRI study using dynamic causal modelling. *Neuroimage* 122, 52–64. doi: 10.1016/j.neuroimage.2015.07.077

Tzvi, E., Verleger, R., Münte, T. F., and Krämer, U. M. (2016). Reduced alpha-gamma phase amplitude coupling over right parietal cortex is associated with implicit visuomotor sequence learning. *Neuroimage* 141, 60–70. doi: 10.1016/j.neuroimage.2016.07.019

Vakil, E., Kahan, S., Huberman, M., and Osimani, A. (2000). Motor and non-motor sequence learning in patients with basal ganglia lesions: the case of serial reaction time (SRT). *Neuropsychologia* 38, 1–10. doi: 10.1016/S0028-3932(99)00058-5

van Mier, H., Tempel, L. W., Perlmutter, J. S., Raichle, M. E., and Petersen, S. E. (1998). Changes in brain activity during motor learning measured with PET: effects of hand of performance and practice. *J. Neurophysiol.* 80, 2177–2199.

Wu, H. G., Miyamoto, Y. R., Gonzalez Castro, L. N., Ölveczky, B. P., and Smith, M. A. (2014). Temporal structure of motor variability is dynamically regulated and predicts motor learning ability. *Nat. Neurosci.* 17, 312–321. doi: 10.1038/nn.3616

Wulf, G., and Shea, C. H. (2002). Principles derived from the study of simple skills do not generalize to complex skill learning. *Psychon. Bull. Rev.* 9, 185–211. doi: 10.3758/BF03196276

Yang, J., and Li, P. (2012). Brain networks of explicit and implicit learning. *PLoS ONE* 7:e42993. doi: 10.1371/journal.pone.0042993

Yen, S.-C., Schmit, B. D., Landry, J. M., Roth, H., and Wu, M. (2012). Locomotor adaptation to resistance during treadmill training transfers to overground walking in human SCI. *Exp. Brain Res.* 216, 473–482. doi: 10.1007/s00221-011-2950-2

Young, J. P., Herath, P., Eickhoff, S., Choi, J., Grefkes, C., Zilles, K., et al. (2004). Somatotopy and attentional modulation of the human parietal and opercular regions. *J. Neurosci.* 24, 5391–5399. doi: 10.1523/JNEUROSCI.4030-03.2004

Conflict of Interest Statement: The authors declare that the research was conducted in the absence of any commercial or financial relationships that could be construed as a potential conflict of interest.

frontiers in Neuroscience

OPINION
published: 05 September 2017
doi: 10.3389/fnins.2017.00491

The Emergent Role of Virtual Reality in the Treatment of Neuropsychiatric Disease

Yacine Benyoucef[*†], *Pierre Lesport*[†] *and Amani Chassagneux*

SPACEMEDEX, Valbonne Sophia-Antipolis, France

Keywords: augmented reality, cybertherapy, neuropsychiatric disorder, pain, rehabilitation medicine, virtual reality

BACKGROUND

The development of outstanding computer science technologies such as virtual reality (VR) and augmented reality (AR) has provided new avenues in order to challenge the functional connectivity disruption seen in neurodegenerative diseases.

Virtually simulating the outside world with high realism, close-to-total immersion and easiness of interaction presents an interesting way to decipher new therapeutic perspectives as a non-invasive and non-pharmacological neuromodulation tool.

As of recently, these cutting-edge techniques already appear to be used in the treatment of some neuropsychiatric disorders, cognitive and behavioral impairments since the patient is placed in an environment virtually yet specifically adapted to his needs. Specific use of VR and AR becomes interesting for both social and functional rehabilitation whether it originates from traumatic situations and injuries or from pathologies known to show from neuromuscular disturbances to decay. Virtual reality is already used in research in combination to rehabilitation adapted treadmills in order to help treat children with cerebral palsy (coordination impairment, stiff and weak muscles, tremors, etc.) that appear in early childhood (Sloot et al., 2015; Cho et al., 2016). However, there is still some work to be done to improve the actual research setups and the reproducibility of results.

Therefore, we will review here the innovative and emergent role of cybertherapies and focus on the possibilities to extend its use as far as rehabilitation centers to everyday well-being.

NEUROPSYCHIATRIC PERSPECTIVES

Nowadays, virtual simulations of our world are created with high realism coupled to immersion techniques. This appears to be a useful tool in the treatment of neuropsychiatric diseases and behavioral disorders which might concern almost 450 million of patients worldwide. Statistically, one out of four people has already or will develop a mental disorder during their lifetime according to the World Health Organization (WHO, 2001). And because virtual reality allows for a wide range of applications, this cutting-edge technology could find its place as a neuromodulator to target a panel of states from wellbeing to mental diseases and pain management.

But, due to its innovative nature, there is a strong need to enhance its development and to standardize applications. So far, specific adaptative environments and serious games are selected as a means to a safe and regular use in clinical medicine. It constitutes in itself a brand new public health approach to help treating brain disorders: troubled thinking and perception disorders, cognitive impairment, disruption of emotions, or behavioral disorders are some of the areas targeted by this cutting-edge treatment using serious games: the patient is in a specific virtual environment and evolves as he would in his real life. The objective is to help him face his fears or behavioral challenge in order to improve his day-to-day life (Malbos et al., 2013; Sarver et al., 2014; Fleming et al., 2017).

OPEN ACCESS

Edited by:
Takashi Hanakawa, National Center of Neurology and Psychiatry, Japan

Reviewed by:
Yutaka Oouchida, Tohoku University, Japan
Shiro Yano, Tokyo University of Agriculture, Japan

****Correspondence:***
Yacine Benyoucef
yacine.benyoucef@spacemedex.com

[†] These authors have contributed equally to this work.

Specialty section:
This article was submitted to Neural Technology, a section of the journal Frontiers in Neuroscience

Received: *14 June 2017*
Accepted: *21 August 2017*
Published: *05 September 2017*

Citation:
Benyoucef Y, Lesport P and Chassagneux A (2017) The Emergent Role of Virtual Reality in the Treatment of Neuropsychiatric Disease. Front. Neurosci. 11:491. doi: 10.3389/fnins.2017.00491

Traditional exposure methods were found in protocols such as gradual *in vivo* exposure, role-playing games and sometimes group therapy but all eventually led to a similar limitation due to systematic desensitization (Cottraux, 1994). Success is often reached with difficulties because of limitations like the lack of imagination for the patient, usually coupled to a lack of intimacy and aversion to participate or the cost of such a therapy. All of which don't appear with the virtual reality, since VR allows for a private use at a lower cost: it has to be used as an additional technique to overcome limitations of traditional psychotherapies. Through VR the idea is to dive deep into an anxiogene and interactive environment with a controlled, safe and ludic protocol. A strong planning is mandatory, as every patient needs a design specifically matched to his pathology. One of the main challenges is to stick to the reality as accurately as possible in order to solve or at least lessen the psychopathological issue caused by the dismemberment of the conscience, which appears like a conflict between stimuli and cognition, between what we sense and what we live. This paradigm could be resolved by a full presence feeling: the more we are in, the less we are in conflict, and the more the treatment is effective.

That presence feeling could be brought by the AR technique, where the system allows inserting virtual contents in the real world as a real time perceived ultra-reality. Virtual elements are superimposed over the real image of the environment, bringing additional information and augmenting our perception. That technology is already powerful in medical training (Cutolo et al., 2017) and as a navigational tool in surgery (Cabrilo et al., 2014), but appears to be useful in the treatment of specific phobia, specifically on the phobia of small animals (Chicchi Giglioli et al., 2015), even if there is still a strong protocols development and clinical tests to do to extend its use not only in phobia but also in other pathologies.

REHABILITATION MEDICINE

Associated with specific exercises, VR assisted rehabilitation becomes interesting for both social and functional rehabilitation (Laver et al., 2015; Dockx et al., 2016; White and Moussavi, 2016; Fernandez Montenegro and Argyriou, 2017). The overall system using a treadmill or an exoskeleton plus a chosen specific virtual environment might have an important impact for post-traumatic injuries or diseases with neuromuscular disturbances and degeneration (Villiger et al., 2013; Pietrzak et al., 2014). Using the specified setup, the patient will be able to walk and move, repeating the exercise and gradually increasing the intensity. Such systems could bring an innovative solution through the use of virtual reality, where objectives, motivation, and targeted exercises could be mixed in a ludic protocol. Indeed, VR assisted rehabilitation allows the patient to work on locomotion disorders, postural rehabilitation, and equilibrium as well as spatial navigation or any other disorders (Chiarovano et al., 2017; Cogné et al., 2017). Patients with memory impairment such as witnessed in Alzheimer's disease could benefit from experiencing a virtual walk outside without putting them at risk of getting lost and VR could help creating familiar environments with for example the incorporation of musicotherapy and family pictures. With an adapted setup, both young patients and senior patients could see their rehabilitation sessions benefiting from a new vision and therefore see a new capacity added to the means accessible to them in order to get better. By targeting specific brain areas and specific training, VR could be used as a cortical reorganization inducer, and trigger new healing neurological and critical pathways in mental health disorders or trauma induced stress and anxiety such as Post-Traumatic Stress Disorder (Maples-Keller et al., 2017; Tielman et al., 2017), to adaptive rehabilitation following stroke induced neurological impairments (Xiao et al., 2017; Yasuda et al., 2017).

The next step would be to integrate haptic control and grabbing of virtual elements for the patient to be immersed in an even more lifelike simulated reality in order to achieve greater stimulation and to obtain enhanced results aiming at improving living conditions for all patients suffering from myopathies.

As of late, software improvements and reduction in the costs of virtual gear transformed VR into a practical tool for immersive multisensory experiences in 3D that can distract patients from their chronic pains. Virtual reality is a promising intervention with several potential applications in the inpatient medical setting. Studies to date demonstrate some efficacy, but there is a need for larger, well-controlled studies to show clinical and cost-effectiveness (Dascal et al., 2017). Several studies aiming to assess the effectiveness of VR in hospitalized patients with chronic pains have been published. The use of VR as a distraction in these patients was effective to a point in reducing pain compared to a control distraction condition (Jin et al., 2016; Jones et al., 2016; Garrett et al., 2017; McSherry et al., 2017; Tashjian et al., 2017), showing that it can be used as a bonus therapy tool for pain management. But these findings are coming in contradiction to other studies that point out that the use of VR didn't change pain thresholds in patients (Smith et al., 2017). VR and AR were also studied in the context of Phantom Limb Pain (PLP). The PLP patients present a perception of discomfort consecutive to amputation of their limb. In such cases, mirror therapy is used and VR and AR therapy can provide an increased level of immersion with customizable environments for the amputee to alleviate the discomfort. They can also use myoelectric sensors to manipulate artificial limbs to perform several tasks, thus limitating their handicap (Ortiz-Catalan et al., 2014; Dunn et al., 2017).

The pain management of patients in hospital could nonetheless benefit from VR as adjunctive therapy if it is used in the right emotional and social context. For example, the qualitative effects of immersive virtual reality therapy during painful procedures are possible in the operating theater environment and could contribute in postoperative satisfaction (Mosso-Vázquez et al., 2014; Chan and Scharf, 2017). More insights will be obtained by future research with more immersive VR technology to explore the potential link between stimuli and the context that changes the value of these stimuli. VR was also successful as adjunct therapy for acute pain management but most of the studies reported very

important individualized responses in patients (Garrett et al., 2017).

CONCLUSION

As such, the efficiency of VR and AR, while attractive due to the increasing levels of immersion, customizable environments, and decreasing costs, is yet to be fully proven and continues to need further research with higher quality studies to fully explore its benefits and democratize its use.

AUTHOR CONTRIBUTIONS

All authors worked from the conception of this article to the final approval, and share the same opinion.

REFERENCES

Cabrilo, I., Bijlenga, P., and Schaller, K. (2014). Augmented reality in the surgery of cerebral arteriovenous malformations: technique assessment and considerations. *Acta Neurochir.* 156, 1769–1774. doi: 10.1007/s00701-014-2183-9

Chan, P. Y., and Scharf, S. (2017). Virtual reality as an adjunctive non-pharmacological sedative during orthopedic surgery under regional anesthesia: a pilot and feasibility study. *Anesth. Analg.* doi: 10.1213/ANE.0000000000002169. [Epub ahead of print].

Chiarovano, E., Wang, W., Rogers, S. J., MacDoughall, H. G., Curthoys, I. S., and De Waele, C. (2017). Balance in virtual reality: effect of age and bilateral vestibular loss. *Front. Neurol.* 8:5. doi: 10.3389/fneur.2017.00005

Chicchi Giglioli, I. A., Pallavicini, F., Pedroli, E., Serino, S., and Riva, G. (2015). Augmented Reality: a brand new challenge for the assessment and treatment of psychological disorders. *Comput. Math. Methods Med.* 2015:862942. doi: 10.1155/2015/862942

Cho, C., Hwang, W., Hwang, S., and Chung, Y. (2016). Treadmill training with virtual reality improves gait, balance and muscle strength in children with cerebral palsy. *Tohoku J. Exp. Med.* 238, 213–218. doi: 10.1620/tjem.238.213

Cogné, M., Taillade, M., N'Kaoua, B., Tarruella, A., Klinger, E., Larrue, F., et al. (2017). The contribution of virtual reality to the diagnosis of spatial navigation disorders and to the study of the role of navigation aids: a systematic literature review. *Ann. Phys. Rehabil. Med.* 60, 164–176. doi: 10.1016/j.rehab.2015.12.004

Cottraux (1994). *Cognitive and Behavioral Therapies*. 3rd Edn. Paris: PUF.

Cutolo, F., Meola, A., Carbone, M., Sinceri, S., Cagnazzo, F., Denaro, E., et al. (2017). A new head-mounted display-based augmented reality system in neurosurgical oncology: a study on phantom. *Comput. Assist. Surg. (Abingdon).* 22, 39–53. doi: 10.1080/24699322.2017.1358400

Dascal, J., Reid, M., Ishak, W., Spiegel, B., Recacho, J., Rosen, B., et al. (2017). Virtual reality and medical inpatients: a systematic review of randomized, controlled trials. *Innov. Clin. Neurosci.* 14, 14–21.

Dockx, K., Bekkers, E. M., Van der Bergh, V., Ginis, P., Rochester, L., Hausdorff J. M. et al. (2016). Virtual reality for rehabilitation in Parkinson's disease. *Cochrane Database Syst. Rev.* 12:CD010760. doi: 10.1002/14651858.CD010760.pub2

Dunn, J., Yeo, E., Moghaddampour, P., Chau, B., and Humbert, S. (2017). Virtual and augmented reality in the treatment of phantom limb pain: a literature review. *NeuroRehabilitation.* 40, 595–601. doi: 10.3233/NRE-171447

Fernandez Montenegro, J. M., and Argyriou, V. (2017). Cognitive evaluation for the diagnosis of Alzheimer's disease based on turing test and virtual environments. *Physiol. Behav.* 2017, 42–51. doi: 10.1016/j.physbeh.2017.01.034

Fleming, T. M., Bavin, L., Stasiak, K., Hermansson-Webb, E., Merry S. N., Cheek, C., et al. (2017). Serious games and gamification for mental health: current status and promising directions. *Front. Psychiatry* 2017:215. doi: 10.3389/fpsyt.2016.00215

Garrett, B., Taverner, T., and McDade, P. (2017). virtual reality as an adjunct home therapy in chronic pain management: an exploratory study. *JMIR Med. Inform.* 5:e11. doi: 10.2196/medinform.7271

Jin, W., Choo, A., Gromala, D., Shaw, C., and Squire, P. (2016). A virtual reality game for chronic pain management: a randomized, controlled clinical study. *Stud. Health Technol. Inform.* 220, 154–160. doi: 10.3233/978-1-61499-625-5-154

Jones, T., Moore, T., and Choo, J. (2016). The impact of virtual reality on chronic pain. *PLoS ONE* 211:e0167523. doi: 10.1371/journal.pone.0167523

Laver, K. E., George, S., Thomas, S., Deutsch, J. E., and Crotty, M. (2015). Virtual reality for stroke rehabilitation. *Cochrane Database Syst. Rev.* 2:CD008349. doi: 10.1002/14651858.CD008349.pub3

Malbos, E., Boyer, L., and Lançon, C. (2013). Virtual reality in the treatment of mental disorders. *Presse Med.* 42, 1442–1452. doi: 10.1016/j.lpm.2013.01.065

Maples-Keller, J. L., Yasinski, C., Manjin, L., and Rothbaum, B. O. (2017). Virtual reality-enhanced extinction of phobias and post-traumatic stress. *Neurotherapeutics* 14, 554–563. doi: 10.1007/s13311-017-0534-y

McSherry, T., Atterbury, M., Gartner, S., Helmold, E., Searles, D. M., and Schulman, C. (2017). Randomized, crossover study of immersive virtual reality to decrease opioid use during painful wound care procedures in adults. *J. Burn Care Res.* doi: 10.1097/BCR.0000000000000589. [Epub ahead of print].

Mosso-Vázquez, J. L., Gao, K., Wiederhold, B. K., and Wiederhold, M. D. (2014). Virtual reality for pain management in cardiac surgery. *Cyberpsychol. Behav. Soc. Netw.* 17, 371–378. doi: 10.1089/cyber.2014.0198

Ortiz-Catalan, M., Sander, N., Kristoffersen, M. B., Håkansson, B., and Brånemark, R. (2014). Treatment of phantom limb pain (PLP) based on augmented reality and gaming controlled by myoelectric pattern recognition: a case study of a chronic PLP patient. *Front. Neurosci.* 8:24. doi: 10.3389/fnins.2014.00024

Pietrzak, E., Pullman, S., and McGuire, A. (2014). Using virtual reality and videogames for traumatic brain injury rehabilitation: a structured literature review. *Games Health J.* 3, 202–214. doi: 10.1089/g4h.2014.0013

Sarver, N. W., Beidel, D. C., and Spitalnick, J. S. (2014). The feasibility and acceptability of virtual environments in the treatment of childhood social anxiety disorder. *J. Clin. Child. Adolesc. Psychol.* 43, 63–73. doi: 10.1080/15374416.2013.843461

Sloot, L. H., Harlaar, J., and Van der Krogt, M. M. (2015). Self-paced versus fixed speed walking and the effect of virtual reality in children with cerebral palsy. *Gait Posture* 42, 498–504. doi: 10.1016/j.gaitpost.2015.08.003

Smith, A., Carlow, K., Biddulph, T., Murray, B., Paton, M., and Harvie, D. S. (2017). Contextual modulation of pain sensitivity utilising virtual environments. *Br. J. Pain.* 11, 71–80. doi: 10.1177/2049463717698349

Tashjian, V. C., Mosadeghi, S., Howard, A. R., Lopez, M., Dupuy, T., Reid, M., et al. (2017). Virtual reality for management of pain in hospitalized patients: results of a controlled trial. *JMIR Ment. Health.* 4:e9. doi: 10.2196/mental.7387

Tielman, M. L., Neerincx, M. A., Bidarra, R., Kybartas, B., and Brinkman, W. P. (2017). A therapy system for post-traumatic stress disorder using a virtual agent and virtual storytelling to reconstruct traumatic memories. *J. Med. Syst.* 41:125. doi: 10.1007/s10916-017-0771-y

Villiger, M., Bohli, D., Kiper, D., Pyk, P., Spillmann, J., Meilick, B., et al. (2013). Virtual reality-augmented neurorehabilitation improves motor function and reduces neuropathic pain in patients with incomplete spinal cord

injury. *Neurorehabil. Neural Repair* 27, 675–683. doi: 10.1177/1545968313490999

White, P. J., and Moussavi, Z. (2016). Neurocognitive treatment for a patient with Alzheimer's disease using a virtual reality navigational environment. *J. Exp. Neurosci.* 2016, 129–135. doi: 10.4137/JEN.S40827

World Health Organization (WHO) (2001). *Mental and Neurological Disorders. The World Health Report, Mental Health: New Understanding, New Hope*. Geneva: NMH Communications.

Xiao, X., Lin, Q., Lo, W.-L., Mao, Y.-R., Shi, X.-C., Cates, R. S., et al. (2017). Cerebral reorganization in subacute stroke survivors after virtual reality-based training: a preliminary study. *Behav. Neurol.* 2017:6261479. doi: 10.1155/2017/6261479

Yasuda, K., Muroi, D., Ohira, M., and Iwata, H. (2017). Validation of an immersive virtual reality system for training near and far space neglect in individuals with stroke: a pilot study. *Top. Stroke Rehabil.* 12, 1–6. doi: 10.1080/10749357.2017.1351069

Conflict of Interest Statement: Spacemedex is a start-up in the field of aerospace medicine, biotechnologies and medical devices. The corresponding author is the founder and chief executive officer. All other authors have worked as consultants in neuroscience and collaborate to the successful development of our research policies.

frontiers in Neuroscience

HYPOTHESIS AND THEORY
published: 16 November 2017
doi: 10.3389/fnins.2017.00637

SSRI and Motor Recovery in Stroke: Reestablishment of Inhibitory Neural Network Tonus

*Camila B. Pinto[1,2], Faddi G. Saleh Velez[1], Fernanda Lopes[1], Polyana V. de Toledo Piza[1,3], Laura Dipietro[4], Qing M. Wang[5], Nicole L. Mazwi[6], Erica C. Camargo[7], Randie Black-Schaffer[6] and Felipe Fregni[1]**

[1] *Laboratory of Neuromodulation and Center for Clinical Research Learning, Department of Physical Medicine and Rehabilitation, Harvard Medical School, Spaulding Rehabilitation Hospital, Harvard University, Boston, MA, United States,* [2] *Department of Neuroscience and Behavior, Psychology Institute, University of São Paulo, São Paulo, Brazil,* [3] *Department of Severe Patients, Hospital Israelita Albert Einstein, São Paulo, Brazil,* [4] *Highland Instruments, Cambridge, MA, United States,* [5] *Stroke Biological Recovery Laboratory, Department of Physical Medicine and Rehabilitation, Harvard Medical School, Spaulding Rehabilitation Hospital, Harvard University, Boston, MA, United States,* [6] *Department of Physical Medicine and Rehabilitation, Harvard Medical School, Spaulding Rehabilitation Hospital, Harvard University, Boston, MA, United States,* [7] *Department of Neurology, Harvard Medical School, Massachusetts General Hospital, Harvard University, Boston, MA, United States*

OPEN ACCESS

Edited by:
Giancarlo Zito, Ospedale San Giovanni Calibita Fatebenefratelli, Italy

Reviewed by:
Leif Hertz, Institute of Metabolic Disease Research and Drug Development, China Medical University, China
Giovanni Assenza, Università Campus Bio-Medico, Italy
Filippo Zappasodi, Università degli Studi "G. d'Annunzio" Chieti - Pescara, Italy

***Correspondence:**
Felipe Fregni
fregni.felipe@mgh.harvard.edu

Specialty section:
This article was submitted to Neural Technology, a section of the journal Frontiers in Neuroscience

Received: *17 May 2017*
Accepted: *02 November 2017*
Published: *16 November 2017*

Citation:
Pinto CB, Saleh Velez FG, Lopes F, de Toledo Piza PV, Dipietro L, Wang QM, Mazwi NL, Camargo EC, Black-Schaffer R and Fregni F (2017) SSRI and Motor Recovery in Stroke: Reestablishment of Inhibitory Neural Network Tonus. Front. Neurosci. 11:637. doi: 10.3389/fnins.2017.00637

Selective serotonin reuptake inhibitors (SSRIs) are currently widely used in the field of the neuromodulation not only because of their anti-depressive effects but also due to their ability to promote plasticity and enhance motor recovery in patients with stroke. Recent studies showed that fluoxetine promotes motor recovery after stroke through its effects on the serotonergic system enhancing motor outputs and facilitating long term potentiation, key factors in motor neural plasticity. However, little is known in regards of the exact mechanisms underlying these effects and several aspects of it remain poorly understood. In this manuscript, we discuss evidence supporting the hypothesis that SSRIs, and in particular fluoxetine, modulate inhibitory pathways, and that this modulation enhances reorganization and reestablishment of excitatory-inhibitory control; these effects play a key role in learning induced plasticity in neural circuits involved in the promotion of motor recovery after stroke. This discussion aims to provide important insights and rationale for the development of novel strategies for stroke motor rehabilitation.

Keywords: stroke, motor rehabilitation, SSRIs, cortical excitability, inhibitory tonus, neuroplasticity

INTRODUCTION

Stroke is the second cause of death worldwide and the leading cause of death in upper-middle income countries; about 6.7 million people died from stroke in 2013 in the US (Mozaffarian et al., 2016). Among stroke survivors, recovery of motor function is frequently incomplete, with the majority of stroke patients unable to perform professional duties or activities of daily living 6 months after the event (Hummel and Cohen, 2005, 2006).

Current conventional therapies rely on behavioral treatments such as physiotherapy and occupational therapy (Winstein et al., 2016); however, these treatments only induce limited plastic and cortical reorganization changes (Veerbeek et al., 2014). Thus, considerable research efforts have been devoted to developing methods for enhancing neuroplasticity in stroke and increasing the efficacy of rehabilitation techniques.

To this end, the use of pharmacological agents such as selective serotonin reuptake inhibitors (SSRIs), in particular fluoxetine, is increasingly being explored by several research groups. It has been shown that SSRIs can modulate neural excitability, promote plastic changes and improve motor rehabilitation after stroke (Chollet et al., 2011; Siepmann et al., 2015). Chollet et al. reported positive results of the Flame (fluoxetine for motor recovery after acute ischemic stroke) trial. They hypothesized that fluoxetine enhances motor recovery after stroke through a coupling of its neuroprotective effect with the serotonergic system capability to enhance motor outputs and facilitate long term potentiation (LTP) (Chollet et al., 2011). The encouraging results of the Flame trial were further supported by the positive results of a Cochrane review of SSRIs for stroke recovery including 52 trials and 4,059 patients (Mead et al., 2013).

The similarity between the processes of stroke recovery and learning has also recently gained increasing attention, and it is being explored by several research groups with the goal of improving the therapeutic efficacy of technologies for stroke rehabilitation (Hogan et al., 2006; Krakauer, 2006). Neural repair and recovery after stroke involve mechanisms of neuronal excitability modulation that are very similar to those involved in memory and learning processes (Krakauer, 2006).

Although their exact function during these processes is still unclear (Clarkson et al., 2010), the important role of inhibitory networks has begun to be acknowledged. These networks are thought to play a key role in both early and late stages of learning-induced plastic circuits. In fact, a strong neural system to promote learning is a system that can rapidly shift between inhibition and excitation (Trevelyan, 2016).

While the exact mechanisms of action of SSRIs on the neural system after stroke are far from being understood, this review aims to discuss the potential role of SSRIs on inhibitory neural circuits as a possible mechanism underlying motor rehabilitation after stroke through cortical reorganization and enhancement of motor learning. We critically analyze evidence regarding: (i) The relationship between inhibitory neural activity and motor learning; (ii) Disruption of inhibitory activity after stroke; (iii) Evidence of SSRIs-induced enhancement of inhibitory tone; and (iv) Evidence of SSRIs-induced enhancement of motor learning through an increase of inhibitory tone in stroke.

Relationship between Inhibitory Neural Activity and Motor Learning

Motor learning leads to alteration in the cortical motor mapping, promoting changes in the motor and somatosensory representations. Motor learning involves neuronal excitability and inhibitory modulatory mechanisms that are very similar to the mechanisms involved in memory and non-motor learning processes (Krakauer, 2006).

Learning a new motor skill shares similar physiological traits with motor recovery from stroke. The similarities between these processes provide us with a model that can be applied to certain processes of functional recovery after stroke (Krakauer, 2006; Rossi et al., 2009; Krakauer and Mazzoni, 2011; Kitago and Krakauer, 2013; Costanzo, 2017). For instance, the modifications of motor behavior after exposure to stimuli or experiences (learning) are similar to those occurring during physical therapy; however, in the latter case the modifications underlie a process of re-learning of behaviors lost due to the structural alteration caused by the cerebrovascular accident (Krakauer, 2006; Krakauer and Mazzoni, 2011).

Additionally, memory plays an important role in the consolidation of newly learned behaviors, therefore the enhancement of mechanisms underlying both learning and memory is crucial for therapies aimed at promoting stroke motor recovery (Krakauer, 2006).

The neurophysiological mechanism underlying learning and memory is synaptic plasticity. Enhanced and more effective synaptic functions largely depend on facilitating the likelihood of neuronal inputs to happen; repeated stimuli generate a pattern of repeated activation on a determined pathway leading to an enhanced responsiveness of the post synaptic neuron (potentiation) (Feldman, 2009; Costanzo, 2017). On a cellular level these processes depend on changes in network excitability as regulated by long-term potentiation (LTP) and long-term depression (LTD) (Hagemann et al., 1998). LTP and LTD can induce changes in synaptic strengthening, thereby shaping learning and memory processing (Bliss and Collingridge, 1993; Lynch, 2004).

Although little is known about the spatiotemporal aspects of motor learning (Berger et al., 2017), the modulation of inhibitory activity is an important mechanism underlying motor cortex plasticity. In fact, inhibitory activity can change during early and late stages of the learning process (See **Figure 1**; Engel et al., 2001; Hensch and Stryker, 2004; Stagg et al., 2011).

The early stage of learning is characterized by reduction in inhibition, facilitating LTP process in the motor cortex (Nudo et al., 1996; Floyer-Lea et al., 2006). Local changes in inhibitory circuits (GABA concentrations) can unmask existent neural pathways within the cortex leading to rapid changes in the sensory and motor representations (Castro-Alamancos et al., 1995; Castro-Alamancos and Connors et al., 1996). It has been shown that during early learning a transient GABA decrease in the motor cortex correlates with the degree of motor learning (Floyer-Lea et al., 2006; Stagg, 2013). Despite the transient impact of lower inhibitory activity in acute phases of learning, this correlation may be inverted in late phases of learning consolidation.

In later stages of motor learning, a partial recovery in inhibitory tonus (restoration of the inhibitory tonus) can be associated with longer-term consolidation of learning (Shadmehr and Holcomb, 1997; Floyer-Lea et al., 2006).

An interesting study using TMS, tDCS and neuroimaging showed that the degree of learning is associated with a decrease in GABA activity induced by tDCS (Johnstone et al., 2016), thus supporting the notion that during early learning stages a decreased and transient inhibitory tone is desirable. However, subsequent inhibition seems necessary for consolidation of learning (Brosh and Barkai, 2009).

Taken all together, these studies suggest that understanding the balance between excitation and inhibition activity during motor learning is key to better understanding the process

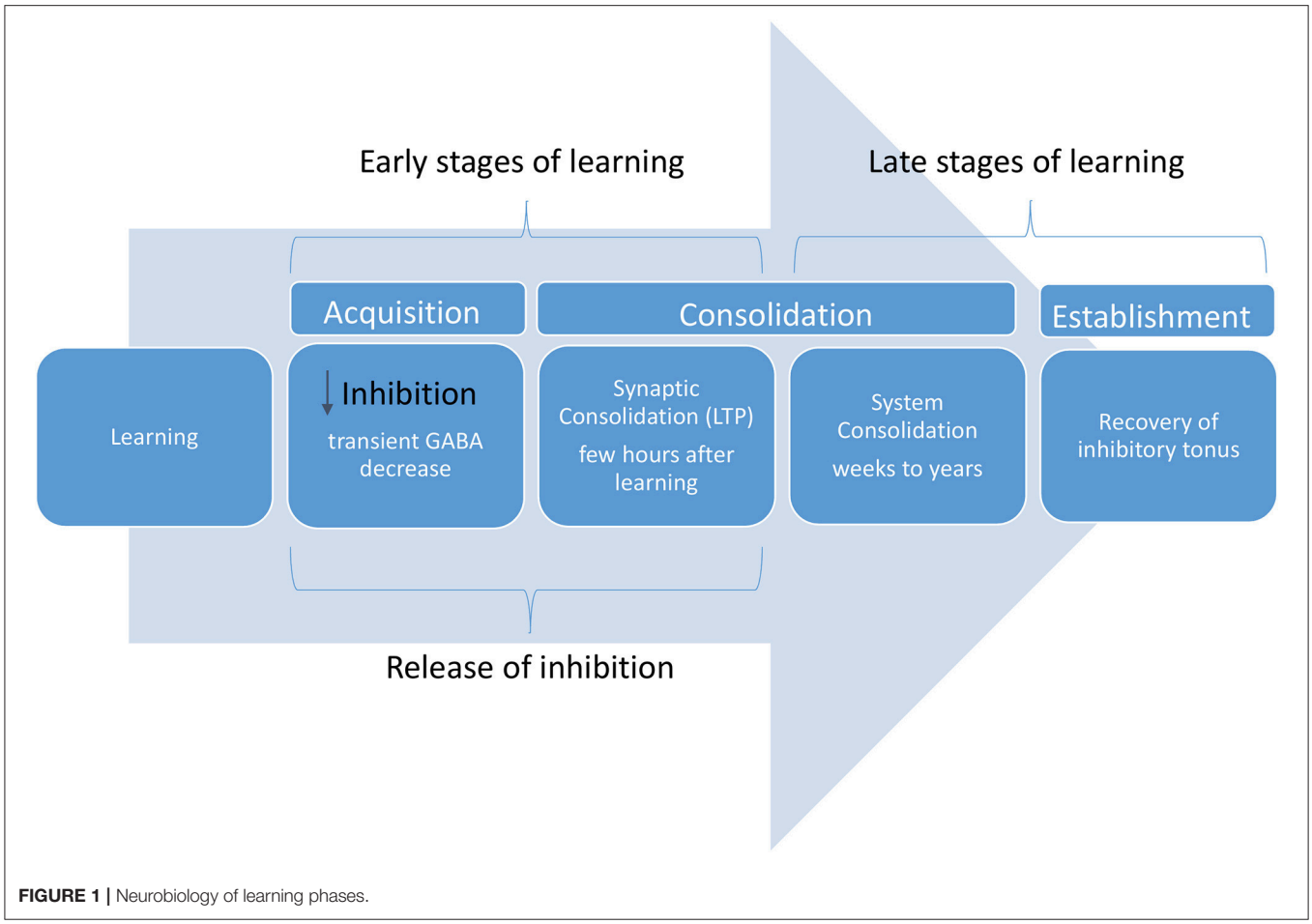

FIGURE 1 | Neurobiology of learning phases.

of motor learning. Assuming that stroke recovery and motor learning are somewhat similar processes (Hogan et al., 2006; Krakauer, 2006), this knowledge may help understand how to improve rehabilitation in stroke patients.

Disruption of Inhibitory Activity after Stroke

Following stroke, several structural and biological changes take place and the interactions between excitatory and inhibitory activity in learning-related circuits are crucial to drive motor cortex plasticity and recovery (Jones, 2017). In the very acute phase of stroke (hours after the event), inhibition of activity of cortical areas surrounding the injured site is a neuroprotective mechanism since increased excitability can result in glutamatergic toxicity and increase apoptosis (Schiene et al., 1996; Floyer-Lea et al., 2006).

After this initial phase, and similarly to early stages of learning, the excitation/inhibition ratio increases (Schiene et al., 1996). Two main neurophysiological changes have been associated with brain remodeling and recovery after stroke: (i) an initial increase in excitability in cortical regions and perilesional areas not affected by the stroke, and (ii) increased activity/excitability in the contralesional hemisphere. In this context, several studies showed that in stroke patients the inhibitory function is globally reduced in both hemispheres suggesting that the modulation of inhibitory circuits might result from a strategy that aims at compensating for motor impairment (Talelli et al., 2006; Di Lazzaro et al., 2012; Takeuchi and Izumi, 2012). Even though this enhanced excitability pattern is related to the enhanced plasticity and functional reorganization, both changes are required to be time dependent.

In the peri-lesional and distant cortical regions the down-regulation of the inhibitory tonus is important for altering cortical maps and promoting neuronal connectivity (*re-hardwiring*) (Schiene et al., 1996). Moreover, manipulation of the inhibitory tone promotes axonal and dendritic growth and guidance, cytoskeletal organization and the expression of genes related with adult brain remodeling (Urban et al., 2012; Nudo, 2013).

Widespread areas of enhanced cortical excitability appear after stroke, and are important for some of the compensatory re-organization (Collins, 2016). For example, Frost et al. (2003) showed that in adult squirrel monkeys an increased hand representation in ventral pre-motor areas (PMv) is observed after an experimental ischemic lesion of 50% of the M1 hand area. Additionally, the amount of reorganization was correlated with the size of the hand area lesion, suggesting that bigger lesions induce greater compensatory reorganization (Frost et al., 2003). Although the development of compensatory reorganization

results in initial gain of function, it may inhibit further gain of function in later phases of stroke rehabilitation (Meintzschel and Ziemann, 2006; Carmichael, 2012).

In this regard, increased disinhibition of the widespread cortical areas increases the risk of competitive interaction between the areas (pre motor cortex and M1), thereby resulting in incomplete motor recovery (Takeuchi et al., 2007). On the other hand, the localized and transient disinhibition of the affected M1 in stroke patients may promote the motor recovery of normal patterns by facilitating M1 plasticity (Takeuchi and Izumi, 2012).

One example is the surrounding inhibitory theory that highlights the importance of inhibitory networks during the initiation of active voluntary tasks. During movement preparation, there is a local decrease of inhibition (decrease in GABAa) and a concomitant increase of inhibition in the brain neighboring areas; these processes avoid competition between local and neighboring areas and allow specific activation of the motor area in charge of generating the desired motor behavior (Pfurtscheller et al., 2005; Klimesch, 2012; Pfurtscheller and Lopes da Silva, 2017). In stroke patients, the local decrease of inhibitory activity prior to movement is reduced and there is a widespread disinhibition in the neighboring areas of the lesion (Reynolds and Ashby, 1999; Zaaroor et al., 2003; Hummel et al., 2009).

Therefore, stronger functional recovery is associated with a time-dependent increase of inhibition. In fact, an important aspect that has not been fully explored in human studies is the modulation of the inhibitory states; varying from disinhibition to inhibition in cortico-subcortical circuits according to the phase of learning. A shift in one direction only (i.e., disinhibitory state) has a low learning efficiency. In fact, that shift may be an index of cortical disorganization.

A Network Example of Disrupted Excitation-Inhibition Balance: Transcallosal Imbalance and Motor Recovery in Stroke

An example of imbalance in the excitation-inhibition ratio can be seen in the transcallosal interaction between motor cortices in stroke (Julkunen et al., 2016). Functional imaging and non-invasive brain stimulation have indicated that ipsilateral motor projections are enhanced early after stroke and that a pattern of hyper-excitation is commonly observed in the unaffected hemisphere (Turton et al., 1996; Netz et al., 1997; Werhahn et al., 2003; Murase et al., 2004; Oh et al., 2010). Although the underlying mechanism remains unclear, it is believed that latent ipsilateral motor projections are activated by disruption of the contralateral corticospinal projections in stroke patients (Feydy et al., 2002; Johansen-Berg et al., 2002). This results in the reconfiguration of motor networks through the establishment of alternative inputs for the cortico-spinal tracts. Then, parallel motor circuits are activated and begin to transfer the impaired functions to unaffected areas of the brain (Feydy et al., 2002; Lindenberg et al., 2010).

In later stages of stroke recovery, better motor recovery and outcome of functional rehabilitation are associated with a shift of activation back to the affected hemisphere by the reestablishment of the inhibitory tonus in the unaffected hemisphere as well as with recovery of connectivity and cessation of imbalance between the two hemispheres (Jaillard et al., 2005; Carter et al., 2010; Park et al., 2011).

A persistent increased activity of the unaffected hemisphere can result in alterations of transcallosal structure and function and it is associated with upper limb motor impairment and greater levels of arm motor dysfunction (Sato et al., 2015) in chronic stroke patients. In this context, several studies showed the importance of inhibition after stroke and the association between increased inhibition of the unaffected hemisphere with better functional outcomes (Conforto et al., 2008; Swayne et al., 2008). Additionally, patients with severe upper limb impairment display higher disinhibition of the unaffected hemisphere compared to patients with mild-moderate impairment (Liepert et al., 2000).

Therefore, it is hypothesized that the balance between excitatory and inhibitory inputs after stroke is crucial for long term stroke recovery and motor re-learning. These time dependent changes in balance between excitatory and inhibitory networks are also seen in healthy subjects (Guerra et al., 2016). However, after a stroke this process can be altered and jeopardize motor recovery. Consequently, longitudinal changes in the regulation of inhibitory functions seem to play a major role in this balance, since the lack of inhibition in later phases of stroke recovery is associated with worse motor function outcomes (see **Figure 2**; Crichton et al., 2016).

Can SSRIs Enhance Inhibitory Tone?

SSRIs are the most common treatment for major depressive disorder (MDD). Clinical and preclinical data of MDD patients indicate imbalanced activity in the right dorsolateral prefrontal cortex (DLPC) compared to the left cortex/counterpart (Grimm et al., 2008). It has been shown that impaired inhibition of the right hemisphere, as indexed by TMS measures such as intracortical inhibition (ICI), intracortical facilitation (ICF) and cortical silent period, is correlated with treatment responsiveness and recovery after depression (Mantovani et al., 2012). Several authors have also demonstrated that adults with MDD present deficits in GABAergic mediated transmission related with the severity of MDD (Robinson et al., 2003; Ye et al., 2008; Croarkin et al., 2014). Moreover, it has been shown that acute (intravenous infusion) (Bhagwagar, 2004) or chronic (2 months) (Sanacora et al., 2002) administration of SSRIs can increase cortical levels of GABA in depressed adults, leading to the normalization of GABA levels and possibly contributing to an antidepressant mechanism.

Besides that, in mouse models of social isolation, fluoxetine treatment can induce stress recovery independently of its serotonergic pathways. In these models, fluoxetine acts by increasing the neurosteroids levels in the brain allowing a normal allosteric increase of GABA-A synapses and therefore restoring inhibition (Matsumoto et al., 2007).

Several neurological conditions seem to depend on a balance between excitatory and inhibitory activity in the brain, and the inhibitory control of excitation may have a key role in this balance. Dysfunction in GABA-controlled inhibition is pathophysiologically correlated with several diseases and

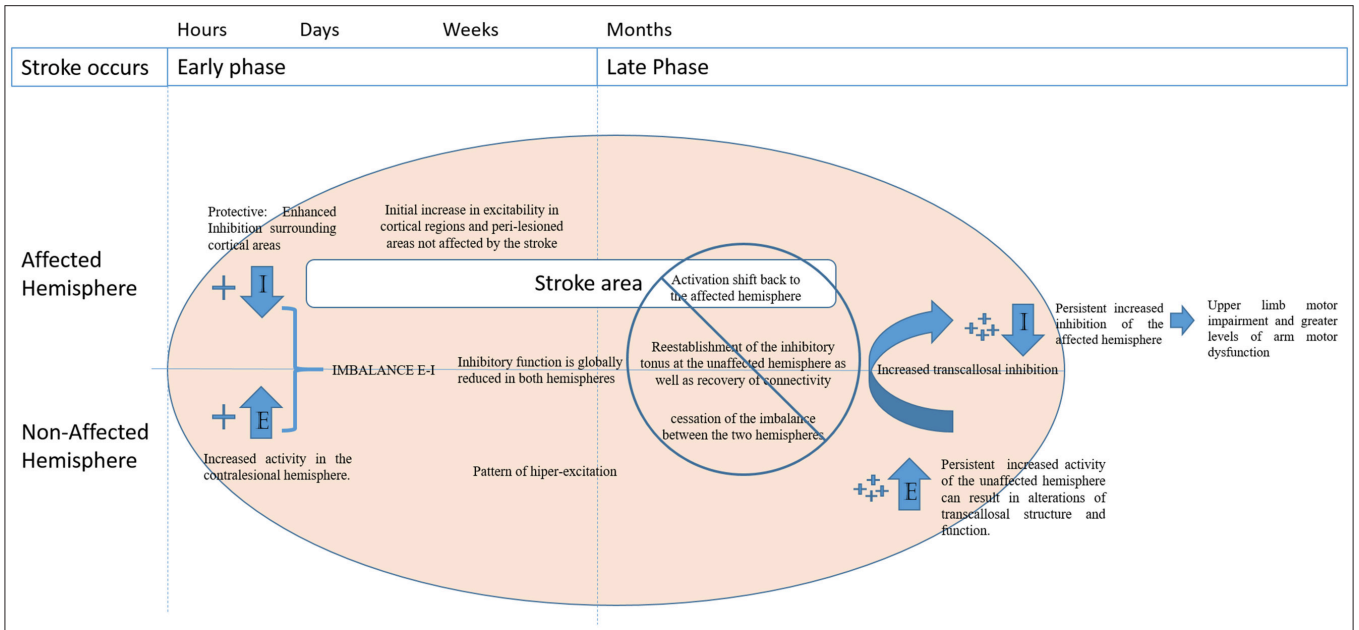

FIGURE 2 | Disruption of balance between excitation (E) and inhibition (I) of the affected and non-lesioned hemispheres throughout the time post stroke.

restoration of functional inhibition leads to better treatment outcomes. In particular, fluoxetine was shown to have positive effects on motor rehabilitation after stroke and preclinical data demonstrated that fluoxetine can directly up regulate GABA, increasing inhibitory activity (Tunnicliff et al., 1999; Robinson et al., 2003). In fact it is possible that one of the mechanisms of SSRIs in improving depression is through a reestablishment of normal learning patterns of prefrontal circuits.

SSRIs and Changes in Inhibitory Activity in Stroke

Inhibitory circuits play an essential role in post-stroke motor learning. SSRIs seem to exert an effect on excitation/inhibition pathways, leading to enhancement of motor function after a stroke. Although this mechanism is still underexplored in stroke, other disease models are clearer; some insights from these conditions can be extrapolated to better understand the potential role of this class of drugs in stroke patients.

Recent studies have shown the effects of drugs that are capable of modulating excitatory and inhibitory pathways and this may be how they facilitate functional recovery after brain lesions. Some of these pharmacological candidates are SSRIs (Pariente et al., 2001; Chollet et al., 2011), dopamine agonist (Scheidtmann et al., 2001), amphetamines (Bütefisch et al., 2002; Sawaki et al., 2002b) and cholinergic substances (ACR) (Sawaki et al., 2002a; Meintzschel and Ziemann, 2006).

Among these drugs, SSRIs have been shown to be able to produce different effects (inhibitory or excitatory) on motor cortex plasticity (Robol et al., 2004). The neuroplastic changes triggered by SSRIs can be responsible for the compensation of some of the neurophysiologic damage caused by the stroke. Several early studies suggested that serotonergic agents such as fluoxetine and citalopram have a positive effect on motor function in hemiplegic patients after stroke (Dam et al., 1996; Pariente et al., 2001; Zittel et al., 2008). The Flame trial, a large randomized placebo-controlled clinical trial, showed that the administration of fluoxetine during the acute stroke phase has a moderate effect size, resulting in improvement of a clinical motor function scale for upper and lower limbs outcome (Fugl-Meyer) (Chollet et al., 2011).

To date, the mechanism by which fluoxetine enhances rehabilitation after stroke remain unclear; however, some insights from animal-based models suggested that SSRIs may enhance overall brain excitability. Additionally, it has been shown that SSRIs can promote neuronal sprouting (Kokoeva et al., 2005; Hourai and Miyata, 2013; Ohira et al., 2013b) and cortical reorganization (26), restore blood flow (Rosenstein et al., 1998; Sun et al., 2003), and enhance neuroprotective mechanism (Lim et al., 2009); thereby improving neuronal survival and protecting cerebral tissue from hypoxia since it regulates the expression of hypoxia-inducible factor-1α (HIF-1α) and of heme oxygense-1 (HO-1) (Shin et al., 2009; Siepmann et al., 2015). Therefore, one hypothesis for the motor rehabilitation induced by fluoxetine is that the blockage of serotonin (5-HT) reuptake due to SSRI administration increases the availability of this neurotransmitter in the synaptic cleft thus enhancing signal transmission (Ganzer et al., 2013; Rief et al., 2016; Stahl, 2017) and consequently, increasing the excitatory input of glutamate and activating the NMDA receptors leading to a cascade of intracellular events. These events might generate synaptic modifications that culminate in a LTP leading synapse reprogramming and strengthening (Stahl, 2017).

Nevertheless, we also believe that this acute effect on enhancement of excitatory activity is followed by an increase in inhibitory activity. Studies exploring the effects exerted by SSRIs over motor cortex plasticity showed that SSRIs can also enhance

inhibitory activity (Etherton et al., 2016). Studies have shown that serotonergic drugs induce changes in inhibitory activity. Indeed inhibition in the motor cortex was observed in healthy subjects 2.5 h after citalopram intake. A single dose of citalopram produced a transient enhanced GABAergic interneuronal control over corticospinal neurons, resulting in increases in the ICI, motor threshold and cortico-silent period (CSP) as well as mild decrease in the ICF (Robol et al., 2004). Therefore, citalopram was able to acutely decrease motor cortex excitability in healthy subjects.

In addition, pre-clinical data suggest that citalopram, fluoxetine and sertraline have anticonvulsive effects in the hippocampus inhibiting seizure like events. The effects of these SSRIs were likely due to regulation of pyramidal cell's excitability leading to vigorous inhibition of repetitive firing (Igelström and Heyward, 2012). However, in clinical studies an increase in seizures after administration of SSRIs was also described (Hill et al., 2015).

Recently, authors have been exploring the role of long term administration of fluoxetine treatment administration (Chen et al., 2011) inducing structural plasticity by promoting neuron "dematuration" (Kobayashi et al., 2010; Ohira et al., 2013a,b). This mechanism consists in a reverse effect on the normal maturate state of cells that can be induced by changes in GABAergic transmission; therefore, culminating in a juvenile-like state of fast-spiking inhibitory interneurons. In several studies, neuronal "dematuration" induced by fluoxetine was identified in different brain regions such as adult dentate granule cells, adult amygdala cells (Karpova et al., 2011), hippocampus, medial pre-frontal cortex (mPFC) (Guirado et al., 2014) and a subset of GABAergic interneurons, generated from Layer 1 inhibitory neuron progenitor cells (L1-INP cells) (Ohira et al., 2013a).

In this context, it is important to acknowledge that the same antidepressant can exert different regulatory effects in different brain regions and these effects vary depending on dose, regimen of use (single dose or prolonged use) and time of administration (in acute or chronic diseases phase). For example, a single dose of paroxetine can improve motor performance and induce hyper activation of the primary sensorimotor cortex (S1M1) (Loubinoux et al., 2005). However, prolonged paroxetine treatment (30 days 20 mg per day) induced hypo activation of S1M1 cells, but still resulted in improvement in finger tapping motor task (Gerdelat-Mas et al., 2005). These results indicate that SSRIs may have an acute effect on excitatory circuits that is led by enhancement of inhibitory activity.

Even though the exact mechanism by which this effect occurs is unknown, prior studies showed that some SSRIs can potentiate GABA-mediated inhibitory neurotransmission. Among SSRIs, fluoxetine's mechanism of action includes its 5-HT2C antagonism. Furthermore, 5-HT2C receptors are expressed on GABAergic neurons (Serrats et al., 2005; Invernizzi et al., 2007).

Furthermore, SSRIs can activate other receptors such as the 5-HT2B receptor that have been identified in multiple brain cells such as neurons, astrocytes, and Purkinje cells (Chen et al., 1995; Peng et al., 2014). However, animal studies have shown that its expression can be twice as much in astrocytes than in neurons (Lovatt et al., 2007; Dong et al., 2015). Astrocytes have a main role in the neuronal metabolic process in the brain and recent evidence shows that fluoxetine can alter this metabolic process through 5-HT2B receptor activity (Peng et al., 2014; Hertz et al., 2015a).

The activation of 5-HT2B leads to a cascade of effects that have been associated with the enhancement of learning and memory. Among those processes, animal studies showed that its activation can lead to raise of intracellular calcium levels in astrocytes and consequent increase of glycogenolysis and glycolysis, causing subsequent increase of lactate release that can either act as extra metabolic fuel for neurons or act in further signaling pathways (Li et al., 2011; Hertz et al., 2015a; Steinman et al., 2016). Other processes such as potassium homeostasis are also enhanced by this activation (Du et al., 2014). In this regard, it is known that lactate has a neuroprotective effects during brain ischemia and that glycogen metabolism have many implications for the brain activities. In addition, it is suggested that the 5-HT2B receptor plays an important role in neurogenesis driven by SSRI treatments since studies in animals lacking this receptor revealed a deficient response to the enhanced effects of fluoxetine in neurogenesis (Diaz et al., 2012, 2016).

Moreover, the effects exert by fluoxetine differ depending on its dose as different responses are seen in glycogen concentration in astrocytes with different doses of fluoxetine. Whereas lower concentration of fluoxetine causes an increase of glycogen in astrocytes the opposite effects are seen with an increased concentration of the drug. It is believe that this dual effect can be associated with aspects of either the therapeutic effect or adverse event of the medication (Bai et al., 2017). The effects of fluoxetine in the 5-HT2B receptor need to be further explored in human studies since its role in plasticity can be used to better explain the mechanism underling this drug effects in neuroplasticity and motor rehabilitation after stroke.

In this context, the astrocytic metabolism could have a role in regulation excitatory and inhibitory mechanism after stroke. The activation of GABA-A receptors in astrocytes can stimulate a similar mechanism enhancing regulation of calcium concentrations and further enhancement of glycogenolysis, a process that has already been associated with learning and memory tasks; therefore relevant in the setting of motor recovery (Hertz et al., 2015b). Finally, the effects of fluoxetine in the 5-HT2B receptor need to be further explored in human studies since its role in plasticity can be used to better explain the mechanism underlying this drug effects in neuroplasticity and motor rehabilitation after stroke.

SSRIs and Safety Considerations

Most studies to date have reported little or no side effects in relation of SSRI use in the stroke population; however, known potential adverse effects on mood disorders should be discussed. Due to their selective action, SSRIs present a more tolerable profile of adverse actions and there are differences between the main side effects of the different selective serotonin reuptake

inhibitors. Overall, the most frequently reported adverse events are nausea, vomiting, abdominal pain, diarrhea, agitation, anxiety, insomnia, cycling for mania, headache, dizziness, fatigue, tremors, extrapyramidal effects, xerostomia, perspiration, loss or weight gain, sexual dysfunction, and dermatological reactions.

Moreover, SSRIs effects on patient with pre-existent cardiac disease or acute coronary syndrome are controversial as they may improve cardiac disease prognosis by inhibiting platelet aggregation but could potentially worsen prognosis by increasing risk of bleeding or of arrhythmias (Rieckmann and Kronish, 2013).

Another important aspect associated with increased serotonergic activity in the central nervous system is the Serotonergic syndrome, a potentially fatal condition (Peng et al., 2014). The most common symptoms include: hyperthermia, agitation, ocular clone, tremor, akathisia, deep tendon hyperreflexia, inducible or spontaneous clonus, muscular rigidity, dilated pupils, dry mucous membranes, increased intestinal sounds, spotted skin and diaphoresis (Boyer and Shannon, 2005). Although, serotonergic syndrome is commonly the result of the combination of SSRIs with drugs or dietary supplements that have a similar effect of increasing serotonin, it may occur after the initiation of a higher doses of single serotonergic drugs or increase of the dose of a serotonergic drug in particularly sensitive individuals. Selective serotonin reuptake inhibitors, such as fluoxetine, are perhaps the most implicitly associated drug group associated with serotonergic syndrome. They may contribute to the development of serotonin syndrome up to several weeks after drug discontinuation (Birmes et al., 2003).

Even though uncommon, the FLAME trial reported that among the 118 participants two in the active fluoxetine group have severe adverse events (hyponatremia and partial seizure). The most frequent adverse events in the active group were transient digestive disorders. To avoid serotonin syndrome, treatment was stopped in patients in the active group who developed depression and required the use of another antidepressant during the study (Chollet et al., 2011). Therefore, if this hypothesis that SSRIs improve motor function by modulating the excitatory-inhibitory balance is confirmed, other interventions that are safer may be best better first alternatives to SSRIs in this context.

SUMMARY

The mechanisms underlying the enhancement of motor learning via SSRIs are still unclear, and the exact effects of fluoxetine in motor recovery after stroke are yet to be proven. We discussed how this class of drugs might help reestablish the excitation-inhibitory balance by initially enhancing excitation that is followed by a compensatory inhibition. Different techniques such as functional magnetic resonance, magnetic resonance spectroscopy, transcranial magnetic stimulation, transcranial direct current stimulation and EEG have been used to show the role of neurochemical and neurophysiological markers as well as to quantify modifications of inhibitory and excitatory responses to several interventions. However, further work needs to be done to develop better methods to assess specific alterations in inhibitory pathways.

Ultimately SSRIs can have a broader action on promoting reorganization of neural activity following brain lesion. With the current evidence it is not possible to conclude whether the increased neural inhibition that follows use of SSRIs is indeed the result of its usage. However further studies can explore further this mechanism as to understand better how to use SSRIs and the potential limitations of this class of drugs that may also be detrimental in some cases.

AUTHOR CONTRIBUTIONS

CP: conception and design of the manuscript, acquisition of data, analysis and interpretation of data reviewed, drafting revising and important intellectual contribution, critical revision and final approval of the version; FS: conception and design of the manuscript, interpretation of data reviewed, drafting revising and important intellectual contribution, and critical revision; FL and PdTP: acquisition of data, analysis, and final review; LdP, NM, RB-S, QW, and EC: critical revision, review, and final approval of the version; FF: conception and design of the manuscript, analysis, critical revision, and final approval of the version.

FUNDING

This research was supported by the NIH R21 Grant 1R21HD079048-01A1.

REFERENCES

Bai, Q., Song, D., Gu, L., Verkhratsky, A., and Peng, L. (2017). Bi-phasic regulation of glycogen content in astrocytes via Cav-1/PTEN/PI3K/AKT/GSK-3β pathway by fluoxetine. *Psychopharmacology* 234, 1069–1077. doi: 10.1007/s00213-017-4547-3

Berger, D. J., Ferrari, F., Esposito, A., Masciullo, M., Molinari, M., Lacquaniti, F., et al. (2017). "Changes in muscle synergy organization after neurological lesions," in *Converging Clinical and Engineering Research on Neurorehabilitation II. Biosystems and Biorobotics,* Vol. 15, eds J. Ibáñez, J. González-Vargas, J. Azorín, M. Akay, and J. Pons (Cham: Springer International Publishing), 939–943.

Bhagwagar, Z. (2004). Increased brain GABA concentrations following acute administration of a selective serotonin reuptake Inhibitor. *Am. J. Psychiatry* 161, 368–370. doi: 10.1176/appi.ajp.161.2.368

Birmes, P., Coppin, D., Schmitt, L., and Lauque, D. (2003). Serotonin syndrome: a brief review. *Can. Med. Assoc. J.* 168, 1439–1442.

Bliss, T. V., and Collingridge, G. L. (1993). A synaptic model of memory: long-term potentiation in the hippocampus. *Nature* 361, 31–39. doi: 10.1038/361031a0

Boyer, E. W., and Shannon, M. (2005). The serotonin syndrome. *N. Engl. J. Med.* 352, 1112–1120. doi: 10.1056/NEJMra041867

Brosh, I., and Barkai, E. (2009). Learning-induced enhancement of feedback inhibitory synaptic transmission. *Learn. Mem.* 16, 413–416. doi: 10.1101/lm.1430809

Bütefisch, C. M., Davis, B. C., Sawaki, L., Waldvogel, D., Classen, J., Kopylev, L., et al. (2002). Modulation of use-dependent plasticity by d-amphetamine. *Ann. Neurol.* 51, 59–68. doi: 10.1002/ana.10056

Carmichael, S. T. (2012). Brain excitability in stroke: the Yin and Yang of stroke progression. *Arch. Neurol.* 69, 161–167. doi: 10.1001/archneurol.2011.1175

Carter, A. R., Astafiev, S. V., Lang, C. E., Connor, L. T., Rengachary, J., Strube, M. J., et al. (2010). Resting interhemispheric functional magnetic resonance imaging connectivity predicts performance after stroke. *Ann. Neurol.* 67, 365–375. doi: 10.1002/ana.21905

Castro-Alamancos, M., A., and Connors, B. W. (1996). Short-term plasticity of a thalamocortical pathway dynamically modulated by behavioral state. *Science* 272, 274–277. doi: 10.1126/science.272.5259.274

Castro-Alamancos, M., A, Donoghue, J. P., and Connors, B. W. (1995). Different forms of synaptic plasticity in somatosensory and motor areas of the neocortex. *J. Neurosci.* 15, 5324–5333.

Chen, J. L., Lin, W. C., Cha, J. W., So, P. T., Kubota, Y., and Nedivi, E. (2011). Structural basis for the role of inhibition in facilitating adult brain plasticity. *Nat. Neurosci.* 14, 587–594. doi: 10.1038/nn.2799

Chen, Y., Peng, L., Zhang, X., Stolzenburg, J. U., and Hertz, L. (1995). Further evidence that fluoxetine interacts with a 5-HT2C receptor in glial cells. *Brain Res. Bull.* 38, 153–159. doi: 10.1016/0361-9230(95)00082-P

Chollet, F., Tardy, J., Albucher, J.-F., Thalamas, C., Berard, E., Lamy, C., et al. (2011). Fluoxetine for motor recovery after acute ischaemic stroke (FLAME): a randomised placebo-controlled trial. *Lancet Neurol.* 10, 123–130. doi: 10.1016/S1474-4422(10)70314-8

Clarkson, A. N., Huang, B. S., Macisaac, S. E., Mody, I., and Carmichael, S. T. (2010). Reducing excessive GABA-mediated tonic inhibition promotes functional recovery after stroke. *Nature* 468, 305–309. doi: 10.1038/nature09511

Collins, K. (2016). *Investigation of Upper Limb Kinematics and Corticospinal Pathway Activity Early after Stroke*. East Angle, CA: Norwich University.

Conforto, A. B., dos Santos, R. L., Farias, S. N., Marie, S. K. N., Mangini, N., and Cohen, L. G. (2008). Effects of somatosensory stimulation on the excitability of the unaffected hemisphere in chronic stroke patients. *Clinics* 63, 735–740. doi: 10.1590/S1807-59322008000600005

Costanzo, L. S. (2017). *Physiology E-Book*. Elsevier Health Sciences. Available online at: https://books.google.com/books?id=H6BcDgAAQBAJ

Crichton, S. L., Bray, B. D., McKevitt, C., Rudd, A. G., and Wolfe, C. D. A. (2016). Patient outcomes up to 15 years after stroke: survival, disability, quality of life, cognition and mental health. *J. Neurol. Neurosurg. Psychiatr.* 87, 1091–1098. doi: 10.1136/jnnp-2016-313361

Croarkin, P. E., Nakonezny, P. A., Husain, M. M., Port, J. D., Melton, T., Kennard, B. D., et al. (2014). Evidence for pretreatment LICI deficits among depressed children and adolescents with nonresponse to fluoxetine. *Brain Stimul.* 7, 243–251. doi: 10.1016/j.brs.2013.11.006

Dam, M., Tonin, P., De Boni, A., Pizzolato, G., Casson, S., Ermani, M., et al. (1996). Effects of fluoxetine and maprotiline on functional recovery in poststroke hemiplegic patients undergoing rehabilitation therapy. *Stroke* 27, 1211–1214. doi: 10.1161/01.STR.27.7.1211

Diaz, S. L., Doly, S., Narboux-Nême, N., Fernández, S., Mazot, P., Banas, S. M., et al. (2012). 5-HT2B receptors are required for serotonin-selective antidepressant actions. *Mol. Psychiatry* 17, 154–163. doi: 10.1038/mp.2011.159

Diaz, S. L., Narboux-Nême, N., Boutourlinsky, K., Doly, S., and Maroteaux, L. (2016). Mice lacking the serotonin 5-HT2B receptor as an animal model of resistance to selective serotonin reuptake inhibitors antidepressants. *Eur. Neuropsychopharmacol.* 26, 265–279. doi: 10.1016/j.euroneuro.2015.12.012

Di Lazzaro, V., Profice, P., Pilato, F., Capone, F., Ranieri, F., Florio, L., et al. (2012). The level of cortical afferent inhibition in acute stroke correlates with long-term functional recovery in humans. *Stroke* 43, 250–252. doi: 10.1161/STROKEAHA.111.631085

Dong, L., Li, B., Verkhratsky, A., and Peng, L. (2015). Cell type-specific *in vivo* expression of genes encoding signalling molecules in the brain in response to chronic mild stress and chronic treatment with fluoxetine. *Psychopharmacology* 232, 2827–2835. doi: 10.1007/s00213-015-3921-2

Du, T., Liang, C., Li, B., Hertz, L., and Peng, L. (2014). Chronic fluoxetine administration increases expression of the L-channel gene Cav1.2 in astrocytes from the brain of treated mice and in culture and augments K+-induced increase in [Ca2+]i. *Cell Calc.* 55, 166–174. doi: 10.1016/j.ceca.2014.01.002

Engel, D., Pahner, I., Schulze, K., Frahm, C., Jarry, H., Ahnert-Hilger, G., et al. (2001). Plasticity of rat central inhibitory synapses through GABA metabolism. *J. Physiol.* 535, 473–482. doi: 10.1111/j.1469-7793.2001.00473.x

Etherton, M., Siddiqui, K. A., Ayres, A., and Schwamm, L. H. (2016). *Abstract WP174: Prestroke Selective Serotonin Reuptake Inhibitor Use and Functional Outcomes in Ischemic Stroke. Stroke 47, AWP174–AWP174*. Available online at: http://stroke.ahajournals.org/content/47/Suppl_1/AWP174

Feldman, D. E. (2009). Synaptic mechanisms for plasticity in neocortex. *Annu. Rev. Neurosci.* 32, 33–55. doi: 10.1146/annurev.neuro.051508.135516

Feydy, A., Carlier, R., Roby-Brami, A., Bussel, B., Cazalis, F., Pierot, L., et al. (2002). Longitudinal study of motor recovery after stroke: recruitment and focusing of brain activation. *Stroke* 33, 1610–1617. doi: 10.1161/01.STR.0000017100.68294.52

Floyer-Lea, A., Wylezinska, M., Kincses, T., and Matthews, P. M. (2006). Rapid modulation of GABA concentration in human sensorimotor cortex during motor learning. *J. Neurophysiol.* 95, 1639–1644. doi: 10.1152/jn.00346.2005

Frost, S. B., Barbay, S., Friel, K. M., Plautz, E. J., and Nudo, R. J. (2003). Reorganization of remote cortical regions after ischemic brain injury: a potential substrate for stroke recovery. *J. Neurophysiol.* 89, 3205–3214. doi: 10.1152/jn.01143.2002

Ganzer, P. D., Moxon, K. A., Knudsen, E. B., and Shumsky, J. S. (2013). Serotonergic pharmacotherapy promotes cortical reorganization after spinal cord injury. *Exp. Neurol.* 241, 84–94. doi: 10.1016/j.expneurol.2012.12.004

Gerdelat-Mas, A., Loubinoux, I., Tombaria, D., Rascolb, O., Cholleta, F., and Simonetta-Moreaua, M. (2005). Chronic administration of selective serotonin reuptake inhibitor (SSRI) paroxetine modulates human motor cortex excitability in healthy subjects. *Neuroimage* 27, 314–322. doi: 10.1016/j.neuroimage.2005.05.009

Grimm, S., Beck, J., Schuepbach, D., Hell, D., Boesiger, P., Bermpohl, F., et al. (2008). Imbalance between left and right dorsolateral prefrontal cortex in major depression is linked to negative emotional judgment: an fMRI study in severe major depressive disorder. *Biol. Psychiatry* 63, 369–376. doi: 10.1016/j.biopsych.2007.05.033

Guerra, A., Pogosyan, A., Nowak, M., Tan, H., Ferreri, F., Di Lazzaro, V., et al. (2016). Phase dependency of the human primary motor cortex and cholinergic inhibition cancelation during beta tACS. *Cereb. Cortex* 26, 3977–3990. doi: 10.1093/cercor/bhw245

Guirado, R., Perez-Rando, M., Sanchez-Matarredona, D., Castrén, E., and Nacher, J. (2014). Chronic fluoxetine treatment alters the structure, connectivity and plasticity of cortical interneurons. *Int. J. Neuropsychopharmacol.* 17, 1635–1646. doi: 10.1017/S1461145714000406

Hagemann, G., Redecker, C., Neumann-Haefelin, T., Freund, H. J., and Witte, O. W. (1998). Increased long-term potentiation in the surround of experimentally induced focal cortical infarction. *Ann. Neurol.* 44, 255–258. doi: 10.1002/ana.410440217

Hensch, T. K., and Stryker, M. P. (2004). Columnar architecture sculpted by GABA circuits in developing cat visual cortex. *Science* 303, 1678–1681. doi: 10.1126/science.1091031

Hertz, L., Rothman, D. L., Li, B., and Peng, L. (2015a). Chronic SSRI stimulation of astrocytic 5-HT2B receptors change multiple gene expressions/editings and metabolism of glutamate, glucose and glycogen: a potential paradigm shift. *Front. Behav. Neurosci.* 9:25. doi: 10.3389/fnbeh.2015.00025

Hertz, L., Xu, J., Song, D., Du, T., Li, B., Yan, E., et al. (2015b). Astrocytic glycogenolysis: mechanisms and functions. *Metab. Brain Dis.* 30, 317–333. doi: 10.1007/s11011-014-9536-1

Hill, T., Coupland, C., Morriss, R., Arthur, A., Moore, M., and Hippisley-Cox, J. (2015). Antidepressant use and risk of epilepsy and seizures in people aged 20 to 64 years: cohort study using a primary care database. *BMC Psychiatry* 15:315. doi: 10.1186/s12888-015-0701-9

Hogan, N., Krebs, H. I., Rohrer, B., Palazzolo, J. J., Dipietro, L., Fasoli, S. E., et al. (2006). Motions or muscles? Some behavioral factors underlying robotic assistance of motor recovery. *J. Rehabil. Res. Dev.* 43, 605–618. doi: 10.1682/JRRD.2005.06.0103

Hourai, A., and Miyata, S. (2013). Neurogenesis in the circumventricular organs of adult mouse brains. *J. Neurosci. Res.* 91, 757–770. doi: 10.1002/jnr.23206

Hummel, F. C., and Cohen, L. G. (2006). Non-invasive brain stimulation: a new strategy to improve neurorehabilitation after stroke? *Lancet Neurol.* 5, 708–712. doi: 10.1016/S1474-4422(06)70525-7

Hummel, F., and Cohen, L. G. (2005). Improvement of motor function with noninvasive cortical stimulation in a patient with chronic stroke. *Neurorehabil. Neural Repair* 19, 14–19. doi: 10.1177/1545968304272698

Hummel, F. C., Steven, B., Hoppe, J., Heise, K., Thomalla, G., Cohen, L. G., et al. (2009). Deficient intracortical inhibition (SICI) during

movement preparation after chronic stroke. *Neurology* 72, 1766–1772. doi: 10.1212/WNL.0b013e3181a609c5

Igelström, K. M., and Heyward, P. M. (2012). Inhibition of hippocampal excitability by citalopram. *Epilepsia* 53, 2034–2042. doi: 10.1111/j.1528-1167.2012.03660.x

Invernizzi, R. W., Pierucci, M., Calcagno, E., Di Giovanni, G., Di Matteo, V., Benigno, A., et al. (2007). Selective activation of 5-HT2C receptors stimulates GABA-ergic function in the rat substantia nigra pars reticulata: a combined *in vivo* electrophysiological and neurochemical study. *Neuroscience* 144, 1523–1535. doi: 10.1016/j.neuroscience.2006.11.004

Jaillard, A., Martin, C. D., Garambois, K., Lebas, J. F., and Hommel, M. (2005). Vicarious function within the human primary motor cortex? a longitudinal fMRI stroke study. *Brain* 128, 1122–1138. doi: 10.1093/brain/awh456

Johansen-Berg, H., Rushworth, M. F., Bogdanovic, M. D., Kischka, U., Wimalaratna, S., and Matthews, P. M. (2002). The role of ipsilateral premotor cortex in hand movement after stroke. *Proc. Natl. Acad. Sci. U.S.A.* 99, 14518–14523. doi: 10.1073/pnas.222536799

Johnstone, A., Hinson, E., and Stagg, C. J. (2016). "tDCS and magnetic resonance imaging," in *Transcranial Direct Current Stimulation in Neuropsychiatric Disorders: Clinical Principles and Management*, eds A. Brunoni, M. Nitsche, and C. Loo (Cham: Springer International Publishing), 169–195.

Jones, T. A. (2017). Motor compensation and its effects on neural reorganization after stroke. *Nat. Rev. Neurosci.* 18, 267–280. doi: 10.1038/nrn.2017.26

Julkunen, P., Määttä, S., Säisänen, L., Kallioniemi, E., Könönen, M., Jäkälä, P., et al. (2016). Functional and structural cortical characteristics after restricted focal motor cortical infarction evaluated at chronic stage – indications from a preliminary study. *Clin. Neurophysiol.* 127, 2775–2784. doi: 10.1016/j.clinph.2016.05.013

Karpova, N. N., Pickenhagen, A., Lindholm, J., Tiraboschi, E., Kulesskaya, N., Agústsdóttir, A., et al. (2011). Fear erasure in mice requires synergy between antidepressant drugs and extinction training. *Science* 334, 1731–1734. doi: 10.1126/science.1214592

Kitago, T., and Krakauer, J. W. (2013). "Chapter 8 - Motor learning principles for neurorehabilitation," in *Neurological Rehabilitation*, *Handbook of Clinical Neurology*, Vol. 110, eds M. P. Barnes and D. C. Good (New York, NY: Elsevier), 93–103. doi: 10.1016/B978-0-444-52901-5.00008-3

Klimesch, W. (2012). Alpha-band oscillations, attention, and controlled access to stored information. *Trends Cogn. Sci.* 16, 606–617. doi: 10.1016/j.tics.2012.10.007

Kobayashi, K., Ikeda, Y., Sakai, A., Yamasaki, N., Haneda, E., Miyakawa, T., et al. (2010). Reversal of hippocampal neuronal maturation by serotonergic antidepressants. *Proc. Natl. Acad. Sci. U.S.A.* 107, 8434–8439. doi: 10.1073/pnas.0912690107

Kokoeva, M. V., Yin, H., and Flier, J. S. (2005). Neurogenesis in the hypothalamus of adult mice: potential role in energy balance. *Science* 310, 679–683. doi: 10.1126/science.1115360

Krakauer, J. W. (2006). Motor learning: its relevance to stroke recovery and neurorehabilitation. *Curr. Opin. Neurol.* 19, 84–90. doi: 10.1097/01.wco.0000200544.29915.cc

Krakauer, J. W., and Mazzoni, P. (2011). Human sensorimotor learning: adaptation, skill, and beyond. *Curr. Opin. Neurobiol.* 21, 636–644. doi: 10.1016/j.conb.2011.06.012

Li, B., Zhang, S., Zhang, H., Hertz, L., and Peng, L. (2011). Fluoxetine affects GluK2 editing, glutamate-evoked Ca^{2+} influx and extracellular signal-regulated kinase phosphorylation in mouse astrocytes. *J. Psychiatry Neurosci.* 36, 322–338. doi: 10.1503/jpn.100094

Liepert, J., Hamzei, F., and Weiller, C. (2000). Motor cortex disinhibition of the unaffected hemisphere after acute stroke. *Muscle Nerve* 23, 1761–1763. doi: 10.1002/1097-4598(200011)23:11<1761::AID-MUS14>3.0.CO;2-M

Lim, C.-M., Kim, S.-W., Park, J.-Y., Kim, C., Yoon, S. H., and Lee, J.-K. (2009). Fluoxetine affords robust neuroprotection in the postischemic brain via its anti-inflammatory effect. *J. Neurosci. Res.* 87, 1037–1045. doi: 10.1002/jnr.21899

Lindenberg, R., Renga, V., Zhu, L. L., Nair, D., and Schlaug, G. (2010). Bihemispheric brain stimulation facilitates motor recovery in chronic stroke patients. *Neurology* 75, 2176–2184. doi: 10.1212/WNL.0b013e318202013a

Loubinoux, I., Tombari, D., Pariente, J., Gerdelat-Mas, A., Franceries, X., Cassol, E., et al. (2005). Modulation of behavior and cortical motor activity in healthy subjects by a chronic administration of a serotonin enhancer. *Neuroimage* 27, 299–313. doi: 10.1016/j.neuroimage.2004.12.023

Lovatt, D., Sonnewald, U., Waagepetersen, H. S., Schousboe, A., He, W., Lin, J. H.-C., et al. (2007). The transcriptome and metabolic gene signature of protoplasmic astrocytes in the adult murine cortex. *J. Neurosci.* 27, 12255–12266. doi: 10.1523/JNEUROSCI.3404-07.2007

Lynch, M. A. (2004). Long-term potentiation and memory. *Physiol. Rev.* 84, 87–136. doi: 10.1152/physrev.00014.2003

Mantovani, A., Pavlicova, M., Avery, D., Nahas, Z., McDonald, W. M., Wajdik, C. D., et al. (2012). Long-term efficacy of repeated daily prefrontal transcranial magnetic stimulation (TMS) in treatment-resistant depression. *Depress. Anxiety* 29, 883–890. doi: 10.1002/da.21967

Matsumoto, K., Puia, G., Dong, E., and Pinna, G. (2007). GABA(A) receptor neurotransmission dysfunction in a mouse model of social isolation-induced stress: possible insights into a non-serotonergic mechanism of action of SSRIs in mood and anxiety disorders. *Stress* 10, 3–12. doi: 10.1080/10253890701200997

Mead, G. E., Hsieh, C.-F., Lee, R., Kutlubaev, M., Claxton, A., Hankey, G. J., et al. (2013). Selective serotonin reuptake inhibitors for stroke recovery: a systematic review and meta-analysis. *Stroke* 44, 844–850. doi: 10.1161/STROKEAHA.112.673947

Meintzschel, F., and Ziemann, U. (2006). Modification of practice-dependent plasticity in human motor cortex by neuromodulators. *Cereb. Cortex* 16, 1106–1115. doi: 10.1093/cercor/bhj052

Mozaffarian, D., Benjamin, E. J., Go, A. S., Arnett, D. K., Blaha, M. J., Cushman, M., et al. (2016). Heart disease and stroke statistics-2016 update a report from the American heart association. *Circulation* 133, e38–e48. doi: 10.1161/CIR.0000000000000366

Murase, N., Duque, J., Mazzocchio, R., and Cohen, L. G. (2004). Influence of interhemispheric interactions on motor function in chronic stroke. *Ann. Neurol.* 55, 400–409. doi: 10.1002/ana.10848

Netz, J., Lammers, T., and Hömberg, V. (1997). Reorganization of motor output in the non-affected hemisphere after stroke. *Brain* 120, 1579–1586. doi: 10.1093/brain/120.9.1579

Nudo, R. J. (2013). Recovery after brain injury: mechanisms and principles. *Front. Hum. Neurosci.* 7:887. doi: 10.3389/fnhum.2013.00887

Nudo, R. J., Milliken, G. W., Jenkins, W. M., and Merzenich, M. M. (1996). Use-dependent alterations of movement representations in primary motor cortex of adult squirrel monkeys. *J. Neurosci.* 16, 785–807.

Oh, B.-M., Kim, D.-Y., and Paik, N.-J. (2010). Disinhibition in the unaffected hemisphere is related with the cortical involvement of the affected hemisphere. *Int. J. Neurosci.* 120, 512–515. doi: 10.3109/00207451003760114

Ohira, K., Takeuchi, R., Iwanaga, T., and Miyakawa, T. (2013a). Chronic fluoxetine treatment reduces parvalbumin expression and perineuronal nets in gamma-aminobutyric acidergic interneurons of the frontal cortex in adult mice. *Mol. Brain* 6:43. doi: 10.1186/1756-6606-6-43

Ohira, K., Takeuchi, R., Shoji, H., and Miyakawa, T. (2013b). Fluoxetine-induced cortical adult neurogenesis. *Neuropsychopharmacology* 38, 909–920. doi: 10.1038/npp.2013.2

Pariente, J., Loubinoux, I., Carel, C., Albucher, J. F., Leger, A., Manelfe, C., et al. (2001). Fluoxetine modulates motor performance and cerebral activation of patients recovering from stroke. *Ann. Neurol.* 50, 718–729. doi: 10.1002/ana.1257

Park, C. H., Chang, W. H., Ohn, S. H., Kim, S. T., Bang, O. Y., Pascual-Leone, A., et al. (2011). Longitudinal changes of resting-state functional connectivity during motor recovery after stroke. *Stroke* 42, 1357–1362. doi: 10.1161/STROKEAHA.110.596155

Peng, L., Gu, L., Li, B., and Hertz, L. (2014). Fluoxetine and all other SSRIs are 5-HT2B agonists - importance for their therapeutic effects. *Curr. Neuropharmacol.* 12, 365–379. doi: 10.2174/1570159X12666140828221720

Pfurtscheller, G., and Lopes da Silva, F. H. (2017). Event-related EEG/MEG synchronization and desynchronization: basic principles. *Clin. Neurophysiol.* 110, 1842–1857. doi: 10.1016/S1388-2457(99)00141-8

Pfurtscheller, G., Neuper, C., Brunner, C., and Lopes Da Silva, F. (2005). Beta rebound after different types of motor imagery in man. *Neurosci. Lett.* 378, 156–159. doi: 10.1016/j.neulet.2004.12.034

Reynolds, C., and Ashby, P. (1999). Inhibition in the human motor cortex is reduced just before a voluntary contraction. *Neurology* 53, 730–735. doi: 10.1212/WNL.53.4.730

Rieckmann, N., and Kronish, I. (2013). Serotonin reuptake inhibitor use, depression, and long-term outcomes after an acute coronary syndrome: a prospective cohort study. *JAMA Intern. Med.* 173, 1150–1151. doi: 10.1001/jamainternmed.2013.910

Rief, W., Barsky, A. J., Bingel, U., Doering, B. K., Schwarting, R., Wöhr, M., et al. (2016). Rethinking psychopharmacotherapy: the role of treatment context and brain plasticity in antidepressant and antipsychotic interventions. *Neurosci. Biobehav. Rev.* 60, 51–64. doi: 10.1016/j.neubiorev.2015.11.008

Robinson, R. T., Drafts, B. C., and Fisher, J. L. (2003). Fluoxetine increases GABAA receptor activity through a novel modulatory site. *J. Pharmacol. Exp. Ther.* 304, 978–984. doi: 10.1124/jpet.102.044834

Robol, E., Fiaschi, A., and Manganotti, P. (2004). Effects of citalopram on the excitability of the human motor cortex: a paired magnetic stimulation study. *J. Neurol. Sci.* 221, 41–46. doi: 10.1016/j.jns.2004.03.007

Rosenstein, J. M., Mani, N., Silverman, W. F., and Krum, J. M. (1998). Patterns of brain angiogenesis after vascular endothelial growth factor administration *in vitro* and *in vivo*. *Proc. Natl. Acad. Sci. U.S.A.* 95, 7086–7091.

Rossi, S., Hallett, M., Rossini, P. M., and Pascual-Leone, A. (2009). Safety, ethical considerations, and application guidelines for the use of transcranial magnetic stimulation in clinical practice and research. *Clin. Neurophysiol.* 120, 2008–2039. doi: 10.1016/j.clinph.2009.08.016

Sanacora, G., Mason, G. F., Rothman, D. L., and Krystal, J. H. (2002). Increased occipital cortex GABA concentrations in depressed patients after therapy with selective serotonin reuptake inhibitors. *Am. J. Psychiatry* 159, 663–665. doi: 10.1176/appi.ajp.159.4.663

Sato, S., Bergmann, T. O., and Borich, M. R. (2015). Opportunities for concurrent transcranial magnetic stimulation and electroencephalography to characterize cortical activity in stroke. *Front. Hum. Neurosci.* 9:250. doi: 10.3389/fnhum.2015.00250

Sawaki, L., Boroojerdi, B., Kaelin-Lang, A., Burstein, A. H., Bütefisch, C. M., Kopylev, L., et al. (2002a). Cholinergic influences on use-dependent plasticity. *J. Neurophysiol.* 87, 166–171. doi: 10.1152/jn.00279.2001

Sawaki, L., Cohen, L. G., Classen, J., Davis, B. C., and Butefisch, C. M. (2002b). Enhancement of use-dependent plasticity by D-amphetamine 7446. *Neurology* 59, 1262–1264. doi: 10.1212/WNL.59.8.1262

Scheidtmann, K., Fries, W., Müller, F., and Koenig, E. (2001). Effect of levodopa in combination with physiotherapy on functional motor recovery after stroke: a prospective, randomised, double-blind study. *Lancet* 358, 787–790. doi: 10.1016/S0140-6736(01)05966-9

Schiene, K., Bruehl, C., Zilles, K., Qü, M., Hagemann, G., Kraemer, M., et al. (1996). Neuronal hyperexcitability and reduction of GABAA-receptor expression in the surround of cerebral photothrombosis. *J. Cereb. Blood Flow Metab.* 16, 906–914. doi: 10.1097/00004647-199609000-00014

Serrats, J., Mengod, G., and Cortés, R. (2005). Expression of serotonin 5-HT2C receptors in GABAergic cells of the anterior raphe nuclei. *J. Chem. Neuroanat.* 29, 83–91. doi: 10.1016/j.jchemneu.2004.03.010

Shadmehr, R., and Holcomb, H. H. (1997). Neural correlates of motor memory consolidation. *Science* 277, 821–825. doi: 10.1126/science.277.5327.821

Shin, T. K., Kang, M. S., Lee, H. Y., Seo, M. S., Kim, S. G., Kim, C. D., et al. (2009). Fluoxetine and sertraline attenuate postischemic brain injury in mice. *Korean J. Physiol. Pharmacol.* 13, 257–263. doi: 10.4196/kjpp.2009.13.3.257

Siepmann, T., Penzlin, A. I., Kepplinger, J., Illigens, B. M., Weidner, K., Reichmann, H., et al. (2015). Selective serotonin reuptake inhibitors to improve outcome in acute ischemic stroke: possible mechanisms and clinical evidence. *Brain Behav.* 5:e00373. doi: 10.1002/brb3.373

Stagg, C. J. (2013). Magnetic Resonance Spectroscopy as a tool to study the role of GABA in motor-cortical plasticity. *Neuroimage* 86, 19–27. doi: 10.1016/j.neuroimage.2013.01.009

Stagg, C. J., Bachtiar, V., and Johansen-Berg, H. (2011). The role of GABA in human motor learning. *Curr. Biol.* 21, 480–484. doi: 10.1016/j.cub.2011.01.069

Stahl, S. M. (2017). Mechanism of action of serotonin selective reuptake inhibitors. *J. Affect. Disord.* 51, 215–235. doi: 10.1016/S0165-0327(98)00221-3

Steinman, M. Q., Gao, V., and Alberini, C. M. (2016). The role of lactate-mediated metabolic coupling between astrocytes and neurons in long-term memory formation. *Front. Integr. Neurosci.* 10:10. doi: 10.3389/fnint.2016.00010

Sun, Y., Jin, K., Xie, L., Childs, J., Mao, X. O., Logvinova, A., et al. (2003). VEGF-induced neuroprotection, neurogenesis, and angiogenesis after focal cerebral ischemia. *J. Clin. Invest.* 111, 1843–1851. doi: 10.1172/JCI200317977

Swayne, O. B., Rothwell, J. C., Ward, N. S., and Greenwood, R. J. (2008). Stages of motor output reorganization after hemispheric stroke suggested by longitudinal studies of cortical physiology. *Cereb. Cortex* 18, 1909–1922. doi: 10.1093/cercor/bhm218

Takeuchi, N., and Izumi, S.-I. (2012). Maladaptive plasticity for motor recovery after stroke: mechanisms and approaches. *Neural Plast.* 2012:359728. doi: 10.1155/2012/359728

Takeuchi, N., Tada, T., Chuma, T., Matsuo, Y., and Ikoma, K. (2007). Disinhibition of the premotor cortex contributes to a maladaptive change in the affected hand after stroke. *Stroke* 38, 1551–1556. doi: 10.1161/STROKEAHA.106.470187

Talelli, P., Greenwood, R. J., and Rothwell, J. C. (2006). Arm function after stroke: neurophysiological correlates and recovery mechanisms assessed by transcranial magnetic stimulation. *Clin. Neurophysiol.* 117, 1641–1659. doi: 10.1016/j.clinph.2006.01.016

Trevelyan, A. J. (2016). Do cortical circuits need protecting from themselves? *Trends Neurosci.* 39, 502–511. doi: 10.1016/j.tins.2016.06.002

Tunnicliff, G., Schindler, N. L., Crites, G. J., Goldenberg, R., Yochum, A., and Malatynska, E. (1999). The GABA(A) receptor complex as a target for fluoxetine action. *Neurochem. Res.* 24, 1271–1276. doi: 10.1023/A:1020977123968

Turton, A., Wroe, S., Trepte, N., Fraser, C., and Lemon, R. N. (1996). Contralateral and ipsilateral EMG responses to transcranial magnetic stimulation during recovery of arm and hand function after stroke. *Electroencephalogr. Clin. Neurophysiol. Electromyogr. Mot. Control* 101, 316–328. doi: 10.1016/0924-980X(96)95560-5

Urban, E. T., Bury, S. D., Barbay, H. S., Guggenmos, D. J., Dong, Y., and Nudo, R. J. (2012). Gene expression changes of interconnected spared cortical neurons 7 days after ischemic infarct of the primary motor cortex in the rat. *Mol. Cell. Biochem.* 369, 267–286. doi: 10.1007/s11010-012-1390-z

Veerbeek, J. M., van Wegen, E., van Peppen, R., van der Wees, P. J., Hendriks, E., Rietberg, M., et al. (2014). What is the evidence for physical therapy poststroke? a systematic review and meta-analysis. *PLoS ONE* 9:e87987. doi: 10.1371/journal.pone.0087987

Werhahn, K. J., Conforto, A. B., Kadom, N., Hallett, M., and Cohen, L. G. (2003). Contribution of the ipsilateral motor cortex to recovery after chronic stroke. *Ann. Neurol.* 54, 464–472. doi: 10.1002/ana.10686

Winstein, C. J., Stein, J., Arena, R., Bates, B., Cherney, L. R., Cramer, S. C., et al. (2016). Guidelines for adult stroke rehabilitation and recovery: a guideline for healthcare professionals from the american heart association/american stroke association. *Stroke* 47, e98–e169. doi: 10.1161/STR.0000000000000098

Ye, Z. Y., Zhou, K. Q., Xu, T., Le, and Zhou, J. N. (2008). Fluoxetine potentiates GABAergic IPSCs in rat hippocampal neurons. *Neurosci. Lett.* 442, 24–29. doi: 10.1016/j.neulet.2008.06.072

Zaaroor, M., Pratt, H., and Starr, A. (2003). Time course of motor excitability before and after a task-related movement. *Neurophysiol. Clin. Neurophysiol.* 33, 130–137. doi: 10.1016/S0987-7053(03)00029-7

Zittel, S., Weiller, C., and Liepert, J. (2008). Citalopram improves dexterity in chronic stroke patients. *Neurorehabil. Neural Repair* 22, 311–314. doi: 10.1177/1545968307312173

Conflict of Interest Statement: The authors declare that the research was conducted in the absence of any commercial or financial relationships that could be construed as a potential conflict of interest.

frontiers in Neuroscience

REVIEW
published: 25 July 2017
doi: 10.3389/fnins.2017.00423

Therapeutic Use of Non-invasive Brain Stimulation in Dystonia

Angelo Quartarone[1,2], Vincenzo Rizzo[3], Carmen Terranova[3], Alberto Cacciola[2], Demetrio Milardi[1,2], Alessandro Calamuneri[1], Gaetana Chillemi[3] and Paolo Girlanda[3]*

[1] Department of Biomedical, Dental Sciences and Morphological and Functional Images, University of Messina, Messina, Italy, [2] Centro Neurolesi Bonino Pulejo (IRCCS), Messina, Italy, [3] Department of Clinical and Experimental Medicine, University of Messina, Messina, Italy

Repetitive transcranial magnetic stimulation (rTMS) and transcranial direct current stimulation (tDCS) are non-invasive methods for stimulating cortical neurons that have been increasingly used in the neurology realm and in the neurosciences applied to movement disorders. In addition, these tools have the potential to be delivered as clinically therapeutic approach. Despite several studies support this hypothesis, there are several limitations related to the extreme variability of the stimulation protocols, clinical enrolment and variability of rTMS and tDCS after effects that make clinical interpretation very difficult. Aim of the present study will be to critically discuss the state of art therapeutically applications of rTMS and tDCS in dystonia.

Keywords: dystonia, neuroplasticity, transcranial magnetic stimulation, basal ganglia, non-invasive brain stimulation

OPEN ACCESS

Edited by:
Takashi Hanakawa, National Center of Neurology and Psychiatry, Japan

Reviewed by:
Shinichi Furuya, Sony Computer Science Laboratories, Japan
Christian K. E. Moll, University Medical Center Hamburg-Eppendorf, Germany

****Correspondence:***
Angelo Quartarone
aquartar65@gmail.com

Specialty section:
This article was submitted to Neural Technology, a section of the journal Frontiers in Neuroscience

Received: *10 May 2017*
Accepted: *06 July 2017*
Published: *25 July 2017*

Citation:
Quartarone A, Rizzo V, Terranova C, Cacciola A, Milardi D, Calamuneri A, Chillemi G and Girlanda P (2017) Therapeutic Use of Non-invasive Brain Stimulation in Dystonia. Front. Neurosci. 11:423. doi: 10.3389/fnins.2017.00423

INTRODUCTION

Dystonia can be defined as a "movement disorder characterized by sustained or intermittent muscle contractions causing abnormal, often repetitive, movements, postures, or both" (Albanese et al., 2013).

Dystonia encompasses a heterogeneous group of syndromes that can be classified per the anatomical distribution in: focal, segmental, multifocal, hemidystonia, and generalized dystonia.

In addition, according to the etiology, dystonia can be categorized in inherited (i.e., autosomal dominant, recessive, X-linked, or mitochondrial), acquired (i.e., vascular, iatrogenic, neoplastic, traumatic, or psychogenic) and idiopathic (sporadic or familiar) (Albanese et al., 2013).

The pathophysiology of dystonia remains highly speculative although clinical heterogeneity suggests that it may be a multifactorial disease.

The paucity of symptomatic animal models is one of the reason why dystonia pathophysiology remains largely obscure (Raike et al., 2005).

Recent developed symptomatic animal models have also established the critical role of the cerebellum in dystonia, suggesting that basal ganglia and cerebellum are nodes in an integrated network that is dysfunctional in dystonia (Wilson and Hess, 2013; Richter and Richter, 2014; Pappas et al., 2015). Dystonia treatment can only partially alleviate symptoms and mainly relies on the injection of botulinum toxin in the hyperactive muscles, while the use of levodopa, anticholinergic and antiepileptic drugs has been proven to be largely ineffective (Albanese et al., 2015).

Deep brain stimulation (DBS) of the internal portion of globus pallidus (GPi) is the gold-standard of functional neurosurgical interventions for dystonia in the most severe patients and there are several evidences providing its efficacy and safety (Moro et al., 2017). On the other hand, it remains an invasive procedure so that alternative treatments are needed (Albanese et al., 2015).

In the last few years, gamma-knife and focused ultrasound lesions, which do not require surgical incision of the skull, have challenged the routine application of both the classic radiofrequency lesions and DBS. However, the application of dystonia is very limited (Higuchi et al., 2016).

Finally, transcranial magnetic stimulation (TMS) has been used in the last 20 years to explore non-invasively cortical excitability, shedding also important new insights into the pathophysiology of dystonia (Quartarone and Hallett, 2013).

In addition, TMS is a valuable technique that can be potentially used for diagnostic and therapeutic purposes in dystonia. However, the inter-subject variability in the TMS after-effects and the different pathophysiological mechanisms in the different form of dystonia, have limited diagnostic and therapeutic applications. Nevertheless, TMS can be used to differentiate between organic and psychogenic dystonia (Quartarone et al., 2009).

TMS has been proposed as noninvasive treatment in focal hand dystonia, where pharmacological options or injections of botulinum toxin are often ineffective. Finally, TMS can be considered as an adjuvant treatment in patients with cervical dystonia in conjunction with botulinum remaining the gold standard of treatment.

Hence in the present narrative review, we will describe how TMS can be used as therapeutic tool in dystonia in comparison with other noninvasive brain techniques such as transcranial direct current stimulation (tDCS).

NON-INVASIVE BRAIN STIMULATION TECHNIQUES

TMS and tDCS can stimulate the cerebral cortex painlessly through the intact skull and can produce long lasting changes in cortical excitability.

TMS was originally conceived as a non-invasive method to test the efficiency of motor pathways from the cortex to spinal cord (Rothwell, 1997).

Several experimental evidences suggest that TMS activates axons of the excitatory and inhibitory interneurons that synapse into pyramidal output neurons. In this way, the responsiveness to TMS may represent an indirect measure of the excitability of intrinsic cortical circuits. TMS can also produce long lasting changes in cortical excitability when the pulses are delivered in a repetitive fashion (Siebner and Rothwell, 2003).

Several protocols of non-invasive brain stimulation (NIBS) have been used in the last 20 years, the most common of whom are: repetitive TMS (rTMS), theta-burst stimulation (TBS) and tDCS. In all these cases, electromyography (EMG) amplitude of the motor evoked potentials (MEP) in response to single TMS stimulus is used as read out of the induced cortical plasticity.

The after effects of rTMS depend on the frequency of stimulation employed: if the pulses are given at frequency of 5 Hz or higher they facilitate excitability, whereas at frequency of 1 Hz, or lower, they depress excitability for at least 30–60 min (Quartarone et al., 2006). Thetaburst stimulation (TBS) is a protocol translated from animal studies characterized by repetitive sequences where short bursts are applied in the frequency range of EEG theta rhythms.

There are two main protocols i) the intermittent TBS (iTBS) which has facilitatory effects and ii) the continuous TBS (cTBS) which instead produces inhibitory effects. Their effect can be long lasting, up to 1 h, after the end of the conditioning protocol (Huang et al., 2005).

tDCS takes advantage of a weak polarizing direct current (1–2 mA) applied via small electrodes on the intact scalp. Several experimental evidences suggest that this small current is sufficient to polarize neurons changing their firing frequency. Anodal stimulation tends to increase cortical excitability while cathodal tends to decrease it (Nitsche and Paulus, 2001).

NIBS has been used to explore therapeutic opportunities in a bewildering variety of neurological conditions. It is now clear that, in order to get more tangible clinical effects, repeated rTMS sessions are needed (Khedr et al., 2005).

The mechanisms of action of TMS responsible for the long-lasting effects on cortical excitability are still sketchy. Changes in the effectiveness of synapses between cortical neurons such as long term depression (LTD) and long term potentiation (LTP) have been postulated based on pharmacological studies in humans. Indeed, the after effects of rTMS are abolished by a single dose of the NMDA antagonist dextromethorphan (Stefan et al., 2002). Similarly, another NMDA-antagonist, the memantine can block the after effects of some rTMS protocols (Huang et al., 2007). In addition the LTD-like depression produced by PAS10 is abolished by nimodipine, an L-type voltage-gated-Ca^{2+}-channel blocker (Weise et al., 2017). Finally, several evidences suggest that TMS modulation of BDNF-TrkB pathway could play a permissive role in determining the NMDA dependent after-effects on synaptic plasticity (Wang et al., 2011).

PATHOPHYSIOLOGY OF DYSTONIA AND THERAPEUTIC NIBS

Since dystonia etiology is very heterogeneous, dystonia pathophysiology can be a very complex puzzle (Marsden et al., 1985).

Despite the basal ganglia have been traditionally involved in dystonia, several evidences in animal models and in humans studies suggest that dystonia can be considered a network disorder (Quartarone and Hallett, 2013).

However, although it is tempting to locate the neuronal damage to a single node of the cortico-sub-cortical loop, there are now compelling evidences suggesting that, in a network perspective, it is also important to consider how remote healthy nodes of the brain may react and rearrange themselves in response to the primary damage. Such plastic reorganization may be either adaptive, compensatory, or maladaptive thus worsening the deficit (Quartarone and Hallett, 2013).

In keeping with this hypothesis, increased glucose metabolism over the striatum and anatomically related cortical motor regions such as supplementary motor area (SMA), lateral premotor cortex (PMC), anterior cingulate cortex (ACC) and dorsolateral

prefrontal cortex (DLPCF) have been reported (Lerner et al., 2004; Asanuma et al., 2005).

However, several evidences suggest also an involvement of the cerebellar cortex and its direct connections with the basal ganglia and the motor cortex (Neumann et al., 2015; Cacciola et al., 2016, 2017; Milardi et al., 2016). This hypothesis is also supported by some neurophysiological data showing an abnormal cerebellar modulation over motor cortex in dystonic patients (Brighina et al., 2009).

Since dystonic patients have not overt cerebellar signs such as incoordination, loss of balance or falling, it has been postulated a compensative role of cerebellum thus pointing it out as a good candidate for therapeutic neuromodulation.

THERAPEUTIC APPROACHES IN DYSTONIA: STATE OF ART

In keeping with the pathophysiological considerations discussed above, NIBS has been applied over primary motor cortex (M1), PMC, ACC and the cerebellar cortex which are important relays of the cortico-striatal and cerebello-thalamic loops.

Since TMS affects the superficial layers of the cerebral cortex it is unlikely that it may stimulate directly basal ganglia structures. On the other hand, it has been demonstrated that rTMS over the human PFC may exert remote effects on the ipsilateral caudate nucleus via a cortico-striatal release of dopamine (Strafella et al., 2001). In addition rTMS over M1 induces a reduction in raclopride binding in the left putamen if compared with rTMS of the left occipital cortex (Strafella et al., 2003).

Therefore, it can be hypothesized that some of the potential therapeutic action in movement disorders are mediated by remote sub-cortical effects.

One possible strategy in dystonia is an increase of inhibitory mechanisms. In keeping with this hypothesis, it has been reported that 30 min of inhibitory low frequency stimulation over M1 may reduce writing pressure for at least 3 h in patients with focal hand dystonia (FHD) (Siebner et al., 1999).

Similarly, 1 Hz rTMS over PMC improved handwriting velocity and hand discomfort during writing (Tyvaert et al., 2006). In addition, the effect of rTMS was compared in three different motor areas including PMC in patients with FHD. This study revealed that rTMS (20 min 0.2 Hz rTMS) over PMC is more effective than M1 and SMA repetitive stimulation (Murase et al., 2005). The clinical effects were paralleled by increased cortical inhibition as indexed by a prolonged cortical silent period (Murase et al., 2005). In the same study the authors did not report any therapeutic effect of rTMS over M1 (Murase et al., 2005); the discrepancy with the study of Siebner could be due to the different parameters of stimulation (Siebner et al., 1999).

A similar beneficial effect was obtained in a subsequent study employing cTBS over the left PMC which however did not restore deficient inhibitory mechanisms (Veugen et al., 2013).

The beneficial effects of PMC stimulation are in keeping with an open trial of epidural PMC stimulation after at least 1 month of stimulation (Lalli et al., 2012).

Another study has used rTMS over PMC (Lefaucheur et al., 2004), however the lack of a placebo arm makes the interpretation of data very difficult. In this study the authors applied inhibitory rTMS over PMC for 5 consecutive days in patients with generalized secondary dystonia showing a significant clinical effect as indexed by the reduction of the Burke-Fahn-Marsden scale (Lefaucheur et al., 2004).

It is interesting to note that the parameters of cortical excitability, tested with TMS, can be used as prognostic markers of response to rTMS. For instance, it has been reported that only patients with a modulation of cortical inhibition do respond to rTMS treatment (Kimberley et al., 2015).

Altogether, these data suggest a potential therapeutic role of rTMS over PMC. The efficacy of PMC neuromodulation is not surprising considering that PMC is implicated in sensory-motor integration and motor learning.

Another potential target of stimulation is the somatosensory cortex (SCC). It has been indeed shown that 5 Hz rTMS may enhance tactile discrimination in healthy subjects (Ragert et al., 2003). In addition, it has been widely reported that patients with FHD have significant alterations of sensory-motor integration (Quartarone et al., 2003) as well as distortion of the fingers representation map in SCC (Butterworth et al., 2003).

High frequency stimulation over SCC is not beneficial in FHD, with no effect on tactile discrimination in comparison to controls (Schneider et al., 2010). In addition, it is interesting to note that the improvement of tactile discrimination in healthy controls after rTMS, was associated with an increased connectivity in the stimulated SCC, bilateral PMC and basal ganglia, which was not the case in FHD. Therefore, it can be postulated that a cortical-subcortical disconnection may be the basis of the ineffectiveness of rTMS (Schneider et al., 2010).

In another placebo controlled study, low frequency 1 Hz stimulation was delivered over SCC 30 min per day for 4 consecutive weeks in 15 patients affected by writer's cramp (Havrankova et al., 2010). The procedure was successful only in 4 out of 15 patients and was strictly related to the precise coil localization of a narrow strip over the post central sulcus (Havrankova et al., 2010).

ACC has been used as another potential target since this area has an increased activation with PET studies in patients with blepharospasm (Ceballos-Baumann and Brooks, 1998; Kerrison et al., 2003). Low frequency stimulation (0.2 Hz), delivered in a randomized controlled study, can significantly reduce eye blink rate, the number of sustained blinks and the time to eye closure (Kranz et al., 2009). This clinical effects was associated with a normalization of the blink recovery cycle (Kranz et al., 2010).

A new appealing target for NIBS is cerebellum since several evidences suggest that the cerebellum may play a compensatory role in dystonia (Jinnah and Hess, 2006; Quartarone and Hallett, 2013).

In a randomized controlled study, iTBS was delivered bilaterally over the cerebellum for 5 consecutive days for 2 weeks in 20 right handed patients affected by cervical dystonia.

This protocol induced a transient improvement of dystonia and was paralleled by a restoration of the topographic specificity

of PAS with a disappearance of the facilitation on Fist Dorsal Interosseus (FDI) (Koch et al., 2014).

On the other hand, tDCS has brought conflicting results, in one study tDCS over the cerebellum was successful in FHD (Bradnam et al., 2015), while in other study it did not work (Sadnicka et al., 2014).

Similarly cathodal tDCS tested over M1 in a randomized double blind sham-controlled study was not successful in a population of writer's cramp patients and musicians cramp (Benninger et al., 2011; Buttkus et al., 2011).

Finally, since there is an enhanced sensory-motor integration, another feasible strategy is to provide independent inputs from dystonic muscles via an asynchronous afferent stimulation avoiding any temporal coupling of the evoked afferent inputs (Schabrun et al., 2009).

The idea is that a period of asynchronous afferent stimulation or non-associative stimulation (NAS) may reverse maladaptive cortical changes and alleviate symptoms.

By using a NAS protocol consisting of asynchronous electrical stimuli (never delivered together with a random inter-stimulus interval ranging from 0.15 to 2.85 as well as with stimulus intensity set to evoke a tiny muscle contraction) applied to the motor points of FDI and abductor pollicis brevis (APB) for 1 h, it has been demonstrated in FHD patients that NAS transiently normalizes the distorted motor map and can significantly reduce movement variability during cycling drawing (Schabrun et al., 2009).

LIMITATIONS AND FUTURE PERSPECTIVES

There are several factors that that strongly limit the interpretation of results after rTMS studies.

Perhaps the most important limitation is the lack of an optimal placebo condition, the so called sham condition. In theory, tilting the coil should dramatically reduce the biological effects of TMS, however several modeling studies in animals are now suggesting that tilting the coil over the skull does not exclude the possibility of a tiny cortical activation (Lisanby et al., 2001).

On the other hand, by using shield equipped coils and a tilt of 90 degrees it is possible to minimize the effective magnetic field (Duecker and Sack, 2013).

Another not risible issue is that active rTMS, besides its cortical effects, is associated with a characteristic click sound and a stimulation of trigeminal afferents. Therefore, to mimic click sound and trigeminal stimulation new dedicated sham shielded coils have been designed with a delivered magnetic field of only 10% compared to active coils.

Another limitation is that most of the studies have addressed primary dystonia while the therapeutic effect of NIBS in secondary dystonia is still unknown.

Despite therapeutic cerebellar stimulation is promising, the gold standard in dystonia is targeting the motor areas strictly connected with basal ganglia (Bharath et al., 2015).

The major limitation of all these studies are the small sample size, the presence of different phenotypes in the same cohort of patients, as well as the fact that several different parameters of stimulation have been adopted across studies.

Despite this extreme variability, it looks like that to be successful NIBS needs to be delivered in a multisession design. Some single session studies have shown positive results that however were not persistent (Murase et al., 2005; Furuya et al., 2014).

There are other possible confounding factors such as preliminary exercise, time of the day and concomitant medications (Ridding and Ziemann, 2010).

Finally, in most studies, stimulation was not performed under neuronavigation to maintain an adequate coil position during stimulation sessions.

Nevertheless, these preliminary results reinforce the idea that NIBS can represent a promising alternative therapeutic opportunity in dystonia.

Several recommendations could be considered in future therapeutic trials: first, it will be important in future studies to determine the best stimulation target, second to use multisession designs with neuronavigation and finally to increase the sample size with multicenter approaches. Another requirement is to design more efficient stimulation protocols to prolong the therapeutic effects. Last but not list, rTMS could be used, soon, to pre-select possible candidates to invasive surgical stimulation approaches.

AUTHOR CONTRIBUTIONS

AQ: work conception and design, drafting the work, work revision, final approval, and global agreement. VR: data interpretation, work revision, final approval, and global agreement. CT, AlbC, DM, AleC: work conception and design, work revision, final approval, GC: data interpretation, drafting the work. PG: work conception and design, guarantor of integrity of entire study, manuscript revision for important intellectual content, final approval.

REFERENCES

Albanese, A., Bhatia, K., Bressman, S. B., Delong, M. R., Fahn, S., Fung, V. S. C., et al. (2013). Phenomenology and classification of dystonia: a consensus update. *Mov. Disord.* 28, 863–873. doi: 10.1002/mds.25475

Albanese, A., Romito, L. M., and Calandrella, D. (2015). Therapeutic advances in dystonia. *Mov. Disord.* 30, 1547–1556. doi: 10.1002/mds.26384

Asanuma, K., Carbon-Correll, M., and Eidelberg, D. (2005). Neuroimaging in human dystonia. *J. Med. Invest.* 52 (Suppl.), 272–279. doi: 10.2152/jmi.52.272

Benninger, D. H., Lomarev, M., Lopez, G., Pal, N., Luckenbaugh, D. A., and Hallett, M. (2011). Transcranial direct current stimulation for the treatment of focal hand dystonia. *Mov. Disord.* 26, 1698–1702. doi: 10.1002/mds.23691

Bharath, R. D., Munivenkatappa, A., Gohel, S., Panda, R., Saini, J., Rajeswaran, J., et al. (2015). Recovery of resting brain connectivity ensuing mild traumatic brain injury. *Front. Hum. Neurosci.* 9:513. doi: 10.3389/fnhum.2015.00513

Bradnam, L. V., Graetz, L. J., McDonnell, M. N., and Ridding, M. C. (2015). Anodal transcranial direct current stimulation to the cerebellum improves handwriting

and cyclic drawing kinematics in focal hand dystonia. *Front. Hum. Neurosci.* 9:286. doi: 10.3389/fnhum.2015.00286

Brighina, F., Romano, M., Giglia, G., Saia, V., Puma, A., Giglia, F., et al. (2009). Effects of cerebellar TMS on motor cortex of patients with focal dystonia: a preliminary report. *Exp. Brain Res.* 192, 651–656. doi: 10.1007/s00221-008-1572-9

Butterworth, S., Francis, S., Kelly, E., McGlone, F., Bowtell, R., and Sawle, G. V. (2003). Abnormal cortical sensory activation in dystonia: An fMRI study. *Mov. Disord.* 18, 673–682. doi: 10.1002/mds.10416

Buttkus, F., Baur, V., Jabusch, H. C., De La Cruz Gomez-Pellin, M., Paulus, W., Nitsche, M. A., et al. (2011). Single-session tDCS-supported retraining does not improve fine motor control in musician's dystonia. *Restor. Neurol. Neurosci.* 29, 85–90. doi: 10.3233/RNN-2011-0582

Cacciola, A., Milardi, D., Livrea, P., Flace, P., Anastasi, G., and Quartarone, A. (2017). The Known and Missing Links Between the Cerebellum, Basal Ganglia, and Cerebral Cortex. *Cerebellum* 16, 753–755. doi: 10.1007/s12311-017-0850-0

Cacciola, A., Milardi, D., and Quartarone, A. (2016). Role of cortico-pallidal connectivity in the pathophysiology of dystonia. *Brain* 139:e48. doi: 10.1093/brain/aww102

Ceballos-Baumann, A. O., and Brooks, D. J. (1998). Activation positron emission tomography scanning in dystonia. *Adv. Neurol.* 78, 135–152.

Duecker, F., and Sack, A. T. (2013). Pre-Stimulus Sham TMS Facilitates Target Detection. *PLoS ONE* 8:e57765. doi: 10.1371/journal.pone.0057765

Furuya, S., Nitsche, M. A., Paulus, W., and Altenmüller, E. (2014). Surmounting retraining limits in Musicians' dystonia by transcranial stimulation. *Ann. Neurol.* 75, 700–707. doi: 10.1002/ana.24151

Havrankova, P., Jech, R., Walker, N. D., Operto, G., Tauchmanova, J., Vymazal, J., et al. (2010). Repetitive TMS of the somatosensory cortex improves writer's cramp and enhances cortical activity. *Neuroendocrinol. Lett.* 31, 73–86.

Higuchi, Y., Matsuda, S., and Serizawa, T. (2016). Gamma knife radiosurgery in movement disorders: indications and limitations. *Mov. Disord.* 32, 28–35. doi: 10.1002/mds.26625

Huang, Y.-Z., Chen, R.-S., Rothwell, J. C., and Wen, H.-Y. (2007). The after-effect of human theta burst stimulation is NMDA receptor dependent. *Clin. Neurophysiol.* 118, 1028–1032. doi: 10.1016/j.clinph.2007.01.021

Huang, Y. Z., Edwards, M. J., Rounis, E., Bhatia, K. P., and Rothwell, J. C. (2005). Theta burst stimulation of the human motor cortex. *Neuron* 45, 201–206. doi: 10.1016/j.neuron.2004.12.033

Jinnah, H. A., and Hess, E. J. (2006). A new twist on the anatomy of dystonia: the basal ganglia and the cerebellum? *Neurology* 67, 1740–1741. doi: 10.1212/01.wnl.0000246112.19504.61

Kerrison, J. B., Lancaster, J. L., Zamarripa, F. E., Richardson, L. A., Morrison, J. C., Holck, D. E. E., et al. (2003). Positron emission tomography scanning in essential blepharospasm. *Am. J. Ophthalmol.* 136, 846–852. doi: 10.1016/S0002-9394(03)00895-X

Khedr, E. M., Ahmed, M. A., Fathy, N., and Rothwell, J. C. (2005). Therapeutic trial of repetitive transcranial magnetic stimulation after acute ischemic stroke. *Neurology* 65, 466–468. doi: 10.1212/01.wnl.0000173067.84247.36

Kimberley, T. J., Borich, M. R., Schmidt, R. L., Carey, J. R., and Gillick, B. (2015). Focal hand dystonia: individualized intervention with repeated application of repetitive transcranial magnetic stimulation. *Arch. Phys. Med. Rehabil.* 96, S122–S128. doi: 10.1016/j.apmr.2014.07.426

Koch, G., Porcacchia, P., Ponzo, V., Carrillo, F., Cáceres-Redondo, M. T., Brusa, L., et al. (2014). Effects of two weeks of cerebellar theta burst stimulation in cervical dystonia patients. *Brain Stimul.* 7, 564–572. doi: 10.1016/j.brs.2014.05.002

Kranz, G., Shamim, E. A., Lin, P. T., Kranz, G. S., and Hallett, M. (2010). Transcranial magnetic brain stimulation modulates blepharospasm: a randomized controlled study. *Neurology* 75, 1465–1471. doi: 10.1212/WNL.0b013e3181f8814d

Kranz, G., Shamim, E. A., Lin, P. T., Kranz, G. S., Voller, B., and Hallett, M. (2009). Blepharospasm and the modulation of cortical excitability in primary and secondary motor areas. *Neurology* 73, 2031–2036. doi: 10.1212/WNL.0b013e3181c5b42d

Lalli, S., Piacentini, S., Franzini, A., Panzacchi, A., Cerami, C., Messina, G., et al. (2012). Epidural premotor cortical stimulation in primary focal dystonia: clinical and 18F-fluoro deoxyglucose positron emission tomography open study. *Mov. Disord.* 27, 533–538. doi: 10.1002/mds.24949

Lefaucheur, J. P., Fnelon, G., Mnard-Lefaucheur, I., Wendling, S., and Nguyen, J. P. (2004). Low-frequency repetitive TMS of premotor cortex can reduce painful axial spasms in generalized secondary dystonia: A pilot study of three patients. *Neurophysiol. Clin.* 34, 141–145. doi: 10.1016/j.neucli.2004.07.003

Lerner, A., Shill, H., Hanakawa, T., Bushara, K., Goldfine, A., and Hallett, M. (2004). Regional cerebral blood flow correlates of the severity of writer's cramp symptoms. *Neuroimage* 21, 904–913. doi: 10.1016/j.neuroimage.2003.10.019

Lisanby, S. H., Gutman, D., Luber, B., Schroeder, C., and Sackeim, H. A. (2001). Sham TMS: Intracerebral measurement of the induced electrical field and the induction of motor-evoked potentials. *Biol. Psychiatry* 49, 460–463. doi: 10.1016/S0006-3223(00)01110-0

Marsden, C. D., Obeso, J. A., Zarranz, J. J., and Lang, A. E. (1985). The anatomical basis of symptomatic hemidystonia. *Brain* 108, 463–483. doi: 10.1093/brain/108.2.463

Milardi, D., Arrigo, A., Anastasi, G., Cacciola, A., Marino, S., Mormina, E., et al. (2016). Extensive direct subcortical cerebellum-basal ganglia connections in human brain as revealed by constrained spherical deconvolution tractography. *Front. Neuroanat.* 10:29. doi: 10.3389/fnana.2016.00029

Moro, E., LeReun, C., Krauss, J. K., Albanese, A., Lin, J. P., Walleser Autiero, S., et al. (2017). Efficacy of pallidal stimulation in isolated dystonia: a systematic review and meta-analysis. *Eur. J. Neurol.* 24, 552–560. doi: 10.1111/ene.13255

Murase, N., Rothwell, J. C., Kaji, R., Urushihara, R., Nakamura, K., Murayama, N., et al. (2005). Subthreshold low-frequency repetitive transcranial magnetic stimulation over the premotor cortex modulates writer's cramp. *Brain* 128, 104–115. doi: 10.1093/brain/awh315

Neumann, W. J., Jha, A., Bock, A., Huebl, J., Horn, A., Schneider, G. H., et al. (2015). Cortico-pallidal oscillatory connectivity in patients with dystonia. *Brain* 138, 1894–1906. doi: 10.1093/brain/awv109

Nitsche, M. A., and Paulus, W. (2001). Sustained excitability elevations induced by transcranial DC motor cortex stimulation in humans. *Neurology* 57, 1899–1901. doi: 10.1212/WNL.57.10.1899

Pappas, S. S., Darr, K., Holley, S. M., Cepeda, C., Mabrouk, O. S., Wong, J. M. T., et al. (2015). Forebrain deletion of the dystonia protein torsinA causes dystonic-like movements and loss of striatal cholinergic neurons. *Elife* 4:e08352. doi: 10.7554/eLife.08352

Quartarone, A., Bagnato, S., Rizzo, V., Siebner, H. R., Dattola, V., Scalfari, A., et al. (2003). Abnormal associative plasticity of the human motor cortex in writer's cramp. *Brain* 126, 2586–2596. doi: 10.1093/brain/awg273

Quartarone, A., and Hallett, M. (2013). Emerging concepts in the physiological basis of dystonia. *Mov. Disord.* 28, 958–967. doi: 10.1002/mds.25532

Quartarone, A., Rizzo, V., Terranova, C., Morgante, F., Schneider, S., Ibrahim, N., et al. (2009). Abnormal sensorimotor plasticity in organic but not in psychogenic dystonia. *Brain* 132, 2871–2877. doi: 10.1093/brain/awp213

Quartarone, A., Siebner, H. R., and Rothwell, J. C. (2006). Task-specific hand dystonia: can too much plasticity be bad for you? *Trends Neurosci.* 29, 192–199. doi: 10.1016/j.tins.2006.02.007

Ragert, P., Dinse, H. R., Pleger, B., Wilimzig, C., Frombach, E., Schwenkreis, P., et al. (2003). Combination of 5 Hz repetitive transcranial magnetic stimulation (rTMS) and tactile coactivation boosts tactile discrimination in humans. *Neurosci. Lett.* 348, 105–108. doi: 10.1016/S0304-3940(03)00745-6

Raike, R. S., Jinnah, H. A., and Hess, E. J. (2005). Animal models of generalized dystonia. *NeuroRx* 2, 504–512. doi: 10.1602/neurorx.2.3.504

Richter, F., and Richter, A. (2014). Genetic animal models of dystonia: common features and diversities. *Prog. Neurobiol.* 121, 91–113. doi: 10.1016/j.pneurobio.2014.07.002

Ridding, M. C., and Ziemann, U. (2010). Determinants of the induction of cortical plasticity by non-invasive brain stimulation in healthy subjects. *J. Physiol.* 588, 2291–2304. doi: 10.1113/jphysiol.2010.190314

Rothwell, J. C. (1997). Techniques and mechanisms of action of transcranial stimulation of the human motor cortex. *J. Neurosci. Methods* 74, 113–122. doi: 10.1016/S0165-0270(97)02242-5

Sadnicka, A., Hamada, M., Bhatia, K. P., Rothwell, J. C., and Edwards, M. J. (2014). Cerebellar stimulation fails to modulate motor cortex plasticity in writing dystonia. *Mov. Disord.* 29, 1304–1307. doi: 10.1002/mds.25881

Schabrun, S. M., Stinear, C. M., Byblow, W. D., and Ridding, M. C. (2009). Normalizing motor cortex representations in focal hand dystonia. *Cereb. Cortex* 19, 1968–1977. doi: 10.1093/cercor/bhn224

Schneider, S. A., Pleger, B., Draganski, B., Cordivari, C., Rothwell, J. C., Bhatia, K. P., et al. (2010). Modulatory effects of 5Hz rTMS over the primary somatosensory cortex in focal dystonia - An fMRI-TMS Study. *Mov. Disord.* 25, 76–83. doi: 10.1002/mds.22825

Siebner, H. R., and Rothwell, J. (2003). Transcranial magnetic stimulation: new insights into representational cortical plasticity. *Exp. Brain Res.* 148, 1–16. doi: 10.1007/s00221-002-1234-2

Siebner, H. R., Tormos, J. M., Ceballos-Baumann, A. O., Auer, C., Catala, M. D., Conrad, B., et al. (1999). Low-frequency repetitive transcranial magnetic stimulation of the motor cortex in writer's cramp. *Neurology* 52, 529–537.

Stefan, K., Kunesch, E., Benecke, R., Cohen, L. G., and Classen, J. (2002). Mechanisms of enhancement of human motor cortex excitability induced by interventional paired associative stimulation. *J. Physiol.* 543, 699–708. doi: 10.1113/jphysiol.2002.023317

Strafella, A. P., Paus, T., Barrett, J., and Dagher, A. (2001). Repetitive transcranial magnetic stimulation of the human prefrontal cortex induces dopamine release in the caudate nucleus. *J. Neurosci.* 21, 1–4.

Strafella, A. P., Paus, T., Fraraccio, M., and Dagher, A. (2003). Striatal dopamine release induced by repetitive transcranial magnetic stimulation of the human motor cortex. *Brain* 126, 2609–2615. doi: 10.1093/brain/awg268

Tyvaert, L., Houdayer, E., Devanne, H., Monaca, C., Cassim, F., and Derambure, P. (2006). The effect of repetitive transcranial magnetic stimulation on dystonia: a clinical and pathophysiological approach. *Neurophysiol. Clin.* 36, 135–143. doi: 10.1016/j.neucli.2006.08.007

Veugen, L. C., Hoffland, B. S., Stegeman, D. F., and Van De Warrenburg, B. P. (2013). Inhibition of the dorsal premotor cortex does not repair surround inhibition in writer's cramp patients. *Exp. Brain Res.* 225, 85–92. doi: 10.1007/s00221-012-3350-y

Wang, H.-Y., Crupi, D., Liu, J., Stucky, A., Cruciata, G., Di Rocco, A., et al. (2011). Repetitive transcranial magnetic stimulation enhances BDNF–TrkB signaling in both brain and lymphocyte. *J. Neurosci.* 31, 11044–11054. doi: 10.1523/JNEUROSCI.2125-11.2011

Weise, D., Mann, J., Rumpf, J.-J., Hallermann, S., and Classen, J. (2017). Differential regulation of human paired associative stimulation-induced and theta-burst stimulation-induced plasticity by L-type and T-type Ca^{2+} channels. *Cereb. Cortex* 27, 4010–4021. doi: 10.1093/cercor/bhw212

Wilson, B. K., and Hess, E. J. (2013). Animal models for dystonia. *Mov. Disord.* 28, 982–989. doi: 10.1002/mds.25526

Conflict of Interest Statement: The authors declare that the research was conducted in the absence of any commercial or financial relationships that could be construed as a potential conflict of interest.

frontiers in Neuroscience

ORIGINAL RESEARCH
published: 12 September 2017
doi: 10.3389/fnins.2017.00508

Cathodal Transcranial Direct Current Stimulation Improves Focal Hand Dystonia in Musicians: A Two-Case Study

Sara Marceglia[1,2†], Simona Mrakic-Sposta[1,3†], Manuela Fumagalli[1], Roberta Ferrucci[1,4], Francesca Mameli[1], Maurizio Vergari[1], Sergio Barbieri[1,4] and Alberto Priori[1,4,5]*

[1] Fondazione IRCCS Ca' Granda Ospedale Maggiore Policlinico, Milan, Italy, [2] Dipartimento di Ingegneria e Architettura, Università degli Studi di Trieste, Trieste, Italy, [3] Istituto di Bioimmagini e di Fisiologia Molecolare, Consiglio Nazionale delle Ricerche, Segrate, Italy, [4] "Aldo Ravelli" Center for Neurotechnology and Experimental Brain Therapeutics, University of Milan, Milan, Italy, [5] Department of Health Sciences, University of Milan and ASST Santi Paolo e Carlo, Milan, Italy

OPEN ACCESS

Edited by:
Takashi Hanakawa, National Center of Neurology and Psychiatry, Japan

Reviewed by:
Shinichi Furuya, Sony Computer Science Laboratories, Japan
Makii Muthalib, Université de Montpellier, France
Milton Cesar Biagioni, NYU School of Medicine, United States

***Correspondence:**
Alberto Priori
alberto.priori@unimi.it

† These authors have contributed equally to this work.

Specialty section:
This article was submitted to Neural Technology, a section of the journal Frontiers in Neuroscience

Received: *27 June 2017*
Accepted: *28 August 2017*
Published: *12 September 2017*

Citation:
Marceglia S, Mrakic-Sposta S, Fumagalli M, Ferrucci R, Mameli F, Vergari M, Barbieri S and Priori A (2017) Cathodal Transcranial Direct Current Stimulation Improves Focal Hand Dystonia in Musicians: A Two-Case Study. Front. Neurosci. 11:508. doi: 10.3389/fnins.2017.00508

Focal hand dystonia (FHD) in musicians is a movement disorder causing abnormal movements and irregularities in playing. Since weak electrical currents applied to the brain induce persistent excitability changes in humans, cathodal tDCS was proposed as a possible non-invasive approach for modulating cortical excitability in patients with FHD. However, the optimal targets and modalities have still to be determined. In this pilot study, we delivered cathodal (2 mA), anodal (2 mA) and sham tDCS over the motor areas bilaterally for 20 min daily for five consecutive days in two musicians with FHD. After cathodal tDCS, both patients reported a sensation of general wellness and improved symptoms of FHD. In conclusion, our pilot results suggest that cathodal tDCS delivered bilaterally over motor-premotor (M-PM) cortex for 5 consecutive days may be effective in improving symptoms in FHD.

Keywords: cathodal transcranial direct current stimulation, neuromodulation, tDCS, focal hand dystonia, musician

INTRODUCTION

Focal hand dystonia (FHD) in musicians is a movement disorder characterized by irregularities in playing due to involuntary muscular activation in both the hand and arms (Cho and Hallett, 2016; Stahl and Frucht, 2017). FHD generally occurs in people who have spent a long period of time performing repetitive skilled motor tasks (Cho and Hallett, 2016). Furthermore, FHD produces excessive co-contraction of agonists and antagonists of hand and forearm muscles resulting in a slow, stiff-appearing movement and causing pain (MacKinnon, 2002; Garraux et al., 2004). Being a network disorder that involves several brain areas, FHD has a complex pathophysiology including several general abnormalities as the loss of inhibition, sensory dysfunction, and abnormal plasticity (Cho and Hallett, 2016). Functional neuroimaging studies showed alterations in the topography and increased activation of somatosensory and motor cortices (Zeuner and Molloy, 2008; Hinkley et al., 2009). Even though the causes of this disabling condition remain unclear, maladaptive plasticity has been proposed as driver for FHD in musicians (Konczak and Abbruzzese, 2013).

Despite several new therapeutic strategies proposed, botulinum toxin injection is the preferred therapy for FHD, even though some results suggest that it does not effectively improve symptoms (Hallett et al., 2009; Lungu and Ahmad, 2016). External shock waves therapy (Trompetto et al., 2009), prolonged immobilization of the affected arm (Priori et al., 2001), thalamic deep brain

stimulation (Cho et al., 2009), repetitive Transcranial Magnetic Stimulation (rTMS) (Edwards et al., 2008), and transcranial Direct Current Stimulation (tDCS) (Cho and Hallett, 2016) are among the alternatives explored.

In particular, tDCS is a non-invasive technique that induces prolonged changes in brain excitability and influences motor and cognitive performances (Nitsche and Paulus, 2000; Priori, 2003; Ardolino et al., 2005; Priori et al., 2008; Brunoni et al., 2013; Zhao et al., 2017). In the past 10 years, tDCS has been proposed as adjunctive treatment for several neurological and neuropsychiatric conditions (Fregni et al., 2006; Ferrucci et al., 2008a,b; Monti et al., 2008; Mrakic-Sposta et al., 2008; Cogiamanian et al., 2009; Lefaucheur et al., 2017).

Cathodal tDCS was applied in FHD, but the results were controversial, mainly for the heterogeneity of the stimulation protocols tested (Buttkus et al., 2010, 2011; Benninger et al., 2011; Furuya et al., 2014), in terms of electrode montage, tDCS duration and intensity, as well as the number of treatments administered. Also, tDCS was either performed when the patient was at rest, or while the patient was trained (Cho and Hallett, 2016). Biparietal tDCS (two electrodes with different polarities on the head) applied over days during neurorehabilitation could improve therapy effectiveness in FHD (Furuya and Altenmüller, 2015; Rosset-Llobet et al., 2015) and bilateral tDCS (two electrodes with the same polarity on the head) is thought to improve symptoms in subjects showing bi-manual impairments (Pixa et al., 2017). Evidence of increased excitability or loss of inhibition at multiple levels including premotor and motor cortex, somatosensory cortex and cerebellum (Beck et al., 2008; Brighina et al., 2009; Delnooz et al., 2012) support the hypothesis that cathodal tDCS could improve symptoms by reducing excitability, even though the optimal protocol is still to be determined (Cho and Hallett, 2016).

In this pilot study, we applied bilateral anodal, cathodal, and sham tDCS over the motor—premotor cortices for 5 consecutive days in two musicians with FHD, to (1) test whether cathodal tDCS was superior to anodal and sham tDCS in controlling FHD symptoms in musicians, and (2) preliminarily assess the use of a 5-days protocol in terms of safety and efficacy.

METHODS

Patients

After signing their informed consent, two musicians with FHD were recruited for tDCS treatment application. The study was approved by the local Ethic Committee and it was in agreement with the principles stated in the Declaration of Helsinki. All the assessments were performed by an experienced neurologist and the diagnosis was made according to the recommendations found in the literature (Rosset-Llobet et al., 2009).

Patient 1

The first patient was a right-handed 38 years-old man, in whom FHD symptoms manifested first at the age of 18. He began playing piano when he was 11 years-old. At present, he teaches in a secondary school and plays as concert pianist.

Musician's FHD was diagnosed at the age of 22, but the disease progressively exacerbated. In the past time, the therapeutic intervention with Transcutaneous Electrical Nerve Stimulator (TENS) did not improve symptoms. Anatomic Magnetic Resonance Imaging (MRI) brain scan was normal and electroencephalogram (EEG) did not show any sign of epileptic seizures. At the time, focal dystonia interested the middle finger of the right hand and the left hand.

Presently, despite the drug treatment (anticholinergics: 12 mg/day, carbidopa/levodopa: 500 mg/day), dystonic tremor is present at rest and when the right hand is tired or weak (Lee et al., 2015).

Patient 2

The second patient was a right-handed, 44-years-old man. He began playing the accordion at the age of 11. At present, he teaches in a secondary school and plays saxophone, accordion, and clarinet.

First symptoms (cramps) appeared on the right hand at the age of 30. The patient was treated with botulinum toxin injections in hand and forearm muscles without any improvement.

At present, FHD symptoms were predominantly on the right hand, particularly the fifth finger with a subjective complaint extending to the wrist and the distal forearm. The patient complained initial symptoms to the left hand, too. The patient is not currently taking any pharmacological treatment. Anatomic MRI was normal and EEG did not show any sign of epileptic seizures. Electroneurography (ENG) showed normal motor and sensory conduction parameters; electromyography (EMG) showed a reduced disynaptic and presynaptic inhibition of H reflex in the right flexor carpi radialis (0 ms = 100%; 20 ms = 86%), compatible with a diagnosis of FHD.

Clinical Assessment at Baseline

Musician's FHD was evaluated at baseline (see **Table 1**) using the following rating scales: the *Symptom Severity Scale (SSS)* that consists of 10 questions that evaluate direct and indirect disease manifestations; the *Functional Status Scale (FSS),* a 12-item disability scale that comprises an assessment of performances

TABLE 1 | Clinical Examination at baseline in both patients.

CLINICAL EXAMINATION T0 (Baseline Evaluation)		
Scale	**Patient 1**	**Patient 2**
FSS	11/36	2/36
TC	3	2
SSS	28/43	24/43
FMS	2	3
MMPI-2	Hy 74 (cut-off $\leq$ 65; $z = 2.6$)	Normal
CBA	IP-F ($z = -1.73$)	Normal
	IP-1 ($z = -1.9$)	
	MOCQ/R1 ($z = 2.23$)	

FSS, Functional Status Scale; TC, Tubiana and Chamagen Scale; SSS, Symptom Severity Scale; FMS, Fahn Marsden Scale; MMPI-2, Minnesota Multiphasic Personality Inventory Scales; [Hy, Hysteri]; CBA, Cognitive Behavioral Assessment [IP-F=Fear; IP-1=Fear: Calamity; MOCQ/R = Obsessions and compulsing:checking].

of daily activities possibly affected by FHD or hand weakness. The SSS and FSS, which were originally designed for carpal tunnel syndrome, were adapted to FHD in order to investigate its manifestations.

The *Fahn Marsden Scale (FMS)* (Fahn, 1989) was used to quantify generalized or focal dystonia in nine body areas, including eyes, mouth, speech and swallowing, neck, trunk, and right and left arm and leg. The *Tubiana and Chamagne (TC)* (Tubiana and Chamagne, 1983) scale is a classification of severity of focal dystonia in musicians, and it was used to monitor the evolution of the treatment. The scale comprises four stages of severity of dystonia.

Psychological assessment was executed using the *Minnesota Multiphasic Personality Inventory Scales (MMPI-2)* (Butcher et al., 2001) and the *Cognitive Behavioural Assessment 2.0 (CBA-2.0)* (Sanavio and Vidotto, 1996). The MMPI-2 is a well-known and widely used psychological test consisting of 567 true-false items. It traditionally yields scores on four validity scales and 10 clinical scales, although numerous other scales may be scored. For this study, the clinical, select content (Anxiety, Depression, Negative Treatment Indicators) and supplementary (Ego Strength) scales were considered. The CBA 2.0 battery includes a series of questionnaires that investigate broad issues of potential clinical interest and identify areas of dysfunction in the current life of the subjects. Subjective mood, wellness and pain at the hands were evaluated using five 100 mm *Visual Analog Scales (VAS)* (happy/unhappy; wellness/unease; left hand pain/no left hand pain; right hand pain/no right hand pain, tired/no tired).

Performance Assessment

The effects of tDCS on FHD were evaluated through the following tasks administered before and after each tDCS treatment:

Copy of an Archimedes Spiral

Patients were asked to copy a spiral template printed in black on a paper with their dominant arm. The template was 132.31 cm long. The quantitative value was defined through the length of the drawn Archimedean spiral: L = pi*N*R with N = R/t; where: t = spiral's step, N = number of rpm, R = max radius of spiral. We compared the spiral template length to the length of the drawn spiral. The presence of tremor was qualitatively evaluated by four independent judges blinded to the stimulation polarity on a 0–3 scale (0 = absence of tremor, 1 = slight tremor, 2 = medium tremor, 3 = important tremor).

Follow with a Pen the Edge of the Spiral

Patients were asked to follow the spiral line with the pen maintaining a constant distance of 2 mm from the printed line. The task was evaluated by four judges blinded to the stimulation polarity on a 0–3 scale about the presence of tremor (0 = absence of tremor; 1 = slight tremor, 2 = medium tremor, 3 = important tremor).

Copy of Sample Pictures

Patients had to copy different figures (cube, pyramid, and more complex figures) and a 10 cm line. Four blind judges evaluated the presence of constructive apraxia on a 0–3 scale (0 = perfect copy; 1 = very similar copy, 2 = incomplete copy, 3 = very incomplete copy) and the presence of tremor (0–3 scale with 0 = absence of tremor, 1 = slight tremor, 2 = medium tremor, 3 = important tremor).

Copy of a List of Words

Eight lists of 33 words were created using the Lists for Writing. Each list was composed by words (verbs, adjectives, concrete and abstract nouns, all of them both regular and irregular) and non-words. Four blind judges evaluated the quality of writing on a 0–1 scale (0 = good writing; 1 = bad writing symptom of a weak and tired hand), and the presence of tremor (0–3 scale with 0 = absence of tremor, 1 = slight tremor, 2 = medium tremor, 3 = important tremor). The % difference from pre-treatment evaluation was considered for the analysis.

Execution of a Musical Scale and Exercises with the Instrument

Patients executed a musical scale and several technical exercises with their instrument. More specifically, for the piano, the patient was asked to play a two-octave C-major scale, right and left hand, 10 sequences; for the clarinet, the patient was asked to play a two-octave C-major scale.

Adverse events were collected throughout the whole session.

Experimental Protocol

This was a double-blind experiment in which both the patients and the judges were blind to the type of stimulation delivered. Both patients underwent three 5-days sessions, one for sham, one for cathodal, and one for anodal tDCS, in random order (**Figure 1**). Three washout weeks elapsed between each session (anodal, cathodal, sham). After a baseline clinical assessment at the beginning of the 5-day session, each day included (1) pre-tDCS performance evaluation; (2) bilateral tDCS at 2 mA intensity per side over the motor/premotor areas (M-PM) of the cerebral cortex (above C3/C4, FC3/FC4 according to the international 10–20 electrode placement system) for 20 min; and (3) post-tDCS performance evaluation. At the end of the 5-days session, FHD symptoms were re-assessed through the SSS, the TC, and the FSS (**Figure 1**).

Follow-up examinations, including both symptom and performance assessments were conducted at 1 (T1) and 10 (T2) days after the end of each 5-days session.

tDCS

tDCS was delivered to the scalp with two "Eldith DC Stimulator" (Neuroconn GmbH, Germany), each connected to a pair of thick (0.3 mm) rounded saline-soaked sponge electrodes, one (active electrode) placed over the scalp and the other (reference electrode) over the right deltoid muscle. Cathodal and anodal tDCS (C-tDCS and A-tDCS) polarity referred to the two electrodes over the scalp. The wide electrode surface (scalp electrodes 48 cm^2; deltoid electrode 64 cm^2) avoided the possible harmful effects of high current density. For sham tDCS (S-tDCS),

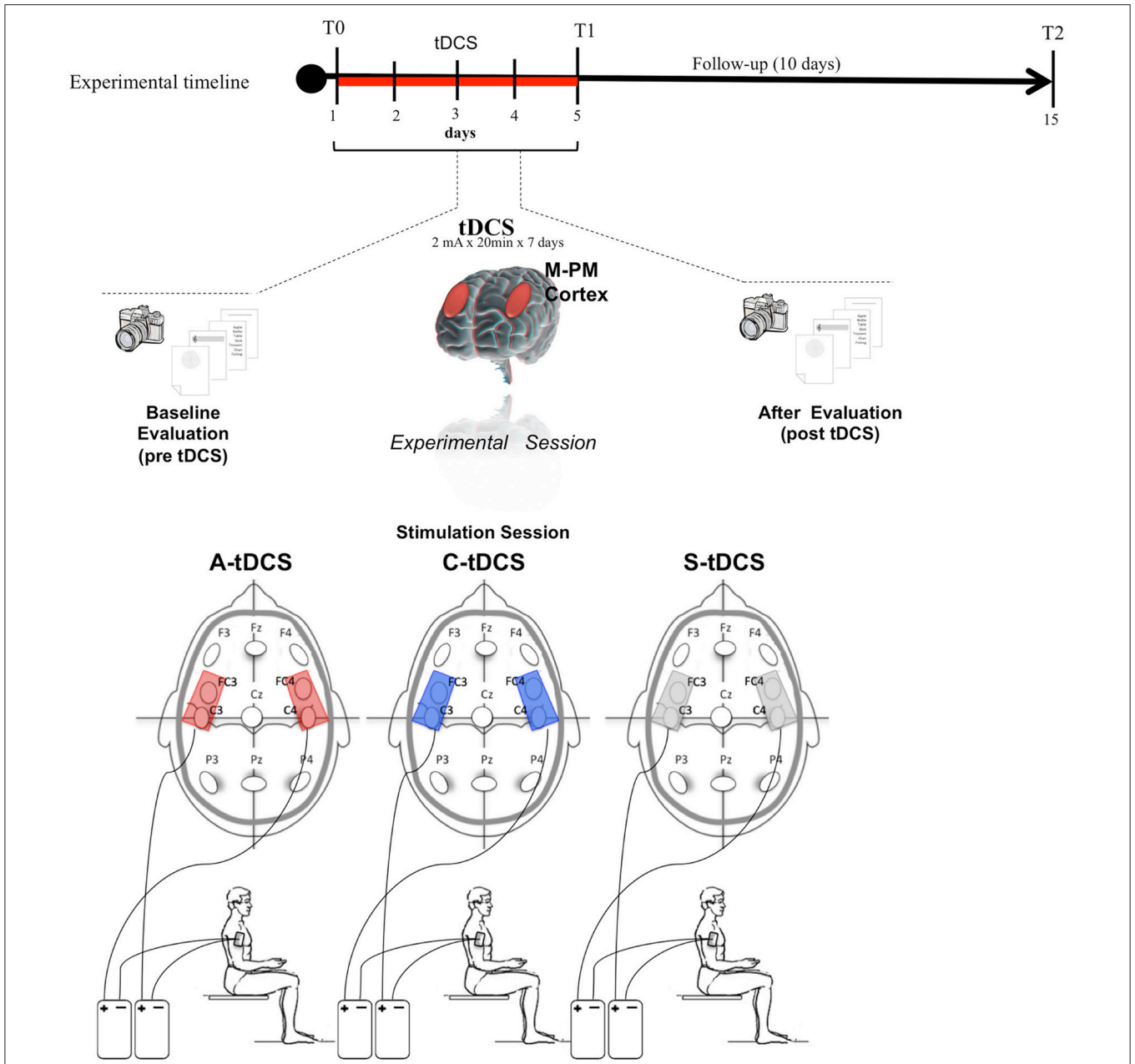

FIGURE 1 | Transcranial Direct Current Stimulation (tDCS) experimental protocol. tDCS was applied bilaterally over the scalp on the motor-premotor cortex (M-PM) for 5 consecutive days. Patients were assessed in the first (T0) and the last day (T1) and after 10 days from ended tDCS (T2).

electrodes were placed as for real stimulation but the stimulator was turned off after 10 s. Hence, the patients felt an initial itching sensation similar to that induced at the beginning of real tDCS but received no stimulation.

To guarantee safety we applied, to each stimulation site, current at a density of 0.0416 mA/cm^2 and delivered a total charge of 0.049 C/cm^2. These intensities are far below the threshold for tissue damage (Nitsche et al., 2003a; Liebetanz et al., 2009; Lefaucheur et al., 2017).

Data Analysis

Considering the low number of subjects reported, we performed only descriptive statistics.

Percentage changes, defined as [(after tDCS-before tDCS)/before tDCS], were used for the analysis to assess tDCS effects. When applicable, the percentage changes of variables evaluated by the independent judges were averaged, to obtain the trend over the entire 5-days session. Data are reported as [mean $\pm$ *SD*].

RESULTS

The patients did not report any adverse effects during stimulation sessions and were not able to distinguish active (anodal or cathodal) and sham stimulation.

Copy of an Archimedes Spiral

Quantitative evaluation showed that whereas S-tDCS and A-tDCS left patients' performance unchanged, after C-tDCS both patients could draw a complete *Copy of an Archimedes spiral* (template length 100%, **Figure 2A**). The time elapsing before each patient could draw a complete spiral differed in the two patients: patient 1 drew a complete spiral 1 day after the entire 5-day C-tDCS session, whereas patient 2 achieved a complete spiral immediately after the first C-tDCS application (day 1) in the post-C-tDCS assessment. Conversely, when sham and anodal sessions ended, both patients could draw a spiral that was 20–30% shorter than the printed one. At T2, the beneficial effect of C-tDCS ended (**Figure 2B**). Qualitative analysis showed that C-tDCS reduced tremor, whereas A-tDCS and S-tDCS did not (**Figures 2C–G**).

Follow with a Pen the Edge of the Spiral and Copy of a Sample Pictures

In the *Follow the edge of a spiral with a pen* task both patients improved at T1 of the C-tDCS session and worsened after A-tDCS (**Figures 3A,B**).

In both patients, tremor decreased (patient 1: −33%; patient 2: −62%) while patients were "*copying sample pictures*" immediately after a single C-tDCS session. At T2, the effect of C-tDCS persisted (% change at T2 C-tDCS, Patient 1: −9%; patient 2: −30%; **Figures 4A,B**).

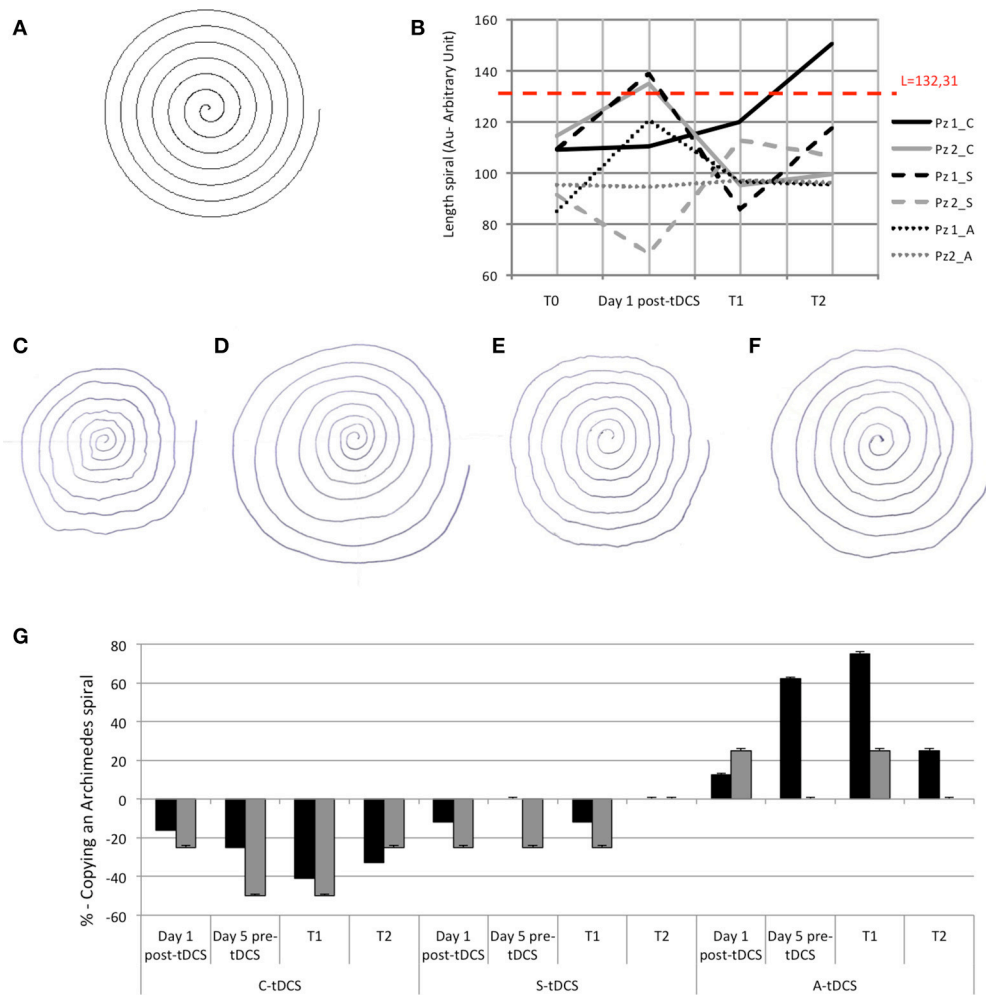

FIGURE 2 | (A) Copy of an Archimedes spiral task: template of Archimedean Spiral; **(B)** The lines show quantitative evaluation in both patients at T0, at day 1 after tDCS, at T1, and at T2. The red dashed line is the length of the sample spiral (132.31 mm), black lines refer to patient 1 and gray lines to patient 2. The full is C-tDCS, the dashed line is A-tDCS and the dotted line s S-tDCS session; **(C)** Copy of Archimedean Spiral the first day after C-tDCS treatment in patient 1; **(D)** Copy of Archimedean Spiral at T1 of the C-tDCS session in patient 1; **(E)** Copy of Archimedean Spiral at the first day after A-tDCS treatment in patient 1; **(F)** Copy of Archimedean Spiral at T1 of the A-tDCS session in patient 1. **(G)** The histogram shows tremor in qualitative analysis in the percentage differences after tDCS in both patients. 0% is baseline (pre-tDCS—T0).

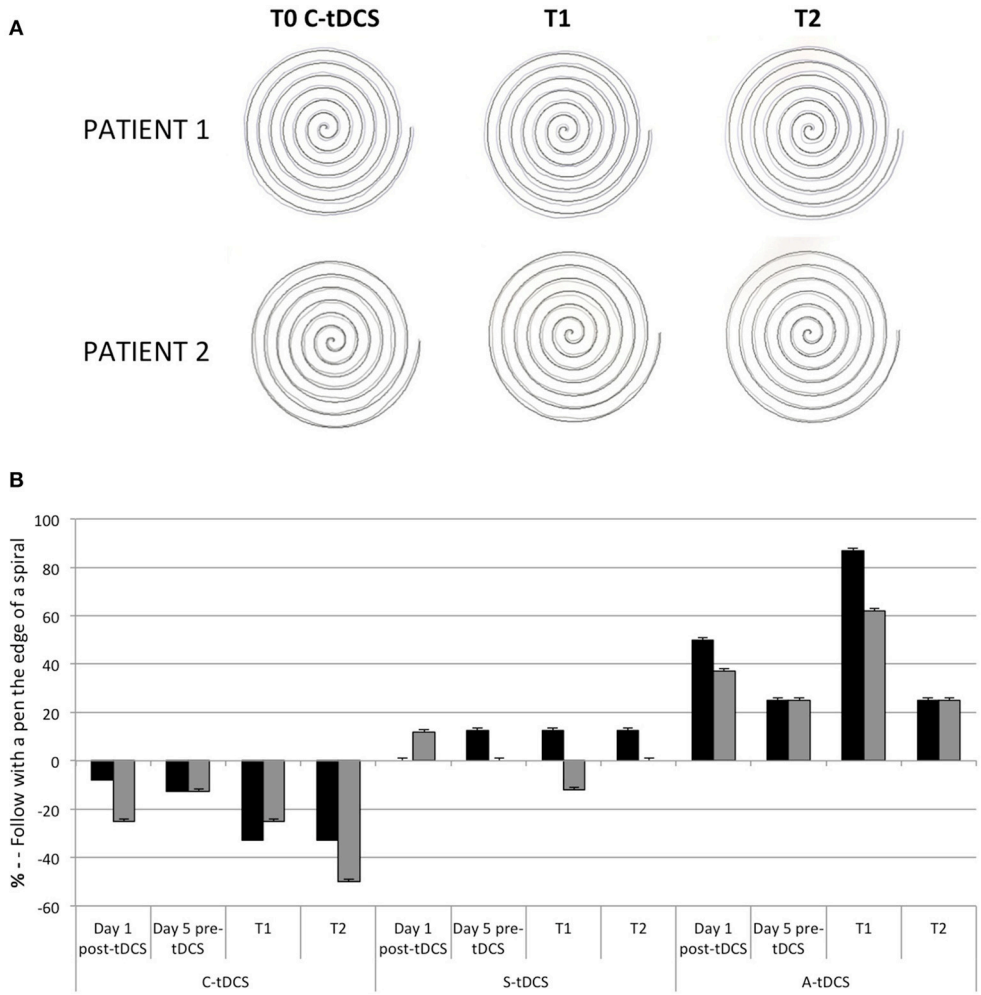

FIGURE 3 | (A) Follow with a pen the edge of the spiral at pre (T0) and post C-tDCS (T1 and T2) in both patients. **(B)** The histogram showed the qualitative analysis in the percentage differences after tDCS in both patients. 0% is baseline (pre-tDCS—T0).

Copy of a List of Words

Either way, before and after tDCS (anodal, cathodal, and sham), the quality of writing was good in both patients, with no presence of bad writing due to a weak or tired hand and tremor.

FHD Symptoms and Playing

FSS, TC, and SSS values improved in both patients after C-tDCS. At T1, FSS decreased by 9% in patient 1 and 100% in patient 2, TC decreased by 33% in patient 1 and 100% in patient 2, SSS decreased by 3% in patient 1 and 46% in patient 2. After A-tDCS, only some values improved: FSS decreased in patient 1 by 35 and 100% in patient 2, TC did not change in patient 1 and 2, SSS decreased by 13% in patient 1 and 5% in patient 2 (**Table 2**).

Patient 1 reported a subjective improvement and decrease of pain at the right hand only after C-tDCS. He also reported subjective improvement of prono-supination movement in the left hand (**Figures 5A,B**).

Patient 2 reported a subjective improvement after cathodal tDCS: the right hand was more toned, he had a better control of the 5th finger, fewer shots, and less hand/art fatigue (**Figures 5C,D**).

VAS

Both patients reported a sensation of general wellness, of happiness, of reduction of hand pain and an improvement of rest particularly after C-tDCS (at T1). In details, for health/wellness: patient 1, 21 vs. 32 vs. 19% (S-C-A-tDCS, respectively); patient 2, 0 vs. 4 vs. 0%; happy/unhappy: patient 1, 20 vs. 55 vs. 43%; patient 2, 0 vs. 8 vs. 2%; pain/no pain right hand patient 1, 13 vs. 37 vs. 0%; patient 2, 0 vs. 0 vs. 0%; pain/no pain left hand patient 1, 2 vs. 68 vs. 3%; patient 2, 0 vs. 0 vs. 0%; tired/not tired patient 1, 18 vs. 42 vs. 24%; patient 2, 0 vs. 5 vs. 7%).

DISCUSSION

Musician's FHD is a difficult disease, with little therapeutic options while bringing to early termination of their professional life. We showed that cathodal tDCS delivered bilaterally for

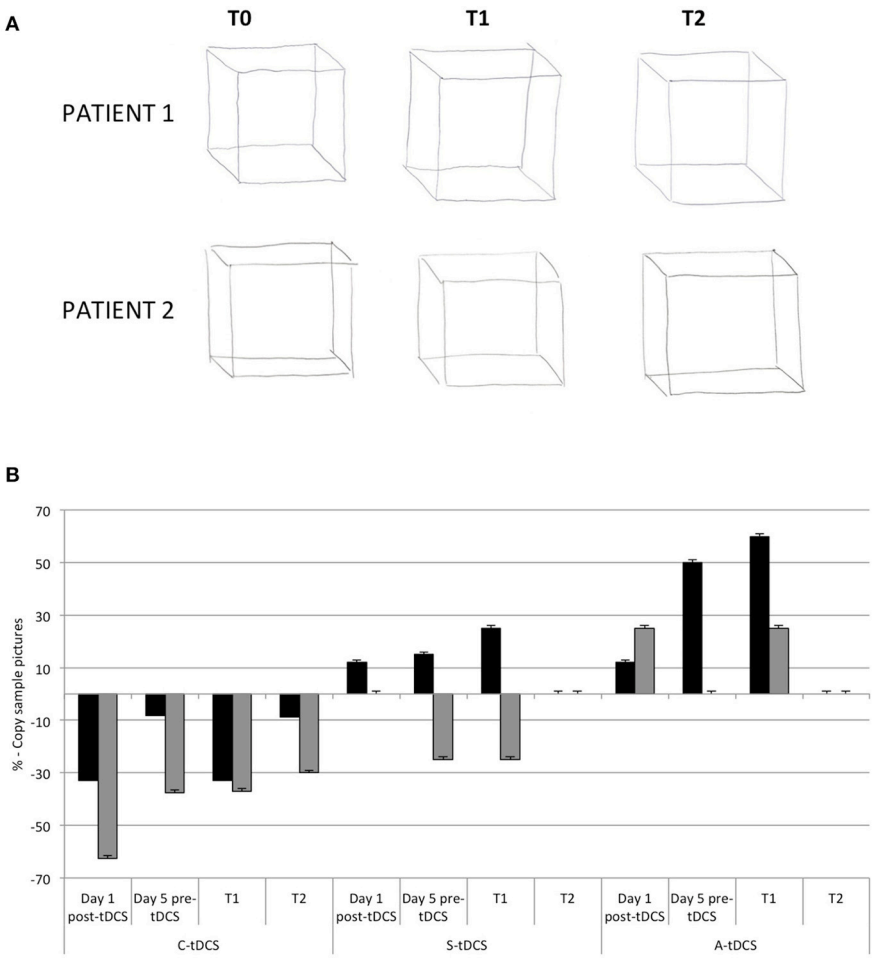

FIGURE 4 | (A) The tremor graft pre (T0), and post (T1 and T2) C-tDCS in both patients. **(B)** The histogram showed qualitative analysis in the percentage differences of tremor after tDCS in both patients. Zero percent is baseline (pre-tDCS—T0).

5 consecutive days is feasible and safe, and that it transiently improves motor performances, subjective perception of pain and fatigue, and subjective perception of playing in two musicians with FHD.

Our findings, while proposing a new stimulation protocol, are in line with the conclusions of the recent review by Cho and Hallet who reported the potential therapeutic use of non-invasive brain stimulation to treat FHD (Cho and Hallett, 2016). Considering the current state-of-the-art, there are few studies investigating the effects of cathodal tDCS in FHD, but none of them applied a 5-days bilateral (two electrodes with the same polarity on the head) M1 tDCS protocol nor it found improvements lasting for 10 days. More specifically, of the seven tDCS studies mentioned in the review (Rosset-Llobet et al., 2009; Buttkus et al., 2010, 2011; Benninger et al., 2011; Furuya et al., 2014; Sadnicka et al., 2014), four have applied electrodes on M1 but only one reported positive effects (Furuya et al., 2014). Unlike the others, the authors combined cathodal tDCS on the affected M1 with anodal tDCS on the unaffected M1 in pianists, finding that rhythmic accuracy of sequential finger movements improved and was retained 4 days after intervention.

Following the Furuya S and colleagues' suggestion of working on the two sides of the head contemporarily, we applied tDCS bilaterally (two electrodes with the same polarity on the two head sides) over the M-PM cortex in two musicians with FHD and bilateral symptoms, sharing the idea of a possible advantage over mono-lateral stimulation. The M-PM cortex was chosen as tDCS target because it is believed to encode the motor programs responsible for skilled finger movement (Karni et al., 1995; Gentner et al., 2010). In addition, bilateral tDCS was shown to improve symptoms occurring on both sides of the body (Pixa et al., 2017), similarly to our two patients, who had both hands affected by symptoms (at least in an initial phase). Then, considering the positive results of applying tDCS for one week (5 days) in other hyperkinetic disorders (Mrakic-Sposta et al., 2008), and considering the boosting effects of tDCS applied over days during neurorehabilitation (Furuya and Altenmüller, 2015; Rosset-Llobet et al., 2015), we chose the 5-days protocol.

After 5 consecutive days of cathodal tDCS, both our patients experienced consistent improvements in tremor, slight improvement of finger postures during playing, and diminished pain in the hands and arms, without experiencing any side

TABLE 2 | Clinical assessment of both patients before and after 5-days tDCS session.

CLINICAL ASSESSMENT												
	T0 (Before tDCS)						T1 (5 days after tDCS)					
Scale	Patient 1			Patient 2			Patient 1			Patient 2		
	C-tDCS	S-tDCS	A-tDCS	C-tDCS	S-tDCS	A-tDCS	C-tDCS	S-tDCS	A-tDCS	C-tDCS	S-tDCS	A-tDCS
FSS	11/36	12/36	17/36	2/36	2/36	2/36	10/36	11/36	11/36	0/36	0/36	0/36
TC	3	3	3	2	2	2	4	3	3	4	2	3
SSS	28/43	28/43	29/43	24/43	17/43	20/43	27/43	29/43	25/43	13/43	18/43	19/43

FSS, Functional Status Scale; TC, Tubiana and Chamagen Scale; SSS, Symptom Severity Scale.

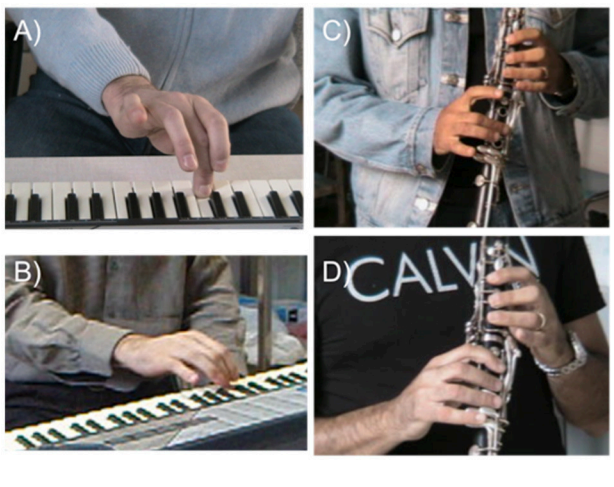

FIGURE 5 | Typical patterns of dystonia posture in a pianist **(A)** and clarinet **(C)** at baseline (T0). In **(B,D)** the patients after 5-days of C-tDCS (T1).

effect. Moreover, our patients, who were blinded to the treatment received, reported a positive subjective impression of how C-tDCS affected their pain, tiredness, mood, and wellness. Conversely, in line with the study by Quartarone et al. (2005), where anodal tDCS was shown to up regulate brain excitability in patients with writer's cramp, A-tDCS worsened the symptoms in our patients. Collectively, our results suggest that cathodal tDCS treatment might help to produce steady, more accurate arm movements, but not to stabilize abnormal fine finger movements. Because cathodal tDCS reduces brain excitability (Nitsche et al., 2003b), bilateral cathodal tDCS delivered over the motor areas could have down regulated excitability in the underlying brain areas by recovering the inadequate motor cortical inhibition responsible for excessive excitation and near synchronous co-contractions of agonists and antagonists (Nitsche et al., 2003b; Ardolino et al., 2005; Byl, 2007). Our application of bi-hemispheric C-tDCS seemed to help recovering patient's bilateral symptoms and overall condition. We can hence hypothesize that, in presence of bilateral symptoms, tDCS should be delivered bilaterally (two electrodes with the same polarity on the two head sides) whereas, in presence of unilateral symptoms (Furuya et al., 2014), tDCS preferable application may be bipolar (two different polarities on the head). Moreover, the 5-days protocol resulted to be effective in providing beneficial effects at least for 2 weeks, confirming that over-days tDCS sessions may be more effective than single-shot tDCS sessions in promoting brain plasticity, especially if combined with neurorehabilitation therapy (Rosset-Llobet et al., 2015).

Finally, our experiment differs from all the others reported in the literature for both the electrode montage (bilateral tDCS) and the stimulation protocol (5 consecutive days). This could partly explain why our results are more consistent than those obtained by other groups (Cho and Hallett, 2016).

However, this was a double-subject studies that allows observing individual responses, but not generalizing its results to the whole population of FHD musicians, as inherent limitation of the experimental design. Although, no definitive conclusions can be derived from 2 subjects, our results should be interpreted in the context of the novel target of stimulation (bilateral M-PM for patients with initial bilateral symptoms) and stimulation protocol (5 consecutive days) that may be considered as new factors in future trials. Also, we haven't assessed any biomarker to better understand the potential pathophysiological mechanisms of tDCS that should be included in further studies.

In conclusion, a 5-days treatment with cathodal tDCS could be a safe and low-cost effective adjuvant in the therapy of involuntary flexion or extension of hand and limbs and in hand pain and the bilateral electrode montage over PM-M areas could favorably impact FHD in musicians with bilateral symptoms.

ETHICS STATEMENT

The study was carried out in accordance with the recommendations of the Ethical Committee of the Fondazione IRCCS Ca'Granda Ospedale Maggiore Policlinico with written informed consent from all subjects. All subjects gave written informed consent in accordance with the Declaration of Helsinki.

AUTHOR CONTRIBUTIONS

SM and SMS designed the study, conducted the experiment, analyzed data, and drafted the manuscript and figures. MF, RF, and FM designed and administered the cognitive tasks and reviewed the manuscript. MV administered tDCS and reviewed

the manuscript. SB evaluated the patients, provided clinical advice and scales, and reviewed the manuscript. AP ideated the study, coordinated the research protocol, and finalized the manuscript.

ACKNOWLEDGMENTS

The work was supported by the grant GR-2011-02352807 from the Italian Ministry of Health.

REFERENCES

Ardolino, G., Bossi, B., Barbieri, S., and Priori, A. (2005). Non-synaptic mechanisms underlie the after-effects of cathodal transcutaneous direct current stimulation of the human brain. *J. Physiol.* 568, 653–663. doi: 10.1113/jphysiol.2005.088310

Beck, S., Richardson, S. P., Shamim, E. A., Dang, N., Schubert, M., and Hallett, M. (2008). Short intracortical and surround inhibition are selectively reduced during movement initiation in focal hand dystonia. *J. Neurosci.* 28, 10363–10369. doi: 10.1523/JNEUROSCI.3564-08.2008

Benninger, D. H., Lomarev, M., Lopez, G., Pal, N., Luckenbaugh, D. A., and Hallett, M. (2011). Transcranial direct current stimulation for the treatment of focal hand dystonia. *Mov. Disord.* 26, 1698–1702. doi: 10.1002/mds.23691

Brighina, F., Romano, M., Giglia, G., Saia, V., Puma, A., Giglia, F., et al. (2009). Effects of cerebellar TMS on motor cortex of patients with focal dystonia: a preliminary report. *Exp. Brain Res.* 192, 651–656. doi: 10.1007/s00221-008-1572-9

Brunoni, A. R., Boggio, P. S., Ferrucci, R., Priori, A., and Fregni, F. (2013). Transcranial direct current stimulation: challenges, opportunities, and impact on psychiatry and neurorehabilitation. *Front. Psychiatry* 4:19. doi: 10.3389/fpsyt.2013.00019

Butcher, J., Graham, J., Ben-Porath, Y., Tellegen, A., Dahlstrom, W., and Kaemmer, B. (2001). *MMPI-2: Manual for Administration and Scoring*. Minneapolis, MN: University of Minnesota Press.

Buttkus, F., Baur, V., Jabusch, H.-C., de la Cruz Gomez-Pellin, M., Paulus, W., Nitsche, M. A., et al. (2011). Single-session tDCS-supported retraining does not improve fine motor control in musician's dystonia. *Restor. Neurol. Neurosci.* 29, 85–90. doi: 10.3233/RNN-2011-0582

Buttkus, F., Weidenmüller, M., Schneider, S., Jabusch, H. C., Nitsche, M. A., Paulus, W., et al. (2010). Failure of cathodal direct current stimulation to improve fine motor control in musician's dystonia. *Mov. Disord. Off. J. Mov. Disord. Soc.* 25, 389–394. doi: 10.1002/mds.22938

Byl, N. N. (2007). Learning-based animal models: task-specific focal hand dystonia. *ILAR J.* 48, 411–431. doi: 10.1093/ilar.48.4.411

Cho, C. B., Park, H. K., Lee, K. J., and Rha, H. K. (2009). Thalamic deep brain stimulation for Writer's Cramp. *J. Korean Neurosurg. Soc.* 46:52. doi: 10.3340/jkns.2009.46.1.52

Cho, H. J., and Hallett, M. (2016). Non-invasive brain stimulation for treatment of focal hand dystonia: update and future direction. *J. Mov. Disord.* 9, 55–62. doi: 10.14802/jmd.16014

Cogiamanian, F., Barbieri, S., and Priori, A. (2009). Novel nonpharmacologic perspectives for the treatment of task-specific focal hand dystonia. *J. Hand Ther.* 22, 156–161. doi: 10.1016/j.jht.2008.11.008

Delnooz, C. C. S., Helmich, R. C., Medendorp, W. P., Van de Warrenburg, B. P. C., and Toni, I. (2012). Writer's cramp: increased dorsal premotor activity during intended writing. *Hum. Brain Mapp.* 34, 613–625. doi: 10.1002/hbm.21464

Edwards, M. J., Talelli, P., and Rothwell, J. C. (2008). Clinical applications of transcranial magnetic stimulation in patients with movement disorders. *Lancet Neurol.* 7, 827–840. doi: 10.1016/S1474-4422(08)70190-X

Fahn, S. (1989). "Assessment of the primary dystonias," in *Quantification of Neurologic Deficit*, ed T. Munsat (Oxford: Butterworths), 241–270.

Ferrucci, R., Mameli, F., Guidi, I., Mrakic-Sposta, S., Vergari, M., Marceglia, S., et al. (2008a). Transcranial direct current stimulation improves recognition memory in Alzheimer disease. *Neurology* 71, 493–498. doi: 10.1212/01.wnl.0000317060.43722.a3

Ferrucci, R., Marceglia, S., Vergari, M., Cogiamanian, F., Mrakic-Sposta, S., Mameli, F., et al. (2008b). Cerebellar transcranial direct current stimulation impairs the practice-dependent proficiency increase in working memory. *J. Cogn. Neurosci.* 20, 1687–1697. doi: 10.1162/jocn.2008.20112

Fregni, F., Boggio, P. S., Lima, M. C., Ferreira, M. J. L., Wagner, T., Rigonatti, S. P., et al. (2006). A sham-controlled, phase II trial of transcranial direct current stimulation for the treatment of central pain in traumatic spinal cord injury. *Pain* 122, 197–209. doi: 10.1016/j.pain.2006.02.023

Furuya, S., and Altenmüller, E. (2015). Acquisition and reacquisition of motor coordination in musicians: virtuosity and disorder of musicians. *Ann. N.Y. Acad. Sci.* 1337, 118–124. doi: 10.1111/nyas.12659

Furuya, S., Nitsche, M. A., Paulus, W., and Altenmüller, E. (2014). Surmounting retraining limits in Musicians' dystonia by transcranial stimulation: noninvasive stimulation for FD. *Ann. Neurol.* 75, 700–707. doi: 10.1002/ana.24151

Garraux, G., Bauer, A., Hanakawa, T., Wu, T., Kansaku, K., and Hallett, M. (2004). Changes in brain anatomy in focal hand dystonia. *Ann. Neurol.* 55, 736–739. doi: 10.1002/ana.20113

Gentner, R., Gorges, S., Weise, D., aufm Kampe, K., Buttmann, M., and Classen, J. (2010). Encoding of motor skill in the corticomuscular system of musicians. *Curr. Biol.* 20, 1869–1874. doi: 10.1016/j.cub.2010.09.045

Hallett, M., Benecke, R., Blitzer, A., and Comella, C. L. (2009). Treatment of focal dystonias with botulinum neurotoxin. *Toxicon* 54, 628–633. doi: 10.1016/j.toxicon.2008.12.008

Hinkley, L. B. N., Webster, R. L., Byl, N. N., and Nagarajan, S. S. (2009). Neuroimaging characteristics of patients with focal hand dystonia. *J. Hand Ther.* 22, 125–134. doi: 10.1016/j.jht.2008.11.002

Karni, A., Meyer, G., Jezzard, P., Adams, M. M., Turner, R., and Ungerleider, L. G. (1995). Functional MRI evidence for adult motor cortex plasticity during motor skill learning. *Nature* 377, 155–158. doi: 10.1038/377155a0

Konczak, J., and Abbruzzese, G. (2013). Focal dystonia in musicians: linking motor symptoms to somatosensory dysfunction. *Front. Hum. Neurosci.* 7:297. doi: 10.3389/fnhum.2013.00297

Lee, A., Schoonderwaldt, E., Chadde, M., and Altenmüller, E. (2015). Analysis of dystonic tremor in musicians using empirical mode decomposition. *Clin. Neurophysiol.* 126, 147–153. doi: 10.1016/j.clinph.2014.04.013

Lefaucheur, J.-P., Antal, A., Ayache, S. S., Benninger, D. H., Brunelin, J., Cogiamanian, F., et al. (2017). Evidence-based guidelines on the therapeutic use of transcranial direct current stimulation (tDCS). *Clin. Neurophysiol.* 128, 56–92. doi: 10.1016/j.clinph.2016.10.087

Liebetanz, D., Koch, R., Mayenfels, S., König, F., Paulus, W., and Nitsche, M. A. (2009). Safety limits of cathodal transcranial direct current stimulation in rats. *Clin. Neurophysiol.* 120, 1161–1167. doi: 10.1016/j.clinph.2009.01.022

Lungu, C., and Ahmad, O. (2016). Update on the use of botulinum toxin therapy for focal and task-specific dystonias. *Semin. Neurol.* 36, 41–46. doi: 10.1055/s-0035-1571211

MacKinnon, S. E. (2002). Pathophysiology of nerve compression. *Hand Clin.* 18, 231–241. doi: 10.1016/S0749-0712(01)00012-9

Monti, A., Cogiamanian, F., Marceglia, S., Ferrucci, R., Mameli, F., Mrakic-Sposta, S., et al. (2008). Improved naming after transcranial direct current stimulation in aphasia. *J. Neurol. Neurosurg. Psychiatr.* 79, 451–453. doi: 10.1136/jnnp.2007.135277

Mrakic-Sposta, S., Marceglia, S., Mameli, F., Dilena, R., Tadini, L., and Priori, A. (2008). Transcranial direct current stimulation in two patients with Tourette syndrome. *Mov. Disord.* 23, 2259–2261. doi: 10.1002/mds.22292

Nitsche, M. A., Liebetanz, D., Lang, N., Antal, A., Tergau, F., and Paulus, W. (2003a). Safety criteria for transcranial direct current

stimulation (tDCS) in humans. *Clin. Neurophysiol.* 114, 2220–2222. doi: 10.1016/S1388-2457(03)00235-9

Nitsche, M. A., Nitsche, M. S., Klein, C. C., Tergau, F., Rothwell, J. C., and Paulus, W. (2003b). Level of action of cathodal DC polarisation induced inhibition of the human motor cortex. *Clin. Neurophysiol.* 114, 600–604. doi: 10.1016/S1388-2457(02)00412-1

Nitsche, M. A., and Paulus, W. (2000). Excitability changes induced in the human motor cortex by weak transcranial direct current stimulation. *J. Physiol.* 527(Pt 3), 633–639. doi: 10.1111/j.1469-7793.2000.t01-1-00633.x

Pixa, N. H., Steinberg, F., and Doppelmayr, M. (2017). Effects of high-definition anodal transcranial direct current stimulation applied simultaneously to both primary motor cortices on bimanual sensorimotor performance. *Front. Behav. Neurosci.* 11:130. doi: 10.3389/fnbeh.2017.00130

Priori, A. (2003). Brain polarization in humans: a reappraisal of an old tool for prolonged non-invasive modulation of brain excitability. *Clin. Neurophysiol.* 114, 589–595. doi: 10.1016/S1388-2457(02)00437-6

Priori, A., Mameli, F., Cogiamanian, F., Marceglia, S., Tiriticco, M., Mrakic-Sposta, S., et al. (2008). Lie-specific involvement of dorsolateral prefrontal cortex in deception. *Cereb. Cortex* 18, 451–455. doi: 10.1093/cercor/bhm088

Priori, A., Pesenti, A., Cappellari, A., Scarlato, G., and Barbieri, S. (2001). Limb immobilization for the treatment of focal occupational dystonia. *Neurology* 57, 405–409. doi: 10.1212/WNL.57.3.405

Quartarone, A., Rizzo, V., Bagnato, S., Morgante, F., Sant'Angelo, A., Romano, M., et al. (2005). Homeostatic-like plasticity of the primary motor hand area is impaired in focal hand dystonia. *Brain J. Neurol.* 128, 1943–1950. doi: 10.1093/brain/awh527

Rosset-Llobet, J., Candia, V., Fàbregas i Molas, S., Dolors Rosinés i Cubells, D., and Pascual-Leone, A. (2009). The challenge of diagnosing focal hand dystonia in musicians. *Eur. J. Neurol.* 16, 864–869. doi: 10.1111/j.1468-1331.2009.02610.x

Rosset-Llobet, J., Fàbregas-Molas, S., and Pascual-Leone, Á. (2015). Effect of transcranial direct current stimulation on neurorehabilitation of task-specific dystonia: a double-blind, randomized clinical trial. *Med. Probl. Perform. Art.* 30, 178–184.

Sadnicka, A., Hamada, M., Bhatia, K. P., Rothwell, J. C., and Edwards, M. J. (2014). Cerebellar stimulation fails to modulate motor cortex plasticity in writing dystonia. *Mov. Disord.* 29, 1304–1307. doi: 10.1002/mds.25881

Sanavio, E., and Vidotto, G. (Eds.). (1996). *CBA-2.0: 10 Anni di Ricerche*. Torino: Upsel.

Stahl, C. M., and Frucht, S. J. (2017). Focal task specific dystonia: a review and update. *J. Neurol.* 264, 1536–1541. doi: 10.1007/s00415-016-8373-z

Trompetto, C., Avanzino, L., Bove, M., Marinelli, L., Molfetta, L., Trentini, R., et al. (2009). External shock waves therapy in dystonia: preliminary results. *Eur. J. Neurol.* 16, 517–521. doi: 10.1111/j.1468-1331.2008.02525.x

Tubiana, R., and Chamagne, P. (1983). Occupational "cramps" of the upper limb. *Ann. Chir. Main* 2, 134–142. doi: 10.1016/S0753-9053(83)80091-X

Zeuner, K. E., and Molloy, F. M. (2008). Abnormal reorganization in focal hand dystonia–sensory and motor training programs to retrain cortical function. *Neurorehabilitation* 23, 43–53.

Zhao, H., Qiao, L., Fan, D., Zhang, S., Turel, O., Li, Y., et al. (2017). Modulation of brain activity with noninvasive transcranial direct current stimulation (tdcs): clinical applications and safety concerns. *Front. Psychol.* 8:685. doi: 10.3389/fpsyg.2017.00685

Conflict of Interest Statement: SM, SMS, RF, MF, MV, and AP are co-founders of Newronika srl, a spin-off company of the Fondazione IRCCS Ca' Granda Ospedale Maggiore Policlinico and the University of Milan, Milan, Italy.

The other authors declare that the research was conducted in the absence of any commercial or financial relationships that could be construed as a potential conflict of interest.

frontiers in Neuroscience

MINI REVIEW
published: 13 December 2017
doi: 10.3389/fnins.2017.00710

Remodeling Functional Connectivity in Multiple Sclerosis: A Challenging Therapeutic Approach

Mario Stampanoni Bassi[1,2], *Luana Gilio*[1,2], *Fabio Buttari*[1,2], *Pierpaolo Maffei*[1], *Girolama A. Marfia*[2], *Domenico A. Restivo*[3], *Diego Centonze*[1,2*] *and Ennio Iezzi*[1]

[1] *Unit of Neurology & Unit of Neurorehabilitation, IRCCS Istituto Neurologico Mediterraneo Neuromed, Pozzilli, Italy,* [2] *Multiple Sclerosis Research Unit, Department of Systems Medicine, Tor Vergata University, Rome, Italy,* [3] *Department of Neurology, Nuovo Garibaldi Hospital, Catania, Italy*

Neurons in the central nervous system are organized in functional units interconnected to form complex networks. Acute and chronic brain damage disrupts brain connectivity producing neurological signs and/or symptoms. In several neurological diseases, particularly in Multiple Sclerosis (MS), structural imaging studies cannot always demonstrate a clear association between lesion site and clinical disability, originating the "clinico-radiological paradox." The discrepancy between structural damage and disability can be explained by a complex network perspective. Both brain networks architecture and synaptic plasticity may play important roles in modulating brain networks efficiency after brain damage. In particular, long-term potentiation (LTP) may occur in surviving neurons to compensate network disconnection. In MS, inflammatory cytokines dramatically interfere with synaptic transmission and plasticity. Importantly, in addition to acute and chronic structural damage, inflammation could contribute to reduce brain networks efficiency in MS leading to worse clinical recovery after a relapse and worse disease progression. These evidence suggest that removing inflammation should represent the main therapeutic target in MS; moreover, as synaptic plasticity is particularly altered by inflammation, specific strategies aimed at promoting LTP mechanisms could be effective for enhancing clinical recovery. Modulation of plasticity with different non-invasive brain stimulation (NIBS) techniques has been used to promote recovery of MS symptoms. Better knowledge of features inducing brain disconnection in MS is crucial to design specific strategies to promote recovery and use NIBS with an increasingly tailored approach.

Keywords: multiple sclerosis, inflammation, brain networks, functional connectivity, synaptic plasticity, non-invasive brain stimulation

OPEN ACCESS

Edited by:
Takashi Hanakawa, National Center of Neurology and Psychiatry, Japan

Reviewed by:
Kazumasa Uehara, Arizona State University, United States
Katsuya Ogata, Kyushu University, Japan

***Correspondence:**
Diego Centonze
centonze@uniroma2.it

Specialty section:
This article was submitted to Neural Technology, a section of the journal Frontiers in Neuroscience

Received: *06 October 2017*
Accepted: *04 December 2017*
Published: *13 December 2017*

Citation:
Stampanoni Bassi M, Gilio L, Buttari F, Maffei P, Marfia GA, Restivo DA, Centonze D and Iezzi E (2017) Remodeling Functional Connectivity in Multiple Sclerosis: A Challenging Therapeutic Approach. Front. Neurosci. 11:710. doi: 10.3389/fnins.2017.00710

INTRODUCTION

Multiple Sclerosis (MS) is an autoimmune inflammatory disease of the central nervous system (CNS) characterized by white matter demyelinating lesions and gray matter atrophy. MS represents one of the most frequent neurological condition associated with clinical disability in young adults. Symptoms include a huge range of manifestations such as motor/sensory deficits, fatigue, spasticity, cognitive dysfunction, and pain, related to the different neural systems involved. In several

neurological disorders, and particularly in MS, structural imaging studies hardly demonstrate clear associations between lesion site and clinical disability. The peculiar discordance between radiological and clinical features is usually referred to as the "clinico-radiological paradox" (Barkhof, 2002). The remote effects of a brain lesion on functionally connected regions and the ongoing rearrangement produced by synaptic plasticity in response to brain damage can concur in determining the discrepancy between structural damage and clinical symptoms.

The concept of diaschisis (von Monakow, 1914; Feeney and Baron, 1986) refers to focal changes in metabolism or neuronal activity in anatomically intact brain regions located away from the lesion (Carrera and Tononi, 2014). Recently, the concept of diaschisis has been applied to complex networks analysis. The connectome is defined as an overall map of neural connections in the brain (Sporns et al., 2005) represented by a set of nodes (i.e., graphs) joined by lines depicted between them (Bullmore and Bassett, 2011). It is possible to explore how network activity is changed by a lesion relying upon its topography within the network architecture (Honey and Sporns, 2008; Alstott et al., 2009; Joyce et al., 2013). Accordingly, the term "connectomal diaschisis" refers to changes in the structural and functional connectome, including disconnections between and reorganization of subgraphs, involving areas located away from the lesion (Carrera and Tononi, 2014). A better definition of diaschisis could contribute to clarify the clinico-radiological paradox in neurological disorders. Understanding how lesions alter brain networks could help to select the appropriate treatment based on the underlying process. However, it is challenging to ascertain whether remote connectivity changes occur following diaschisis or rely on other recovery mechanisms, such as plasticity (either positive or maladaptive) and vicariation (Carrera and Tononi, 2014).

Clinical improvement after brain lesions mainly depends on structural and functional connectivity restoring. Synaptic plasticity is the main mechanism involved, both promoting spontaneous recovery and mediating the beneficial effects of rehabilitation. Non-invasive brain stimulation (NIBS) techniques such as repetitive transcranial magnetic stimulation (rTMS) and transcranial direct current stimulation (tDCS) perturbing local neural activity can subsequently affect the function of distributed brain regions located away from the stimulated area. Therefore, NIBS can be successfully used for testing and modulating brain networks dynamics in physiological and in a number of neuropsychiatric conditions (Shafi et al., 2012).

A number of studies suggest that inflammatory molecules released during MS relapses alter neuronal functioning acting both on synaptic transmission and plasticity (Stampanoni Bassi et al., 2017b). It is therefore reasonable to assume that inflammation in MS could disrupt brain connectivity, even regardless of demyelinating white matter lesions and gray matter atrophy. In addition, as inflammation could restrain brain network reorganization inducing synaptic plasticity alterations, promoting beneficial synaptic plasticity through NIBS could represent a promising therapeutic approach in MS.

In this paper, the main studies exploring brain connectivity in MS with different techniques will be overviewed. We performed a literature search in PubMed in August 2017 using the terms "connectivity" and "multiple sclerosis." We looked for original case-control studies, case series, or cohort studies. We also examined many of the references of the articles found. We excluded studies not available in English language, studies conducted in animals, studies published more than 10 years before, and studies including patients with age <18 years. We will also overview the alterations of synaptic transmission and plasticity described in a MS experimental model (i.e., experimental autoimmune encephalomyelitis, EAE) and in human MS using TMS. The findings supporting the role of inflammation in inducing connectivity dysfunction and the possible role of NIBS in promoting beneficial connectivity for recovery will be discussed.

CONNECTIVITY IN MS

In MS, alterations of brain connectivity have been studied with different techniques. TMS has been used to test cortico-cortical connectivity, checking how a stimulus delivered on a given brain region can influence the excitability of a different region and providing information on effective connectivity (Gerstein and Aertsen, 1985; Friston et al., 1993). Inhibitory connectivity between homologous regions of both primary motor cortices (M1) has been assessed using either a single coil or a double-coil (d-c) approach (**Figure 1**). With a single suprathreshold magnetic pulse given over M1, it is possible to induce inhibitory influences in the contralateral M1 measurable as a suppression of the tonic muscle voluntary activity ipsilateral to the stimulated cortex (ipsilateral silent period, iSP; Wassermann et al., 1991). Interhemispheric inhibition (IHI) can be also studied with d-c TMS when a suprathreshold stimulus delivered over one M1 is able to suppress the test response elicited by a suprathreshold stimulus given over the contralateral M1 at short (10 ms) or longer (40 ms) interstimulus intervals (Ferbert et al., 1992; Murase et al., 2004; Uehara et al., 2013). The two subtypes of IHI are likely mediated by different physiological mechanisms, both depending on GABAB transmission (Kukaswadia et al., 2005; Radhu et al., 2012). IHI40 could depend on an overlapping population of inhibitory neurons activated by the excitatory input from the contralateral M1 (Kukaswadia et al., 2005) whereas IHI10 may be mediated by transcallosal fibers passing through the posterior body and the isthmus of the corpus callosum (CC, Ni et al., 2009). In MS, owing to high prevalence of lesions within the CC, most TMS approaches mainly focused on interhemispheric connectivity (Boroojerdi et al., 1998; Schmierer et al., 2000; Codecà et al., 2010; Wahl et al., 2011). In MS, altered iSP correlated with clinical disability (Schmierer et al., 2000, 2002; Llufriu et al., 2012; Neva et al., 2016) and with central motor conduction time prolongation (Jung et al., 2006). Whereas, some studies showed a correlation between CC lesions and iSP alterations (Lenzi et al., 2007; Llufriu et al., 2012), other studies found that reduced iSP did not correlate with magnetic resonance imaging (MRI) alterations of the CC (Jung et al., 2006). One study reported reduced IHI in early RR-MS even without detectable CC lesions at conventional MRI, making IHI

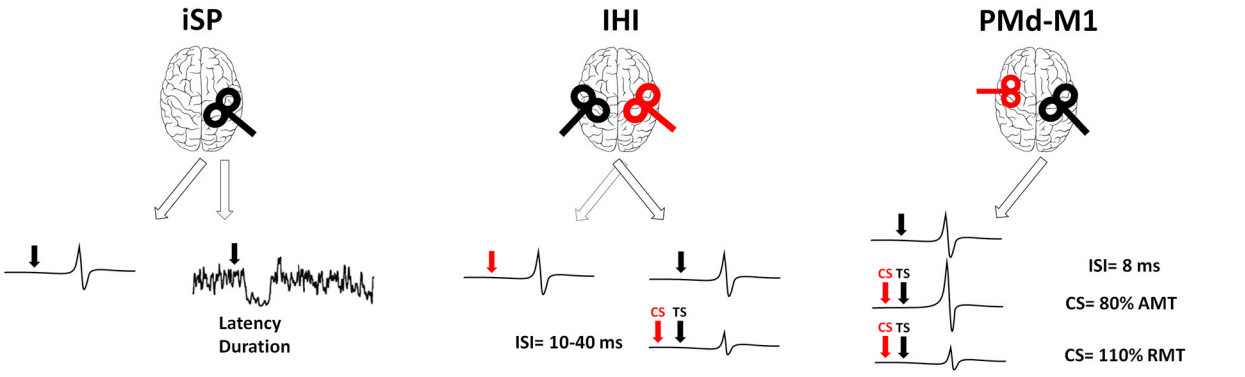

- Slower transcallosal conduction in MS patients ***(Boroojerdi et al., 1998)***
- Abnormalities of iSP in 80% of MS patients ***(Schmirer et al., 2000)***
- Abnormal iSP and CMCT correlated with EDSS. In PP-MS patients only altered iSP correlated with EDSS ***(Schmirer et al., 2002)***
- iSP duration correlated with CMCT and did not correlate with MRI alterations of the CC ***(Jung et al., 2006)***
- iSP duration was negatively correlated with activation in the iM1 on fMRI. iM1 activation correlated with T1-LL and CC alterations ***(Lenzi et al., 2007).***
- iSP latency correlated with EDSS and SDMT. iSP latency correlated with CC area and volume ***(Llufriu et a., 2012).***

- IHI_{10} was reduced in early RR-MS compared with HC. The correlation between CC microstructure and IHI_{10} observed in HC was lacking in MS. These alterations were observed in the absence of macroscopic CC lesions, motor hand/arm dysfunction in the nine-hole-peg test and prolonged CMCT ***(Wahl et al., 2011)***

- MS patients had reduced facilitation compared with HS. Only disabled MS patients showed less inhibition. PMd–M1 interactions did not differ between patients with or without lesions in the CC ***(Codecà et al., 2010)***

FIGURE 1 | Results of the main studies investigating interhemispheric connections in MS. Red coils and arrows represent CS, black coils and arrows depict TS. AMT, active motor threshold; CC, corpus callosum; CMCT, central motor conduction time; CS, conditioning stimulus; EDSS, expanded disability status scale; fMRI, functional magnetic resonance imaging; HC, healthy controls; IHI, interhemispheric inhibition; iM1, ipsilateral primary motor cortex; ISI, interstimulus interval; iSP, ipsilateral silent period; M1, primary motor cortex; PMd, dorsal premotor cortex; PP-MS, primary progressive multiple sclerosis; RMT, resting motor threshold; RR-MS, relapsing-remitting multiple sclerosis; SDMT, symbol digit modality test; T1-LL, T1 lesion load; TS, test stimulus.

failure a possible marker of callosal disconnection also at earlier disease stages (Wahl et al., 2011). Finally, altered connectivity between dorsal premotor cortex and contralateral M1 suggests that also excitatory transcallosal connectivity may be impaired independently of lesion load and site, and even in the absence of clinical disability (Codecà et al., 2010).

Recently, functional MRI (fMRI) gave the opportunity to study the activity of a large number of brain regions. FMRI is a tool able to reveal dynamic changes in brain tissue occurring whilst the subject is awake and fully relaxed (i.e., resting state fMRI, rs-fMRI), or in response to specific behavioral tasks (i.e., task-based fMRI). In MS, task-based fMRI showed increased and widespread brain activations compared to healthy controls, particularly at disease onset (Rocca et al., 2005). Increased activation is generally interpreted as adaptive plastic changes aimed at preventing the clinical manifestations (Pantano et al., 2006; Filippi and Rocca, 2013). Nevertheless, overactivation does not consequently denote adaptive plasticity, as it may be associated to high disability. For instance, diffuse microstructural damage—as shown by combined diffusion tensor imaging (DTI) and fMRI- correlated with increased sensorimotor network activation (Rocca et al., 2002; Lenzi et al., 2007). Intriguingly, increased activation of ipsilateral M1 during hand movements correlated with CC damage and loss of transcallosal inhibition (Lenzi et al., 2007) suggesting that ipsilateral M1 hyperactivation could likely represent a simple epiphenomenon of disease.

The development of methods testing brain connectivity at rest helped to avoid behavioral confounding related to task. In particular, the temporal correlation between neural or hemodynamic spontaneous activity arising from distinct brain regions, namely functional connectivity (FC), describes the intrinsic property of a given area or the influences of a particular area over another region, independently of external stimuli (Biswal et al., 1995; Fox and Raichle, 2007; van den Heuvel and Hulshoff Pol, 2010). In brain networks analysis different types of connectivity can be explored. Structural connectivity is usually referred to the anatomical connections and is evaluated by fiber tractography from DTI to obtain a reliable map of anatomical connection between brain areas. The relationship between structural and functional brain networks has not been yet completely elucidated (Rubinov et al., 2009; Honey et al., 2010; Ponten et al., 2010). Whereas, areas anatomically connected show a greater FC (Honey et al., 2007, 2009; Rubinov et al., 2009; Hermundstad et al., 2013), functional interactions are not limited to directly connected areas (Honey et al., 2007, 2009). A better definition of the complex relationship between structural and

functional brain networks could predict how structural damage alters network dynamics (Honey and Sporns, 2008; Kaiser, 2013; van Dellen et al., 2013).

In MS, several studies have described rs-fMRI alterations involving different networks. Increased or decreased FC have been related to disease phenotype, clinical characteristics and neuroradiological findings (**Table 1**). Overall, findings apparently contrast likely due to different methodological approaches, and different clinical phenotypes. In addition, whether FC changes could be compensatory or maladaptive is not yet clear. Longitudinal studies or combining different experimental techniques could contribute to clarify the clinical implications of connectivity changes in MS. In addition, standardized measures should be properly identified to predict the effect of damage, evaluate symptoms evolution and compare the effect of different treatment protocols. Recently, graph based rs-fMRI studies showed that analyzing properties of large-scale brain networks could help to identify reliable measures of brain network functioning. Parameters such as clustering coefficient, path length, network centrality, and modularity, show that brain networks magnify cost efficiency of parallel information processing (Achard and Bullmore, 2007). Moreover, these properties contribute to protect networks from damage (Achard et al., 2006; Achard and Bullmore, 2007). Accordingly, clinical symptoms may occur in MS when structural damage raises to a critical level reducing overall network efficiency (Schoonheim et al., 2015).

INFLAMMATION ALTERS SYNAPTIC TRANSMISSION AND BRAIN CONNECTIVITY

In MS, brain connectivity disruption could rely on the acute and chronic structural damage and also on inflammation. In MS experimental models, inflammatory cytokines induce alterations of synaptic transmission of both glutamatergic and GABAergic transmission, causing synaptic hyperexcitability (Rossi et al., 2011; Mandolesi et al., 2013; Stampanoni Bassi et al., 2017a). Interleukin (IL)-1β represents one of the main inflammatory cytokines involved (Mandolesi et al., 2013).

Synaptic transmission can be explored in humans with TMS and specific protocols are related to different features of synaptic transmission (Ziemann et al., 2008; Rossini et al., 2015). Studies in MS showed that the same inflammatory cytokines induce synaptic alterations similar to those seen in EAE (Rossi et al., 2012a); moreover, the magnitude of these alterations correlated with CNS levels of IL-1β. Furthermore, cerebrospinal fluid from MS patients in active phase of the disease reproduced *in vitro* both the glutamatergic and GABAergic alterations and the neuronal degeneration observed in EAE (Rossi et al., 2012a,b). In addition, different phases and disease phenotypes are associated to specific patterns of alterations. In particular, the relapsing phase of MS is characterized by cortical disinhibition as indexed by reduced contralateral silent period duration and reduced short-interval intracortical inhibition (Caramia et al., 2004).

As inflammatory cytokines alter synaptic functioning, a direct role of neuroinflammation in connectivity dysfunction occurring in MS may be hypothesized. To support this view, few studies showed that in patients with clinically isolated syndrome (CIS) significant FC alterations develop even without white matter lesions or brain atrophy. One study showed significant rs-fMRI changes in a group of patients with CIS manifesting as acute optic neuritis, involving both left and right primary visual cortices and extravisual regions (Wu et al., 2015). Another study explored FC alterations in a group of RR-MS patients and in a group of patients with CIS without brain lesions (Liu et al., 2016), including patients with optic neuritis or spinal cord syndromes. CIS patients showed significantly decreased FC in the visual areas and increased FC in the temporal lobes. It should be highlighted that in both studies altered FC developed also in networks other than the visual system, likely suggesting that acute inflammation may induce diffuse connectivity changes.

It is important to mention another study exploring FC in CIS and RR-MS patients considering graph-based network analysis (Liu et al., 2017). As expected, in RR-MS patients decreased whole brain network efficiency, reduced nodal efficiency, and impaired FC were found. In addition, patients with CIS displayed a similar pattern of alterations. In particular, impaired FC involved the occipital, temporal, and frontal cortices and the insula. Finally, changes in RR-MS did not correlate with white matter lesion load and site, and with gray matter atrophy.

A number of studies showed that also systemic inflammation could affect brain FC. For instance, in healthy individuals, experimental inflammation influences brain activity in the insula and in the cingulate cortex (Hannestad et al., 2012) and alters resting connectivity between the left thalamus and the right posterior cingulate cortex (Labrenz et al., 2016). Furthermore, a study using graph analysis showed that in patients with Hepatitis C the administration of IFN α reduced whole brain network connectivity and efficiency (Dipasquale et al., 2016). Recently, a study showed that IL-6 blood levels covaried with connectivity in the default mode network (Marsland et al., 2017). These studies are in line with previous reports showing that peripheral cytokines may modulate central synaptic transmission altering task-based fMRI (Capuron et al., 2005; Harrison et al., 2009).

Overall, these data suggest that inflammation in MS, altering synaptic transmission, may represent an additional key feature contributing to network dysfunction. It may be hypothesized that, in addition to structural damage, network efficiency can be dramatically disrupted by inflammatory cytokines.

INFLAMMATION, SYNAPTIC PLASTICITY, AND CLINICAL RECOVERY

Recovery after brain injury mainly depends on the ability of surviving neurons to undergo long-term functional changes (Floel and Cohen, 2006). Long-term potentiation (LTP), the most studied form of synaptic plasticity, consists of enduring enhancement of synaptic strength followed by structural rearrangements (Bliss and Gardner-Medwin, 1973). LTP can be virtually induced in all brain areas and may reduce the clinical

TABLE 1 | Main results of studies investigating rs-FC in MS.

Authors	Study population	Main findings
Roosendaal et al., 2010	14 CIS, 31 RR-MS, 41 HCs	Increased rs-FC in several RSNs, including the DMN and sensorimotor network, in CIS compared to HCs and RR-MS. In RR-MS GM atrophy and abnormal WM diffusivity compared to HCs. No changes in CIS. rs-FC and structural MRI or clinical disability did not correlate in CIS and RR-MS.
Rocca et al., 2010	33 SP-MS (18 CI), 24 PP-MS (12 CI), 24 HCs	In SP-MS reduced activity in the DMN, in the medial prefrontal cortex and precentral gyrus, compared with HCs. In PP-MS reduced activity in the precentral gyrus and the ACC compared with HCs. In SP-MS increased ACC activity compared with PP-MS. RS activity in the ACC was reduced particularly in CI. DMN abnormalities correlated with cognitive test and DTI changes in the CC and the cingulum.
Bonavita et al., 2011	36 RR-MS (18 CI and 18 CP), 18 HCs	In RR-MS reduced DMN connectivity in the ACC, reduced in the core and increased at the periphery of the PCC. No correlations between FC changes and global atrophy or T2-LL, but association with regional GM loss. The findings were more marked in CP than CI.
Faivre et al., 2012	13 early RR-MS, 14 HCs	Increased rs-FC in several RSNs in early RR-MS compared with HCs. No correlations between RSNs connectivity and T2-LL or disease duration. Increased rs-FC in cognitive and sensorimotor networks negatively correlated with different cognitive and motor tasks and MSFC scores.
Rocca et al., 2012	85 RR-MS, 40 HCs	In RR-MS decreased rs-FC in different RSNs (salience, executive control, working memory, default mode, sensorimotor, and visual) and increased rs-FC in regions of the executive control and auditory RSNs. Decreased rs-FC was correlated with disability and T2 lesion volumes.
Tona et al., 2014	48 RR-MS, 24 HCs	In RR-MS both increased and decreased connectivity within the thalamic RSN. No significant correlation between thalamic FC and radiologic variables. Increased thalamocortical FC correlated with decreased cognitive performance.
Cruz-Gómez et al., 2014	60 RR-MS (30 CI and 30 CP), 18 HCs	Decreased rs-FC in the DMN in CI compared with CP and HCs. Decreased rs-FC in the LFPN in both CI and CP compared with HCs. Decreased rs-FC in the RFPN and salience network in CI compared with CP. BPF correlated with rs-FC in the DMN, LFPN and RFPN. T1-LL negatively correlated with rs-FC in all explored RSNs.
Louapre et al., 2014	35 RR-MS (15 CI and 20 CP), 20 HCs	In CI decreased rs-FC in DMN and ATT compared with CP. In CI decreased rs-FC particularly between the medial prefrontal cortex and the PCC, predicted by PCC atrophy. In CI higher WM LL and more severe GM atrophy in cognitive networks compared with CP. In CP increased rs-FC in ATT compared with HCs.
Zhou et al., 2014	24 RR-MS and 24 HC	The connections of paired DMN subregions showed decreased SC and increased FC in RR-MS patients. SC alterations correlated with EDSS. Decreased SC was correlated to atrophy.
Rocca et al., 2015	69 CP MS, 42 HCs	In CP MS decreased rs-FC between the hippocampi and several cortical–subcortical regions within the DMN. Reduced hippocampal rs-FC correlated with T2-LL, disease duration, depression and disability.
Sbardella et al., 2015	30 RR-MS and 24 HCs	In RR-MS decreased rs-FC in several networks (cerebellar, executive-control, medial-visual, basal ganglia and sensorimotor) and changes in inter-network correlations. CC microstructural damage correlated with FC in cerebellar and auditory networks. No correlations between rs-FC in all explored RSNs and T2-LL.
Liu et al., 2015	35 RR-MS, 35 HC	Compared to HC, the MS group showed significantly decreased FC between thalamus and several brain regions including right middle frontal and parahippocampal gyri, and the left inferior parietal lobule. Increased intra and inter-thalamic FC was observed in MS compared to HC. FC alterations were not correlated with T2-LL, thalamic volume or the presence of thalamic lesions.
Baltruschat et al., 2015	17 RR-MS, 15 HCs	In RR-MS increased FC between left posterior cingulate gyrus/precuneus, and left middle temporal gyrus and left cerebellum. In RR-MS GM bilateral atrophy in posterior cingulate gyrus/precuneus. BPF negatively correlated with FC between left posterior cingulate gyrus/precuneus and left cerebellum.
Rocca et al., 2016	214 MS patients (RR-MS and SP-MS), 55 HC	Global network properties (network degree, global efficiency, hierarchy, path length and assortativity) were abnormal in MS compared with HC and contributed to distinguish CI MS patients from HC, but not the main MS phenotypes. In MS, global and regional network properties were not correlated with T2-LL and normalized brain volume.
d'Ambrosio et al., 2017	187 MS patients (136 RR-MS, 42 SP-MS and 9 PP- MS), (122 CP and 65 CI); 94 HCs	In patients lower GM, WM and thalamic volumes compared with HCs. In patients decreased rs-FC between thalamic subregions and the caudate, cingulate cortex and cerebellum correlated with worse motor performance. Increased rs-FC with the insula correlated with better motor performance. In CI increased rs-FC between thalamic subregions and temporal areas compared with CP. No correlations between thalamic rs-FC and T2-LL.

ACC, anterior cingulate cortex; ATT, attentional network; CC, corpus callosum; CI, cognitive-impaired patients; CIS, clinically isolated syndrome; CP, cognitive-preserved patients; DMN, Default Mode Network; DTI, Diffusion Tensor Imaging; FC, functional connectivity; GM, gray matter; HCs, healthy controls; LFPN, left fronto-parietal network; LL, lesion load; MRI, Magnetic Resonance Imaging; MS, Multiple Sclerosis; MSFC, Multiple Sclerosis Functional Composite Score; PCC, posterior cingulate cortex; PP-MS, primary-progressive MS patients; RFPN, right fronto-parietal network; RR-MS, relapsing-remitting MS patients; rs-FC, resting-state Functional Connectivity; RSN, resting state network; SC, structural connectivity; SP-MS, secondary-progressive MS patients; WM, white matter.

expression of neuronal damage likely restoring the excitability of neurons deprived of their synaptic inputs. Promoting LTP could therefore contribute to maximize network efficiency restoring, delaying the clinical expression of brain damage. The link between LTP and clinical recovery after acute brain lesion first came from animal studies. In rats, neurological deficit after experimental ischemia partly improved 7 days after the infarction and correlated with increased glutamatergic excitatory transmission in surviving neurons, suggesting that recovery was driven by increased excitatory synaptic activity surrounding

the damaged area (Centonze et al., 2007c). In humans, the evidence that LTP could be crucial for clinical recovery was first showed in acute stroke patients, comparing the amount of TMS-induced LTP-like plasticity with the degree of recovery 6 months later. Patients with higher TMS-induced LTP displayed a better recovery (Di Lazzaro et al., 2010a). Accordingly, the term LTP reserve has been proposed to indicate the amount of LTP induced by different TMS protocols as significant predictor of clinical recovery.

Physical rehabilitation represents the main treatment option to enhance spontaneous recovery of neurological deficits Albeit early rehabilitation after acute brain lesions can facilitate recovery, the optimal treatment type is still poorly defined (Morreale et al., 2016). It is likely that the beneficial effect of rehabilitation could be mediated by LTP, as shown in animals and also in human studies by the findings that learning a motor skill engages LTP mechanisms triggered by motor practice (Rioult-Pedotti et al., 2000; Muellbacher et al., 2001; Ziemann et al., 2004).

Different studies reported alterations of synaptic plasticity in EAE and MS (Mori et al., 2011, 2012; Di Filippo et al., 2013; Nisticò et al., 2013). An early finding was that MS relapses are associated with impaired LTP-like plasticity as assessed with intermittent theta-burst stimulation (iTBS) (Mori et al., 2011). In a further study, iTBS-induced LTP-like plasticity was explored in RR-MS patients either in acute or stable disease phase, confirming that LTP-like plasticity is reduced in relapsing patients compared to remitting patients (Mori et al., 2012) Remarkably, in the same study, 6-months treatment with interferon (IFN) beta 1-a improved LTP-like plasticity in relapsing patients (Mori et al., 2012).

The association between LTP reserve and clinical recovery has been explored in RR-MS patients using the paired associative stimulation protocol (Mori et al., 2014). In this study, LTP reserve tested at the time of a clinical relapse correlated with clinical recovery 3 months later. Patients with greater LTP reserve showed a better recovery whereas patients with absent or poor LTP reserve displayed partial or absent clinical recovery, further suggesting the crucial role of LTP taking place in surviving neurons to compensate coexisting neuronal loss (Mori et al., 2014). Overall, these studies suggest that CNS inflammation in MS patients negatively influences pathways involved in LTP induction and maintenance (Tongiorgi et al., 2012; Stampanoni Bassi et al., 2017a). In addition, some studies suggest that negative impact of acute inflammation on LTP may be reduced by immune-modulating therapies (Mori et al., 2012; Di Filippo et al., 2016). In MS, it is likely that inflammation-induced LTP alterations could lessen brain network reorganization influencing clinical recovery after a relapse and disease progression and that resolving inflammation could positively influence clinical recovery.

NIBS AND SYMPTOMS RECOVERY IN MS

NIBS has been used in healthy subjects for enhancing motor skills and cognitive functions, and in neurological and psychiatric patients for therapeutic purposes (Hummel et al., 2005; Miniussi et al., 2008). Different studies showed that focal perturbation of neural activity by NIBS selectively modulates functional and effective connectivity in different connected networks (Grefkes et al., 2010; Eldaief et al., 2011; Grefkes and Fink, 2011; Cocchi et al., 2016). Furthermore, as inflammation alters synaptic plasticity, boosting LTP through NIBS could help to improve recovery in MS patients.

rTMS and tDCS represent the most commonly used NIBS techniques able to induce LTP-like plasticity (Ziemann et al., 2008). In M1, this plastic effect can be generally measured as an increase of the peak-to-peak amplitude of the motor evoked potentials (MEPs) after the plasticity-inducing protocol, likely coming from enhanced excitability of the cortico-cortical facilitatory synaptic inputs onto the corticospinal cells (Di Lazzaro et al., 2010b). A number of rTMS protocols are able to induce persistent changes in cortical excitability depending on the intensity, frequency and number of stimuli applied, frequency playing a pivotal role. In particular, high-frequency (i.e., $\geq$5 Hz) rTMS protocols produce LTP-like plasticity (Siebner and Rothwell, 2003; Ziemann et al., 2008). Subsequently, new rTMS protocols have been introduced to modulate cortical plasticity, including TBS. In particular, iTBS produces excitatory after-effects through LTP-like plasticity (Huang et al., 2005). tDCS employs weak transcranial currents to induce changes in cortical excitability depending on stimulation polarity (Nitsche and Paulus, 2000). In particular, anodal tDCS may entail LTP-like mechanisms (Liebetanz et al., 2002; Nitsche et al., 2003).

NIBS techniques have been applied to treat different symptoms in MS patients. Spasticity is considered as the consequence of the hyperexcitability of the stretch reflex secondary to corticospinal tract lesions and reduced supraspinal inhibitory input (Young, 1994). In MS, a single session of 5 Hz rTMS over M1 reduced stretch reflex hyperexcitability (Centonze et al., 2007a). Moreover, daily application for 2 weeks of both 5 Hz rTMS and iTBS can be useful to reduce lower limb spasticity in MS (Centonze et al., 2007a; Mori et al., 2010a). Noticeably, one longitudinal study showed that repeated daily iTBS sessions associated with physical rehabilitation may induce functional reorganization of M1 connectivity. In particular, reduced spasticity was associated with both changes in local connectivity and in the inter-hemispheric balance (Boutière et al., 2017). Conversely, one study reported that anodal tDCS on M1 for 5 consecutive days had no clinical impact on spasticity in MS patients (Iodice et al., 2015).

Some studies explored the effects of both anodal tDCS and 5 Hz rTMS over M1 to reduce motor deficits in MS (Koch et al., 2008; Cuypers et al., 2013; Meesen et al., 2014; Elzamarany et al., 2016). It has been shown that 5 Hz rTMS over M1 improved hand dexterity in MS patients with cerebellar symptoms (Koch et al., 2008). Intriguingly, the beneficial effect of high frequency rTMS may have raised from enhanced M1 excitatory drive onto the pontine nuclei modulating the cerebro-pontine-cerebellar network (Schwarz and Thier, 1999) and possibly counteracting the reduced cerebellar inputs to these structures due to demyelination. Similarly, another study showed that two consecutive daily sessions of 5 Hz rTMS on M1

improved hand dexterity in a group of RR and progressive MS patients, with a more pronounced effect in RR-MS (Elzamarany et al., 2016). Of the two studies exploring the effects of anodal tDCS, one study evidenced that anodal tDCS could increase cortico-spinal output (Cuypers et al., 2013) and the other study showed that a single concurrent M1 anodal tDCS session had no beneficial effects on a unimanual motor sequence task in a group of RR-MS and progressive MS (Meesen et al., 2014). In addition, repeated 5 Hz rTMS on M1 for 5 consecutive days over 2 weeks may induce beneficial effects also in other dysfunctions, such as lower urinary tract involvement (Centonze et al., 2007b). Notably, other motor symptoms including gait disturbances may respond to NIBS, as five consecutive sessions of high frequency rTMS over the left dorsolateral prefrontal cortex (DLPFC) improved gait in a RR-MS patient (Burhan et al., 2015).

In MS, neuropathic pain and both positive and negative sensory symptoms, including paresthesia and hypoanestesia, are frequently observed and scarcely responsive to pharmacological treatment. It has been reported that 5 consecutive days of anodal tDCS on M1 may improve neuropathic pain in MS (Mori et al., 2010b). In addition, another study reported that 3 consecutive days of anodal tDCS over the DLPFC reduced neuropathic pain in MS (Ayache et al., 2016). Finally, tactile hypoanesthesia improved in RR-MS after 5 consecutive days of anodal tDCS over the somatosensory cortex (Mori et al., 2013).

Fatigue represents another disabling symptom frequently observed in MS patients, occurring in all disease stages (Krupp and Pollina, 1996; Kos et al., 2004; Lerdal et al., 2007). The nature of fatigue in MS is multifactorial and it has been related to different pathophysiological mechanisms, including structural or functional brain alterations (Ayache and Chalah, 2017). Different studies explored the effects of anodal tDCS on fatigue in MS. The available studies differ in terms of parameters and stimulation sites, including M1 (Ferrucci et al., 2014), somatosensory cortex (Tecchio et al., 2014), left DLPFC (Saiote et al., 2014; Chalah et al., 2015, 2017), and right posterior parietal cortex (Chalah et al., 2017). Overall, whereas the results suggest that tDCS may represent a promising approach to treat fatigue, further studies are needed to define the optimal stimulation parameters and site (Lefaucheur et al., 2017).

Finally, only few studies explored the use of NIBS for treating cognitive deficits associated with MS. One study showed that 10 daily sessions of anodal tDCS over the left DLPFC significantly improved concurrent cognitive training (Mattioli et al., 2016). Another study explored the effects of 5 Hz rTMS over the right DLPFC on working memory deficits (Hulst et al., 2016). In that study, cognitive performance improvement was associated with a reduced aberrant hyperactivation of the prefrontal areas observed in MS patients. It is worth noting that although cognitive activities are subserved by diffuse networks, focal modulation of a node may induce functional changes in remote regions (Siebner et al., 2009).

CONCLUSIONS

Improved understanding of features inducing brain disconnection in MS (i.e., demyelination, neurodegeneration, inflammation) and those influencing recovery (i.e., plasticity) may help to characterize the underlying pathophysiology. As neuroinflammation could induce brain connectivity dysfunction and impair network reorganization, contrasting inflammation may hinder connectivity disruption in MS. Furthermore, strategies aimed at promoting plasticity could be particularly relevant in MS, as plasticity reserve is reduced in these patients. Although NIBS could represent a promising approach for treating different symptoms in MS, it will be useful to identify the brain areas that should be stimulated and relate the lesion site to therapeutic response, establish the need to perform consecutive stimulation sessions and better predict the individual response to NIBS, also considering that in MS plasticity is altered in response to inflammation. It is therefore crucial to understand how focal modulation of brain activity by NIBS can enhance network efficiency. In particular, identifying anatomical and functional principles determining how local perturbations affect large-scale neural activity (Sale et al., 2015) may help to predict the impact of NIBS on brain network reorganization (Gollo et al., 2017). This could help to define whether restoring the original networks or promoting alternative circuits could be the best strategy for recovery, and therefore to use NIBS with an increasingly tailored approach.

AUTHOR CONTRIBUTIONS

MS and EI: work conception and design, drafting the work, work revision, final approval and global agreement; LG: work conception and design, work revision, final approval and global agreement; FB, PM, GM, and DR: work revision, final approval and global agreement; DC: work conception and design, guarantor of integrity of entire study, manuscript revision for important intellectual content, final approval.

FUNDING

This research did not receive any specific grant from funding agencies in the public, commercial, or not-to-profit sectors.

REFERENCES

Achard, S., and Bullmore, E. (2007). Efficiency and cost of economical brain functional networks. *PLoS Comput. Biol.* 3:e17. doi: 10.1371/journal.pcbi.0030017

Achard, S., Salvador, R., Whitcher, B., Suckling, J., and Bullmore, E. D. (2006). A resilient, low-frequency, small-world human brain functional network with highly connected association cortical hubs. *J. Neurosci.* 26, 63–72. doi: 10.1523/JNEUROSCI.3874-05.2006

d'Ambrosio, A., Hidalgo de la Cruz, M., Valsasina, P., Pagani, E., Colombo, B., Rodegher, M., et al. (2017). Structural connectivity-defined thalamic subregions have different functional connectivity abnormalities in multiple sclerosis patients: implications for clinical correlations. *Hum. Brain Mapp.* 38, 6005–6018. doi: 10.1002/hbm.23805

Alstott, J., Breakspear, M., Hagmann, P., Cammoun, L., and Sporns, O. (2009). Modeling the impact of lesions in the human brain. *PLoS Comput. Biol.* 5:e1000408. doi: 10.1371/journal.pcbi.1000408

Ayache, S. S., and Chalah, M. A. (2017). Fatigue in multiple sclerosis–Insights into evaluation and management. *Neurophysiol. Clin.* 47, 139–171. doi: 10.1016/j.neucli.2017.02.004

Ayache, S. S., Palm, U., Chalah, M. A., Al-Ani, T., Brignol, A., Abdellaoui, M., et al. (2016). Prefrontal tDCS decreases pain in patients with multiple sclerosis. *Front. Neurosci.* 10:147. doi: 10.3389/fnins.2016.00147

Baltruschat, S. A., Ventura-Campos, N., Cruz-Gómez, Á. J., Belenguer, A., and Forn, C. (2015). Gray matter atrophy is associated with functional connectivity reorganization during the Paced Auditory Serial Addition Test (PASAT) execution in Multiple Sclerosis (MS). *J. Neuroradiol.* 42, 141–149. doi: 10.1016/j.neurad.2015.02.006

Barkhof, F. (2002). The clinico-radiological paradox in multiple sclerosis revisited. *Curr. Opin. Neurol.* 15, 239–245. doi: 10.1097/00019052-200206000-00003

Biswal, B., Yetkin, F. Z., Haughton, V. M., and Hyde, J. S. (1995). Functional connectivity in the motor cortex of resting human brain using echo-planar MRI. *Magn. Reson. Med.* 34, 537–541. doi: 10.1002/mrm.1910340409

Bliss, T. V., and Gardner-Medwin, A. R. (1973). Long-lasting potentiation of synaptic transmission in the dentate area of the unanaesthetized rabbit following stimulation of the perforant path, *J. Physiol.* 232, 357–374. doi: 10.1113/jphysiol.1973.sp010274

Bonavita, S., Gallo, A., Sacco, R., Corte, M. D., Bisecco, A., Docimo, R., et al. (2011). Distributed changes in default-mode resting-state connectivity in multiple sclerosis. *Mult. Scler.* 17, 411–422. doi: 10.1177/1352458510394609

Boroojerdi, B., Hungs, M., Mull, M., Töpper, R., and Noth, J. (1998). Interhemispheric inhibition in patients with multiple sclerosis. *Electroencephalogr. Clin. Neurophysiol.* 109, 230–237. doi: 10.1016/S0924-980X(98)00013-7

Boutière, C., Rey, C., Zaaraoui, W., Le Troter, A., Rico, A., Crespy, L., et al. (2017). Improvement of spasticity following intermittent theta burst stimulation in multiple sclerosis is associated with modulation of resting-state functional connectivity of the primary motor cortices. *Mult. Scler.* 23, 855–863. doi: 10.1177/1352458516661640

Bullmore, E. T., and Bassett, D. S. (2011). Brain graphs: graphical models of the human brain connectome. *Annu. Rev. Clin. Psychol.* 7, 113–140. doi: 10.1146/annurev-clinpsy-040510-143934

Burhan, A. M., Subramanian, P., Pallaveshi, L., Barnes, B., and Montero-Odasso, M. (2015). Modulation of the left prefrontal cortex with high frequency repetitive transcranial magnetic stimulation facilitates gait in multiple sclerosis. *Case Rep. Neurol. Med.* 2015:251829. doi: 10.1155/2015/251829

Capuron, L., Pagnoni, G., Demetrashvili, M., Woolwine, B. J., Nemeroff, C. B., Berns, G. S., et al. (2005). Anterior cingulate activation and error processing during interferon-alpha treatment. *Biol. Psychiatry* 58, 190–196. doi: 10.1016/j.biopsych.2005.03.033

Caramia, M. D., Palmieri, M. G., Desiato, M. T., Boffa, L., Galizia, P., Rossini, P. M., et al. (2004). Brain excitability changes in the relapsing and remitting phases of multiple sclerosis: a study with transcranial magnetic stimulation. *Clin. Neurophysiol.* 115, 956–965. doi: 10.1016/j.clinph.2003.11.024

Carrera, E., and Tononi, G. (2014). Diaschisis: past, present, future. *Brain* 137, 2408–2422. doi: 10.1093/brain/awu101

Centonze, D., Koch, G., Versace, V., Mori, F., Rossi, S., Brusa, L., et al. (2007a). Repetitive transcranial magnetic stimulation of the motor cortex ameliorates spasticity in multiple sclerosis. *Neurology* 68, 1045–1050. doi: 10.1212/01.wnl.0000257818.16952.62

Centonze, D., Petta, F., Versace, V., Rossi, S., Torelli, F., Prosperetti, C., et al. (2007b). Effects of motor cortex rTMS on lower urinary tract dysfunction in multiple sclerosis. *Mult. Scler.* 13, 269–271. doi: 10.1177/1352458506070729

Centonze, D., Rossi, S., Tortiglione, A., Picconi, B., Prosperetti, C., De Chiara, V., et al. (2007c). Synaptic plasticity during recovery from permanent occlusion of the middle cerebral artery. *Neurobiol. Dis.* 27, 44–53. doi: 10.1016/j.nbd.2007.03.012

Chalah, M. A., Riachi, N., Ahdab, R., Créange, A., Lefaucheur, J. P., and Ayache, S. S. (2015). Fatigue in multiple sclerosis: neural correlates and the role of non-invasive brain stimulation. *Front. Cell. Neurosci.* 9:460. doi: 10.3389/fncel.2015.00460

Chalah, M. A., Riachi, N., Ahdab, R., Mhalla, A., Abdellaoui, M., Créange, A., et al. (2017). Effects of left DLPFC vs. right PPC tDCS on multiple sclerosis fatigue. *J. Neurol. Sci.* 372, 131–137. doi: 10.1016/j.jns.2016.11.015

Cocchi, L., Sale, M. V., Gollo, L. L., Bell, P. T., Nguyen, V. T., Zalesky, A., et al. (2016). A hierarchy of timescales explains distinct effects of local inhibition of primary visual cortex and frontal eye fields. *Elife* 5:e15252. doi: 10.7554/eLife.15252

Codecà, C., Mori, F., Kusayanagi, H., Monteleone, F., Boffa, L., Paolillo, A., et al. (2010). Differential patterns of interhemispheric functional disconnection in mild and advanced multiple sclerosis. *Mult. Scler.* 16, 1308–1316. doi: 10.1177/1352458510376957

Cruz-Gómez, Á. J., Ventura-Campos, N., Belenguer, A., Ávila, C., and Forn, C. (2014). The link between resting-state functional connectivity and cognition in MS patients. *Mult. Scler.* 20, 338–348. doi: 10.1177/1352458513495584

Cuypers, K., Leenus, D. J., Van Wijmeersch, B., Thijs, H., Levin, O., Swinnen, S. P., et al. (2013). Anodal tDCS increases corticospinal output and projection strength in multiple sclerosis. *Neurosci. Lett.* 554, 151–155. doi: 10.1016/j.neulet.2013.09.004

Di Filippo, M., Chiasserini, D., Gardoni, F., Viviani, B., Tozzi, A., Giampà, C., et al. (2013). Effects of central and peripheral inflammation on hippocampal synaptic plasticity. *Neurobiol. Dis.* 52, 229–236. doi: 10.1016/j.nbd.2012.12.009

Di Filippo, M., de Iure, A., Giampà, C., Chiasserini, D., Tozzi, A., Orvietani, P. L., et al. (2016). Persistent activation of microglia and NADPH oxidase drive hippocampal dysfunction in experimental multiple sclerosis. *Sci. Rep.* 18:20926. doi: 10.1038/srep20926

Di Lazzaro, V., Profice, P., Pilato, F., Capone, F., Ranieri, F., Pasqualetti, P., et al. (2010a). Motor cortex plasticity predicts recovery in acute stroke. *Cereb. Cortex* 20, 1523–1528. doi: 10.1093/cercor/bhp216

Di Lazzaro, V., Profice, P., Pilato, F., Dileone, M., Oliviero, A., and Ziemann, U. (2010b). The effects of motor cortex rTMS on corticospinal descending activity. *Clin. Neurophysiol.* 121, 464–473. doi: 10.1016/j.clinph.2009.11.007

Dipasquale, O., Cooper, E. A., Tibble, J., Voon, V., Baglio, F., Baselli, G., et al. (2016). Interferon-α acutely impairs whole-brain functional connectivity network architecture–A preliminary study. *Brain Behav. Immun.* 58, 31–39. doi: 10.1016/j.bbi.2015.12.011

Eldaief, M. C., Halko, M. A., Buckner, R. L., and Pascual-Leone, A. (2011). Transcranial magnetic stimulation modulates the brain's intrinsic activity in a frequency-dependent manner. *Proc. Natl. Acad. Sci. U.S.A.* 108, 21229–21234. doi: 10.1073/pnas.1113103109

Elzamarany, E., Afifi, L., El-Fayoumy, N. M., Salah, H., and Nada, M. (2016). Motor cortex rTMS improves dexterity in relapsing-remitting and secondary progressive multiple sclerosis. *Acta Neurol. Belg.* 116, 145–150. doi: 10.1007/s13760-015-0540-y

Faivre, A., Rico, A., Zaaraoui, W., Crespy, L., Reuter, F., Wybrecht, D., et al. (2012). Assessing brain connectivity at rest is clinically relevant in early multiple sclerosis. *Mult. Scler.* 18, 1251–1258. doi: 10.1177/1352458511435930

Feeney, D. M., and Baron, J. C. (1986). Diaschisis. *Stroke* 17, 817–830. doi: 10.1161/01.STR.17.5.817

Ferbert, A., Priori, A., Rothwell, J. C., Day, B. L., Colebatch, J. G., and Marsden, C. D. (1992). Interhemispheric inhibition of the human motor cortex. *J. Physiol.* 453, 525–546. doi: 10.1113/jphysiol.1992.sp019243

Ferrucci, R., Vergari, M., Cogiamanian, F., Bocci, T., Ciocca, M., Tomasini, E., et al. (2014). Transcranial direct current stimulation (tDCS) for fatigue in multiple sclerosis. *Neuro Rehabil.* 34, 121–127. doi: 10.3233/NRE-131019.

Filippi, M., and Rocca, M. A. (2013). Present and future of fMRI in multiple sclerosis. *Expert Rev. Neurother.* 13, 27–31. doi: 10.1586/14737175.2013.865871

Floel, A., and Cohen, L. G. (2006). Translational studies in neurorehabilitation: from bench to bedside. *Cogn. Behav. Neurol.* 19, 1–10. doi: 10.1097/00146965-200603000-00001

Fox, M. D., and Raichle, M. E. (2007). Spontaneous fluctuations in brain activity observed with functional magnetic resonance imaging. *Nat. Rev. Neurosci.* 8, 700–711. doi: 10.1038/nrn2201

Friston, K. J., Frith, C. D., and Frackowiak, R. S. J. (1993). Time-dependent changes in effective connectivity measured with PET. *Hum. Brain Mapp.* 1, 69–79. doi: 10.1002/hbm.460010108

Gerstein, G. L., and Aertsen, A. M. (1985). Representation of cooperative firing activity among simultaneously recorded neurons. *J. Neurophysiol.* 54, 1513–1528.

Gollo, L. L., Roberts, J. A., and Cocchi, L. (2017). Mapping how local perturbations influence systems-level brain dynamics. *Neuroimage* 160, 97–112. doi: 10.1016/j.neuroimage.2017.01.057

Grefkes, C., and Fink, G. R. (2011). Reorganization of cerebral networks after stroke: new insights from neuroimaging with connectivity approaches. *Brain* 134, 1264–1276. doi: 10.1093/brain/awr033

Grefkes, C., Nowak, D. A., Wang, L. E., Dafotakis, M., Eickhoff, S. B., and Fink, G. R. (2010). Modulating cortical connectivity in stroke patients by rTMS assessed with fMRI and dynamic causal modeling. *Neuroimage* 50, 233–242. doi: 10.1016/j.neuroimage.2009.12.029

Hannestad, J., Gallezot, J. D., Schafbauer, T., Lim, K., Kloczynski, T., Morris, E. D., et al. (2012). Endotoxin-induced systemic inflammation activates microglia:[11C] PBR28 positron emission tomography in nonhuman primates. *Neuroimage* 63, 232–239. doi: 10.1016/j.neuroimage.2012.06.055

Harrison, N. A., Brydon, L., Walker, C., Gray, M. A., Steptoe, A., Dolan, R. J., et al. (2009). Neural origins of human sickness in interoceptive responses to inflammation. *Biol. Psychiatry* 66, 415–422. doi: 10.1016/j.biopsych.2009.03.007

Hermundstad, A. M., Bassett, D. S., Brown, K. S., Aminoff, E. M., Clewett, D., Freeman, S., et al. (2013). Structural foundations of resting-state and task-based functional connectivity in the human brain. *Proc. Natl. Acad. Sci. U.S.A.* 110, 6169–6174. doi: 10.1073/pnas.1219562110

Honey, C. J., Kötter, R., Breakspear, M., and Sporns, O. (2007). Network structure of cerebral cortex shapes functional connectivity on multiple time scales. *Proc. Natl. Acad. Sci. U.S.A.* 104, 10240–10245. doi: 10.1073/pnas.0701519104

Honey, C. J., and Sporns, O. (2008). Dynamical consequences of lesions in cortical networks. *Hum. Brain Mapp.* 29, 802–809. doi: 10.1002/hbm.20579

Honey, C. J., Sporns, O., Cammoun, L., Gigandet, X., Thiran, J. P., Meuli, R., et al. (2009). Predicting human resting-state functional connectivity from structural connectivity. *Proc. Natl. Acad. Sci. U.S.A.* 106, 2035–2040. doi: 10.1073/pnas.0811168106

Honey, C. J., Thivierge, J. P., and Sporns, O. (2010). Can structure predict function in the human brain? *Neuroimage* 52, 766–776. doi: 10.1016/j.neuroimage.2010.01.071

Huang, Y. Z., Edwards, M. J., Rounis, E., Bhatia, K. P., and Rothwell, J. C. (2005). Theta burst stimulation of the human motor cortex. *Neuron* 45, 201–206. doi: 10.1016/j.neuron.2004.12.033

Hulst, H. E., Goldschmidt, T., Nitsche, M. A., de Wit, S. J., van den Heuvel, O. A., Barkhof, F., et al. (2016). rTMS affects working memory performance, brain activation and functional connectivity in patients with multiple sclerosis. *J. Neurol. Neurosurg. Psychiatr.* 88, 386–394. doi: 10.1136/jnnp-2016-314224

Hummel, F., Celnik, P., Giraux, P., Floel, A., Wu, W. H., Gerloff, C., et al. (2005). Effects of non-invasive cortical stimulation on skilled motor function in chronic stroke. *Brain* 128, 490–499. doi: 10.1093/brain/awh369

Iodice, R., Dubbioso, R., Ruggiero, L., Santoro, L., and Manganelli, F. (2015). Anodal transcranial direct current stimulation of motor cortex does not ameliorate spasticity in multiple sclerosis. *Restor. Neurol. Neurosci.* 33, 487–492. doi: 10.3233/RNN-150495

Joyce, K. E., Hayasaka, S., and Laurienti, P. J. (2013). The human functional brain network demonstrates structural and dynamical resilience to targeted attack. *PLoS Comput. Biol.* 9:e1002885. doi: 10.1371/journal.pcbi.1002885

Jung, P., Beyerle, A., Humpich, M., Neumann-Haefelin, T., Lanfermann, H., and Ziemann, U. (2006). Ipsilateral silent period: a marker of callosal conduction abnormality in early relapsing–remitting multiple sclerosis? *J. Neurol. Sci.* 250, 133–139. doi: 10.1016/j.jns.2006.08.008

Kaiser, M. (2013). The potential of the human connectome as a biomarker of brain disease. *Front. Hum. Neurosci.* 7:484. doi: 10.3389/fnhum.2013.00484

Koch, G., Rossi, S., Prosperetti, C., Codecà, C., Monteleone, F., Petrosini, L., et al. (2008). Improvement of hand dexterity following motor cortex rTMS in multiple sclerosis patients with cerebellar impairment. *Mult. Scler.* 14, 995–998. doi: 10.1177/1352458508088710

Kos, D., Kerckhofs, E., Ketelaer, P., Duportail, M., Nagels, G., D'Hooghe, M., et al. (2004). Self-report assessment of fatigue in multiple sclerosis: a critical evaluation. *Occup. Ther. Health Care* 17, 45–62. doi: 10.1080/J003v17n03_04

Krupp, L. B., and Pollina, D. A. (1996). Mechanisms and management of fatigue in progressive neurological disorders. *Curr. Opin. Neurol.* 9, 456–460. doi: 10.1097/00019052-199612000-00011

Kukaswadia, S., Wagle-Shukla, A., Morgante, F., Gunraj, C., and Chen, R. (2005). Interactions between long latency afferent inhibition and interhemispheric inhibitions in the human motor cortex. *J. Physiol.* 563, 915–924. doi: 10.1113/jphysiol.2004.080010

Labrenz, F., Wrede, K., Forsting, M., Engler, H., Schedlowski, M., Elsenbruch, S., et al. (2016). Alterations in functional connectivity of resting state networks during experimental endotoxemia–an exploratory study in healthy men. *Brain Behav. Immun.* 54, 17–26. doi: 10.1016/j.bbi.2015.11.010

Lefaucheur, J. P., Chalah, M. A., Mhalla, A., Palm, U., Ayache, S. S., and Mylius, V. (2017). The treatment of fatigue by non-invasive brain stimulation. *Neurophysiol. Clin.* 47, 173–184. doi: 10.1016/j.neucli.2017.03.003

Lenzi, D., Conte, A., Mainero, C., Frasca, V., Fubelli, F., Totaro, P., et al. (2007). Effect of corpus callosum damage on ipsilateral motor activation in patients with multiple sclerosis: a functional and anatomical study. *Hum. Brain Mapp.* 28, 636–644. doi: 10.1002/hbm.20305

Lerdal, A., Celius, E. G., Krupp, L., and Dahl, A. A. (2007). A prospective study of patterns of fatigue in multiple sclerosis. *Eur. J. Neurol.* 14, 1338–1343. doi: 10.1111/j.1468-1331.2007.01974.x

Liebetanz, D., Nitsche, M. A., Tergau, F., and Paulus, W. (2002). Pharmacological approach to the mechanisms of transcranial DC-stimulation-induced after-effects of human motor cortex excitability. *Brain* 125, 2238–2247. doi: 10.1093/brain/awf238

Liu, Y., Dai, Z., Duan, Y., Huang, J., Ren, Z., Liu, Z., et al. (2016). Whole brain functional connectivity in clinically isolated syndrome without conventional brain MRI lesions. *Eur. Radiol.* 26, 2982–2991. doi: 10.1007/s00330-015-4147-8

Liu, Y., Liang, P., Duan, Y., Huang, J., Ren, Z., Jia, X., et al. (2015). Altered thalamic functional connectivity in multiple sclerosis. *Eur. J. Radiol.* 84, 703–708. doi: 10.1016/j.ejrad.2015.01.001

Liu, Y., Wang, H., Duan, Y., Huang, J., Ren, Z., Ye, J., et al. (2017). Functional brain network alterations in clinically isolated syndrome and multiple sclerosis: a graph-based connectome study. *Radiology* 282, 534–541. doi: 10.1148/radiol.2016152843

Llufriu, S., Blanco, Y., Martinez-Heras, E., Casanova-Molla, J., Gabilondo, I., Sepulveda, M., et al. (2012). Influence of corpus callosum damage on cognition and physical disability in multiple sclerosis: a multimodal study. *PLoS ONE* 7:e37167. doi: 10.1371/journal.pone.0037167

Louapre, C., Perlbarg, V., García-Lorenzo, D., Urbanski, M., Benali, H., Assouad, R., et al. (2014). Brain networks disconnection in early multiple sclerosis cognitive deficits: an anatomofunctional study. *Hum. Brain Mapp.* 35, 4706–4717. doi: 10.1002/hbm.22505

Mandolesi, G., Musella, A., Gentile, A., Grasselli, G., Haji, N., Sepman, H., et al. (2013). Interleukin-1β alters glutamate transmission at purkinje cell synapses in a mouse model of multiple sclerosis. *J. Neurosci.* 33, 12105–12121. doi: 10.1523/JNEUROSCI.5369-12.2013

Marsland, A. L., Kuan, D. C. H., Sheu, L. K., Krajina, K., Kraynak, T. E., Manuck, S. B., et al. (2017). Systemic inflammation and resting state connectivity of the default mode network. *Brain Behav. Immun.* 62, 162–170. doi: 10.1016/j.bbi.2017.01.013

Mattioli, F., Bellomi, F., Stampatori, C., Capra, R., and Miniussi, C. (2016). Neuroenhancement through cognitive training and anodal tDCS in multiple sclerosis. *Mult. Scler.* 22, 222–2230. doi: 10.1177/1352458515587597

Meesen, R. L., Thijs, H., Leenus, D. J., and Cuypers, K. (2014). A single session of 1 mA anodal tDCS-supported motor training does not improve motor performance in patients with multiple sclerosis. *Restor. Neurol. Neurosci.* 32, 293–300. doi: 10.3233/RNN-130348

Miniussi, C., Cappa, S. F., Cohen, L. G., Floel, A., Fregni, F., Nitsche, M. A., et al. (2008). Efficacy of repetitive transcranial magnetic stimulation/transcranial direct current stimulation in cognitive neurorehabilitation. *Brain Stimul.* 1, 326–336. doi: 10.1016/j.brs.2008.07.002

Mori, F., Codecà, C., Kusayanagi, H., Monteleone, F., Boffa, L., Rimano, A., et al. (2010a). Effects of intermittent theta burst stimulation on spasticity in patients with multiple sclerosis. *Eur. J. Neurol.* 17, 295–300. doi: 10.1111/j.1468-1331.2009.02806.x

Mori, F., Codecà, C., Kusayanagi, H., Monteleone, F., Buttari, F., Fiore, S., et al. (2010b). Effects of anodal transcranial direct current stimulation on chronic neuropathic pain in patients with multiple sclerosis. *J. Pain.* 11, 436–442. doi: 10.1016/j.jpain.2009.08.011

Mori, F., Kusayanagi, H., Buttari, F., Centini, B., Monteleone, F., Nicoletti, C. G., et al. (2012). Early treatment with high-dose interferon beta-1a reverses

cognitive and cortical plasticity deficits in multiple sclerosis. *Funct. Neurol.* 27, 163–168.

Mori, F., Kusayanagi, H., Nicoletti, C. G., Weiss, S., Marciani, M. G., and Centonze, D. (2014). Cortical plasticity predicts recovery from relapse in multiple sclerosis. *Mult. Scler.* 20, 451–457. doi: 10.1177/1352458513512541

Mori, F., Nicoletti, C. G., Kusayanagi, H., Foti, C., Restivo, D. A., Marciani, M. G., et al. (2013). Transcranial direct current stimulation ameliorates tactile sensory deficit in multiple sclerosis. *Brain Stimul.* 6, 654–659. doi: 10.1016/j.brs.2012.10.003

Mori, F., Rossi, S., Sancesario, G., Codecà, C., Mataluni, G., Monteleone, F., et al. (2011). Cognitive and cortical plasticity deficits correlate with altered amyloid-β CSF levels in multiple sclerosis. *Neuropsychopharmacology* 36, 559–568. doi: 10.1038/npp.2010.187

Morreale, M., Marchione, P., Pili, A., Lauta, A., Castiglia, S. F., Spallone, A., et al. (2016). Early vs. delayed rehabilitation treatment in hemiplegic patients with ischemic stroke: proprioceptive or cognitive approach? *Eur. J. Phys. Rehabil. Med.* 52, 81–89.

Muellbacher, W., Ziemann, U., Boroojerdi, B., Cohen, L., and Hallett, M. (2001). Role of the human motor cortex in rapid motor learning. *Exp. Brain Res.*136, 431–438. doi: 10.1007/s002210000614

Murase, N., Duque, J., Mazzocchio, R., and Cohen, L. G. (2004). Influence of interhemispheric interactions on motor function in chronic stroke. *Ann. Neurol.* 55, 400–409. doi: 10.1002/ana.10848

Neva, J. L., Lakhani, B., Brown, K. E., Wadden, K. P., Mang, C. S., Ledwell, N. H. M., et al. (2016). Multiple measures of corticospinal excitability are associated with clinical features of multiple sclerosis. *Behav. Brain Res.* 297, 187–195. doi: 10.1016/j.bbr.2015.10.015

Ni, Z., Gunraj, C., Nelson, A. J., Yeh, I. J., Castillo, G., Hoque, T., et al. (2009). Two phases of interhemispheric inhibition between motor related cortical areas and the primary motor cortex in human. *Cereb. Cortex* 19, 1654–1665. doi: 10.1093/cercor/bhn201

Nisticò, R., Mango, D., Mandolesi, G., Piccinin, S., Berretta, N., Pignatelli, M., et al. (2013). Inflammation subverts hippocampal synaptic plasticity in experimental multiple sclerosis. *PLoS ONE* 8:e54666. doi: 10.1371/journal.pone.0054666

Nitsche, M. A., Fricke, K., Henschke, U., Schlitterlau, A., Liebetanz, D., Lang, N., et al. (2003). Pharmacological modulation of cortical excitability shifts induced by transcranial direct current stimulation in humans. *J. Physiol.* 553, 293–301. doi: 10.1113/jphysiol.2003.049916

Nitsche, M. A., and Paulus, W. (2000). Excitability changes induced in the human motor cortex by weak transcranial direct current stimulation. *J. Physiol.* 527, 633–639. doi: 10.1111/j.1469-7793.2000.t01-1-00633.x

Pantano, P., Mainero, C., and Caramia, F. (2006). Functional brain reorganization in multiple sclerosis: evidence from fMRI studies. *J. Neuroimaging* 16, 104–114. doi: 10.1111/j.1552-6569.2006.00029.x

Ponten, S. C., Daffertshofer, A., Hillebrand, A., and Stam, C. J. (2010). The relationship between structural and functional connectivity: graph theoretical analysis of an EEG neural mass model. *Neuroimage* 52, 985–994. doi: 10.1016/j.neuroimage.2009.10.049

Radhu, N., Ravindran, L. N., Levinson, A. J., and Daskalakis, Z. J. (2012). Inhibition of the cortex using transcranial magnetic stimulation in psychiatric populations: current and future directions. *J. Psychiatry Neurosci.* 37, 369–378. doi: 10.1503/jpn.120003

Rioult-Pedotti, M. S., Friedman, D., and Donoghue, J. P. (2000). Learning-induced LTP in neocortex. *Science* 290, 533–536. doi: 10.1126/science.290.5491.533

Rocca, M. A., Colombo, B., Falini, A., Ghezzi, A., Martinelli, V., Scotti, G., et al. (2005). Cortical adaptation in patients with MS: a cross-sectional functional MRI study of disease phenotypes. *Lancet Neurol.* 4, 618–626. doi: 10.1016/S1474-4422(05)70171-X

Rocca, M. A., Falini, A., Colombo, B., Scotti, G., Comi, G., and Filippi, M. (2002). Adaptive functional changes in the cerebral cortex of patients with non-disabling multiple sclerosis correlate with the extent of brain structural damage. *Ann. Neurol.* 51, 330–339. doi: 10.1002/ana.10120

Rocca, M. A., Pravatà, E., Valsasina, P., Radaelli, M., Colombo, B., Vacchi, L., et al. (2015). Hippocampal-DMN disconnectivity in MS is related to WM lesions and depression. *Hum. Brain Mapp.* 36, 5051–5063. doi: 10.1002/hbm.22992

Rocca, M. A., Valsasina, P., Absinta, M., Riccitelli, G., Rodegher, M. E., Misci, P., et al. (2010). Default-mode network dysfunction and cognitive impairment in progressive MS. *Neurology* 74, 1252–1259. doi: 10.1212/WNL.0b013e3181d9ed91

Rocca, M. A., Valsasina, P., Martinelli, V., Misci, P., Falini, A., Comi, G., et al. (2012). Large-scale neuronal network dysfunction in relapsing-remitting multiple sclerosis. *Neurology* 79, 1449–1457. doi: 10.1212/WNL.0b013e31826d5f10

Rocca, M. A., Valsasina, P., Meani, A., Falini, A., Comi, G., and Filippi, M. (2016). Impaired functional integration in multiple sclerosis: a graph theory study. *Brain Struct. Funct.* 221, 115–131. doi: 10.1007/s00429-014-0896-4

Roosendaal, S. D., Schoonheim, M. M., Hulst, H. E., Sanz-Arigita, E. J., Smith, S. M., Geurts, J. J., et al. (2010). Resting state networks change in clinically isolated syndrome. *Brain* 133, 1612–1621. doi: 10.1093/brain/awq058

Rossi, S., Furlan, R., De Chiara, V., Motta, C., Studer, V., Mori, F., et al. (2012a). Interleukin-1β causes synaptic hyperexcitability in multiple sclerosis. *Ann. Neurol.* 71, 76–83. doi: 10.1002/ana.22512

Rossi, S., Muzio, L., De Chiara, V., Grasselli, G., Musella, A., Musumeci, G., et al. (2011). Impaired striatal GABA transmission in experimental autoimmune encephalomyelitis. *Brain Behav. Immun.* 25, 947–956. doi: 10.1016/j.bbi.2010.10.004

Rossi, S., Studer, V., Motta, C., De Chiara, V., Barbieri, F., Bernanrdi, G., et al. (2012b). Inflammation inhibits GABA transmission in multiple sclerosis. *Mult. Scler.* 18, 1633–1635. doi: 10.1177/1352458512440207

Rossini, P. M., Burke, D., Chen, R., Cohen, L. G., Daskalakis, Z., Di Iorio, R., et al. (2015). Non-invasive electrical and magnetic stimulation of the brain, spinal cord, roots and peripheral nerves: basic principles and procedures for routine clinical and research application. An updated report from an IFCN Committee. *Clin. Neurophysiol.* 126, 1071–1107. doi: 10.1016/j.clinph.2015.02.001

Rubinov, M., Sporns, O., van Leeuwen, C., and Breakspear, M. (2009). Symbiotic relationship between brain structure and dynamics. *BMC Neurosci.* 10:55. doi: 10.1186/1471-2202-10-55

Saiote, C., Goldschmidt, T., Timäus, C., Steenwijk, M. D., Opitz, A., Antal, A., et al. (2014). Impact of transcranial direct current stimulation on fatigue in multiple sclerosis. *Restor. Neurol. Neurosci.* 32, 423–436. doi: 10.3233/RNN-130372

Sale, M. V., Mattingley, J. B., Zalesky, A., and Cocchi, L. (2015). Imaging human brain networks to improve the clinical efficacy of non-invasive brain stimulation. *Neurosci. Biobehav. Rev.* 57, 187–198. doi: 10.1016/j.neubiorev.2015.09.010

Sbardella, E., Tona, F., Petsas, N., Upadhyay, N., Piattella, M. C., Filippini, N., et al. (2015). Functional connectivity changes and their relationship with clinical disability and white matter integrity in patients with relapsing–remitting multiple sclerosis. *Mult. Scler.* 21, 1681–1692. doi: 10.1177/1352458514568826

Schmierer, K., Irlbacher, K., Grosse, P., Röricht, S., and Meyer, B. U. (2002). Correlates of disability in multiple sclerosis detected by transcranial magnetic stimulation. *Neurology* 59, 1218–1224. doi: 10.1212/WNL.59.8.1218

Schmierer, K., Niehaus, L., Röricht, S., and Meyer, B. U. (2000). Conduction deficits of callosal fibres in early multiple sclerosis. *J. Neurol. Neurosurg. Psychiatr.* 68, 633–638. doi: 10.1136/jnnp.68.5.633

Schoonheim, M. M., Meijer, K. A., and Geurts, J. J. (2015). Network collapse and cognitive impairment in multiple sclerosis. *Front. Neurol.* 6:82. doi: 10.3389/fneur.2015.00082.

Schwarz, C., and Thier, P. (1999). Binding of signals relevant for action: towards a hypothesis of the functional role of the pontine nuclei. *Trends Neurosci.* 22, 443–451. doi: 10.1016/S0166-2236(99)01446-0

Shafi, M. M., Westover, M. B., Fox, M. D., and Pascual-Leone, A. (2012). Exploration and modulation of brain network interactions with noninvasive brain stimulation in combination with neuroimaging. *Eur. J. Neurosci.* 35, 805–825. doi: 10.1111/j.1460-9568.2012.08035.x

Siebner, H. R., Hartwigsen, G., Kassuba, T., and Rothwell, J. C. (2009). How does transcranial magnetic stimulation modify neuronal activity in the brain? Implications for studies of cognition *Cortex* 45, 1035–1042. doi: 10.1016/j.cortex.2009.02.007

Siebner, H., and Rothwell, J. (2003). Transcranial magnetic stimulation: new insights into representational cortical plasticity. *Exp. Brain Res.* 148, 1–16. doi: 10.1007/s00221-002-1234-2

Sporns, O., Tononi, G., and Kötter, R. (2005). The human connectome: a structural description of the human brain. *PLoS Comput. Biol.* 1:e42. doi: 10.1371/journal.pcbi.0010042

Stampanoni Bassi, M., Leocani, L., Comi, G., Iezzi, E., and Centonze, D. (2017a). Can pharmacological manipulation of LTP favor the effects of motor rehabilitation in multiple sclerosis? *Mult. Scler.* doi: 10.1177/1352458517721358. [Epub ahead of print].

Stampanoni Bassi, M., Mori, F., Buttari, F., Marfia, G. A., Sancesario, A., Centonze, D., et al. (2017b). Neurophysiology of synaptic functioning in multiple sclerosis. *Clin. Neurophysiol.* 128, 1148–1157 doi: 10.1016/j.clinph.2017.04.006

Tecchio, F., Cancelli, A., Cottone, C., Zito, G., Pasqualetti, P., Ghazaryan, A., et al. (2014). Multiple sclerosis fatigue relief by bilateral somatosensory cortex neuromodulation. *J. Neurol.* 261, 1552–1558. doi: 10.1007/s00415-014-7377-9

Tona, F., Petsas, N., Sbardella, E., Prosperini, L., Carmellini, M., Pozzilli, C., et al. (2014). Multiple sclerosis: altered thalamic resting-state functional connectivity and its effect on cognitive function. *Radiology* 271, 814–821. doi: 10.1148/radiol.14131688

Tongiorgi, E., Sartori, A., Baj, G., Bratina, A., Di Cola, F., Zorzon, M., et al. (2012). Altered serum content of brain-derived neurotrophic factor isoforms in multiple sclerosis. *J. Neurol. Sci.* 320, 161–165. doi: 10.1016/j.jns.2012.07.016

Uehara, K., Morishita, T., Kubota, S., and Funase, K. (2013). Neural mechanisms underlying the changes in ipsilateral primary motor cortex excitability during unilateral rhythmic muscle contraction. *Behav. Brain Res.* 240, 33–45. doi: 10.1016/j.bbr.2012.10.053

van Dellen, E., Hillebrand, A., Douw, L., Heimans, J. J., Reijneveld, J. C., and Stam, C. J. (2013). Local polymorphic delta activity in cortical lesions causes global decreases in functional connectivity. *Neuroimage* 83, 524–532. doi: 10.1016/j.neuroimage.2013.06.009

van den Heuvel, M. P., and Hulshoff Pol, H. E. (2010). Exploring the brain network: a review on resting-state fMRI functional connectivity. *Eur. Neuropsychopharmacol.* 20, 519–534. doi: 10.1016/j.euroneuro.2010.03.008

von Monakow, C. (1914). *Die Localization im Grosshirn und der Abbau der Funktion Durch Korticale Herde*. Wiesbaden: JF Bergmann.

Wahl, M., Hübers, A., Lauterbach-Soon, B., Hattingen, E., Jung, P., Cohen, L. G., et al. (2011). Motor callosal disconnection in early relapsing-remitting multiple sclerosis. *Hum. Brain Mapp.* 32, 846–855. doi: 10.1002/hbm.21071

Wassermann, E. M., Fuhr, P., Cohen, L. G., and Hallett, M. (1991). Effects of transcranial magnetic stimulation on ipsilateral muscles. *Neurology* 41, 1795–1799. doi: 10.1212/WNL.41.11.1795

Wu, G. F., Matthew, R., Parks, C. A. L., Ances, B. M., and Van Stavern, G. P. (2015). An eye on brain integrity: acute optic neuritis affects resting state functional connectivity impact of acute on on rs-fcMRI. *Invest. Ophthalmol. Vis. Sci.* 56, 2541–2546. doi: 10.1167/iovs.14-16315

Young, R. R. (1994). Spasticity: a review. *Neurology* 44, 12–20.

Zhou, F., Zhuang, Y., Gong, H., Wang, B., Wang, X., Chen, Q., et al. (2014). Altered inter-subregion connectivity of the default mode network in relapsing remitting multiple sclerosis: a functional and structural connectivity study. *PLoS ONE* 9:e101198. doi: 10.1371/journal.pone.0101198

Ziemann, U., Iliać, T. V., Pauli, C., Meintzschel, F., and Ruge, D. (2004). Learning modifies subsequent induction of long-term potentiation-like and long-term depression-like plasticity in human motor cortex. *J. Neurosci.* 24, 1666–1672. doi: 10.1523/JNEUROSCI.5016-03.2004

Ziemann, U., Paulus, W., Nitsche, M. A., Pascual-Leone, A., Byblow, W. D., Berardelli, A., et al. (2008). Consensus: motor cortex plasticity protocols. *Brain Stimul.* 1, 164–182. doi: 10.1016/j.brs.2008.06.006

Conflict of Interest Statement: The authors declare that the research was conducted in the absence of any commercial or financial relationships that could be construed as a potential conflict of interest.

frontiers in Neuroscience

TECHNOLOGY REPORT
published: 16 May 2018
doi: 10.3389/fnins.2018.00284

MRI-Guided Regional Personalized Electrical Stimulation in Multisession and Home Treatments

Andrea Cancelli[1], *Carlo Cottone*[1], *Alessandro Giordani*[2], *Giampiero Asta*[1], *Domenico Lupoi*[2], *Vittorio Pizzella*[3,4] and *Franca Tecchio*[1,5]*

[1] Laboratory of Electrophysiology for Translational Neuroscience, Istituto di scienze e tecnologie della cognizione (ISTC), Consiglio Nazionale Delle Ricerche (CNR), Rome, Italy, [2] AFaR Division, Fatebenefratelli Foundation for Health Research and Education, Rome, Italy, [3] Department of Neuroscience, Imaging and Clinical Sciences, Università degli Studi G. d'Annunzio Chieti e Pescara, Chieti, Italy, [4] Institute for Advanced Biomedical Technologies, Università degli Studi G. d'Annunzio Chieti e Pescara, Chieti, Italy, [5] Institute of Neurology, Catholic University of the Sacred Heart, Rome, Italy

The shape and position of the electrodes is a key factor for the efficacy of transcranial electrical stimulations (tES). We have recently introduced the Regional Personalized Electrode (RePE), a tES electrode fitting the personal cortical folding, that has been able to differentiate the stimulation of close by regions, in particular the primary sensory (S1) and motor (M1) cortices, and to personalize tES onto such an extended cortical district. However, neuronavigation on individual brain was compulsory for the correct montage. Here, we aimed at developing and testing a neuronavigation-free procedure for easy and quick positioning RePE, enabling multisession RePE-tES at home. We used off-line individual MRI to shape RePE via an *ad-hoc* computerized procedure, while an *ad-hoc* developed Adjustable Helmet Frame (AHF) was used to properly position it in multisession treatments, even at home. We used neuronavigation to test the RePE shape and position obtained by the new computerized procedure and the re-positioning obtained via the AHF. Using Finite Element Method (FEM) model, we also estimated the intra-cerebral current distribution induced by transcranial direct current stimulation (tDCS) comparing RePE vs. non-RePE with fixed reference. Additionally, we tested, using FEM, various shapes, and positions of the reference electrode taking into account possible small displacements of RePE, to test feasibility of RePE-tES sessions at home. The new RePE neuronavigation-free positioning relies on brain MRI space distances, and produced a mean displacement of 3.5 ± 0.8 mm, and the re-positioning of 4.8 ± 1.1 mm. Higher electric field in S1 than in M1 was best obtained with the occipital reference electrode, a montage that proved to feature low sensitivity to typical RePE millimetric displacements. Additionally, a new tES accessory was developed to enable repositioning the electrodes over the scalp also at home, with a precision which is acceptable according to the modeling-estimated intracerebral currents. Altogether, we provide here a procedure to simplify and make easily applicable RePE-tDCS, which enables efficacious personalized treatments.

Keywords: regional personalized electrode (RePE), transcranial electrical stimulation (tES), computational modeling, primary somatosensory and motor cortex (S1, M1), tDCS home treatments, non-invasive brain stimulation (NIBS)

OPEN ACCESS

Edited by:
Takashi Hanakawa, National Center of Neurology and Psychiatry, Japan

Reviewed by:
Satoshi Tanaka, Hamamatsu University School of Medicine, Japan
Nico Sollmann, Technische Universität München, Germany

***Correspondence:**
Franca Tecchio
franca.tecchio@cnr.it

Specialty section:
This article was submitted to Neural Technology, a section of the journal Frontiers in Neuroscience

Received: *30 January 2018*
Accepted: *11 April 2018*
Published: *16 May 2018*

Citation:
Cancelli A, Cottone C, Giordani A, Asta G, Lupoi D, Pizzella V and Tecchio F (2018) MRI-Guided Regional Personalized Electrical Stimulation in Multisession and Home Treatments. Front. Neurosci. 12:284. doi: 10.3389/fnins.2018.00284

INTRODUCTION

Advances in analyzing structural and functional brain features using powerful non-invasive neuroimaging methods are nowadays yielding intriguing insights into brain circuits, their variability across individuals, and their relationship to behavior (Van Essen, 2013; Kopell et al., 2014). If properly exploited, this knowledge can enhance the neuromodulation efficacy of transcranial Electrical Stimulation (tES), and transcranial Direct Current Stimulation (tDCS) in particular, by tuning the dimension, position and shape of the electrodes to the brain networks of interest (Murphy et al., 2009; Tecchio et al., 2014; Galletta et al., 2015; Cancelli et al., 2016, 2017; Grimaldi et al., 2016).

Following the need to concentrate the stimulation on the entire bilateral primary somatosensory representation of the whole body (S1), we recently introduced a new MRI-based neuronavigated procedure to customize brain stimulation through the use of the Regional Personalized Electrode (RePE) (Tecchio et al., 2013). The higher efficacy of personalized vs. non-personalized electrode in targeting the whole region was demonstrated experimentally (Cancelli et al., 2015a), and further confirmed by a recent modeling study (Parazzini et al., 2017). RePE targeting S1 (RePE-S1) was employed in two randomized clinical trials (RCT) showing an efficacy of this personalized 5-day tDCS against fatigue in multiple sclerosis (MS), thus we called the treatment Fatigue Relief in Multiple Sclerosis, FaReMuS (Tecchio et al., 2014; Cancelli et al., 2017). In the 2014 group, the mean fatigue reduction was 28% of the baseline after Real stimulation and 8% after Sham, $p = 0.016$. In the 2017 group, the fatigue symptoms reduction were 42% after Real and 20% after Sham, $p = 0.012$. We observed 7 responders, defined as the patients who changed the fatigue level more or equal to 20% of her/his baseline, in the 2014 group, and 9 in the 2017 one. The relevance of the target selection to effectively relieve fatigue can be perceived from the fact that other two tDCS trials, in which every parameter but the electrode shape and position were identical to those of the efficacious FaReMuS neuromodulation (Tecchio et al., 2014; Cancelli et al., 2017), did not produce the desired effects (Ferrucci et al., 2014; Saiote et al., 2014).

RePE-S1 electrode is shaped according to the projection onto the scalp of the individual cortical folding of the Rolandic sulcus. The projection was obtained by a neuronavigated procedure as the minimal distance from the scalp of the central sulcus reconstructed from the individual brain MRI (Tecchio et al., 2013). We conceived that the treatment should target the entire body somatosensory representation, as both limbs are impaired in people with MS and typically both sides. For this reason we decided to target the entire Rolandic sulcus post-central wall (Fischl et al., 2004; Destrieux et al., 2010). For simplicity, we selected from the left to the right Sylvian sulci, including the secondary somatosensory representation. In fact, as discussed above our main aim was to avoid frontal motor areas, while a wider parietal involvement was acceptable consistently with the literature (Pellicano et al., 2010; Engström et al., 2013; Vecchio et al., 2017).

Despite the promising results in relieving fatigue in people with multiple sclerosis (Tecchio et al., 2014; Cancelli et al., 2017), the application of RePE is still difficult because of the burdensome and complicated set up, that requires an experienced operator for the manually neuronavigated shaping of RePE with the patient affected by multiple sclerosis present along the entire shaping procedure, and an accurate neuronavigated positioning at the beginning of every stimulation session.

The tDCS treatments typically require multiple sessions. In fact, the duration of tES treatments, with one stimulation per day, ranges from 2 sessions (against alcohol or smoke craving, Boggio et al., 2008; Fregni et al., 2008) to 30 sessions (to support motor function in stroke patients, Hesse et al., 2011). In clinical contexts, the 5 consecutive day application is common in several diseases, including depression (Fregni et al., 2006b; Nitsche et al., 2009), pain (Zhu et al., 2017), and stroke (Boggio et al., 2007). The possibility of a simple home treatment set-up, easily manageable by the patient without special assistance, would therefore greatly increase the impact of RePE.

By theoretical computational modeling analysis, we tested here the relevance of RePE shape and position in terms of the tDCS differential efficacy on S1 with respect to primary motor cortex (M1) using a personalized vs. a non-personalized electrode. Computational modeling exploits high resolution MRI and accurate brain models based on Finite Element Method (FEM) to predict the electric field induced in each voxel of the brain during tDCS, thus allowing for an optimization of the tDCS montage, i.e., the maximization of the current flowing in the target region with respect to the other brain areas; in other words the maximization of the target region dosage (Antal et al., 2017).

We first aimed here to present and test a new MRI-based procedure to shape a RePE without the need for the neuronavigation technique, therefore bypassing the simultaneous presence of the patient and the experienced operator. Furthermore, we present a positioning technique that takes advantage of the scalp-space distances calculated on the 3D MRI reconstruction of the subject's head.

In the perspective of applying FaReMus at people home, we had here the second aim of introducing a procedure for easy and accurate repositioning of the electrode in a domiciliary environment (Pérez-Borrego et al., 2014; Charvet et al., 2015). We developed an adjustable helmet frame (AHF) to maintain the position of RePE during stimulation, and to allow an easy repositioning of RePE in multisession tDCS treatments even at the patient's home.

METHODS

The whole procedure was tested on 14 healthy volunteers (10 females, 4 males; age range 25–56 years, mean age 33.9 $\pm$ 11.0 years), eligible to the study in absence of clinical evidence or history of neurological or vascular diseases and with no pharmacological treatments. All participants provided written informed consent for participation in the study, as

approved by the "Lazio 1-San Camillo Forlanini" Ethics Committee.

Each subject underwent a structural brain MRI exam with a 1.5 T scanner (Achieva, Philips Medical Systems, Best, The Netherlands). The acquisition protocol consisted of one 3D high resolution anatomical sequence empirically optimized to increase gray/white matter image contrast (T1-weighted Turbo Field Echo TR/TE/FA = 9.5 ms/4 ms/8°; 2,562 matrix resulting in an in-plane resolution 0.98 × 0.98 mm, slice thickness 1.2 mm, 160 coronal contiguous slice).

Computerized RePE-S1 Shape

As a preliminary step, we manually traced the central sulcus on the standard MNI152_T1_1 mm_brain MR template, thus avoiding the use of neuronavigation in shaping the RePE-S1. A total of 123 points were selected in the middle of the pre- and post-central sulcus (CS) walls, one for each of the 123 sagittal slices passing across the template central sulcus. These points span from the Sylvian sulcus of the left hemisphere to the same sulcus of the right hemisphere (MNI_CS).

The computerized process for shaping the individual RePE-S1 electrode (**Figure 1**) from her/his brain MRI consisted of the following steps:

1. Scalp and brain tissues were segmented from individual original MRIs (iMRI) using the Brain Extraction Tool (BET) of FSL (iBrain and iScalp);
2. iBrain images were spatially normalized with respect to the standard MNI152_T1_1 mm_brain MR template by means of the FMRIB's Linear Image Registration Tool (FLIRT) and the related transformation was saved as a matrix (TM);
3. The 123 MNI_CS points were automatically mapped onto the iMRI of each subject using the inverted spatial normalization matrix [TM^{-1}, convert xfm & img2img] to obtain the 123 points on iMRI (iCS);
4. The iCS was projected onto the external surface of the 3D iScalp using an in-house software (iCSS), applying the minimal distance brain-scalp tissues for each point.
5. The iCSS were then projected to a plan, performing the iCSS on a plan (iCSSp).
6. RePE-S1 was designed using AutoCAD software (Autodesk AutoCAD 2017). The iCCSp coordinates were imported into the software in the native space and replicated at a distance of 2 cm from the original trace. Then, the two 2D iCCS were connected laterally to form a polygon.
7. The shape of RePE was exported in the PDF format and printed to be cut into sponge or conductive silicon electrodes.

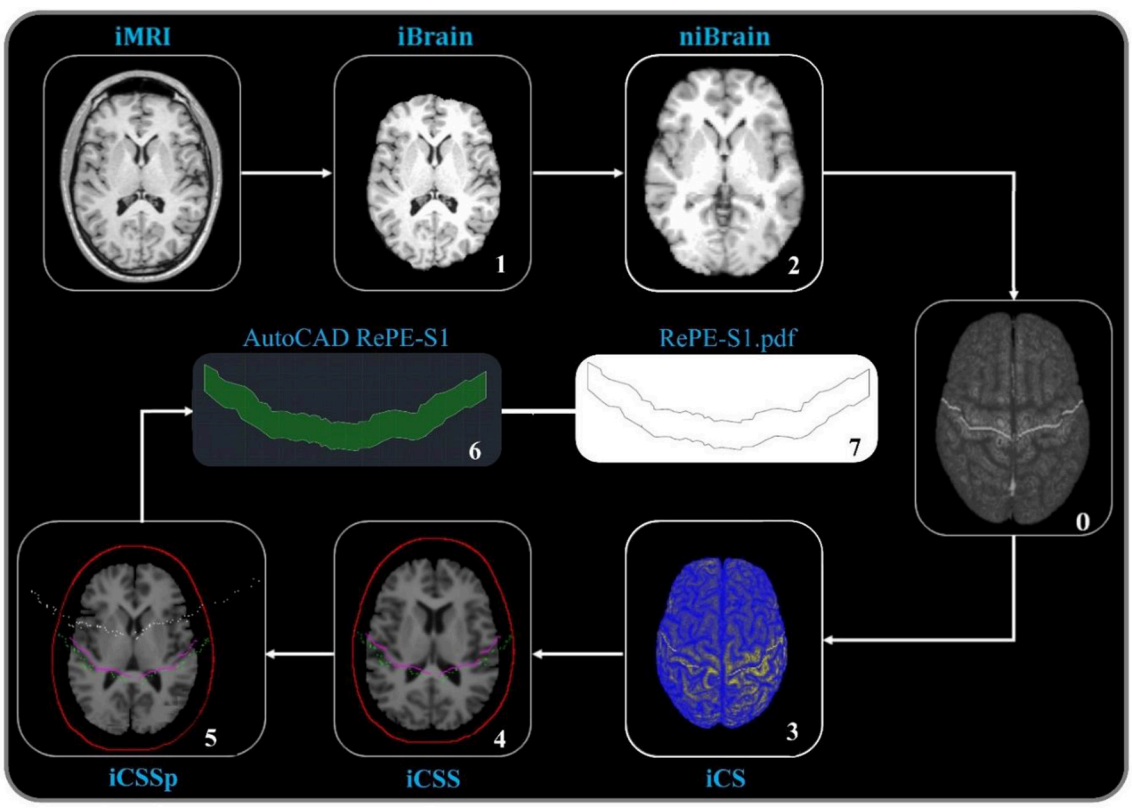

FIGURE 1 | Computerized procedure to shape RePE. As detailed in the Methods, the steps from the individual brain MRI (iMRI), with segmentation of the brain (iBrain, 1), transformed into MNI standard model (niBrain, 2), where the central sulcus identified points are stored (once for every person, thus no number in the process applied in individual subject, 0) and retro projected obtaining the individual central sulcus (iCS, 3), projected on the scalp (iCSS, 4), and further projected on a planar surface (iCSSp, 5) so that by AutoCAD the RePE area is obtained (6) and printed (7).

RePE Positioning Based on the 3D MRI Head Model

To position RePE-S1 over the scalp of each subject in a way that the electrode would overlap her/his iCCS coordinates (minimal distance to the target region), we developed an MRI-based procedure to place each RePE-S1 in relation to the selected external landmarks on the subject's scalp. In particular, we used the following individual head points: Nasion (N, **Figure 2A**); Inion (I, **Figure 2B**); the central and lateral points of RePE-S1 located on the iCSS (RePE-S1_C, RePE-S1_L, RePE-S1_R, **Figure 2C**) with RePE-S1_C positioned on the line connecting Nasion and Inion. Then, over the 3D-rendered head, we measured the distances between N and the above defined three points: N-RePE-S1_C, N-RePE-S1_L, N-RePE-S1_R (**Figures 2D–F**). Given these three values, an operator can position RePE-S1 using the following procedure. She/he should place the zero (0) of a flexible meter on N and extend the meter to I (**Figure 2G**). Then he/she can center RePE-S1_C at distance N-RePE-S1_C from N, along the N-I line. Then he/she can adjust the RePE orientation through the N-RePE-S1_L and RePE-S1_R distances (**Figures 2H,I**).

An Adaptable Helmet Frame [AHF] for the Electrode Repositioning in Multisession tDCS Treatment

We developed an Adaptable Helmet Frame (AHF) using a plastic cyclist helmet (**Figure 3**). The helmet frame was equipped with an adjustable mechanism to comfortably fit the individual head of

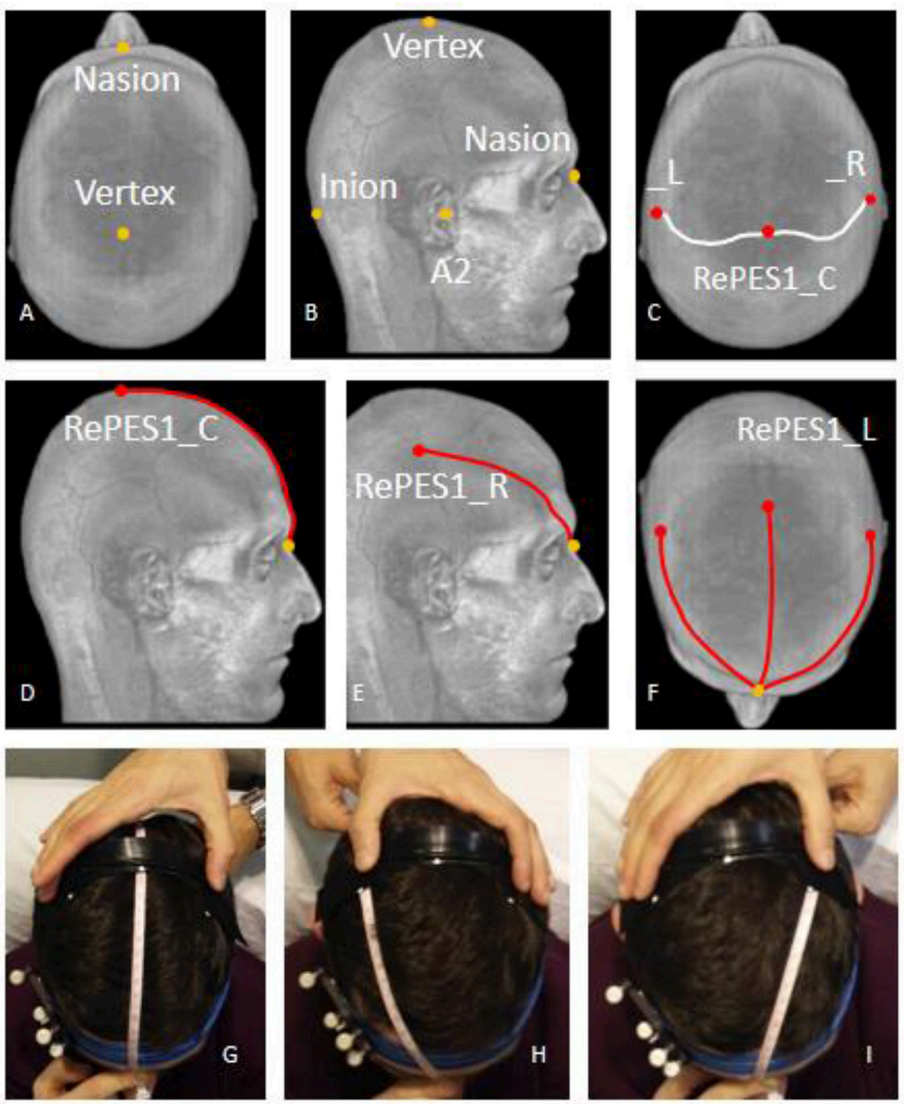

FIGURE 2 | RePE positioning with 3D MRI-derived head space distances. As detailed in the Method section, representation of the curves on the scalp **(A–F)**, whose lengths derived from the individual 3D head model allow positioning RePE **(G–I)**.

FIGURE 3 | AHF for multisession RePE repositioning. Left: Adaptable Helmet Frame (AHF) without (left) and with (right) the Velcro strips to fix RePE. The occipital cathode electrode is fixed under the adjustable mechanism. Right: As detailed in the Methods, steps **(A,B)** allow positioning and re-positioning the AHF in same position. **(C,D)** fix the RePE position with respect to the AHF. Informed consent was obtained from the participant wearing the AHF to publish the image.

the subject, and it was integrated with a nasal support and Velcro bands to firmly fix the electrodes in the desired position.

Once RePE has been properly positioned, the operator can fix the AHF taking care not to move RePE electrode. In detail, (1) she/he positions the AHF so that the nasal support rests well on the nose (**Figure 3A**) and the inferior border lays over the top of the ears (**Figure 3B**). In this way, the AHF is always set in the same position. Thereafter, she/he (2) adapts the circumference to the individual head using the adjustment mechanism, and (3) fixes the electrode to the AHF stably with the two coronal Velcro strips (**Figures 3C,D**).

Neuronavigated Procedure to Evaluate the RePE Positioning and Re-positioning

We used neuronavigation (SofTaxic Neuronavigation System ver. 2.0, www.softaxic.com, E.M.S., Bologna, Italy) to test the repeatability of the RePE positioning based on the 3D MRI head model (**Figure 4A**), and to test the stability of the RePE AHF repositioning (**Figure 4B**).

We marked 27 points along the entire length of the electrode: the central point, 13 points on the left and 13 on the right of the central point (0.5 cm between points, RePEpoints, **Figure 4C**).

We collected the coordinates of RePEpoints in the individual MRI space, after positioning the electrode along the central sulcus projected on the scalp using the 3D-head space anatomical landmarks system, and repeated the procedure five times. For comparison, we also collected the RePEpoints positions when positioning RePE using the neuronavigated procedure. Finally, we calculated the distances between the corresponding RePEpoints and the points of the central sulcus projected onto the scalp (**Figure 1**).

To test the repeatability of the repositioning tool, we properly fixed the electrode into the AHF, we digitized the RePEpoints coordinates, and then we removed the AHF. We repeated the digitization of the RePE position after wearing AHF over 5 consecutive days.

Statistical Analysis

Evaluation of the Identification of the Computerized Individual Central Sulcus

To evaluate the ability of the computerized procedure to locate the individual central sulcus, we compared the 123 iCSS points with those obtained by manually tracing the central sulcus on individual MRIs projected on the scalp (Manual iCSS).

Two independent researchers (a neuroradiologist—DL and a biomedical engineer with specific training in MRI data analysis—AC) selected every sagittal image where the central sulcus appeared on the individual segmented brain and recorded one point (X, Y, Z) for each slice. Accordingly, the number of points of Manual iCSS varied across subjects between a minimum of 102 and a maximum of 117. We projected the Manual iCS onto the external surface of the 3D iScalp using the same software that was used for the Computerized procedure (Manual iCSS).

We quantified the accuracy of the Computerized iCSS identification as the point-to-point Euclidean distance to the Manual iCSS set (nearest points) and the Intra-Class Correlation (ICC) between Computerized iCSS and Manual iCSS.

RePE Position Accuracy

We evaluated the repeatability of RePE position using the Euclidean distances of the RePEpoints from the corresponding projections on the scalp of the central sulcus points. In order to detect possible systematic positioning errors, we submitted the differences of the 3D coordinates (x, y, z) for the 27 points in successive positions to an analysis of variance (ANOVA) with the Positioning Error (Rep2-1, Rep3-1, Rep4-1, Rep5-1) and Positioning Method (Neuronavigation, 3D MRI-head distances) as within-subject factors. Any systematic displacement will correspond with significant Positioning Error effect. We performed all statistical analysis using SPSS (IBM).

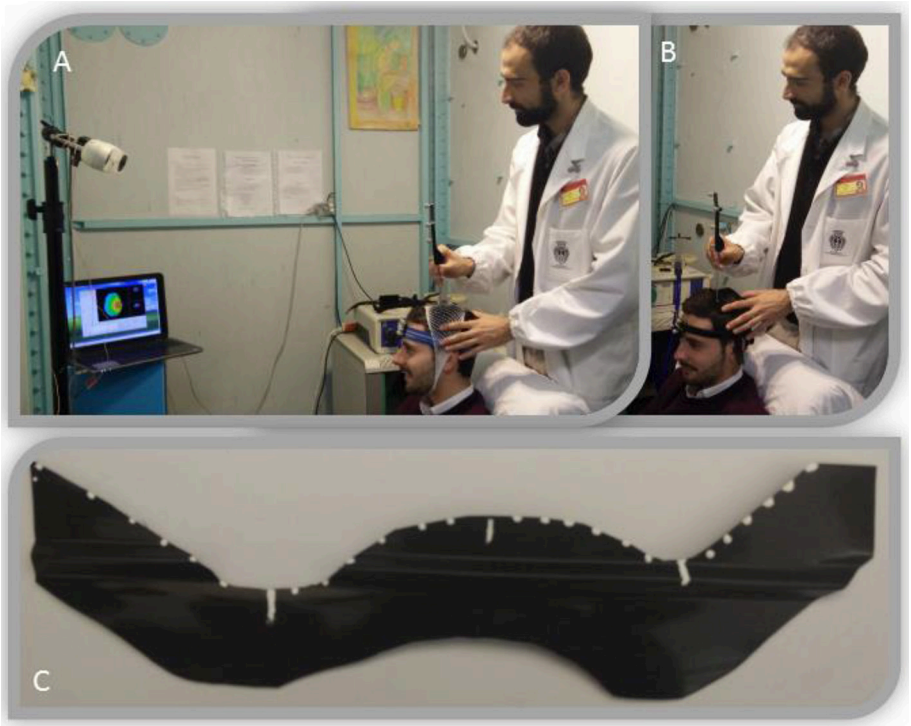

FIGURE 4 | Neuronavigation setup used to estimate RePE positioning systems. Top: As detailed in the Methods, experimental neuronavigated procedure to test the RePE positioning via the MRI-derived 3D-head model measures **(A)** and via the AHF **(B)**. Informed consent was obtained from the participants executing the procedure and wearing RePE to publish the image. **(C)** RePE with the testing point used for the neuronavigated procedure.

Intracerebral Current Induced by RePE: MRI-Derived Finite Element Method

The electric field (EF) distributions induced into the brain by RePE-S1 and non-RePE were computed using a FEM forward model. Several configurations were analyzed: different positions of RePE-S1 and different return electrode locations. One MRI scan of a 39 year old adult male head was segmented using an algorithm developed in-house for automated tissue compartment segmentation (Huang et al., 2013). Adaptive volumetric meshing was applied to the tissue segmentation in ScanIP (Simpleware Ltd, Exeter, UK) with a compound coarseness of −15 (maximum edge length 1.85 mm, target minimum 0.775 mm, target Jacobian minimum 0.1). The resulting meshes consisted of $>10^7$ quadratic tetrahedral elements and $>1.5{\cdot}10^6$ degrees of freedom. Further refined meshes were found to have no noticeable effect on simulation results. The mesh was imported into COMSOL Multiphysics 4.3 (Burlington, MA) to simulate quasi-static volume conductor physics, since this approximation is acceptable for tES (Smith, 1992; Nathan et al., 1993; Eshel et al., 1995). The overall volume was divided in seven compartments with different electrical conductivity (Datta et al., 2011; Parazzini et al., 2011; Wagner et al., 2014; Galletta et al., 2015; Cancelli et al., 2016) representing: gray matter ($\sigma = 0.276$ S·m^{-1}), white matter ($\sigma = 0.126$ S·m^{-1}), cerebral spinal fluid (CSF, $\sigma = 1.65$ S·m^{-1}), skull ($\sigma = 10^{-2}$ S·m^{-1}), air ($\sigma = 10^{-4}$ S·m^{-1}), fat $\sigma = 0.025$ S·m^{-1}), and skin ($\sigma = 0.465$ S·m^{-1}). Two additional masks including the Post and Anterior Central Gyruses were created and intersected with gray matter to segment the Primary Somatosensory and Motor Area, respectively, for a quantitative evaluation of the electric field generated at the target. The electrodes were imported into ScanCAD (Simpleware Ltd, Exeter, UK) for manual positioning over the scalp of the 3D model. During transcranial electrical stimulation (tES), a conductive gel ($\sigma = 0.3$ S·m^{-1}) is interposed between the silicon electrode and the scalp. The adopted model was modified accordingly.

Within COMSOL, the Laplace equation $\nabla(\sigma\nabla V) = 0$, with σ being the electric conductivity and V the electric potential, was solved considering the Neumann boundary conditions. COMSOL implemented a linear system solver of conjugate gradients with a relative tolerance of 10^{-6} mA of current stimulation which was applied for all the montages, so a boundary condition of orthogonal current density was implemented to the anode and the cathode. For each electrode, the current value was divided by the skin-electrode contact area and was applied as a current density boundary condition and assigned to the mesh nodes as current loads representing the right-hand-side of the linear system of equations.

RePE-S1 vs. Non-RePE-S1 Bilateral Stimulation

Two different electrodes of 35 cm^2, RePE over S1 and a non-personalized electrode (semi-curved pad 17.5 × 2 cm, Cancelli et al., 2015a; Parazzini et al., 2017) placed in three different

locations were examined as anodes (**Figure 5**). A standard electrode with twice the area of the anodes [70 cm^2, in order to decrease the current density under the return electrode (Tecchio et al., 2014, 2015; Cancelli et al., 2015a,b, 2017)] was used as a cathode centered over Oz.
We examined four montages:

- Montage RePE A: RePE-S1 designed and positioned over S1 as detailed in sections Computerized RePE-S1 shape and RePE Positioning Based on the 3D MRI Head Model;
- Montage Non-RePE A: non-RePE over hand/mouth S1;
- Montage Non-RePE B: non-RePE centered on Cz of the 10–10 International System (IS);
- Montage Non-RePE C: non-RePE centered on CPz of the IS.

Reference Electrode Evaluation

Following the results of the montages described in section Reference Evaluation in RePE tDCS, no more computations involving either the non-RePE anode or positions behind the Central Sulcus of RePE-S1 were run. Sixteen montages with RePE-S1 were evaluated with the aim of optimizing the RePE stimulation: four different reference electrodes (pad over Oz, Neck, Shoulders and a strip around the head, **Figure 6**), each with four different positions of RePE-S1, with the anterior border of RePE-S1 overlapping the CS scalp projection (RePE A), 0.5 cm ahead of the CS scalp projection (RePE B), or 1 and 1.5 cm ahead (RePE C and RePE D).

RESULTS

Computerized RePE Design

Computerized Individual Central Sulcus on the Scalp

The mean average distance across points and subjects of iCSS and manual iCSS sets was 2.9 ± 3.2 mm, and the mean intra-class correlation was 0.999 ± 0.0013 (ICC).

RePE Positioning and Re-positioning

RePE Position Based on Head Fiducials

The coordinates of the RePE position did not differ between neuronavigated positioning and new computerized positioning based on the distances derived from the 3D-head model, as indicated by the *Positioning Method* factor [$F_{(3, 3)} = 0.263$, $p = 0.849$]. The mean repetition error in terms of the Euclidean distance was 3.0 mm for neuronavigation and 3.5 mm for anatomical landmark-system across all repetitions (**Table 1**). When compared with paired-sample *t*-test, no differences were found [$t_{(9)} = -1.110$, $p = 0.296$]. No systematic displacement occurred in any direction, as indicated by the *Positioning Error* factor [$F_{(9, 45)} = 0.768$, $p = 0.646$].

Adaptable Helmet Frame [AHF] for the Electrode Repositioning in Multisession tDCS Treatment

The mean repositioning error in terms of the Euclidean distance was 4.8 ± 1.1 mm across all repetitions and subjects. The ANOVA design analyzing the coordinate differences displayed that no systematic displacement occurred in any direction (**Table 2**). In fact, *Positioning Error* factor was [$F_{(3, 24)} = 0.086$, $p = 0.967$].

Electric Field Distribution Analysis

RePE-S1 vs. Non-RePE-S1 Bilateral Stimulation

The different shape and position of the electrode used as anode and cathode (**Figure 5**) played a key role in determining the boundaries of the cortical area that was stimulated. Specifically, RePE A generated a cortical EF diffused uniformly from the central sulcus to the occipital area, position of the return electrode. Therefore, the stimulation affected the entire S1 with an average EF (EF_{AVE}) of 0.152 V/m for the 1.5 mA/35 cm^2 current density, while the EF was minimized in M1 ($EF_{AVE} = 0.134$ V/m). In the montage non-RePE A the non–personalized electrode was placed ahead of the Central Sulcus and the stimulation involved both the entire S1 ($EF_{AVE} = 0.153$ V/m) and M1 ($EF_{AVE} = 0.140$ V/m). The montage non-RePE B generated a similar EF magnitude to that of RePE A in the central section of S1, but decreasing toward the Sylvian Fissure (**Figure 5**). This is conceivably because the non-personalized electrode didn't follow the convolutions of the entire Post Central Gyrus. Thus, the resulting average EF in S1 was lower than RePE A, $EF_{AVE} = 0.114$ V/m. The montage non-RePE C was placed posteriorly to S1 so the stimulation barely affected both S1 ($EF_{AVE} = 0.083$ V/m) and M1 ($EF_{AVE} = 0.078$ V/m).

The maximum ratio between the EF induced in S1 and M1, was obtained by montage RePE A ($EF_{AVE}{}^{S1} > 13\%\ EF_{AVE}{}^{M1}$).

Reference Evaluation in RePE tDCS

The computational analysis using various positions of the RePE anode with different cathodes revealed that the highest efficacy is obtained using a standard reference electrode on Oz, placed oppositely to the area in which the induced EF is required to be low (in this case, M1). The average EF obtained with all the RePE positions with Oz reference (**Figure 6** bottom, **Table 3**) is the highest (0.91 V/m) in the Left, Central and Right part of S1, even if the effect in the central part is similar in M1. Indeed, the other reference choices cannot discriminate between the EF in M1 and S1 at all. In particular the Neck and Shoulder reference induced maximal EF only in the lateral parts (L and R, 0.09 V/m) of the target region. The strip reference causes a low EF from Left to Right both in S1 and M1 (0.58 V/m).

Comparing the positions of the RePE anode over the scalp, best efficacy is obtained by the RePE A position ($EF_{S1}/EF_{M1} = 1.13$). RePE B, with a slip of 5 mm from Position A toward the projection of M1, generated similar EF at the target ($EF_{S1}/EF_{M1} = 1.12$), while RePE C and RePE D (1 and 1.5 cm form Position A) significantly decreased performances.

DISCUSSION

The main achievement of this study is the double development of an easy and effective tool to shape and position a tES electrode personalized for stimulating a specific cortical district, and for repositioning it for a multi-sessions protocol, specifically designed to be used by the patient at home.

When the stimulation target is a limited cortical area, modeling suggests that a ring configuration of HD electrodes is the most appropriate montage for focusing current into such area

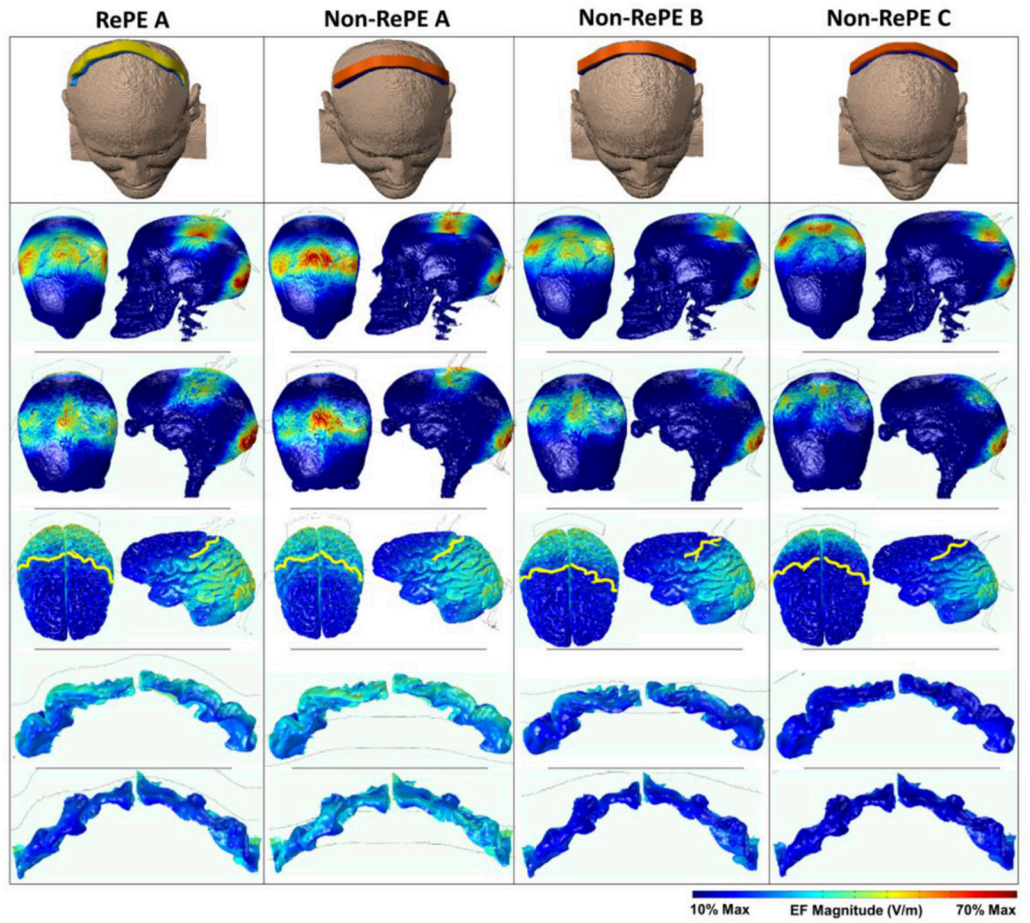

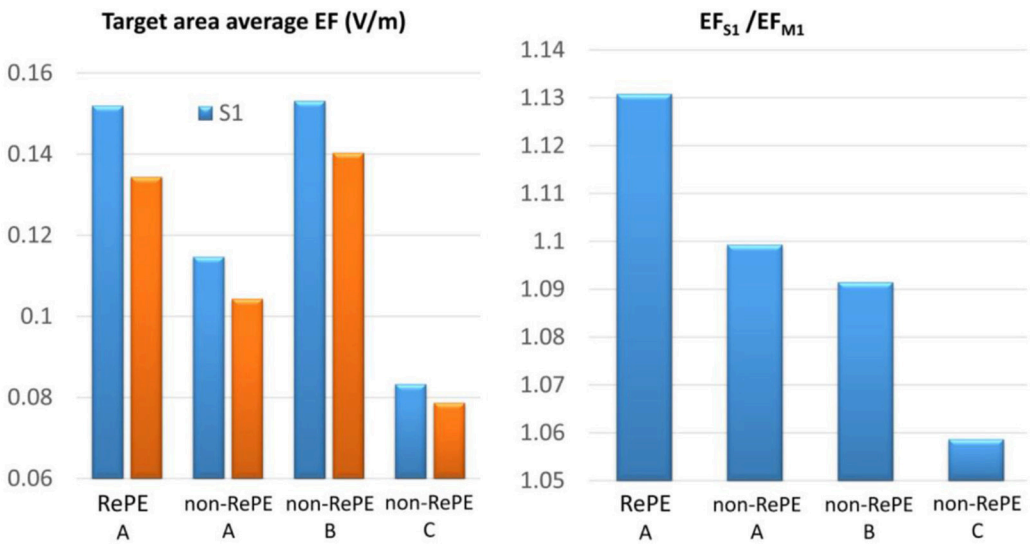

FIGURE 5 | Modeling: RePE-S1 vs. non-RePE-S1 comparison. Top: First row: The four anodal electrodes tested against the same reference with twice the RePE's area positioned on Oz: personalized S1 electrode positioned 0.5 cm frontal to the scalp projection of the central sulcus (RePE A), the non-personalized strip shaped to overlay Cz and from C3 to C4 (Non-RePE) with a part on hand/mouth S1 (A), on Cz (B), or on CPz (C). From the second row: electric field amplitude (EF) on the scalp (second row), dura mater (third row), cortical surface (fourth row), and S1 post-central (fifth row) and M1 pre-central gyri (sixth row). Bottom: Average EF (V/m) in the whole body S1 (light blue) and M1 (orange) for the four montages (Left) and the ratio in S1 with respetct to M1 (Right).

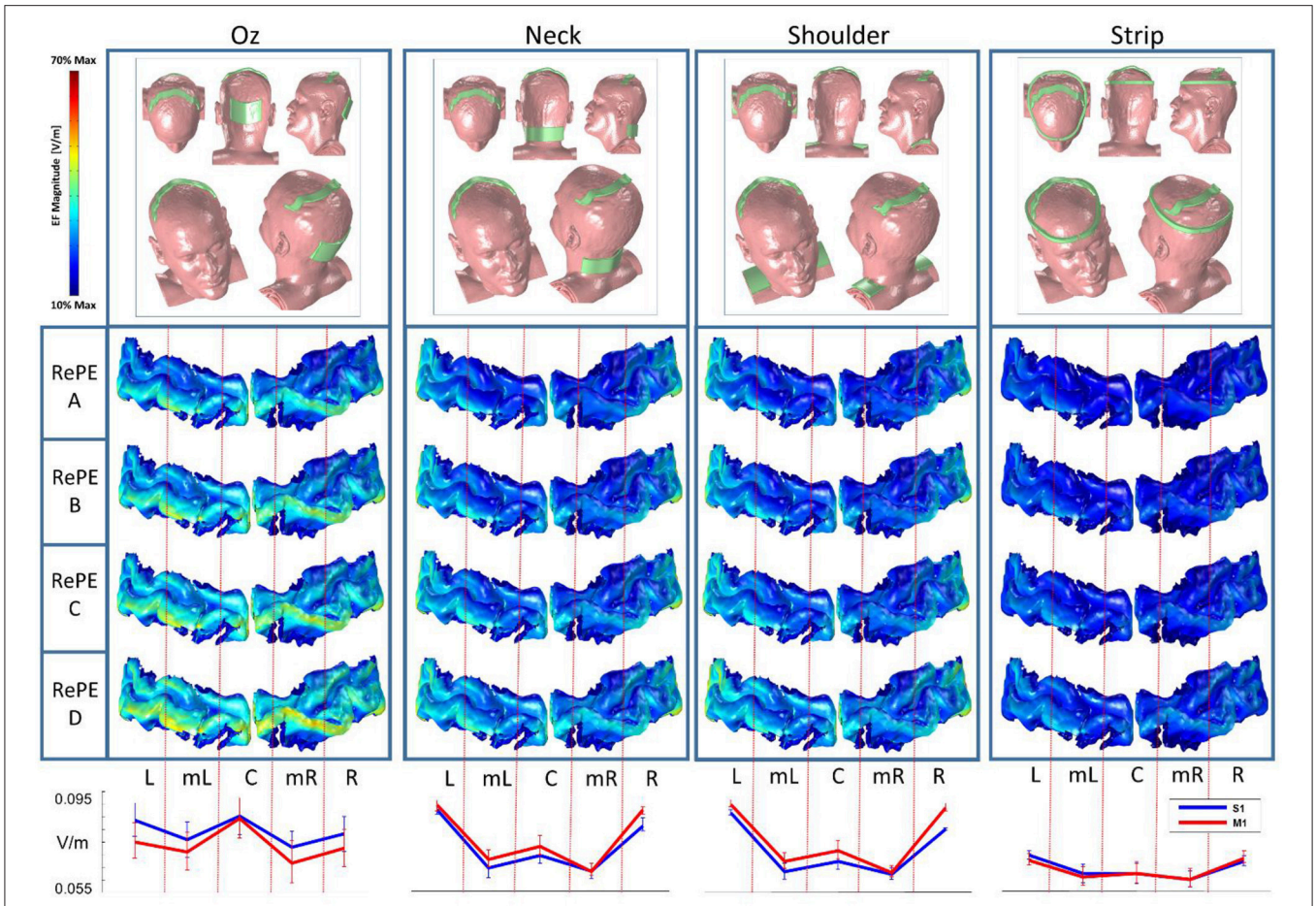

FIGURE 6 | Modeling: Reference evaluation in RePE tDCS. **(Top)** For each of the reference electrode position (Oz, neck, shoulders, and a ring centered on RePE) the electric field amplitude (EF) on the cortical strip including the S1 and M1 cortical gyri for the four RePE positions: with the anterior border fitting the CS scalp projection (RePE A), 0.5 cm (RePE B), or 1 cm (RePE C) and 1.5 cm ahead (RePE D). **(Bottom)** Average EF (V/m) in the five sections (Left L, medio-Left mL, central C, medio-Right mR, and Right R) of S1 (blue) and M1 (red), averaged across the RePE positions, for the four reference electrodes.

TABLE 1 | RePE positioning via 3D head MRI distances vs. Neuronavigation.

Session	Neuronavigation (mm)				3D head model MRI distances (mm)			
	Distance	***X***	***Y***	***Z***	**Distance**	***X***	***Y***	***Z***
1	3.1 ± 1.4	1.1 ± 2.9	0.5 ± 2.8	−0.8 ± 2.7	3.7 ± 0.6	1.9 ± 2.7	−3.1 ± 4.1	2.0 ± 3.9
2	2.6 ± 1.5	0.4 ± 3.0	−0.6 ± 3.1	−0.4 ± 2.2	2.5 ± 0.5	1.5 ± 2.7	−2.3 ± 4.3	2.8 ± 4.9
3	2.7 ± 1.3	0.9 ± 2.1	−1.9 ± 1.6	0.7 ± 2.3	3.7 ± 0.5	−2.0 ± 3.7	2.3 ± 4.4	0.9 ± 3.7
4	3.4 ± 1.1	1.4 ± 3.3	0.0 ± 2.2	0.5 ± 2.4	4.2 ± 0.7	2.0 ± 3.0	2.0 ± 2.7	−3.9 ± 2.6
5	3.0 ± 0.6	1.3 ± 2.7	−1.4 ± 4.2	1.2 ± 3.6	3.8 ± 1.2	0.8 ± 3.5	−0.2 ± 4.6	2.5 ± 5.0
Overall	3.0 ± 1.2	1.0 ± 2.8	−0.7 ± 2.8	0.2 ± 2.6	3.5 ± 0.8	0.8 ± 3.3	−2.8 ± 4.3	0.3 ± 2.1

Mean displacements between each of the 27 RePEpoints in each electrode and the corresponding point of the scalp projection of the central sulcus, both as Euclidean distance (Distance) and the differences of each of the three Cartesian coordinates (x, y, z), when the personalized electrode was positioned either using the neuronavigated procedure or the distances derived from the 3D-head model from individual MRI.

(Datta et al., 2009; Cancelli et al., 2016). On the contrary, the idea of the RePE-tDCS came out from the necessity to uniformly stimulate an extended cortical region (S1) and to minimize the degree to which EF was induced in the adjacent region (M1). The present procedure makes this personalized stimulation more easy and affordable.

The results obtained through computational modeling support the idea that RePE-tDCS is a valid montage for

TABLE 2 | RePE position by adaptable helmet frame [AHF].

Day	Distance	*X*	*Y*	*Z*
1	4.8 ± 1.4	−2.0 ± 1.9	0.9 ± 1.4	0.8 ± 1.2
2	4.9 ± 1.1	−0.7 ± 3.6	3.0 ± 3.1	−1.0 ± 2.4
3	4.7 ± 1.0	0.8 ± 1.2	2.8 ± 0.4	0.7 ± 2.3
4	4.9 ± 1.1	−2.1 ± 2.8	0.6 ± 3.8	1.1 ± 2.4
5	4.6 ± 0.7	−2.0 ± 3.9	0.8 ± 4.2	0.5 ± 2.8
Overall	4.8 ± 1.1	−0.7 ± 2.7	1.6 ± 2.6	0.4 ± 2.4

Mean displacements between each of the 27 RePEpoints in each electrode positioning with the AHF and the corresponding point of the scalp projection of the central sulcus, both as Euclidean distance (Distance) and the differences of each of the three Cartesian coordinates (x, y, z).

differentiating the tDCS dose between two contiguous areas. A non-RePE electrode cannot reach the same efficiency in terms of local specificity of the induced EF, regardless of its position on the scalp. On the other hand, it is clear that in any standard tDCS montage, i.e., with 2 electrodes, the position of the second electrode is crucial in managing the direction of the current flow. Because of the high conductivity of the CSF, the EF generated by tDCS is diffused between the two electrodes. Therefore, the electrode shape is not the unique parameter which should be considered in a RePE-montage optimization. To realize a correct RePE-tDCS, the shape and position of the reference electrode are essential (**Figure 6**). In both extra-cephalic standard electrode references—neck and shoulders—and a strip around the head, the current flow did not affect the cortex as much as utilizing an occipital electrode. The four positions used to test RePE suggest that the tDCS dose is more differentiated between the two areas when the edge of the electrode, opposite to the reference, is close to the boundary delimiting the two areas (RePE A). On the other hand, a similar EF magnitude is obtained using a position of the anode that is 0.5 cm away (RePE B). This suggests that a position displacement of <5 mm does not affect the stimulation.

The computerized procedure we developed to design RePE identifies the edge of the target area on the MNI model and retro-transforms it onto the individual MRI coordinates. We evaluated the accuracy of this step through a control test, and we observed errors to the order of 2–3 mm with respect to the visual inspection of manual tracing, as tested by two independent MRI analysis experts.

The computerized procedure, processing the individual MRI using standard well-tested software, offers multiple advantages relative to manual protocols including:

(1) a significant time reduction in the electrode preparation; (2) no need to have the patient in the laboratory for the RePE preparation; (3) no need for a neuronavigation system; (4) the reduction of the variability in the RePE shape, depending on the experience of the researcher or technician who prepares the electrode.

In the present investigation, we used a 3D T1 sequence (MPRAGE) on a 1.5 T MRI scanner to obtain anatomical scans. In some experiments we tested lower resolution images in order to consider the minimal requirement of the quality of scans necessary to apply the proposed computerized procedure. The

TABLE 3 | Reference evaluation in RePE tDCS.

Montage	Oz					Neck					Shoulders					Strip				
	L	mL	C	mR	R	L	mL	C	mR	R	L	mL	C	mR	R	L	mL	C	mR	R
RePE A	1.135	1.090	1.029	1.144	1.101	0.993	0.945	0.960	0.991	0.967	0.974	0.942	0.946	0.992	0.923	1.071	1.038	1.008	1.003	1.006
RePE B	1.139	1.091	1.026	1.124	1.093	0.994	0.964	0.960	1.026	0.932	0.977	0.948	0.950	1.006	0.916	1.065	1.056	1.016	1.026	0.983
RePE C	1.126	1.076	1.022	1.103	1.094	0.991	0.967	0.961	1.024	0.929	0.974	0.952	0.952	1.008	0.912	1.057	1.056	1.011	1.022	0.980
RePE D	1.106	1.062	1.011	1.061	1.073	0.981	0.962	0.960	1.006	0.919	0.966	0.950	0.952	0.996	0.902	1.036	1.040	1.000	0.991	0.964

Electric field in S1 and M1 ratio delivered by the 16 montages in the five different portions of the target regions.

scans do not require high-resolution 3D sequences, but the sulcus can be well identified using almost any acquisition sequence (i.e., T1, T2, Flair) in any direction axial, sagittal and coronal, with a voxel resolution around 1 mm^2 and maximum 3 mm of slice thickness.

The present paper provides a simple and low-cost procedure for the tES electrode positioning and re-positioning (AHF), using easily recognizable anatomical scalp landmarks in any tES multisession treatments. Being a non-invasive brain stimulation, tDCS painlessly delivers electrical current of low intensity through the skull to selected areas of the brain (Nitsche et al., 2000; Antal et al., 2017), and offers a very high safety profile. Several double-blind studies proved multisession tDCS treatments to have negligible side effects offering an analgesic effect against chronic pain (Soler et al., 2010; Brietzke et al., 2016), to relieve symptoms in attention deficits and depression (Gögler et al., 2016; Cachoeira et al., 2017), in addition to relieving fatigue in multiple sclerosis. The suitability and repeatability consistent with those obtained via neuronavigation further simplify tES procedures, making them largely suitable for multisession home treatments and clinical protocols (Pérez-Borrego et al., 2014; Amatya et al., 2015; Charvet et al., 2015).

The test of the whole procedure is performed only for the single post-central gyrus RePE shape and position. This is a limitation of the present study. However, it is conceivable that the presented procedure can be easily exported to other extended cortical targets, like (almost) all bilateral associative cortices. While in the case of the central sulcus we proved that our procedure was appropriate, for different sulci that show greater variability between individuals other brain normalization procedures that take into account all cortical folding (Destrieux et al., 2010) might be evaluated. In the present work, we developed an automatized procedure to shape and position an electrode to focus the neuromodulation effect on a cortical area, limiting as much as possible the direct effects on contiguous cortical areas. We developed this procedure, based on individual brain MRI, since we documented that the personalization of the electrode is necessary to modify the excitability of the entire area of the postcentral gyrus from the left to the right Silvian sulcus (Cancelli et al., 2015a).

Future perspectives in the field of transportation research will consider to build and strengthen easy to use methods for other personalized tES. The relevance of the homologous areas balance in different neurological and psychiatric disorders (Fregni et al., 2006a; Ferrucci et al., 2009; Nitsche et al., 2009), and the indication that equal bilateral stimulation impinge positively counteracting pathological imbalances (Pahor and Jaušovec, 2018; Tseng et al., 2018), suggests that developing electrodes to target such bilateral representations will be more frequent in future. Conceivably, to build electrodes that take into account the specific individual cortical folding is an advantage in focusing the stimulation of high-definition tES (Edwards et al., 2013; Moreno-Duarte et al., 2014; Malavera et al., 2015; De Ridder et al., 2017). In fact, we devoted this work to develop an easy applicable tool to stimulate a specific cortical region in individual patients, without the need of neuronavigation, and we underlined that other RePE to target other cortical folding can be shaped and positioned via the procedure offered in the present work. Nevertheless, specific cases require proper modeling analyses in selecting the proper montage, specifically defining the reference in use.

CONCLUSIONS

We provide a model-based investigation of the RePE tDCS accompanied by a simple, low-cost procedure to easily apply it. We tested the technique for the stimulation of the primary somatosensory area, but the procedure, if supported by a correct application of the return electrode, can potentially be applied to any cortical region to differentiate the EF induced at the target region. Furthermore, as a complete and computerized design, positioning and re-positioning of the electrodes establishes a relevant advancement for any home tES treatment.

AUTHOR CONTRIBUTIONS

FT and AC: contributed to conception and design of the study; AC, GA, CC, AG, and DL: acquired and analyzed the data; AC, FT, and VP: drafted and finally revised the manuscript and the figures.

ACKNOWLEDGMENTS

The authors are sincerely grateful to all involved for the time and cooperation required to participate in the study and thank Massimiliano Marconi and Daniele Spizzichino for the support in collecting MRI and Prof. Filippo Carducci and Eng. Giulia Santi for important steps in the computerized procedure of the RePE shaping. This work was supported by:

1) FISM—Fondazione Italiana Sclerosi Multipla—Cod. 2014/R/22 [FaReMuS CuNeH], and
2) PNR-CNR Aging Program 2012–2018.

REFERENCES

Amatya, B., Galea, M. P., Kesselring, J., and Khan, F. (2015). Telerehabilitation for persons with multiple sclerosis. *Cochrane Database Syst. Rev.* 4:CD010508. doi: 10.1002/14651858.CD010508.pub2

Antal, A., Alekseichuk, I., Bikson, M., Brockmöller, J., Brunoni, A. R., Chen, R., et al. (2017). Low intensity transcranial electric stimulation: safety, ethical, legal regulatory and application guidelines. *Clin. Neurophysiol.* 128, 1774–1809. doi: 10.1016/j.clinph.2017.06.001

Boggio, P. S., Nunes, A., Rigonatti, S. P., Nitsche, M. A., Pascual-Leone, A., and Fregni, F. (2007). Repeated sessions of noninvasive brain DC stimulation is associated with motor function improvement in stroke patients. *Restor. Neurol. Neurosci.* 25, 123–129.

Boggio, P. S., Sultani, N., Fecteau, S., Merabet, L., Mecca, T., Pascual-Leone, A., et al. (2008). Prefrontal cortex modulation using transcranial DC stimulation

reduces alcohol craving: a double-blind, sham-controlled study. *Drug Alcohol Depend.* 92, 55–60. doi: 10.1016/j.drugalcdep.2007.06.011

Brietzke, A. P., Rozisky, J. R., Dussan-Sarria, J. A., Deitos, A., Laste, G., Hoppe, P. F., et al. (2016). Neuroplastic effects of transcranial direct current stimulation on painful symptoms reduction in chronic hepatitis C: a phase II randomized, double blind, sham controlled trial. *Front. Neurosci.* 9:498. doi: 10.3389/fnins.2015.00498

Cachoeira, C. T., Leffa, D. T., Mittelstadt, S. D., Mendes, L. S. T., Brunoni, A. R., Pinto, J. V., et al. (2017). Positive effects of transcranial direct current stimulation in adult patients with attention-deficit/hyperactivity disorder – A pilot randomized controlled study. *Psychiatry Res.* 247, 28–32. doi: 10.1016/j.psychres.2016.11.009

Cancelli, A., Cottone, C., Di Giorgio, M., Carducci, F., and Tecchio, F. (2015a). Personalizing the electrode to neuromodulate an extended cortical region. *Brain Stimul.* 8, 555–560. doi: 10.1016/j.brs.2015.01.398

Cancelli, A., Cottone, C., Giordani, A., Migliore, S., Lupoi, D., Porcaro, C., et al. (2017). Personalized bilateral whole body somatosensory cortex stimulation to relieve fatigue in multiple sclerosis. *Mult. Scler.* doi: 10.1177/1352458517720528. [Epub ahead of print].

Cancelli, A., Cottone, C., Tecchio, F., Truong, D. Q., Dmochowski, J., and Bikson, M. (2016). A simple method for EEG guided transcranial electrical stimulation without models. *J. Neural Eng.* 13:36022. doi: 10.1088/1741-2560/13/3/036022

Cancelli, A., Cottone, C., Zito, G., Di Giorgio, M., Pasqualetti, P., and Tecchio, F. (2015b). Cortical inhibition and excitation by bilateral transcranial alternating current stimulation. *Restor. Neurol. Neurosci.* 33, 105–114. doi: 10.3233/RNN-140411

Charvet, L. E., Kasschau, M., Datta, A., Knotkova, H., Stevens, M. C., Alonzo, A., et al. (2015). Remotely-supervised transcranial direct current stimulation (tDCS) for clinical trials: guidelines for technology and protocols. *Front. Syst. Neurosci.* 9:26. doi: 10.3389/fnsys.2015.00026

Datta, A., Baker, J. M., Bikson, M., and Fridriksson, J. (2011). Individualized model predicts brain current flow during transcranial direct-current stimulation treatment in responsive stroke patient. *Brain Stimul.* 4, 169–174. doi: 10.1016/j.brs.2010.11.001

Datta, A., Bansal, V., Diaz, J., Patel, J., Reato, D., and Bikson, M. (2009). Gyri-precise head model of transcranial direct current stimulation: improved spatial focality using a ring electrode versus conventional rectangular pad. *Brain Stimul.* 2, 201–207. doi: 10.1016/j.brs.2009.03.005

De Ridder, D., Perera, S., and Vanneste, S. (2017). State of the art: novel applications for cortical stimulation. *Neuromodulation* 20, 206–214. doi: 10.1111/ner.12593

Destrieux, C., Fischl, B., Dale, A., and Halgren, E. (2010). Automatic parcellation of human cortical gyri and sulci using standard anatomical nomenclature. *Neuroimage* 53, 1–15. doi: 10.1016/j.neuroimage.2010.06.010

Edwards, D., Cortes, M., Datta, A., Minhas, P., Wassermann, E. M., and Bikson, M. (2013). Physiological and modeling evidence for focal transcranial electrical brain stimulation in humans: a basis for high-definition tDCS. *Neuroimage* 74, 266–275. doi: 10.1016/j.neuroimage.2013.01.042

Engström, M., Flensner, G., Landtblom, A. M., Ek, A. C., and Karlsson, T. (2013). Thalamo-striato-cortical determinants to fatigue in multiple sclerosis. *Brain Behav.* 3, 715–728. doi: 10.1002/brb3.181

Eshel, Y., Witman, S., Rosenfeld, M., and Abboud, S. (1995). Correlation between skull thickness asymmetry and scalp potential estimated by a numerical model of the head. *IEEE Trans. Biomed. Eng.* 42, 242–249. doi: 10.1109/10.364510

Ferrucci, R., Bortolomasi, M., Vergari, M., Tadini, L., Salvoro, B., Giacopuzzi, M., et al. (2009). Transcranial direct current stimulation in severe, drug-resistant major depression. *J. Affect. Disord.* 118, 215–219. doi: 10.1016/j.jad.2009.02.015

Ferrucci, R., Vergari, M., Cogiamanian, F., Bocci, T., Ciocca, M., Tomasini, E., et al. (2014). Transcranial direct current stimulation (tDCS) for fatigue in multiple sclerosis. *Neuro Rehabilitation* 34, 121–127. doi: 10.3233/NRE-131019

Fischl, B., van der Kouwe, A., Destrieux, C., Halgren, E., Ségonne, F., Salat, D. H., et al. (2004). Automatically parcellating the human cerebral cortex. *Cereb. Cortex* 14, 11–22. doi: 10.1093/cercor/bhg087

Fregni, F., Boggio, P. S., Nitsche, M. A., Marcolin, M. A., Rigonatti, S. P., and Pascual-Leone, A. (2006a). Treatment of major depression with transcranial direct current stimulation. *Bipolar Disord.* 8, 203–204. doi: 10.1111/j.1399-5618.2006.00291.x

Fregni, F., Gimenes, R., Valle, A. C., Ferreira, M. J., Rocha, R. R., Natalle, L., et al. (2006b). A randomized, sham-controlled, proof of principle study of transcranial direct current stimulation for the treatment of pain in fibromyalgia. *Arthritis Rheum.* 54, 3988–3998. doi: 10.1002/art.22195

Fregni, F., Liguori, P., Fecteau, S., Nitsche, M. A., Pascual-Leone, A., and Boggio, P. S. (2008). Cortical stimulation of the prefrontal cortex with transcranial direct current stimulation reduces cue-provoked smoking craving: a randomized, sham-controlled study. *J. Clin. Psychiatry* 69, 32–40. doi: 10.4088/JCP.v69n0105

Galletta, E. E., Cancelli, A., Cottone, C., Simonelli, I., Tecchio, F., Bikson, M., et al. (2015). Use of computational modeling to inform tDCS electrode montages for the promotion of language recovery in post-stroke aphasia. *Brain Stimul.* 8, 1108–1115. doi: 10.1016/j.brs.2015.06.018

Gögler, N., Willacker, L., Funk, J., Strube, W., Langgartner, S., Napiórkowski, N., et al. (2016). Single-session transcranial direct current stimulation induces enduring enhancement of visual processing speed in patients with major depression. *Eur. Arch. Psychiatry Clin. Neurosci.* 267, 671–686. doi: 10.1007/s00406-016-0761-y

Grimaldi, G., Argyropoulos, G. P., Bastian, A., Cortes, M., Davis, N. J., Edwards, D. J., et al. (2016). Cerebellar Transcranial Direct Current Stimulation (ctDCS): a novel approach to understanding cerebellar function in health and disease. *Neuroscientist* 22, 83–97. doi: 10.1177/1073858414559409

Hesse, S., Waldner, A., Mehrholz, J., Tomelleri, C., Pohl, M., and Werner, C. (2011). Combined transcranial direct current stimulation and robot-assisted arm training in subacute stroke patients: an exploratory, randomized multicenter trial. *Neurorehabil. Neural Repair* 25, 838–846. doi: 10.1177/15459683114 13906

Huang, Y., Dmochowski, J. P., Su, Y., Datta, A., Rorden, C., and Parra, L. C. (2013). Automated MRI segmentation for individualized modeling of current flow in the human head. *J. Neural Eng.* 10:066004. doi: 10.1088/1741-2560/10/6/066004

Kopell, N. J., Gritton, H. J., Whittington, M. A., and Kramer, M. A. (2014). Beyond the connectome: the dynome. *Neuron* 83, 1319–1328. doi: 10.1016/j.neuron.2014.08.016

Malavera, A., Vasquez, A., and Fregni, F. (2015). Novel methods to optimize the effects of transcranial direct current stimulation: a systematic review of transcranial direct current stimulation patents. *Expert Rev. Med. Devices* 12, 679–688. doi: 10.1586/17434440.2015.1090308

Moreno-Duarte, I., Morse, L. R., Alam, M., Bikson, M., Zafonte, R., and Fregni, F. (2014). Targeted therapies using electrical and magnetic neural stimulation for the treatment of chronic pain in spinal cord injury. *Neuroimage* 85, 1003–1013. doi: 10.1016/j.neuroimage.2013.05.097

Murphy, D. N., Boggio, P., and Fregni, F. (2009). Transcranial direct current stimulation as a therapeutic tool for the treatment of major depression: insights from past and recent clinical studies. *Curr. Opin. Psychiatry* 22, 306–311. doi: 10.1097/YCO.0b013e32832a133f

Nathan, S. S., Sinha, S. R., Gordon, B., Lesser, R. P., and Thakor, N. V (1993). Determination of current density distributions generated by electrical stimulation of the human cerebral cortex. *Electroencephalogr. Clin. Neurophysiol.* 86, 183–192. doi: 10.1016/0013-4694(93)90006-H

Nitsche, M. A., Boggio, P. S., Fregni, F., and Pascual-Leone, A. (2009). Treatment of depression with transcranial direct current stimulation (tDCS): a review. *Exp. Neurol.* 219, 14–19. doi: 10.1016/j.expneurol.2009.03.038

Nitsche, M. A., Nitsche, M. A., Paulus, W., and Paulus, W. (2000). Excitability changes induced in the human motor cortex by weak transcranial direct current stimulation. *J. Physiol.* 527(Pt 3), 633–639. doi: 10.1111/j.1469-7793.2000.t01-1-00633.x

Pahor, A., and Jaušovec, N. (2018). The effects of theta and gamma tACS on working memory and electrophysiology. *Front. Hum. Neurosci.* 11:651. doi: 10.3389/fnhum.2017.00651

Parazzini, M., Fiocchi, S., Cancelli, A., Cottone, C., Liorni, I., Ravazzani, P., et al. (2017). A computational model of the electric field distribution due to regional personalized or nonpersonalized electrodes to select transcranial electric stimulation target. *IEEE Trans. Biomed. Eng.* 64, 184–195. doi: 10.1109/TBME.2016.2553177

Parazzini, M., Fiocchi, S., Rossi, E., Paglialonga, A., and Ravazzani, P. (2011). Transcranial direct current stimulation: estimation of the electric field and of the current density in an anatomical human head model. *IEEE Trans. Biomed. Eng.* 58, 1773–1780. doi: 10.1109/TBME.2011.2116019

Pellicano, C., Gallo, A., Li, X., Ikonomidou, V. N., Evangelou, I. E., Ohayon, J. M., et al. (2010). Relationship of cortical atrophy to fatigue in patients with multiple sclerosis. *Arch. Neurol.* 67, 447–453. doi: 10.1001/archneurol.2010.48

Pérez-Borrego, Y. A., Campolo, M., Soto-León, V., Rodriguez-Matas, M. J., Ortega, E., and Oliviero, A. (2014). Pain treatment using tDCS in a single patient: telemedicine approach in non-invasive brain simulation. *Brain Stimul.* 7, 334–335. doi: 10.1016/j.brs.2013.11.008

Saiote, C., Goldschmidt, T., Timäus, C., Steenwijk, M. D., Opitz, A., Antal, A., et al. (2014). Impact of transcranial direct current stimulation on fatigue in multiple sclerosis. *Restor. Neurol. Neurosci.* 32, 423–436. doi: 10.3233/RNN-130372

Smith, W. E. (1992). Estimation of the spatio-temporal correlations of biological electrical sources from their magnetic fields. *IEEE Trans. Biomed. Eng.* 39, 997–1004. doi: 10.1109/10.161331

Soler, M. D., Kumru, H., Pelayo, R., Vidal, J., Tormos, J. M., Fregni, F., et al. (2010). Effectiveness of transcranial direct current stimulation and visual illusion on neuropathic pain in spinal cord injury. *Brain* 133, 2565–2577. doi: 10.1093/brain/awq184

Tecchio, F., Cancelli, A., Cottone, C., Ferrucci, R., Vergari, M., Zito, G., et al. (2015). Brain plasticity effects of neuromodulation against multiple sclerosis fatigue. *Front. Neurol.* 6:141. doi: 10.3389/fneur.2015.00141

Tecchio, F., Cancelli, A., Cottone, C., Tomasevic, L., Devigus, B., Zito, G., et al. (2013). Regional personalized electrodes to select transcranial current stimulation target. *Front. Hum. Neurosci.* 7:131. doi: 10.3389/fnhum.2013.00131

Tecchio, F., Cancelli, A., Cottone, C., Zito, G., Pasqualetti, P., Ghazaryan, A., et al. (2014). Multiple sclerosis fatigue relief by bilateral somatosensory cortex neuromodulation. *J. Neurol.* 261, 1552–1558. doi: 10.1007/s00415-014-7377-9

Tseng, P., Iu, K. C., and Juan, C. H. (2018). The critical role of phase difference in theta oscillation between bilateral parietal cortices for visuospatial working memory. *Sci. Rep.* 8:349. doi: 10.1038/s41598-017-18449-w

Van Essen, D. C. (2013). Cartography and connectomes. *Neuron* 80, 775–790. doi: 10.1016/j.neuron.2013.10.027

Vecchio, F., Miraglia, F., Porcaro, C., Cottone, C., Cancelli, A., Rossini, P. M., et al. (2017). Electroencephalography-derived sensory and motor network topology in multiple sclerosis fatigue. *Neurorehabil. Neural Repair* 31, 56–64. doi: 10.1177/1545968316656055

Wagner, S., Rampersad, S. M., Aydin, Ü., Vorwerk, J., Oostendorp, T. F., Neuling, T., et al. (2014). Investigation of tDCS volume conduction effects in a highly realistic head model. *J. Neural Eng.* 11:016002. doi: 10.1088/1741-2560/11/1/016002

Zhu, C. E., Yu, B., Zhang, W., Chen, W., Qi, Q., and Miao, Y. (2017). Effiectiveness and safety of transcranial direct current stimulation in fibromyalgia: a systematic review and meta-analysis. *J. Rehabil. Med.* 49, 2–9. doi: 10.2340/16501977-2179

Conflict of Interest Statement: The authors declare that the research was conducted in the absence of any commercial or financial relationships that could be construed as a potential conflict of interest.

Advantages of publishing in Frontiers

OPEN ACCESS
Articles are free to read for greatest visibility and readership

FAST PUBLICATION
Around 90 days from submission to decision

HIGH QUALITY PEER-REVIEW
Rigorous, collaborative, and constructive peer-review

TRANSPARENT PEER-REVIEW
Editors and reviewers acknowledged by name on published articles

Frontiers
Avenue du Tribunal-Fédéral 34
1005 Lausanne | Switzerland

Visit us: www.frontiersin.org
Contact us: info@frontiersin.org | +41 21 510 17 00

REPRODUCIBILITY OF RESEARCH
Support open data and methods to enhance research reproducibility

DIGITAL PUBLISHING
Articles designed for optimal readership across devices

FOLLOW US
@frontiersin

IMPACT METRICS
Advanced article metrics track visibility across digital media

EXTENSIVE PROMOTION
Marketing and promotion of impactful research

LOOP RESEARCH NETWORK
Our network increases your article's readership